ENGINEERING SERVICE CENTER
Port Hueneme, California 93043-4370

TECHNICAL REPORT
TR-2366-ENV

REACTIVE CAPPING MAT DEVELOPMENT AND EVALUATION FOR SEQUESTERING CONTAMINANTS IN SEDIMENT

FINAL REPORT
PROJECT NO: ER-1493

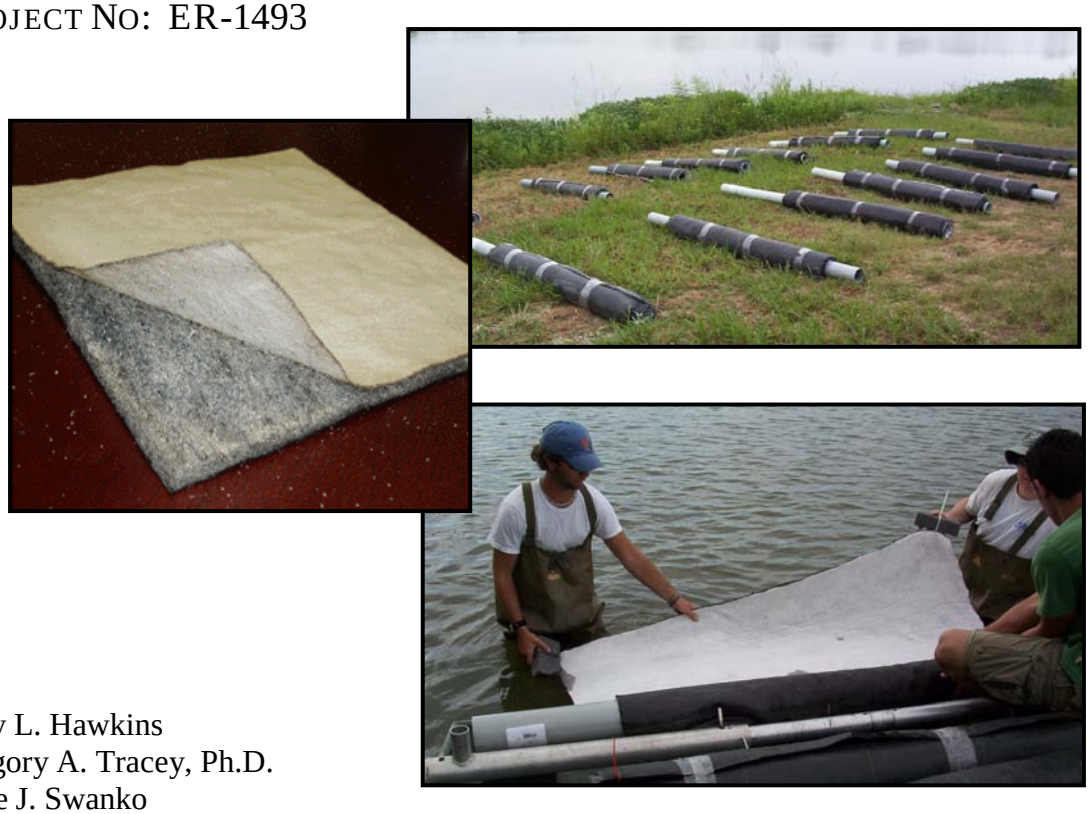

By

Amy L. Hawkins
Gregory A. Tracey, Ph.D.
Jesse J. Swanko
Kevin H. Gardner, Ph.D.
Jeffrey S. Melton, Ph.D.

August 2011

This page is intentionally left blank

REPORT DOCUMENTATION PAGE (SF 298)	Form Approved OMB No. 0704-0811

1. REPORT DATE *(DD-MM-YYYY)*	2. REPORT TYPE	3. DATES COVERED *(From – To)*
20-07-2010	Final Report	

4. TITLE AND SUBTITLE

Reactive Capping Mat Development and Evaluation for Sequestering Contaminants in Sediment

5a. CONTRACT NUMBER

5b. GRANT NUMBER

5c. PROGRAM ELEMENT NUMBER

6. AUTHOR(S)

Amy L. Hawkins, NAVFAC
Gregory A. Tracy, Ph.D., SAIC
Jesse J. Swanko, SAIC
Kevin H. Gardner, Ph.D., UNH
Jeffrey S. Melton, Ph.D., UNH

5d. PROJECT NUMBER

ER-1493

5e. TASK NUMBER

5f. WORK UNIT NUMBER

7. PERFORMING ORGANIZATION NAME(S) AND ADDRESSES

Naval Facilities Engineering Service Center
1100 23rd Avenue, Port Hueneme, CA 93043

8. PERFORMING ORGANIZATION REPORT NUMBER

9. SPONSORING/MONITORING AGENCY NAME(S) AND ADDRESS(ES)

Strategic Environmental Research and Development Program (SERDP)

10. SPONSOR/MONITORS ACRONYM(S)

11. SPONSOR/MONITOR'S REPORT NUMBER(S)

12. DISTRIBUTION/AVAILABILITY STATEMENT

13. SUPPLEMENTARY NOTES

14. ABSTRACT

Strategic Environmental Research and Development Program (SERDP) Project Number ER-1493 (Reactive Capping Mat Development and Evaluation for Sequestering Contaminants in Sediment) was implemented by a collaborative team from the NAVFAC Engineering Service Center (NAVFAC ESC), Science Applications International Corporation (SAIC) and the University of New Hampshire (UNH). The project consisted of developing a reactive geotextile mat system to serve as a chemically effective, mechanically stable, and cost efficient technology for reducing ecological risks by sequestering contaminants in sediment. Use of reactive mat systems could provide an alternative to costly dredging and offsite disposal, and a more stable solution for standard capping approaches. The mat system, if deemed successful, would be deployed in a wide variety of environmental settings to prevent both metals and organic contaminants from entering overlying surface waters while simultaneously allowing both groundwater flux and surficial biological colonization.

15. SUBJECT TERMS

16. SECURITY CLASSIFICATION OF:			17. LIMITATION OF ABSTRACT	18. NUMBER OF PAGES	19a. NAME OF RESPONSIBLE PERSON
a. REPORT	b. ABSTRACT	c. THIS PAGE			19b. TELEPHONE NUMBER *(include area code)*
U	U	U			

This page is intentionally left blank.

EXECUTIVE SUMMARY

Strategic Environmental Research and Development Program (SERDP) Project Number ER-1493 (Reactive Capping Mat Development and Evaluation for Sequestering Contaminants in Sediment) was implemented by a collaborative team from the NAVFAC Engineering Service Center (NAVFAC ESC), Science Applications International Corporation (SAIC) and the University of New Hampshire (UNH). The project consisted of developing a reactive geotextile mat system to serve as a chemically effective, mechanically stable, and cost efficient technology for reducing ecological risks by sequestering contaminants in sediment. Use of reactive mat systems could provide an alternative to costly dredging and offsite disposal, and a more stable solution for standard capping approaches. The mat system, if deemed successful, would be deployed in a wide variety of environmental settings to prevent both metals and organic contaminants from entering overlying surface waters while simultaneously allowing both groundwater flux and surficial biological colonization.

Laboratory Studies. Various mixtures of reactive amendments to potentially adsorb sediment contamination were evaluated in a laboratory setting to determine the optimal combination of reactive core materials (activated carbon, apatite, and organoclay) to be placed within prototype mats with woven geotextile tops and non-woven geotextile backs to be positioned on top of sediments of concern. Laboratory data from amendment isotherm experiments and kinetics studies identified CETCO Sediment Remediation Technologies organoclay containing bentonite as the base clay and coconut shell activated carbon as the optimal amendments for achieving maximum contaminant sequestration (as compared to other types of organoclay and activated carbon). Preloading studies with humic acid on activated carbon generally indicated negligible effects, but similar tests on organoclay showed that preloading with humic acid did change the relative adsorption capacity of individual PAHs and that the long term exposure of organoclay to natural organic matter might also affect mat performance by causing increased desorption of target compounds.

Gradient ratio testing and finite element modeling were conducted in a laboratory setting using both clean geotextiles and field weathered small-scale (6 ft x 6 ft) test mats to identify the non-woven geotextile most resistant to biofouling (8 oz/yd^2 polypropylene with 80 apparent opening size) for construction of the prototype mat system. These results along with numerical modeling showed that the coarser geotextiles (AOS 70 and 80) did not clog and did not lose amendment under controlled laboratory conditions while also experiencing relatively little sediment transport into the cap. Gas permeability testing also showed that these coarser geotextiles would allow the maximum methane levels produced in a freshwater environment to pass through the reactive mat without creating uplift as long as additional weight was supplied by an overlying sand cap. Based on these cumulative laboratory results, a reactive mat featuring a 0.28 lb/ft^2 activated carbon, 0.23 lb/ft^2 apatite, 0.28 lb/ft^2 organoclay amendment mixture and an AOS 80 geotextile was recommended for the treatment of metals and organics in aquatic environments of low to moderate dissolved organic matter levels.

Site Selection. Following an extensive desktop site selection process, Cottonwood Bay in Grand Prairie, Texas was selected as the most suitable project test site based on a variety of chemical, physical, biological and logistical factors. A comprehensive geophysical investigation, including

bathymetry, side-scan sonar, sediment profile imaging and groundwater seep surveys was conducted to characterize the site and identify a specific target area with a substantial groundwater plume for mat system placement. These surveys confirmed that the site was free of obstacles that would impede mat performance and provided baseline topography information for comparison to the sediment landscape following mat deployment. Groundwater seepage results identified an area of relatively high groundwater flow potential in the center of the bay as defined by average subsurface porewater temperatures 1.61ºC cooler and average subsurface porewater conductivity 0.71 mS/cm greater than corresponding surface water; known groundwater plumes were integral to the site selection process.

Prototype Testing. A prototype mat system was deployed in Cottonwood Bay in April 2008, featuring four 25 ft x 25 ft test arrangements (bare single layer geotextile, single layer geotextile with sand cap, bare double layer geotextile, sand cap only) and an undisturbed control. In fall 2008, following five months of soak time, the effectiveness of the various test arrangements for contaminant sequestration was monitored with passive samplers (peepers, semi-permeable membrane devices). The passive samplers were strategically placed at specific interfaces of interest in the various mat system treatments and allowed to soak for 50 days. Concurrent with the passive sampler recovery in December 2008, a post-construction geophysical investigation of the full scale mat system was conducted to evaluate the geophysical properties (*e.g.*, acoustic signature, sand cap placement, microorganism activity) of the various treatments. In summer 2009, approximately one year after deployment of the full scale mat system (six months after deployment of the passive samplers), Ultraseep and Trident Probe porewater measurements were collected to quantify water flux from sediments through the various treatments and identify any change in contaminant concentration with respect to potential overlying sources (*e.g.*, groundwater fluxing out of the mat versus overlying water penetrating the mat). Passive contaminant sampling at the prototype mat system was repeated in fall 2009 to provide comparative second year contaminant sequestration results. Sediment cores were also collected from each treatment area at that time to characterize the sediment from which previous porewater samples had been extracted and to establish the vertical chemical gradient in the natural sediments for confirmation of previous porewater sampler results.

Overall prototype field data indicated that below treatment porewater chemistry correlated to surface sediment trends across treatments, thus providing a reliable indicator of localized contaminant partitioning below the mat interfaces. Porewater flux (*i.e.*, Ultraseep) results showed that metals concentrations passing through the mats were comparable to above treatment peeper results, thus indicating that the mats are sequestering deep metal porewater concentrations observed in the Trident Probe dataset. In general the geophysical data revealed changes within the range of modeled expectations and exhibited sufficient sensitivity to be a useful tool for monitoring mat conditions. Mat uplift due to gas buildup beneath the geotextile was observed in the summer months for the mat only treatments, but these conditions were not found in the mat treatment with an additional sand cap providing sufficient weight, thus confirming the predicted results of the gas permeability testing.

Finally, the passive sampler (*i.e.*, peeper, SPMD) data showed generally consistent and statistically significant (at 90-95% confidence) two- to four-fold below/above reductions in primarily two treatments (mat/sand and double mat) between years for certain metals (nickel,

zinc, barium, silver, vanadium) and several polycyclic aromatic hydrocarbons (benzo[b]fluoranthene, indeno[1,2,3-c,d]pyrene, benzo[g,h,i]perylene, anthracene, benzo[a]anthracene), thus demonstrating that contaminant sequestration had occurred. Performance for other metals (*e.g.*, copper) was less robust and limited by overall low environmental concentrations relative to detection limits.

Conclusions and Recommendations. The selected implementation method including mat with sand cover is recommended as an effective technology to sequester contaminants in sediments while preventing uplift due to gas accumulation. Unlike the low level concentrations observed in surface sediments of the present study, the future candidate site sediments should contain contamination in the ecological effects range and be confirmed by an advance site chemical characterization study of the specific placement area (not performed in the present study). Laboratory verification via chemical testing and geotechnical modeling using methods developed in the present study should also be performed to predict mat performance metrics. These data will ensure that field passive sampler measurements (with an appropriate degree of sample replication) can reliably confirm/refute whether a broad suite of chemical gradients (as opposed to the limited metals and PAHs of the present study) are being better controlled by the mat treatment as opposed to a traditional capping approach (*i.e.*, sand/mix only covers). Based on the results of the present study, the project goal of further evaluating the reactive capping mat technology via a large-scale (~10,000 ft^2) implementation at a selected remediation site is recommended.

This page is intentionally left blank.

ACRONYMS AND ABBREVIATIONS

AldHA	Aldrich Humic Acid
AOS	Apparent Opening Size
AUS	American Underwater Services, Inc.
BET	Brunauer, Emmett and Teller
CMA	Coastal Monitoring Associates, Inc.
CoC	Contaminant of Concern
DOC	Dissolved Organic Carbon
DoD	Department of Defense
ESTCP	Environmental Security Technology Certification Program
FA	Fulvic Acid
FEA	Finite Element Analysis
FS	Feasibility Study
GC/MS	Gas Chromatograph/Mass Spectrometer
GR	Gradient Ratio
HOC	Hydrophobic Organic Contaminant
ICP-MS	Inductively Coupled Plasma-Mass Spectrometry
LCL	Lower Confidence Limit
LL	Liquid Limit
MDL	Method Detection Limit
MNA	Monitored Natural Attenuation
NAS	Naval Air Station
NAVFAC	Naval Facilities Engineering Command
NFESC	Naval Facilities Engineering Service Center
NOM	Natural Organic Matter
NWIRP	Naval Weapons Industrial Reserve Plant
PAH	Polycyclic Aromatic Hydrocarbons
PCB	Polychlorinated Biphenyls
PED	Polyethylene Device
PI	Plasticity Index
PMDS	Polydimethylsiloxan
QA/QC	Quality Assurance/Quality Control
SAIC	Science Applications International Corporation
SDI	Specialty Devices, Inc.
SEC	Size Exclusion Chromatography
SERDP	Strategic Environmental Research and Development Program
SPI	Sediment Profile Imaging
SPME	Solid Phase Micro-Extraction
SPMD	Semi-Permeable Membrane Device
SRHA	Suwannee River Humic Acid
SRFA	Suwannee River Fulvic Acid
SRNOM	Suwannee River Natural Organic Matter
TCMX	Tetrachlorometaxylene
TNRCC	Texas Natural Resource Conservation Commission

LIST OF ACRONYMS AND ABBREVIATIONS (Continued)

TOC	Total Organic Carbon
TRRP	Texas Risk Reduction Program
UCL	Upper Confidence Limit
UNH	University of New Hampshire
USEPA	United States Environmental Protection Agency
USGS	United States Geological Survey
WAAS	Wide Area Augmentation System

TABLE OF CONTENTS

Page

LIST OF TABLES xiii
LIST OF FIGURES xv
1.0 INTRODUCTION 1
2.0 OBJECTIVE 1
3.0 BACKGROUND 1
4.0 MATERIALS AND METHODS 2
4.1 Task 1: Composite Material Testing 3
4.1.1 Amendment Adsorption Capacity 4
4.1.2 Amendment Adsorption Kinetics 6
4.1.3 Combined Effects of Humic Acid, Fulvic Acid and Natural Organic Matter 6
4.1.4 Column Testing 6
4.2 Task 2: Pilot Site Selection 7
4.2.1 Strategy Overview 7
4.2.2 Primary Site Selection Criteria 8
4.2.3 Geophysical Surveys 9
4.3 Task 3: Geotextile Testing 11
4.3.1 Field Evaluation 11
4.3.2 Gradient Ratio Testing 16
4.3.3 Finite Element Analysis 19
4.3.4 Gas Permeability Testing 24
4.4 Task 4: Prototype Mat System Testing 26
4.4.1 Prototype Mat System Design 26
4.4.2 Mat System Deployment 28
4.4.3 Geophysical Investigation 31
4.4.4 Passive Contaminant Sampling 31
4.4.5 Chemical Flux Survey 37
4.4.6 Sediment Coring 40
5.0 RESULTS AND DISCUSSION 41
5.1 Task 1: Composite Material Testing 41
5.1.1 Amendment Adsorption Capacity 42
5.1.2 Amendment Adsorption Kinetics 43
5.1.3 Combined Effects of Humic Acid, Fulvic Acid and Natural Organic Material 44
5.2 Task 2: Pilot Site Selection 47
5.2.1 Site Selection Overview 47
5.2.2 Selected Site Background Assessment 48
5.2.3 Geophysical Surveys 52
5.2.4 Target Area Establishment 57
5.3 Task 3: Geotextile Testing 59
5.3.1 Field Evaluation 59
5.3.2 Gradient Ratio Testing 59
5.3.3 Consolidation Testing 70
5.3.4 Finite Element Analysis 75
5.3.5 Gas Permeability Testing 84
5.4 Task 4: Prototype Mat Testing 87

TABLE OF CONTENTS
(Continued)

Page

5.4.1 Geophysical Investigation 87
5.4.2 Diffusion Sampling Results 92
5.4.3 Volumetric Sampling Results 107
5.4.4 Sediment Coring 112
5.4.5 Sources of Uncertainty 114
6.0 CONCLUSIONS AND IMPLICATIONS FOR FUTURE RESEARCH/IMPLEMENTATION 117
ACKNOWLEDGEMENTS 120
REFERENCES 122

LIST OF APPENDICES

Appendix A. SERDP Project Number ER-1493 First Year Annual Progress Report (December 2006) A-1

Appendix B. SERDP Project Number ER-1493 Second Year Annual Progress Report (December 2007) B-1

Appendix C. Mat System Consolidation and Groundwater Flow Modeling Results C-1

Appendix D. Prototype Mat System Geophysical Results (December 2008) D-1

Appendix E. First and Second Year Peeper Analytical Results (December 2008 & December 2009) E-1

Appendix F. First and Second Year Semi-Permeable Membrane Device (SPMD) Analytical Results (December 2008 & December 2009) F-1

Appendix G. Prototype Mat System Ultraseep Flow and Analytical Data (June 2009) G-1

Appendix H. Prototype Mat System Trident Probe Analytical Results (June 2009) H-1

Appendix I. Prototype Mat System Sediment Core Results (October 2009) I-1

LIST OF ATTACHMENTS

Attachment 1. Sharma, B. 2008. Evaluation of Reactive Cap Sorbents for In-Situ Remediation of Contaminated Sediments. Submitted to the University of New Hampshire. September. J-1

LIST OF TABLES

Table 4.3-1. Material design summary of small-scale geotextile test mats. 12

Table 4.3-2. Characteristics of clean representative mats used in gradient ratio experiments. 19

Table 4.3-3. Summary of average geotechnical property estimates for finite element modeling. 22

Table 4.4-1. Report outline for design element experimental results used to guide construction of the final prototype mat system. 26

Table 4.4-2. Ultraseep sampling summary for the Cottonwood Bay prototype mat system. 38

Table 5.2-1. Select sediment data available from historic Cottonwood Bay samples showing elevated concentrations of contaminants of interest for the site selection process. 50

Table 5.2-2. Sediment core characteristics at two stations in Cottonwood Bay West. 54
Table 5.2-3. Trident Probe subsurface temperature and conductivity results for Cottonwood Bay. 56
Table 5.3-1. List of non-woven geotextiles used for reactive core gradient ratio testing applications. 60
Table 5.3-2. Approximate gas bubble volume over time during the gas permeability test. 85
Table 5.4-1. Summary of first year (top) and second year (bottom) peeper mean analytical results for all metals of concern at the prototype mat system. 93
Table 5.4-2. Results of hypothesis testing to determine the statistical significance of contaminant reductions across treatment boundaries for all metals of concern at the prototype mat system. 94
Table 5.4-3. Suspected outliers for metals of concern in the peeper dataset identified at the sub-replicate level. 97
Table 5.4-4. Results of hypothesis testing to determine the statistical significance of contaminant reductions across treatment boundaries for all metals of concern at the prototype mat system with the exclusion of sub-replicate outliers.....97
Table 5.4-5. Comparison of “below treatment” peeper concentrations with and without non-detect values included in the mean calculations. 100
Table 5.4-6. Summary of first year (top) and second year (bottom) SPMD mean analytical results for all PAHs at the prototype mat system. 102
Table 5.4-7. Results of hypothesis testing to determine the statistical significance of contaminant reductions across treatment boundaries for PAHs at the prototype mat system. 103
Table 5.4-8. Summary of Trident Probe mean analytical results for all metals of concern at the prototype mat system. 109
Table 5.4-9. Summary of Ultraseep mean analytical results for all metals of concern at the prototype mat system adjusted to reflect the discharge sample. 111
Table 5.4-10. Summary of sediment core chemistry for all metals of concern and PAHs at the prototype mat system. 112
Table 5.4-11. Ultraseep, deep Trident Probe and “below treatment” peeper results for zinc in the prototype mat system. 115
Table 5.4-12. Comparison of Year One and Year Two “above treatment” peeper concentrations with background water column peeper concentrations. 117

LIST OF FIGURES

Figure 4.1-1. Experimental column for reactive mat flow-through testing. 7

Figure 4.2-1. Overview of the Cottonwood Bay site. 10

Figure 4.3-1. Construction diagram of small-scale geotextile test mats. 12

Figure 4.3-2. Small-scale geotextile test mat deployment. 13

Figure 4.3-4. Geotextile sediment gradient ratio column experimental setup. 15

Figure 4.3-5. Detailed photograph of geotextile gradient ratio test column showing (a) permeameter for gradient ratio tests, (b) geotextile-sediment contact and (c) mat-sediment contact. 17

Figure 4.3-6. Comparative images of a geotextile sample before (left) and after (right) a gradient ratio test. 17

Figure 4.3-7. Sediment that has passed through the geotextile during a gradient ratio test. 18

Figure 4.3-8. Geometry of a typical reactive mat application for finite element modeling. 21

Figure 4.3-9. Summary of the boundary conditions for finite element modeling. 21

Figure 4.3-10. Permeameter setup for gas permeability testing. 25

Figure 4.4-1. Construction and layout diagrams of prototype geotextile test mats. 27

Figure 4.4-2. Various arrangements for prototype mat system testing. 27

Figure 4.4-3. Vertical passive sampler layout in Cottonwood Bay. 32

Figure 5.1-1. Adsorption of 2,2’,5,5’-tetrachlorobiphenyl on bare activated carbon in the presence of Passaic River and Hudson River porewaters. 46

Figure 5.1-2. Adsorption of 2,2’,5,5’-tetrachlorobiphenyl on virgin sorbent mixture (virgin SM) and weathered sorbent mixture after six months in Cottonwood Bay (CB SM). 46

Figure 5.2-1. Conceptual model of the hydrogeologic setting of the Cottonwood Bay site (modified from Barker and Braun 2000). 49

Figure 5.2-2. Historic Cottonwood Bay sampling stations used in the site background assessment (modified from EnSafe 2001). 51

Figure 5.2-3. Locations of remedial wells and trenches at the Cottonwood Bay site (modified from Barker and Braun 2000). 52

Figure 5.2-4. Trident Probe stations for the Cottonwood Bay groundwater seepage survey. 56

Figure 5.2-5. Potential groundwater discharge zones for Cottonwood Bay. 57

Figure 5.2-6. Preferred target areas for prototype mat system deployment based on the results of the Cottonwood Bay geophysical surveys. 58

Figure 5.3-1. Gradient ratio test results for geotextile GT-1 (AOS 170). 61
Figure 5.3-2. Gradient ratio test results for geotextile GT-2 (AOS 70). 61
Figure 5.3-3. Gradient ratio test results for geotextile GT-3 (AOS 80). 62
Figure 5.3-4. Gradient ratio test results for geotextile GT-4 (AOS 170). 62
Figure 5.3-5. Gradient ratio test results for clean mats featuring the GT-2 (AOS 70) geotextile and containing organoclay and activated carbon as the reactive material. 64
Figure 5.3-6. Gradient ratio test results for weathered geotextile mat RCM-1 after six months of soak time in Cottonwood Bay. 64
Figure 5.3-7. Gradient ratio test results for weathered geotextile mat RCM-3 after six months of soak time in Cottonwood Bay. 65
Figure 5.3-8. Gradient ratio test results for weathered geotextile mat RCM-5 after six months of soak time in Cottonwood Bay. 65
Figure 5.3-9. Long-term gradient ratio test results for geotextiles GT-2 and GT-3. 66
Figure 5.3-10. Evidence of wall seepage near the manometer port during the long-term gradient ratio test for single geotextile GT-3. 67
Figure 5.3-11. Example of sediment passing through the geotextile during a typical gradient ratio test. 68
Figure 5.3-12. Sediment mass passing through different geotextiles and reactive core mats during gradient ratio tests starting at hydraulic gradient of $i = 5$. 69
Figure 5.3-13. Consolidation of Cottonwood Bay sediment; strain versus effective stress. 71
Figure 5.3-14. Consolidation of Cottonwood Bay sediment; void ratio versus effective stress. 71
Figure 5.3-15. Coefficient of consolidation of Cottonwood Bay sediment. 72
Figure 5.3-16. Coefficient of volumetric compressibility of Cottonwood Bay sediment. 72
Figure 5.3-17. Variation in coefficient of consolidation with void ratio for Cottonwood Bay sediment. 73
Figure 5.3-18. Variation in coefficient of volumetric compressibility for Cottonwood Bay sediment. 73
Figure 5.3-19. Permeability versus effective stress for Cottonwood Bay sediment. 74
Figure 5.3-20. Void ratio versus permeability for Cottonwood Bay sediment. 74
Figure 5.3-21. Excess pore pressure dissipation in the underlying sediment for the uncoupled consolidation finite element model. 76
Figure 5.3-22. Settlement due to mat deployment after 95% sediment consolidation under the uncoupled model. 76
Figure 5.3-23. Horizontal profile of maximum sediment displacement under the uncoupled consolidation model. 77

Figure 5.3-24. Volumetric strain after 95% consolidation under the uncoupled consolidation model. 77
Figure 5.3-25. Total water pore pressure for an unclogged mat (a) and a clogged mat (b) under the uncoupled seepage model. 79
Figure 5.3-26. Specific discharge for an unclogged mat (a) and a clogged mat (b) under the uncoupled seepage model. 80
Figure 5.3-27. Sediment settlement due to mat deployment under the coupled model....81
Figure 5.3-28. Horizontal profile of the maximum sediment displacement under the coupled model. 82
Figure 5.3-29. Volumetric strain under the coupled model. 82
Figure 5.3-30. Biogas bubble flow/dissipation at Day 0 (left) and Day 12 (right) of the gas permeability test. 85
Figure 5.3-31. Volume of the gas bubble beneath the geotextile versus time. 86
Figure 5.3-32. Flow/dissipation rate of gas versus time per square meter of geotextile. 86
Figure 5.4-1. Water depth comparison in Cottonwood Bay from bathymetry collected both before and after placement of the prototype mat system. 91
Figure 5.4-2. First year (left column) and second year (right column) peeper analytical results for select metals (nickel, zinc, copper) at the prototype mat system. 95
Figure 5.4-3. First year (left column) and second year (right column) peeper analytical results for select metals (nickel, zinc, copper) at the prototype mat system with the exclusion of sub-replicate outliers. 98
Figure 5.4-4. Second year vertical peeper analytical results for select metals (cadmium, chromium) at the prototype mat system. 101
Figure 5.4-5 First year (left column) and second year (right column) SPMD analytical results for select low molecular weight (anthracene), high molecular weight (benzo[a]anthracene) and total PAHs at the prototype mat system. 106
Figure 5.4-6. Trident Probe analytical results for a select metal (nickel) at the prototype mat system relative to the treatment-water interface (thickness of mat included where applicable). 109
Figure 5.4-7. Reduction factors for deep (-11”) versus shallow (-3.5”, directly below treatment) porewater concentrations for various metals below the mat system treatments as measured by the Trident Probe. 110
Figure 5.4-8. Ultraseep analytical results for select metals for the prototype mat system treatments. Discharge fraction (%) values indicated in text boxes (see text). 111
Figure 5.4-9. Sediment core analytical results in surface (0-4”) and subsurface (4-8”) layers for select metals (nickel, copper, zinc) and PAHs (anthracene, benzo[a]anthracene) at various treatments in the prototype mat system. 113

Figure 5.4-10. Historic and recent bulk sediment analytical results for select metals and organics at the prototype mat system area in Cottonwood Bay. 115

1.0 INTRODUCTION

Strategic Environmental Research and Development Program (SERDP) Project Number ER-1493 (Reactive Capping Mat Development and Evaluation for Sequestering Contaminants in Sediment) was implemented by a collaborative team from the NAVFAC Engineering Service Center (NAVFAC ESC), Science Applications International Corporation (SAIC) and the University of New Hampshire (UNH). The project consisted of developing a reactive geotextile mat system to serve as a chemically effective, mechanically stable, and cost efficient technology for reducing ecological risks by sequestering contaminants in sediment. Use of reactive mat systems could provide an alternative to costly dredging and offsite disposal, and a more stable solution for standard capping approaches. The mat system, if deemed successful, would be deployed in a wide variety of environmental settings to prevent both metals and organic contaminants from entering overlying surface waters while simultaneously allowing both groundwater flux and surficial biological colonization.

2.0 OBJECTIVE

The objective of SERDP Project Number ER-1493 is to develop and test a mixture of chemically reactive materials suitable for incorporation within an engineered geotextile mat to create a composite active capping system capable of deployment in a wide variety of environmental settings in order to effectively sequester both metal and organic contaminants in sediments.

3.0 BACKGROUND

In situ capping has frequently been used to physically separate contaminated sediments from the aquatic environment above the cap and, in some cases, to act as an impermeable barrier to groundwater flux. Sequestration based on physical separation alone, however, is not always desirable because it does not ensure that dissolved phase contaminant flux is eliminated as a transport pathway either through or around the cap. More recently, *in situ* capping with chemically reactive materials has been explored as an option to provide a physical barrier to remobilization of sediment-bound contaminants while at the same time sequestering dissolved contaminants as they flow through the cap via groundwater flux (Knox *et al*. 2008, McDonough *et al*. 2007, Zhao *et al*. 2007, Reible *et al*. 2006). To date, studies of these reactive capping methods have largely focused on applying one type of reactive material to treat one particular class of contaminant and have typically involved deploying relatively thick layers of unconsolidated material (6 to 12 inches) over the bottom to accomplish this goal. Such an approach may not be effective at many sites with physically challenging conditions, multiple classes of contaminants or concerns with cap stability due to erosive forces. Loosely applied amendment caps may also be prohibitively expensive due to the increased costs associated with broadcasting larger amounts of coarsely applied reactive materials to achieve the desired cap thickness.

In contrast to thick layers of reactive material, *in situ* capping with a reactive geotextile mat may be a more practical means of sequestering sediment contaminants at many sites by preventing physical contact between biota and sediment and retarding leaching of chemicals into overlying waters while simultaneously allowing natural groundwater flow. The mixed reactive capping

materials developed in this project will satisfy these conditions when incorporated into a functional mat system. Overall, the reactive mats would be non-intrusive, would simultaneously address multiple contaminant classes, would be easily deployed and would offer greater permeability to natural groundwater flow than a thick layer of unconsolidated reactive material. These benefits also expand the utility of the reactive mat system to intertidal and sloped environments where the stability and effectiveness of either a traditional sand cap or unconstrained reactive materials would be diminished due to dynamic conditions. Finally, reactive mats can be fabricated on land to control mat thickness (0.5 inch) and amendment proportions, thus minimizing the amount and cost of composite material as compared to the current practice of placing large amounts of unconsolidated substrate cap material through the water column which can result in uncertain and variable layers.

Year One activities for SERDP Project Number ER-1493 were described in the First Year Annual Progress Report prepared in December 2006 (NAVFAC 2006). The first year actions involved separating the project into four separate tasks, performing composite material testing, identifying a primary pilot site, and fabricating small-scale test mats. Year Two activities were described in the Second Year Annual Progress Report prepared in December 2007 (NAVFAC 2007), including continued composite material testing, final pilot site selection, geophysical surveys for target area establishment and small-scale test mat deployment. This final report summarizes these results, describes additional year three and year four monitoring activities and provides final conclusions regarding the overall mat system effectiveness in achieving project goals. A final summary is also provided to outline the potential transition of this technology to future full-scale ESTCP remediation efforts. The Year One and Year Two Progress Reports are provided as Appendix A and Appendix B, respectively.

4.0 MATERIALS AND METHODS

This section provides a comprehensive description of how scientific questions were approached and addressed for each of four tasks established in the technical proposal. Based on the overall goal of developing a chemically effective, mechanically stable and cost efficient technology that could be deployed in a wide variety of environmental settings, the laboratory and field studies were designed to increase understanding of the practical effectiveness and limitations of this technology. The following sections summarize the experimental design of each investigation as well as associated desktop audits, field work, and laboratory analyses; detailed descriptions are referenced in appropriate Appendices. The considerable and important steps discussed in these sections include the following.

- ***Composite Material Testing***. Laboratory tests were designed and performed to identify the mixture of amendment materials to be incorporated into the reactive mats that most effectively sequesters contaminants of interest. The results of these experiments were used to design various small-scale test mats used for preliminary evaluation as well as to construct the prototype mats used for long-term monitoring and evaluation.
- ***Pilot Site Establishment.*** Desktop audits were performed to identify a project location (water body) that could be used as a pilot site for in-situ testing of various reactive mat and amendment arrangements. A subsequent geophysical investigation was then performed at this pilot site to select a particular area within the water body to serve as the

target location for long-term field testing of the prototype mat system constructed to the specifications of the composite material testing results. All field efforts for this project were performed at the selected pilot site.

- ***Geotextile Testing.*** Small-scale test mats featuring different types of geotextile materials were tested under controlled laboratory conditions as well as deployed at the selected pilot site and recovered after two predetermined soak times to assess the potential effects of biofouling, biofilm formation and weathering on final mat design and efficacy. The geotextile type found to be most resistant to biofouling while still maintaining proper integrity and porosity as determined from these tests was ultimately used to construct the prototype mat system used for long-term monitoring and evaluation.
- ***Prototype Mat Testing.*** Variations on a prototype mat system were constructed at the selected pilot site to include various treatments (*e.g.*, single mat, double mat, mat with sand cap) of a reactive mat featuring the most resistant geotextile as recommended by the results of the geotextile testing as well as the optimum amendment mixture as determined by the results of the composite material testing. This mat system was monitored and evaluated over a period of two years to determine the effectiveness of the proposed technology in achieving project goals.

4.1 Task 1: Composite Material Testing

The purpose of composite material testing for this project was to determine the optimal mixture of reactive sequestering materials to be incorporated in the final geotextile mat design. To accomplish this goal, many laboratory studies were required to empirically assess the adsorption behavior of various amendments primarily on different classes of organic compounds.

The first year effort for Task 1 primarily involved testing coconut shell-based activated carbon and three different formulations of brand name organoclays as potential sorbents for organic compounds; additional studies with apatite were conducted as the default sorbent for metals. The sorbent materials were exposed to several common contaminants of interest including five coplanar and non-coplanar polychlorinated biphenyls (PCBs), three polycyclic aromatic hydrocarbons (PAHs) of different ring structures and water solubilities and two heavy metals. Batch studies were performed as both single contaminant systems and multi-contaminant competitive systems. The methods for these initial experiments are discussed in detail in the First Year Annual Progress Report for this project (NAVFAC 2006).

Year two composite material testing investigated the interference caused by humic acid on the adsorption of coplanar and non-coplanar PCBs and PAHs onto activated carbons and organoclays, the two types of sorbents considered for incorporation into the final reactive mat design. To accomplish this goal, several additional kinetic and isotherm studies were conducted using various formulations of activated carbon and organoclay. The methods for these follow-up experiments are discussed in detail in the Second Year Annual Progress Report for this project (NAVFAC 2007).

Early in the third year of the project, laboratory studies were completed to determine the optimal mixture of reactive sequestering materials to be incorporated in the final geotextile mat design.

The results of previous investigations had already identified CETCO Sediment Remediation Technologies organoclay containing bentonite as the base clay and coconut shell activated carbon as the optimal amendments for achieving maximum contaminant sequestration (as compared to other types of organoclay and activated carbon).

Complete methods for the composite material testing activities are provided in the dissertation "Evaluation of Reactive Cap Sorbents for In-Situ Remediation of Contaminated Sediments" submitted to the University of New Hampshire by doctoral candidate Bhawana Sharma in 2008 (Sharma 2008, attached). Summaries of these methods as they pertain to SERDP Project Number ER-1493 are presented in the following sections.

4.1.1 Amendment Adsorption Capacity

Isotherm Experiments. Isotherm experiments for the characterization of the adsorption capacities of CETCO organoclay and coconut shell activated carbon were conducted in separate 125 mL batches with select concentrations of naphthalene, phenanthrene and pyrene, respectively, in contact with the sorbent phase. All the batch experiments were conducted using methanol and deionized water and were carried out at different loading rates of the select contaminants with both bare amendment and amendment preloaded with humic acid to obtain adsorption isotherms. The studies were conducted with an adsorption equilibration time of 48 hours for organoclay and 72 hours for activated carbon; previous experiments conducted as part of this project had shown these durations represented reasonable equilibration periods for adsorption of the select contaminants onto these types of amendments.

Batch adsorption experiments were also conducted with the field-conditioned sorbent mixture (0.28 lb/ft^2 activated carbon, 0.23 lb/ft^2 apatite, 0.28 lb/ft^2 organoclay) obtained from the small-scale test mat recovered from Cottonwood Bay (the selected mat system pilot site) after six months of soak time. These experiments were conducted for a duration of one week at five loadings of a contaminant mixture containing both 2,2',5,5'-tetrachlorobiphenyl and phenanthrene.

As the most favorable mixture of amendment materials was still uncertain after year two, additional batch isotherm experiments were conducted to evaluate the performance of CETCO organoclay and coconut shell activated carbon regarding the adsorption capacity of select PCBs (2-chlorobiphenyl, 2,2',5,5'-tetrachlorobiphenyl, 2,2',4,4',5,5'-hexachlorobiphenyl) and PAHs (naphthalene, phenanthrene, and pyrene) in the presence and absence of humic acid. Kinetics experiments were also conducted to determine the adsorption equilibration time for pyrene and phenanthrene on CETCO organoclay and coconut shell activated carbon. Finally, based on the adsorption equilibration time obtained for pyrene, additional isotherm studies were conducted to determine the desorption properties of naphthalene, phenanthrene and pyrene on CETCO organoclay and activated carbon when these amendments are treated as bare sorbents and preloaded with humic acid.

In addition to these adsorption studies, structural analyses for activated carbon and organoclay were conducted using scanning electron microscopy and x-ray diffractometry, atomic force microscopy and scanning electron microscopy, respectively. The purpose of the structural

analyses was to observe physical differences caused by humic acid on the surfaces of the sorbent material molecules. The Brunauer, Emmett and Teller (BET) surface area analysis was also conducted to determine the surface area of activated carbon and organoclay particles. These structural analyses were conducted as part of standard laboratory QA/QC practices defined for the study and the resulting characterization could serve to explain unexpected behavior in the amendment test experiments. As unexpected amendment behavior was not observed during the laboratory tests, the structural results were not pivotal to the conclusions of this report. Thermogravimetric analyses of organoclays were also performed to determine the percent organic content that increases the hydrophobicity, and thus adsorption capacity, of this type of material.

Humic Acid Preloading. The preloading of both organoclay and activated carbon for the batch isotherm experiments was done with 1 g/L of humic acid solution prepared in deionized water. A sodium azide solution was added to the humic acid solution and the sorbent samples were equilibrated for 48 hours at 150 rpm on a rotary shaker to ensure thorough mixing. In the preloaded amendment samples, humic acid was present in two forms: (i) humic acid adsorbed due to preloading and (ii) humic acid in dissolved form in a deionized water matrix.

Sample Extraction. When the equilibrium time was reached for each batch experiment, the supernatant was extracted into hexane by the vial liquid-liquid extraction method with tetrachlorometaxylene (TCMX) as a surrogate standard. Twenty mL of sample and 10 mL of hexane were transferred into a 40 mL vial. The vials were sealed with Teflon®-lined screw caps and shaken vigorously for 30 seconds on three separate occasions. The vials were then stored for 24 hours at 4˚C, at which point the extracts were passed through sodium sulfate to remove any chemically bound water prior to analysis with gas chromatograph columns.

Gas Chromatographic Analysis. All sample extracts were analyzed for naphthalene, phenanthrene, pyrene and 2,2',5,5'-tetrachlorobiphenyl adsorption using a Varian CP3800 Gas Chromatograph (GC)/Saturn 2200 Ion Trap Mass Spectrometer (MS) with a CP8400 Auto Sampler. The GC column used was a DB-5 type capillary column (Varian Factor Four VF-5ms), 30 m long, 0.25 mm internal diameter and 0.5 µm thick. The ion-trap was operated in selected scan mode (MS/MS) for each PCB congener. The column oven temperature was programmed to hold at 40˚C for two minutes followed by a temperature ramp up to 184˚C at the rate of 12˚C per minute and then up to 280˚C at the rate of 4˚C per minute with the final hold time of two minutes.

Desorption Studies. When the kinetic (adsorption) experiments were completed for the CETCO organoclay and coconut shell activated carbon amendments, additional isotherm studies were conducted to determine the desorption properties of the same organic contaminants of concern (naphthalene, phenanthrene and pyrene). For these studies, humic acid was spiked into previously equilibrated samples of amendment-contaminant mixtures to determine whether continued exposure to high concentrations of organic acids would result in contaminant desorption into porewater.

4.1.2 Amendment Adsorption Kinetics

Kinetic Studies. In addition to the amendment adsorption studies (Section 4.1.1), batch kinetic experiments were conducted to evaluate the adsorption equilibrium times of pyrene and phenanthrene onto CETCO organoclay and coconut shell activated carbon. The experiment was conducted for 15 day durations in both the presence and absence of humic acid. Samples were spiked with the selected PAHs after preloading with humic acid (including a non-loaded control sample) and continuously mixed on a rotary shaker at 150 rpm for the duration of the experiment. The concentrations of the experimental PAH solutions were 0.16 mg/L for pyrene and 1.6 mg/L for phenanthrene. Humic acid preloading, sample extraction and GC analysis were accomplished in the same manner as described above for the batch isotherm experiments.

4.1.3 Combined Effects of Humic Acid, Fulvic Acid and Natural Organic Matter

Batch Experiments. Supplemental experiments were conducted to determine the effects on chemical adsorption of fulvic acid (FA) and natural organic matter (NOM) isolated from sediment pore water. These results supported the understanding of the influence that different fractions of dissolved organic carbon (DOC) would be expected to have on the sorbent properties of potential reactive mat amendments under real site conditions. Batch experiments were conducted to evaluate the adsorption of phenanthrene and 2,2',5,5'-tetrachlorobiphenyl on CETCO organoclay and coconut shell activated carbon in the presence and absence of two humic acids (Aldrich humic acid, Suwannee River (Georgia) humic acid), a fulvic acid (Suwannee River) and natural organic matter (Suwannee River) in a solution at neutral pH in order to assess the combined effects of these substances on overall amendment performance. All organic acid sources were purchased from appropriate vendors. Experiments were conducted in 40 ml vials with varying loading rates of 2,2',5,5'-tetrachlorobiphenyl and phenanthrene, and remaining free-phase concentrations were measured at 72 hours (determined in previous experiments to be sufficient to approximate equilibrium) in order to obtain the data for determination of adsorption isotherms. All batch experiments were conducted using methanol and deionized water as the stock solution for organoclay and acetone and deionized water as the stock solution for activated carbon.

Preloading Process. The preloading of organoclay and activated carbon was achieved by soaking these materials within varying solutions (1, 100 and 1000 mg/L) containing two natural organic matter (NOM) types (humic acid and fulvic acid). A 10% sodium azide was then added to the organic acid solutions to prevent bacterial degradation of the material. Finally, the sorbent samples were mixed for 48 hours at 150 rpm on a rotary shaker to ensure homogeneity.

4.1.4 Column Testing

Column Testing. During year three, project personnel designed and fabricated a stainless steel column specific to mat technology in order to better understand the treatment capabilities of reactive mats deployed in the field (Figure 4.1-1). In these studies, a solution containing select PAHs (naphthalene and phenanthrene) and PCBs (2-chlorobiphenyl and 2,2',5,5'-tetrachlorobiphenyl) was pumped upward through a reactive mat specimen at a flow rate similar to potential hydraulic flux expected under field conditions. Selected concentrations

were scaled to the solubility of each test contaminant (naphthalene: 31 mg/L, phenanthrene: 1.26 mg/L, 2-chlorobiphenyl: 3.35 mg/L, 2,2',5,5'-tetrachlorobiphenyl: 0.06 mg/L), and all contaminants were present as a mixture. Upflow velocity through the columns was 7.9 cm/day, which was higher than measured at the pilot site. The experiment duration was 7 days, and samples were taken once per day. Samples were extracted and analyzed for dissolved phase PCB and PAH as described in Section 4.1.1.

Figure 4.1-1. Experimental column for reactive mat flow-through testing.

4.2 Task 2: Pilot Site Selection

The purpose of selecting a pilot site for this project was to identify a location for the field testing of small-scale geotextile mats The site selection process consisted of screening a number of possible sites based on chemical, biological, and logistical factors, followed by focused geophysical surveys at the selected site to determine a specific area within the site that would serve as the location for prototype mat system deployment.

4.2.1 Strategy Overview

Pilot site selection was initiated in year one by conducting a review of data on potential sites to assess compatibility with expected mat performance characteristics. The pilot site selection process was two-phased, with the first objective being the identification of the most advantageous location from a "long list" of prospective Navy sites. Two sites, Cottonwood Bay in Grand Prairie, Texas and Pearl Harbor in Honolulu, Hawaii, were identified as potential pilot sites based on the criteria described in the First Year Annual Progress Report (NAVFAC 2006). Based on a comprehensive review of chemical, biological and logistical factors, Cottonwood Bay was ultimately chosen as the primary pilot site.

The second objective of the site selection process was to further characterize the geophysical properties of the primary pilot site (Cottonwood Bay) with the goal of defining a specific target

area for deployment of the prototype test mat system. The geophysical investigation included bathymetry, sub-bottom, side-scan sonar, sediment profile imaging (SPI) and groundwater seepage surveys completed during Year Two as described in the Second Year Annual Progress Report (NAVFAC 2007).

4.2.2 Primary Site Selection Criteria

During the Year One effort, a series of criteria were generated in order to screen many prospective sites for characteristics that would allow for the most comprehensive understanding of the field dynamics of the reactive mats. The criteria for phase one site selection included an evaluation of chemical, physical, and biological data as well as site management and logistical considerations. The desirable characteristics for each of these parameters were provided in a series of tables in the First Year Annual Progress Report (NAVFAC 2006).

While these criteria were not quantitatively weighted, priority was given to the presence of both metals and organics in sediment, and groundwater flux and biological colonization conditions suitable for comparing pre- and post-mat deployment conditions. Other practical criteria for initial screening included the chronology and direction of risk assessment remedial management plans. The ideal location would be a near-term candidate for remedial dredging or traditional capping for which it would be possible to evaluate a reactive mat as a more effective, stable and economically advantageous alternative. Additional logistic considerations included accessibility of the site, availability of information to characterize existing conditions and cooperation of site/program management staff with at least some minimal availability to support project planning and execution.

When the two most suitable pilot sites were established (Cottonwood Bay and Pearl Harbor), a comprehensive review of the literature for each location was performed to determine if remediation was planned and if contaminants of potential concern (CoPCs) had been established for metals and organics. Other site factors that were sought in the literature included the absence of major obstructions such as rocks and/or debris that would make deployment of the mats in direct contact with the sediments difficult. Also, it was deemed desirable to have a site with active groundwater seepage and associated contaminant transport to surface waters, wherein the mats would provide active contaminant sequestration while allowing the natural advective flow conditions to occur unimpeded. Additionally, a site with an energetic hydrodynamic environment, such as an intertidal zone or a shoal environment, would be an advantageous site because of the challenges of designing a traditional stable sand cap in such a setting. Other salient characteristics of the prospective pilot site included factors that would affect the bioavailability of contaminants and/or the reactive capacity of the apatite, organic carbon and organoclay to bind the contaminants. Findings from the Task 1 laboratory studies were considered in the evaluation of pilot site suitability because elevated organic carbon and humic acid in sediments could reduce contaminant bioavailability. Therefore, suitable pilot sites would not have high concentrations of these constituents for an optimal demonstration of reactive mat effectiveness. Finally, the availability of transportation facilities and shoreside infrastructure were also evaluated for each site in order to assess the ability to accommodate mat deployment and monitoring.

The results of this comprehensive review indicated that Cottonwood Bay would be the primary pilot site for future activities. A detailed description of Cottonwood Bay is provided in Section 5.2.2. This water body is situated between Routes I-30 and I-20 in Dallas County and is adjacent to the Vought Aircraft Industries plant (formerly the Naval Weapons Industrial Reserve Plant) and Naval Air Station Dallas (NAS). It is connected to the larger Mountain Creek Lake by a man-made diversion channel that transects NAS property, running underneath the entrance bridge and alongside the former base airstrip. Cottonwood Bay is divided into two main portions (East and West) by a causeway running from Vought property to NAS property. These two portions are hereafter referred to as "Cottonwood Bay East" and "Cottonwood Bay West" (Figure 4.2-1). Recent data for this site were provided by the USGS and included a computer model analysis of groundwater flow and the simulated effects of contaminant remediation (Barker and Braun 2000). In summary, concentrations of chromium and PCBs were generally higher adjacent to the current Vought shoreline while concentrations of PAHs (*e.g.*, fluoranthene) increased with proximity to the NAS. Concentrations of metals and organics were found to be generally lower by a factor of five in Cottonwood Bay West compared to stations in Cottonwood Bay East on the opposite side of the causeway. A series of wells and trenches were installed on the NWIRP (now Vought) property with the goal of removing groundwater from the local aquifer before it reaches Cottonwood Bay. Remedial action planning for Cottonwood Bay by NAVFAC Southeast on behalf of the Texas Natural Resource Conservation Commission (TNRCC) is ongoing.

4.2.3 Geophysical Surveys

An extensive geophysical investigation was conducted in Year Two to characterize Cottonwood Bay site conditions including water depth, habitat characteristics and lake sediment properties with the goal of selecting a specific location for future prototype mat system deployment. The evaluation consisted of bathymetry, sub-bottom profiling, side-scan sonar and sediment profile imaging (SPI) surveys conducted by SAIC. Coastal Monitoring Associates, Inc. (CMA) conducted a follow-up groundwater seepage survey to define the extent of sub-surface groundwater plumes that may be radiating from adjacent Vought property and serving as contaminant transport pathways into the bay.

All aspects of the Cottonwood Bay geophysical investigation were completed from July-September 2007 following the detailed methodology described in the Second Year Annual Progress Report (NAVFAC 2007). All pilot site selection activities for this project were completed by Year Two and no additional methodologies for this task are included in this final report.

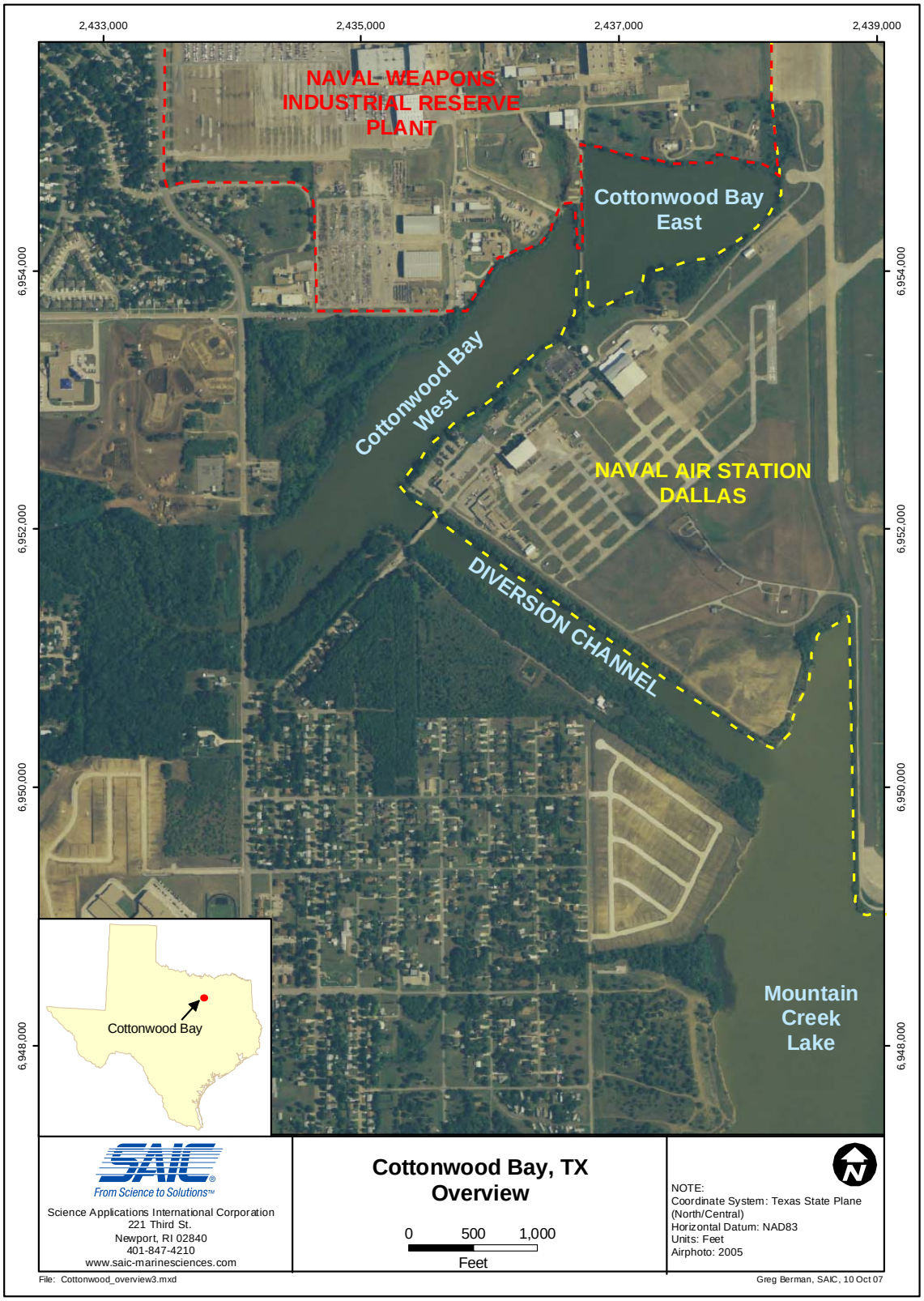

Figure 4.2-1. Overview of the Cottonwood Bay site.

4.3 Task 3: Geotextile Testing

The purpose of the geotextile testing task for this project was to field test different types of geotextile material at the selected pilot site in order to assess: (i) whether sediment clogging, biofouling and biofilm formation will adversely affect the ability of the fabric to allow water to pass through the final mat design, (ii) whether environmental weathering compromises the ability of the mat to retain the amendment material and (iii) whether environmental weathering compromises the reactivity of the sequestration agents. The geotextile found to be most resistant to biofouling after a specified soak period as determined from this small-scale field test was ultimately used for construction of the prototype mat system.

The geotextile testing task included the construction and deployment of small-scale test mats of different compositions (July 2007), six-month retrieval (December 2007), initial laboratory study (January-March 2008), one-year retrieval (October 2008), two-year retrieval (June 2009) and final laboratory study. While the test mats were soaking, laboratory gradient ratio testing and finite element analyses were conducted for clean, non-fouled mats to develop initial results regarding stability, clogging potential and prospective sediment deformation leading to excess pore water pressure as described in the Second Year Annual Progress Report (NAVFAC 2007). These laboratory testing and modeling procedures were continued in year three to incorporate field data from the recovered test mats. Results from the composite material testing and gradient ratio testing performed on these weathered mats were used to determine and confirm both the amendment mixture and the geotextile type most unaffected by biofouling to be used for prototype mat system testing.

4.3.1 Field Evaluation

Fabrication. During Year One of this project, the project team worked with the CETCO company of Arlington Heights, Illinois, to fabricate a total of 14 small-scale test mats of properties, each measuring 6 ft x 6 ft (Figure 4.3-1). These mats were designed and constructed by CETCO such that the amendment material was bound within a high loft core "sandwich" between a woven backing geotextile (silt curtain) and a non-woven top geotextile (fabric). This arrangement was chosen to allow the principal investigators the ability to assess how material type and apparent opening size affect biofouling and sediment clogging. Twelve of the mats contained a mixed core composite consisting of apatite (0.23 lb/ft^2), activated carbon (0.28 lb/ft^2) and organoclay (0.28 lb/ft^2). The maximum achievable loading rate for this mixture was ~0.8 lb/ft^2 due to the light density of activated carbon and associated volume limitations. The remaining two mats contained an Ottawa sand core to serve as a replicated control.

Table 4.3-1 below summarizes the properties of the small-scale test mats. Design variables for these mats included non-woven geotextile material (polyester or polypropylene), amendment core density (expressed as mass per unit area; oz/yd^2) and geotextile apparent opening size (AOS). The AOS for a particular geotextile (expressed as a US Sieve Number) reflects the approximate largest opening dimension available for soil/sediment to pass through as determined by dry sieving uniform sized glass beads of a known standard sieve size through the geotextile until the weight of beads passing through the geotextile is 5% or less. Because sieve numbers are inversely proportional to opening size, a geotextile with a larger AOS value will theoretically be

more susceptible to long-term clogging or blinding. The AOS values of 70, 80 and 170 used for construction of the small-scale test mats represent specified sieve opening sizes of 210, 177 and 88 microns, respectively.

Geotextile material was included as a test variable because different fabric types were expected to show different breakdown and clogging properties when exposed to field conditions. Core density was a test variable in order to evaluate the precise amount of amendment material needed per unit area of a reactive mat to achieve the most efficient chemical sequestration while minimizing clogging. Finally, AOS was a test variable in order to determine the relationship between mat porosity and performance and to evaluate the potential effects of clogging.

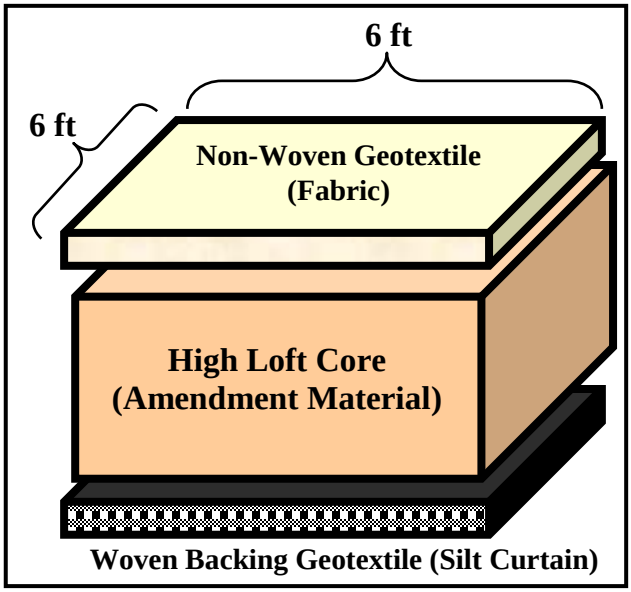

Figure 4.3-1. Construction diagram of small-scale geotextile test mats.

Table 4.3-1. Material design summary of small-scale geotextile test mats.

Total of 14 Test Mats Constructed			
Material	**Core / Mass Per Area**	**AOS**	**Quantity**
Polyester	Mixed - 5 oz/yd^2	170	4
Polypropylene	Mixed - 6 oz/yd^2	70	4
Polypropylene	Mixed - 8 oz/yd^2	80	4
Polypropylene	Ottawa Sand - 6 oz/yd^2	70	2

Deployment. In June 2007, the 14 small-scale mats were placed in Cottonwood Bay East in two rows of seven near the northern shore of the bay adjacent to the Vought property. Each of these rows consisted of two polyester test mats with a 170 apparent opening size and mixed core, two polypropylene test mats with a 70 apparent opening size and mixed core, two polypropylene test mats with an 80 apparent opening size and mixed core and one polypropylene control mat with a 70 apparent opening size and sand core.

All of the test mats contained the same amendment core mixture featuring a combination of apatite, activated carbon and organoclay. For the similar mats in each row, one replicate was deployed with the woven backing geotextile (silt curtain) face down and the other replicate was deployed with the woven backing geotextile face up. This arrangement was selected to investigate how the different geotextiles behave under direct contact with the sediment surface. The control mats were deployed with the woven backing geotextile face down in both rows.

All mats were weighted to the sediment surface with ceramic bricks tethered to each corner with plastic zip ties and the location of the southwest corner of each mat was marked with an aluminum stake. Each mat was also tagged with a colored zip tie to aid in differentiating each replicate during the evaluation process. Approximately five feet of space was left between each mat to reduce possible interference associated with edge effects (*e.g.*, suppression of groundwater flux by nearby mats). Field photographs of the small-scale test mat deployment process are shown in Figure 4.3-2.

Figure 4.3-2. Small-scale geotextile test mat deployment.

Monitoring. A preliminary field evaluation of the small-scale mat deployments was conducted in July 2007 (approximately one month after initial placement) by wading near the mats and observing whether any had substantially shifted position or become subject to any unexpected deterioration. It was noted at this time that Mat 1 in Row 1 (the westernmost mat in the row closer to shore) had accumulated gas underneath that was causing the mat to float off the lake floor. Similar conditions were also noted in Mat 2 and Mat 3 in Row 2 (the second and third westernmost mats in the row further from shore). The source of the gas was most likely a build-up of methane moving up through the sediments beneath the mat or gas being produced by biological activity taking place beneath the mat. Because the westernmost mats in each row featured the smallest apparent opening size (either 5 oz/yd^2 or 6 oz/yd^2), it was postulated that these gaseous accumulations were not able to pass through the small AOS. Whether the mat was deployed with the woven backing geotextile up or down did not appear to affect gas accumulation. Prior to concluding the field evaluation, field personnel released the bubbles from the mats in question by lightly stepping on them to force all gas accumulation out the side until they were again laying flat against the sediment.

Retrieval. The small-scale test mats were recovered after predetermined soak times to assess potential hydraulic conductivity changes due to biofouling and potential reactivity changes due to biofilm growth. Field personnel returned to Cottonwood Bay in December 2007 to conduct the six-month retrieval of the first set of the small-scale (6 ft x 6 ft) geotextile test mats that had been soaking in the eastern portion of the bay since June 2007. At this time, the first row of seven mats (six test mats and one control mat) were lifted from the lake floor and hoisted as flat as possible onto the deck of a dual Jon-boat shallow draft vessel. In contrast to the previous monitoring event, all seven mats were found to be laying flat on the lake floor with no noticeable gas buildup.

The mats were transported to shore and placed flat on a sheet of clear plastic and photographed. Colored zip ties were attached to the mats to identify the different test treatments in terms of geotextile material, apparent opening size and whether the mat was placed with the non-woven geotextile facing up or down. All mats were then covered on both sides with clear plastic, rolled around a 5 ft long 2 in x 3 in piece of wood, sealed in commercial grade garbage bags and encased in 12 in diameter cardboard sonotubes for shipping. This packing process was intended to preserve, to the greatest extent possible, any biofilm and sediment accumulation that had accumulated on each side of the mat during the six month soak time. All seven mats were then shipped at room temperature to UNH for controlled laboratory testing. Preliminary observations of the small-scale test mats following recovery indicated a moderate level of biofouling and the presence of several small red worms that appeared to have burrowed into the non-woven geotextile.

A similar retrieval event for the second set of small-scale test mats was conducted in October 2008 concurrently with deployment of passive contaminant samplers at the prototype mat system (see Section 4.4.4). At this time, two of the original four replicates of the 170 AOS, 5 oz/yd^2 non-woven geotextile test mats, (one each placed with woven geotextile up and down) were retrieved from Row 2 (further from shore) for repeat laboratory testing. These replicates were recovered after only one year of soak time because previous laboratory testing on similar test mats recovered after six-months of soak time had already indicated that this type of non-woven geotextile exhibited increased clogging and was unlikely to be used for full-scale implementation (see Section 5.3.2). The five remaining small-scale mats were left in place for an additional year in accordance with the project work plan. Small-scale test mats were packaged and shipped during all subsequent recovery efforts in the same manner as described above for the initial recovery effort. At the time of the second recovery effort, all remaining small-scale test mats were observed for gas buildup and none were found to be affected as evidenced by their laying flat on the lake floor with minimal floating.

The retrieval event for the five remaining small-scale test mats was conducted in June 2009 concurrent with the Ultraseep and Trident Probe surveys of the prototype mat system (see Section 4.4.5). At the time of this final recovery effort, a moderate level of gas buildup, lifting approximately 25% of each mat off the substrate, was observed immediately prior to test mat retrieval. Although the presence of this gas buildup was unlikely to effect the properties of the small-scale test mats, it did serve as an indicator of a proportional amount of buildup that could be expected below the larger prototype test mats at that time of year, which could in turn effect contaminant sequestration performance by reducing direct contact between the mat and the

sediment-water interface unless a corrective action was taken. This issue was addressed further during the placement and monitoring of full scale mats, discussed in Section 4.4.2.

Performance Evaluation. Following the initial test mat retrieval event, laboratory performance evaluations were conducted to investigate whether biofouling and/or surficial material accumulation which had occurred in the field resulted in changes in mat permeability and hydraulic conductivity. Parallel laboratory testing was also conducted to assess the effects of biofouling on amendment reactivity to determine if the presence of natural organic matter affects adsorption properties (see Section 5.1.3). The ultimate goal of these performance evaluations was to select the geotextile that offered the best balance between fouling resistance and amendment material effectiveness for design of the prototype mat system.

For geotechnical performance testing, a test column system was utilized following American Society of Testing and Materials (ASTM) method 5101 (Figure 4.3-4). Method 5101 is typically used to directly measure the clogging potential of a soil/geotextile system *(i.e.*, a layer of soil in contact with a geotextile such as in a landfill cap situation) and was adopted here to assess the impacts of sediment settlement/biofouling found to cover the reactive mats in the field. Accordingly, adoption of ASTM 5101 for this purpose was assumed to provide a realistic estimate of the actual cap performance with regard to clogging and sediment infiltration.

Figure 4.3-4. Geotextile sediment gradient ratio column experimental setup.

When the small-scale test mats were received at the UNH laboratory, initial observations were made regarding relative percent fouling of the geotextile material. Gradient ratio tests were then performed by placing a section of mat sample into the column and measuring the time required for static head pressure of an underlying water column to flux through the mat surface. The elapsed time was compared to the flux time of a clean, non-fouled mat.

Another concern for the mat performance evaluation was the growth of biofilms on the surface of the reactive materials themselves, regardless of specific type of amendment used in the mat.

These colonies may not be sufficient to cause biofouling by clogging geotextile pore spaces, but could influence the chemistry at the surface of the amendments and thus impact contaminant uptake. To investigate the potential for such interference, samples of biofilm coated materials were collected from the recovered mat segments and tested with the same column testing techniques described in Section 4.1.5 to quantify how biofilms may enhance or diminish amendment effectiveness (Mariah Arias-Thode, SERDP ER-1551); little influence of biofilms was observed.

4.3.2 Gradient Ratio Testing

General Procedure. The purpose of gradient ratio testing is to evaluate the stability and clogging potential of a sediment-geotextile filter system. Different flow rates are tested to determine whether the geotextile is likely to become impermeable to flow under a range of natural field conditions. Using the geotextile permeability column shown in Figure 4.3-4, water was pumped downward through the sediment perpendicular to the plane of the geotextile. The test scenario was inverted from field conditions (i.e., tested using downward flow) because initial experiments showed that pumping water up through the sediment into the cap led to sediment instability and collapse before any meaningful data could be collected. When evaluating the cap samples, the system was allowed to equilibrate under no flow conditions for 24 hours. Then an initial gradient (hydraulic head over the height of the sample) of 1 was applied. After 24 hours, the gradient was increased to 4, and then to 8 after another 24 hours. The onset of clogging can be determined by comparing the ratio of the hydraulic gradient in the geotextile-sediment system to the gradient in the sediment alone. In addition, the gradient ratio test was done in a closed, transparent system, so sediment transported through the geotextile could be observed and also collected when the test was completed. A detailed picture of the gradient ratio column showing geotextile-sediment contact and reactive mat-sediment contact is provided in Figure 4.3-5. Comparative images of a geotextile sample before and after a gradient ratio test are shown in Figure 4.3-6 and accumulated sediment that has passed through the geotextile during a test is shown in Figure 4.3-7.

The gradient ratio value is defined as the ratio of hydraulic gradient in the sediment-geotextile section of the test column to the hydraulic gradient in the sediment-only section of the test column as shown in the following equation:

$$GR = \frac{i_{\text{sediment-geotextile}}}{i_{\text{sediment}}} \begin{matrix} >1 \\ <1 \end{matrix} \begin{matrix} \text{Clogging} \\ \text{Piping} \end{matrix}$$

Values lower than unity (<1) indicate piping conditions along the walls of the chamber, or possibly at the geotextile-sediment interface, while values larger than unity (>1) indicate increased hydraulic pressure across the geotextile. A value greater than or equal to three is defined as a clogged geotextile. Values slightly less than one are generally preferred for a reactive mat system since they show a stable system allowing low flow without clogging. When evaluating the effectiveness of a geotextile, the stability of the gradient ratio value might be as important as the value itself because it denotes a stable filter system without further particle transport.

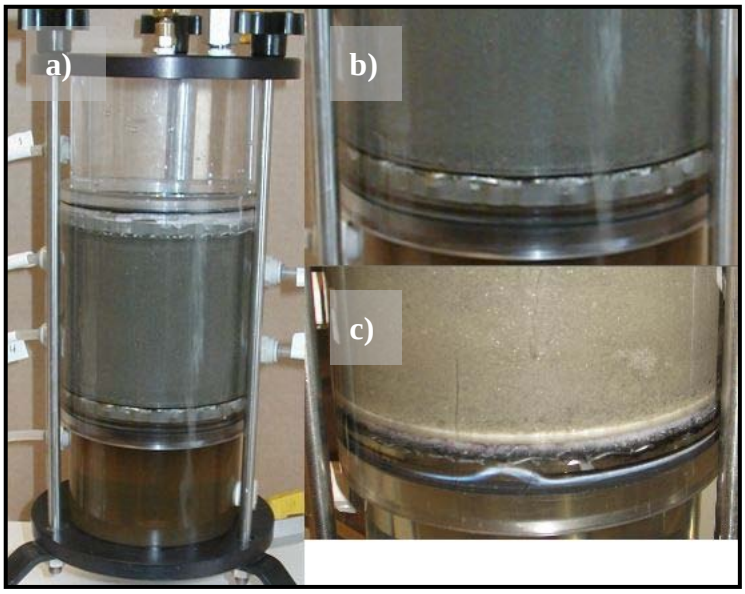

Figure 4.3-5. Detailed photograph of geotextile gradient ratio test column showing (a) permeameter for gradient ratio tests, (b) geotextile-sediment contact and (c) mat-sediment contact.

Figure 4.3-6. Comparative images of a geotextile sample before (left) and after (right) a gradient ratio test.

Figure 4.3-7. Sediment that has passed through the geotextile during a gradient ratio test.

Stock Geotextile Evaluation. Preliminary gradient ratio testing conducted on various stock geotextiles during Year One showed that bubbles trapped in the sediment matrix and under the geotextile sample are an impediment to groundwater flux through the system in a fine grained matrix such as the sediment expected to be encountered in Cottonwood Bay. Experiments were conducted to determine if sample preparation in a nitrogen atmosphere would help eliminate bubbles being trapped in the test column, but results indicated that such a process had negligible effects. The bubble trapping problem was ultimately corrected by refining sample preparation techniques to remove bubbles from the sediment prior to sealing the test column.

In Year Two, gradient ratio testing was continued on stock geotextiles as well as on clean, non-fouled mats in order to establish baseline stability and clogging conditions to which results from similar tests on field weathered geotextile mats would ultimately be compared. As mentioned earlier, vertical upward flow through the sediment-mat interface was planned for the testing process to provide consistency between the experimental conditions and the natural field conditions, but hydraulic consolidation occurred due to the effective stress variation with time and a separation between the sediment and the geotextile eventually developed. Thus downward water flow was used instead for all subsequent tests. Due to the low permeability of the sediment in the test column, it was not possible to measure the flow rate of the entire system according to the ASTM-D 5101 standard. Instead, clogging potential was evaluated using the gradient ratio value only. This procedure was repeated in year three using segments of the field-weathered small-scale test mats to determine whether biofouling increases the likelihood of clogging compared to a clean mat under similar hydraulic conditions.

The stock geotextiles used in the Year Two gradient ratio tests were the same three CETCO geotextiles (in terms of material, mass per area and AOS) used to construct the small-scale test mats (Table 4.3-1). These CETCO geotextiles were selected to cover a wide range of AOS and mass per area for practical applications as well as to mimic the arrangements being tested in the field, which was necessary to collect baseline data on the unweathered condition.

In addition to geotextiles, complete bare reactive mats were also subjected to gradient ratio testing for baseline clogging potential evaluation. The characteristics of the clean, non-fouled reactive mats used in these experiments are presented in Table 4.3-2. These representative mats contained various mixtures of the amendment materials that were considered for the final reactive mat design. As expected, preliminary results indicated that the reactive mats let less material pass through than the single sheet geotextiles.

Table 4.3-2. Characteristics of clean representative mats used in gradient ratio experiments.

Sample ID	Mass Per Area [kg/m^2]	Thickness [cm]	Reactive Material
RCM-1	4.0	~0.10	Organoclay
RCM-3	4.6	~0.10	Organoclay/Apatite
RCM-5	0.4	~0.10	Activated Carbon

Test Mat Performance Evaluation. Upon receipt at the UNH laboratory, the weathered small-scale test mats were cut into manageable pieces to be used for flow-through column gradient ratio testing following the same procedures described above. The goal of these laboratory tests was to assess whether biofouling and biofilm formation on weathered mats would adversely affect the ability of the fabric to allow water to pass through the final mat design and whether environmental weathering compromises the ability of the mat to retain the amendment material. Baseline data for these parameters to which the field data would ultimately be compared were previously established by gradient ratio tests performed on unweathered single sheet geotextiles and bare reactive mats similar to the small-scale test mats that were deployed in the field.

4.3.3 Finite Element Analysis

General Procedure. The main goal of finite element analysis (FEA) was to understand the potential sediment deformation (consolidation) that would be caused by the weight of the reactive mat as well as the resulting pressure increase that would force porewater out of the underlying sediment, potentially altering natural seepage and contamination patterns. Consolidation of the sediment would also change the ground water flow through the affected sediment. The use of FEA allows for a modeling evaluation of two-dimensional transport with regard to flow through the consolidated sediment and around the mat edges. A groundwater component was added to see how this edge flow affects advective transport.

Preliminary finite element models were constructed in Year One with Plaxis (v. 8.0) software using a simulated symmetrical half-sand cap 5 m in length placed over sediment that was treated as an elastic-plastic material with no creep. This elastic-plastic (or Mohr-Coulomb) model was a simple representation of soil/sediment behavior under loading in which the stress-strain behavior is treated as reversible (elastic) until the stress from loading reaches the failure point, at which time the soil/sediment cannot support any further load and the deformation is permanent (plastic behavior). The “no creep” condition requires that the soil/sediment does not undergo any time-dependent deformation in this model. After initial data were collected under this basic sand cap

model, a more complex sediment model was generated that considered both consolidation and secondary creep.

The simulated sand cap (protective layer) for the elastic-plastic model had a thickness of 30 cm (~1 ft). Because PLAXIS (v. 8.0) does not allow for changes in the permeability of geotextile elements, water was assumed to flow freely through the geotextile. To adjust for this deficiency and allow for the goal of evaluating varying permeability, the model was manipulated by adding a thin layer of low weight sand over the geotextile. The permeability of this thin sand layer was then adjusted to effectively change the permeability of the geotextile.

In Year Two, various geotextile mat components were added to the finite element model runs to assess increasingly sophisticated scenarios. These geotextile-inclusive models started with a hypothetical clean mat with the goal of investigating if and how flow patterns would be substantially affected by the level of clogging anticipated to occur under field conditions.

In year three, biofouling data obtained from the recovered small-scale test mats and sediment properties observed at the Cottonwood Bay pilot site were used to modify the finite element models with actual permeability values. Sediment samples were sent to a standardized laboratory for Atterberg limits and organic content testing. Results for Cottonwood Bay sediment indicated a liquid limit (LL) of 155-164 and a plasticity index (PI) of 121-125. These values were relatively high in comparison to an estuarine site (Piscataqua River, NH) where similar analyses indicated a LL of 33-34 and PI of 6-10. This difference may be related to the higher organic matter content observed for Cottonwood Bay sediments (4.3-5.8%) vs. Piscataqua sediment (4.1-4.2%). These data were ultimately applied to the FEA process to generate comparative finite element models for each site and therefore help define the operational range of the mat technology in both freshwater and estuarine conditions.

Geometry and Boundary Conditions. Geometry and boundary conditions were defined to constrain general field conditions and to promote applicability to different circumstances for the reactive mat finite element model. Field information obtained on a similar cap test project on the Anacostia River in Washington D.C. was used to develop the typical geometry for the initial model as shown in Figure 4.3-8.

This model was symmetrical with respect to the vertical left axis. The sediment region was 45 m long by 10 m deep and the reactive mat was defined as an overlying layer of sandy material 15 m long by 0.3 m thick. The mat permeability was used to simulate its clogged state, while the unit weight was used to simulate the weight of the mat's protective layer. The depth of water was set at 4.21 m, which was equivalent to the average depth observed at Cottonwood Bay.

The boundary conditions for the model included the displacement (flux rate) conditions as shown in Figure 4.3-9. The displacement boundary conditions fix any displacement at the base and the horizontal displacement on both sides of the model. The flux boundary conditions control the pressure head at the top of the sediment-mat regions based on the water level (static or tide variation). Flux was prohibited on both vertical sides of the model. The average flux rate (3.3 cm/day) observed on one of the evaluation mats of the Anacostia River was used to produce the groundwater flow for this seepage analysis. Because all the boundary conditions can only

coexist in a fully coupled analysis, they are not all required on each step of the uncoupled solutions.

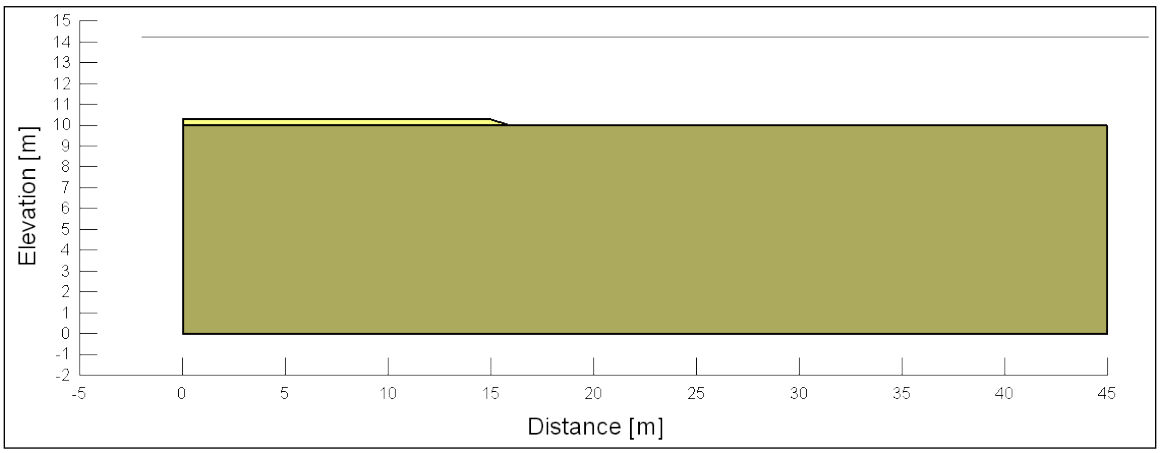

Figure 4.3-8. Geometry of a typical reactive mat application for finite element modeling.

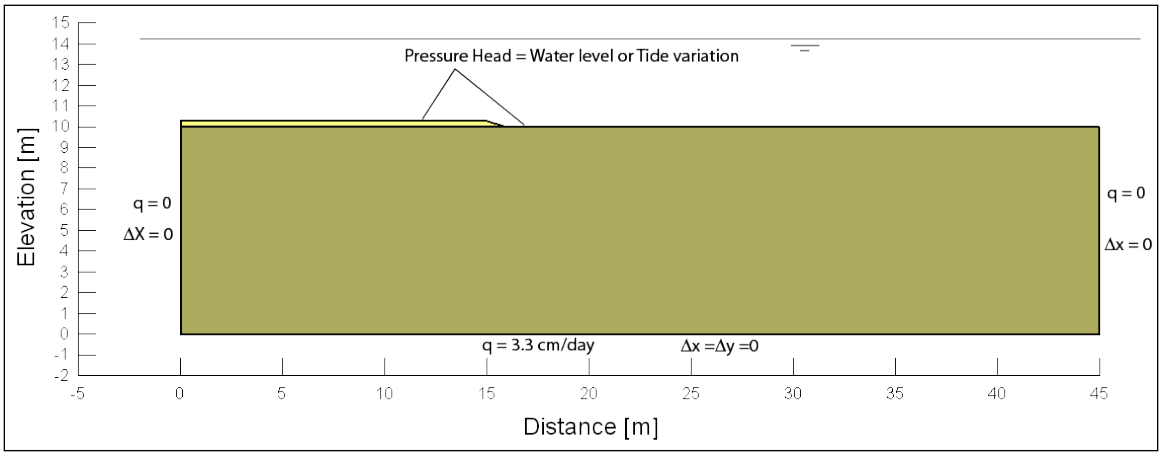

Figure 4.3-9. Summary of the boundary conditions for finite element modeling.

Geotechnical Parameters. For the initial finite element model, reliable estimates of soft sediment geotechnical properties were initially used for qualitative analyses in the absence of field data from the Cottonwood Bay pilot site. Table 4.3-3 shows a summary of the geotechnical property estimates.

The Young's modulus had a constant value from the sediment surface to a depth of 1 m to avoid numerical complications due to small or zero stiffness values. The high Young's modulus of sand was used to avoid numerical complications at the sloped end of the mat. A linear elastic model was used for a first approximation to the final configuration.

Consolidation and triaxial tests were simulated using various constitutive soil models which allowed for the calibration of geotechnical parameters and the definition of the best modeling procedure to simulate a reactive core mat deployment over soft sediment. Additional models

were also developed to calibrate contaminant transport during both soft sediment consolidation and potential geotextile permeability reduction.

Table 4.3-3. Summary of average geotechnical property estimates for finite element modeling.

Property	Sediment	Reactive Mat
Permeability, *k* [cm/s]	1.5×10^{-5}	1.0×10^{-3}
Initial void ratio, e	1.6	0.7
Unsaturated unit weight, γ_{unsat} [kN/m^3]	11	15
Saturated unit weight, γ_{sat} [kN/m^3]	14	17
Poisson's ratio, ν	0.3	0.25
Young's modulus at 1 m, E_{ref}[kN/m^2]	163.41	10000
Increment of Eper meter depth [kN/m^2]	163.41	0

Numerical solutions for the individual analyses of consolidation, seepage, and contaminant transport cases were available in the technical literature. Some finite element software includes these individual solutions but the fully coupled analysis is not available in the literature and is part of ongoing research. Consequently, the uncoupled solutions were employed in the initial model since they have been proven to be useful in understanding the individual contributions to the overall final configuration. They can also produce computationally more efficient results similar to those obtained using the coupled solution. The following sub-sections present uncoupled and coupled solutions to the consolidation-seepage problem.

Uncoupled Consolidation Model. The uncoupled consolidation model shows potential sediment deformation following mat placement independent of groundwater flow. This model was solved in two stages with the first stage computing the *in-situ* stress state of the sediment including the pore pressure distribution. The model assumed no steady state or transient groundwater flow and only the hydrostatic pressure was included. The geometry and boundary conditions of the model were the same as those shown in Figure 4.3-8 and Figure 4.3-9 above, but the flux rate at the base was q = 0 m^3/s to avoid groundwater flow through the sediment.

Consolidation time is the time required to dissipate the excess pore pressure induced by the weight of the mat. For practical purposes, 90-95% of the dissipation was defined as the end point of consolidation. A point was selected at mid-depth of the sediment layer to verify the excess pore pressure dissipation.

Uncoupled Seepage Model. The uncoupled seepage model shows potential changes in pore water properties and groundwater flow following mat placement independent of sediment consolidation. Two models were generated to assess post-mat groundwater seepage. The first model assumed the same permeability for the mat and the sediment. This scenario represented the case of an unclogged mat since the water drains freely from the sediment into the mat and out to the bay. The second model assumed a mat permeability one order of magnitude less than the sediment in order to simulate a clogged mat through which groundwater would not move freely.

Coupled Model. The coupled solution of the consolidation-seepage case is defined in three stages:

- Stage 1. Initial *in-situ* stress state without groundwater flow.
- Stage 2. Groundwater flow is applied by defining a flux rate at the base of the model and the total head at the sediment surface. A new initial stress state is achieved.
- Stage 3. Mat deployment and consolidation under groundwater flow conditions. Coupled solution.

The stages of the coupled modeling process were solved in sequence to simulate the real field conditions expected following mat deployment. No information was available from the consolidation tests to simulate the change of the sediment permeability during consolidation. Therefore, the time required to dissipate the excess pore pressure due to the mat deployment may be higher than the value estimated here. If a longer time is truly required to consolidate the sediment, that means that the lower permeability layer (filter cake) expected to develop beneath the mat will also take longer to develop. Again, a linear stress-strain relationship was used to simulate soil behavior. Field displacements were thus generally overestimated.

Oedometer Consolidation Testing. The geotechnical properties of soft sediment typical of that needed to calibrate the finite element model as appropriate for the Cottonwood Bay pilot site were determined by oedometer and seepage consolidation tests. During year three, two preliminary oedometer consolidation tests were carried out on sediment samples of similar properties collected from the Piscataqua River in New Hampshire. Loading, unloading, and reloading stages were fully completed and the results provide information about the primary consolidation and change of permeability of the sediment, as well as the secondary compression coefficient required for the numerical simulations. Given the soft nature of the sediment, and that information about the secondary compression is required for the reactive mat project, each consolidation test lasted 13 to 14 days. These results were used to guide oedometer testing on a sediment sample collected from Cottonwood Bay.

Seepage Consolidation Testing. Continued low stress sediment consolidation tests were performed during year three on unweathered geotextiles in order to provide compression curves (e vs. σ') that indicate a reduction of the void ratio as effective stress increases. The seepage consolidation test provided information about the behavior of sediment from Cottonwood Bay at 0.64, 1.1 and 2.1 kPa of effective stress which is not possible to obtain on oedometer consolidation tests. The results of the seepage consolidation were used to help calibrate the finite element models depicting a coupled solution featuring consolidation and advective flow contaminant transport.

Sediment Seepage Comparison. Test samples were extracted from the small-scale test mats recovered from Cottonwood Bay after approximately one year of soak time to investigate the amount of material that was able to seep into the mat under field conditions. This material was characterized and the results compared to the seepage properties of stock geotextiles as determined by the previous gradient ratio tests.

Consolidation Modeling. A detailed two-dimensional model was developed to simulate sediment consolidation beneath a reactive mat using the geotechnical properties of fine grained sediment as identified from the Cottonwood Bay sediment sample. The model assumed a sediment bed 8 m thick and 25 m wide where only 5 m of the sediment surface were capped using a 0.3 m layer of sand. The Modified Cam-Clay constitutive model was used to simulate soil behavior.

Groundwater Flow Modeling. A detailed two-dimensional model was developed to simulate groundwater flow through fine grained sediment. Similar to the sediment consolidation model, the groundwater flow model assumed a sediment bed 8 m thick and 25 m wide where only 5 m of the sediment surface was capped using a 0.3 m layer of sand. The reactive mat was simulated as a 1 cm thick layer of material with variable permeability to simulate clogging of the geotextile.

4.3.4 Gas Permeability Testing

As described during the test mat monitoring and retrieval phases, the buildup of methane gas beneath the reactive mats was observed during the field evaluation. The potential impacts of this gas buildup on reactive mat performance thus became an important parameter in further mat testing. Following prototype mat system observations in Cottonwood Bay that indicated potential gas buildup beneath the mats during the summer months that could be detrimental to mat performance, the SERDP review board requested additional laboratory testing to investigate the possible effects of gas accumulation under a reactive cap.

That bacterial activity in sediment can lead to the generation of significant volumes of gas, generally a mixture of methane and carbon dioxide with some other gases such as hydrogen sulfide in smaller amounts, has been well documented. The accumulation of gas underneath geotextile caps has the potential to cause cap instability if the buoyant force of the gas exceeds the submerged weight of the cap. These conditions have occurred in some caps where the geotextile layer was not covered with sand or armored with sufficient weight to offset the buoyancy of the gas. Gas production depends on the temperature of the site, water type and characteristics of the organic matter in the sediment. An upper estimate of biogenic methane gas production in marine sediments has been reported as 4.25 x 10-15 mol/day per gram (8.963 x 10-5 cm^3/day per square meter) of sediment (Colwell *et al*. 2008). However, a literature review showed reported gas production rates from wetland sediments, paddy soil, and other freshwater sediments in the range of 0.3 to 2640 cm^3/day per square meter of sediment surface, which is more than five orders of magnitude greater than production in marine sediments. Gas production rates in freshwater sediment also vary significantly with temperature from 0.3, to 341 to 917 cm^3/day, at 4, 22 and 35°C respectively (Qingzhong *et al*. 2007).

Gas does not exit the sediment in a uniform, steady flow, but rather typically builds up in the sediment and then escapes in large bubbles through a preferential path. Thus gas loading underneath a cap is in the form of sudden bubbles trapped at the geotextile layer. An important question for mat performance then becomes whether these gas bubbles have time to pass through the geotextile or do they continue to build until the cap becomes unstable. In order to address this question, an apparatus and test technique was designed to simulate a gas bubble trapped

under the geotextile and investigate how easily this bubble would migrate through the geotextile under a given hydraulic gradient simulating the rate of gas generation in natural sediment.

The gas permeability test was constructed using the same permeameter/geotextile setup as the gradient ratio test, but without the sediment sample. Water pressure and temperature alone influenced the gas dissolution in water. The purified deionized water used for the experiments remained at room temperature (20-22°C) to minimize variations of its influence on the results. In order to minimize the influence of water pressure on the gas dissipation rate, the water pressure on the gas bubble was held constant at 1" and no water flow was induced through the geotextile.

The geotextile samples were prepared by submerging the geotextile for a period of 24 hr in purified deionized water prior to assembling the permeameter. The fully saturated geotextile was then placed in the permeameter and the system was filled with purified deionized water from the bottom up to prevent trapping of gas bubbles in the system. The permeameter used to carry out the gas permeability test is shown in Figure 4.3-10, including the port used to inject the gas bubble and the location of the geotextile.

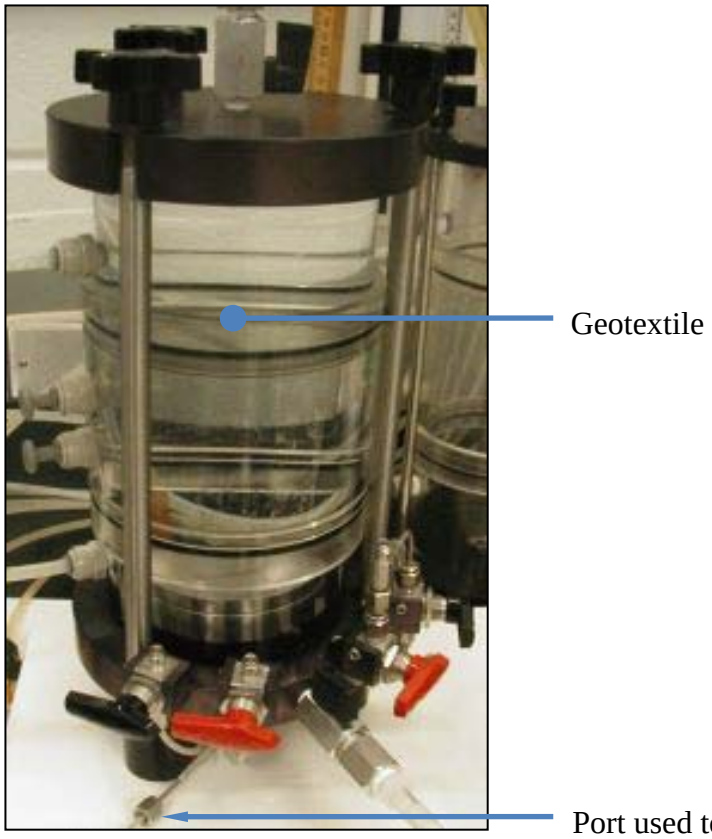

Figure 4.3-10. Permeameter setup for gas permeability testing.

After complete assembly of the permeameter, a 1 cm^3 gas bubble was injected beneath the geotextile and left to pass through the geotextile without any water flow in the permeameter. The gas bubble was monitored daily until it passed through and/or was dissolved in the water. Biogas collected from the Turnkey landfill in Rochester, NH was used for these tests since its

composition is typical of the gas produced by bacterial activity in freshwater sediment (methane, carbon dioxide, nitrogen, oxygen, hydrogen sulfide, and hydrogen). The gas permeability test was carried out using a fine geotextile of greater weight (AOS 170, 8 oz/yd^2) because if the gas flow/dissipation rate for this material was found sufficient to prevent significant gas accumulation beneath the geotextile, then no additional tests would be required on coarser and lighter geotextiles which would be assumed to have greater permeability. The geotextile used in these permeability tests corresponded to samples of the GT-4 geotextile used in the gradient ratio tests.

4.4 Task 4: Prototype Mat System Testing

The purpose of this task was to field test a prototype mat system constructed of different arrangements of the most effective amendment (identified in Task 1) and the geotextile most resistant to fouling (identified in Task 3) in order to assess *in-situ* chemical sequestration effectiveness and flux properties. To accomplish this task, larger prototype mats were constructed per proposed specifications and deployed at the target area in Cottonwood Bay. The Task 4 effort occurred entirely during years three and four of the project. Construction and deployment of the prototype mat system was completed in April 2008 and, the mat arrangements were monitored for contaminant adsorption and flux properties by various techniques through December 2009.

4.4.1 Prototype Mat System Design

Laboratory data from the ongoing composite material testing and gradient ratio testing were used to identify the most adsorbent amendment and the geotextile most unaffected by biofouling for construction of a prototype mat system to be deployed at the selected pilot site and used for long-term monitoring and evaluation of this technology. These design element results are discussed in detail in subsequent sections of this report as outlined in the following table.

Table 4.4-1. Report outline for design element experimental results used to guide construction of the final prototype mat system.

Design Element	Report Section
Amendment Core Mixture	5.1.1. Amendment Adsorption Capacity; 5.1.2. Amendment Adsorption Kinetics
Geotextile Material	5.3.2. Gradient Ratio Testing
Geotextile Apparent Opening Size	5.3.2. Gradient Ratio Testing
Geotextile Mass Per Area	5.3.2. Gradient Ratio Testing
Hydraulic Conductivity	5.3.2. Gradient Ratio Testing
Biofouling/Clogging Resistance	5.3.2. Gradient Ration Testing
Sediment Deformation	5.3.3. Consolidation Testing

The final mats created by CETCO for prototype testing were comprised of an 80 AOS and 8 oz/yd^2 polypropylene non-woven geotextile, a woven backing geotextile and a mixed amendment core made up of 0.23 lb/ft^2 crushed apatite, 0.28 lb/ft^2 coconut shell activated carbon and 0.28 lb/ft^2 CETCO organoclay. Each individual mat was made up of two 25 ft x 15 ft panels

to be placed with a five foot overlap for an overall footprint of 25 ft x 25 ft (Figure 4.4-1). The entire mat system was designed to consist of four test treatments including a single layer mat (T1), a single layer mat with sand cover (T2), a double layer mat (T3) and an area of sand cover only (T4), as well as a similar sized area of undisturbed lake floor (T5, not shown) to serve as a control for the test data (Figure 4.4-2). Where applicable, the sand cover component consisted of an approximately three-inch layer of clean material of moderate grain size to provide a substrate for recolonization of the benthos while at the same time protecting the mat from bioturbation.

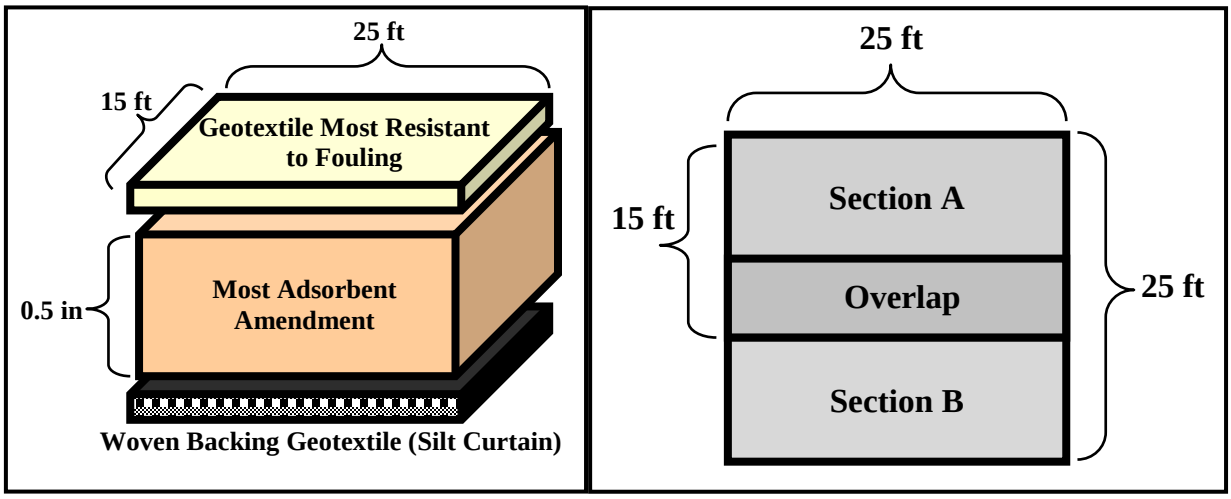

Figure 4.4-1. Construction and layout diagrams of prototype geotextile test mats.

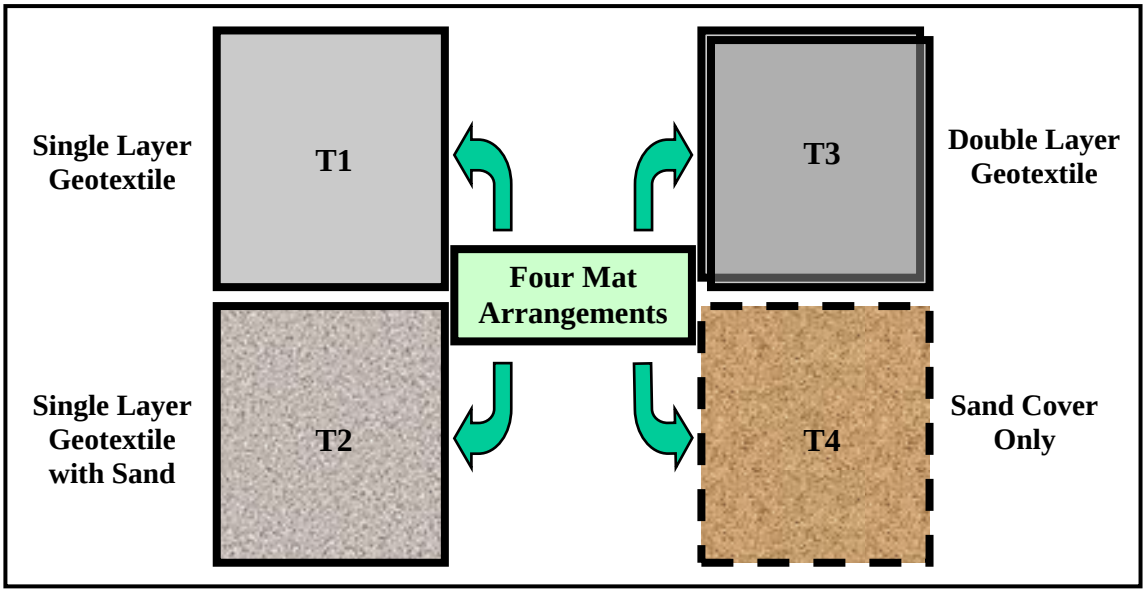

Figure 4.4-2. Various arrangements for prototype mat system testing.

4.4.2 Mat System Deployment

Mobilization. Deployment of the prototype mat system occurred during April 2008, with assistance from personnel from SAIC, UNH, and subcontractors American Underwater Services, Inc. (AUS) and Specialty Devices, Inc. (SDI). Equipment used for deployment included a dive platform, portable work platform, roll-off box, Bobcat loader, dredge pumps and a 12' dual Jon-boat vessel. The dive platform and work platform were delivered on trailers and lowered into the water from the shoreline staging area with a Sky-Trac telescoping forklift capable of extending 30 ft. The roll-off box was delivered and positioned using a dedicated flatbed truck and the dredge pumps were delivered on "gooseneck" trailers towed by heavy-duty pickup trucks. The Sky-Trac forklift and a smaller Bobcat loader were delivered to the site by a local rental company. The dual Jon-boat vessel was delivered on a dedicated trailer and assembled and launched by hand from the staging area shoreline.

Target Area Layout. Prior to mat deployment, personnel used the dual Jon-boat vessel and Hypack software interfaced with a laptop computer and DGPS antenna to mark off the precise target mat deployment area as well as a separate control area for baseline monitoring. The perimeter of the circular target area was marked with temporary open-cell orange foam floats attached to bricks by approximately 12 ft of line. The corners of the control area were marked to the east of the target area using higher grade permanent closed-cell orange foam floats also attached to bricks by approximately 12 ft of line. The temporary floats were intended to be removed when the different mat treatments had been deployed and the permanent floats were intended to remain throughout the course of the long-term monitoring process.

Mat Deployment. The entire prototype mat system was made up of four test areas and an undisturbed control area as discussed above and depicted in Figure 4.4-2. Approximately 25 ft of undisturbed sediment (*i.e.*, the length of one mat) was left between each test area to minimize interference and potential edge effects. The single layer mats were both placed with the non-woven geotextile side facing up (in contact with the water column). The double layer area, however, featured the non-woven geotextile side facing down (in contact with the sediment) on the bottom layer and the non-woven geotextile side facing up (in contact with the water column) on the top layer.

During mat deployment, AUS personnel towed the dive platform into the target area and anchored it in place with several Danforth-style anchors. High winds (20-40 kt) throughout the duration of the project necessitated the use of multiple anchors and spud poles to keep all vessels and barges in place while working. Reactive mat panels were transported to the target area on the portable work platform, which was then tied up alongside the dive platform. Two AUS divers attached to a surface supply airline system entered the water to place the mats while two AUS dive monitors remained on the dive barge to observe the compressor and communicate to the divers via the relay system in their helmets. Project personnel provided support and instruction from the dual Jon-boat vessel anchored nearby in the target area.

While the large mats were rolled up on the portable work platform, small lengths of polypropylene line were attached to the four corners of the individual 25 ft x 15 ft reactive mat panels to attach to the mats to the anchoring mechanism. One diver then screwed 36-inch screw

anchors into the sediment within the target area and the first mat panel was dropped in the water and floated into place. Based on previous work with small-scale test mats, the original anticipation was that the individual mat rolls would sink and they could be unrolled by divers while on the lake floor. However, air trapped in the roll prevented the mats from sinking until they were fully unfurled on the surface. Thus the polypropylene lines on one end of the mat were lashed by one diver to the screw anchors already in place while the other diver pushed the fabric on the surface, receiving assistance from personnel on the dual Jon-boat. The mats were unrolled, allowed to sink, and the divers smoothed the mats and secured the corners to the screw anchors.

Once the first 25 ft x 15 ft mat panel was secured in each test area, the process was repeated for the second 25 ft x 15 ft mat panel with polypropylene lines being positioned approximately four feet from the edge to account for the planned overlap and then lashed to the same screw anchors already under the water. Polypropylene lines attached to the far corners and the overlapping corners of the second panel were then fed through four additional screw anchors in order to pull the overlapping panel tight. For the test area featuring the double layer mat, the four individual panels were placed with an alternating overlap (*i.e.*, like a deck of cards). The upper layer was secured to the same screw anchors as the lower layer to limit both the dive time and the amount of anchors left at the site. When pulled tight to the screw anchors, the mat panels were brought into alignment with 100% overlap and no gaps in mat coverage present along the middle seam of the mat area.

The two single layer mat areas (T1, T2) and the double layer mat area (T3) were marked with a closed-cell orange foam float attached by a diver to the northwest screw anchor. In addition, the divers placed a screw anchor with a fourth float in the center of the sand only test area. These floats were color-coded to differentiate the test areas in the field log and were intended to remain in the water for the duration of long-term monitoring. All PVC pipes and other packing material used to transport the mat rolls were removed from the project site and discarded.

Sand Placement. Following the placement of the mats, AUS personnel assembled a sand slurry system to move capping material from the staging area on the NAS shoreline to two of the test areas in Cottonwood Bay. This slurry system consisted of a steel roll-off box serving as a hopper for the sand/water mix, one 6-inch hydraulic pump to move water from the lake into the roll-off box, a second 6-inch hydraulic pump to move slurry discharge from the roll-off box to the target area and a smaller submersible pump placed in the lake to provide a second water intake with a more concentrated stream for stirring the slurry. The hydraulic pumps used were both Holland Model H6TMS-D8 with a Perkins 1104.44 standard diesel engine power unit capable of moving up to 730 gal/min with a 50-ft head. The pumps used vegetable oil rather than typical hydraulic fluid to turn the impellers in order to minimize environmental impact and cleanup requirements should there be a breach in the line. The submersible pump used to stir the slurry was a 4-inch Honda gas-powered trash pump with a 16 hp engine capable of moving up to 705 gal/min. The approximately 600 ft discharge line consisted of 20-ft lengths of 6-inch diameter rigid pipe connected with buckle clamps and floated at the surface using 30 air-filled plastic barrels. The discharge impeller weighed several hundred pounds and was moved around the roll-off box using the Sky-Trac forklift to capture all available slurry material.

Fourteen cubic yards of "Cushion #1" screened fine sand was purchased from a local dealer to provide approximately three inches of cover on two 25 ft x 25 ft test areas (single layer mat, sand cover only). This material was delivered to the project site in a dump truck and unloaded on top of plastic sheeting to minimize impact on the local environment. During active slurry operations, the sand was transferred from the pile into the roll-off box using the Bobcat loader. The mixture was then stirred with the concentrated stream intake hose to ensure an adequate amount of material was discharged through the hose. The initial sand placement attempt was unsuccessful due to a prevalence of fine-grained material that was dispersed rather than deposited in the target area due to wind wave action. The decision was made to cease slurry operations with the "Cushion #1" sand and purchase a coarser grained material that would have a faster settling rate and be easier to control under the water.

To correct this problem, an additional ten cubic yards of coarser grained masonry sand was obtained from a second local dealer. This material would be left in the roll-off box and mixed with the remainder of the "Cushion #1" sand to achieve the planned three inches of cover on the two test areas. Rather than have a diver attempt to maneuver the discharge hose under the water, the decision was also made to shorten the pipeline by 20 ft, add a 45° angle spigot on the end facing down and hold the end in place using lines tied to the dive platform and the dual Jon-boats anchored nearby. By pulling on the lines, personnel on the dive platform and the Jon-boats could sweep the discharge pipe back and forth to ensure coverage of the entire test area.

The second sand placement attempt involved water being pumped into the roll-off box at 600 psi hydraulic pressure and slurry being discharged at 900 psi hydraulic pressure (corresponding to flow rates of approximately 400 gal/min and 600 gal/min, respectively, at 20-ft head according to Holland manufacturer specifications) over the T2 test area to feature a single layer mat with sand cap. These values were determined by trial and error to be the optimal pump settings for moving masonry sand slurry through 600 ft of pipeline without particles settling out in the hose or water overflowing the roll-off box while still being able to predict and control the discharge plume. Once discharged, the masonry sand settled much more quickly than the "Cushion #1" sand and produced only a small plume at the surface. Divers monitored the pumping effort periodically to ensure sand was being contained over the test area, but extremely poor visibility precluded the use of underwater video to document the sand placement and final site conditions. After 78 minutes of continuous pumping, diver measurements confirmed the presence of a uniform layer of sand approximately 2-3 inches thick over approximately 80% of the single layer mat. The remaining areas of the mat, encompassing the southernmost six feet (approximately 15% of the total) and the extreme southeastern corner (6 ft x 6 ft; approximately 5% of the total), were covered by ½ inch sand and a thin layer of rubble, respectively. There was also an approximately two foot overcast area covered by 2-3 inches of sand beyond the northern edge of the mat and a one foot undercast area covered by ¼ inch of the finest sand particles. This deviation from the planned three inch overall coverage with no overcast resulted both from an inability to gauge how far sand would settle from the end of the pipeline at the chosen discharge rate. The general bottom topography on which the mat was resting also contributed to variable sand thickness as some particles tended to accumulate in natural sinks.

With the single layer mat area (T2) covered, the discharge spigot was positioned over the T4 area (marked by a screw anchor and single float in the center) to receive sand cover only (no mat).

Again, water was pumped into the roll-off box at 600 psi (400 gal/min) and slurry was discharged at 900 psi (600 gal/min) and divers monitored the effort periodically. After 88 minutes of continuous pumping, divers confirmed that a 3-4 inch layer of sand extended approximately 10 ft to the east and west of the screw anchor and approximately 20 ft to the north and south. This layer tapered off to approximately once inch at the northernmost boundary of the test area. Samples of capping material were obtained from both test areas by the divers after placement as well as from the sand pile on shore for grain size analysis.

Demobilization. Following completion of the sand placement process, GPS locations of the permanent floats used to mark the four test areas were recorded, and all temporary floats were removed. Following project completion, the only visible materials left at the project site were four color-coded floats attached to screw anchors marking the four test areas and four additional floats attached to brick anchors marking the corners of the control area.

4.4.3 Geophysical Investigation

Geophysical Investigation. In December 2008, following approximately eight months of soak time, a small-scale geophysical investigation including bathymetry, sub-bottom, side-scan sonar and SPI surveys was conducted over the prototype mat system test area to record properties such as surface roughness and benthic colonization that could not otherwise be observed from above the water. The bathymetry and sub-bottom surveys were conducted with a single-beam echo-sounder interfaced with a BSS+3 survey computer featuring HYPACK v.4.3 software. The side-scan survey was conducted with an IMAGINEX dual frequency digital side-scan sonar transducer ("fish") also interfaced with a BSS+3 survey computer featuring HYPACK v.4.3 software. Both transducers were deployed from a small dual Jon-boat survey craft and several passes were made over the prototype mat system to ensure complete coverage of the study area. The highest resolution side-scan results were achieved with a start gain of 30 dB and a pulse link of 150 µs. Raw bathymetry, sub-bottom and side-scan data were processed to identify the post-impoundment and pre-impoundment surfaces and provide a pictorial view of the prototype mat system area. The final side-scan mosaic produced a clear image of the prototype mat layout and the distribution of sand capping material, which previously had been confirmed only by diver observations.

Sediment profile imaging technology utilizes an underwater still camera-mirror system to take cross-sectional pictures of the sediment-water interface and the upper six inches of sediment (or 3" in cases of sand over mats) in order to assess biological conditions at the sediment water interface. Several replicate SPI photographs were taken over the five test areas (including control) to analyze benthic habitat conditions that had developed after approximately six months of soak time. Cursory analyses of these images were performed to provide an evaluation of sediment buildup on the mats, confirmation of sand capping thickness in appropriate areas and a description of control area conditions.

4.4.4 Passive Contaminant Sampling

Monitoring Device Deployment – Year 1. In October 2008, after approximately six months of soak time, divers installed three types of in-situ passive diffusion samplers at the prototype mat

system to measure the sequestration of contaminants by each test treatment. The passive contaminant sampling devices included dialysis samplers ("peepers"), semi-permeable membrane devices (SPMDs) and solid phase micro-extraction (SPME) fibers. Peepers are expression samplers constructed of polyethylene plastic casing fitted with a nucleopore membrane used to evaluate metals in pore water. In contrast, SPMDs are permeable tube-like bags containing a high molecular weight lipid (triolein) attached to an aluminum deployment device that are used to simulate accumulation of organic contaminants in fish organs. The SPME fibers are coated with a liquid polymer that allows organic contaminants to establish equilibria between the fiber and the sample matrix. Because the utility of SPME devices in aquatic environments is still in the research and developmental phase, the data from these samplers were intended to provide a side-by-side comparison with similar data obtained from the SPMDs through more established techniques.

To install the peepers, SPMDs and SPMEs, divers peeled back a section of mat and placed the devices at least three feet from the edge in predetermined sampling locations. All samplers were attached to aluminum deployment rods that were custom fabricated to meet the specific needs of this project. These rods were then tethered to the screw-anchors that were already holding the mats in place. Precise sampler locations (*i.e.*, which specific corners of the treatment) were carefully selected to maximize interaction with the desired interface (*i.e.*, presence of sand cap) and avoid any anomalous features such as the sand cap overcast and undercast areas adjacent to the single layer mat area covered with sand, T2 (see Section 4.4.2).

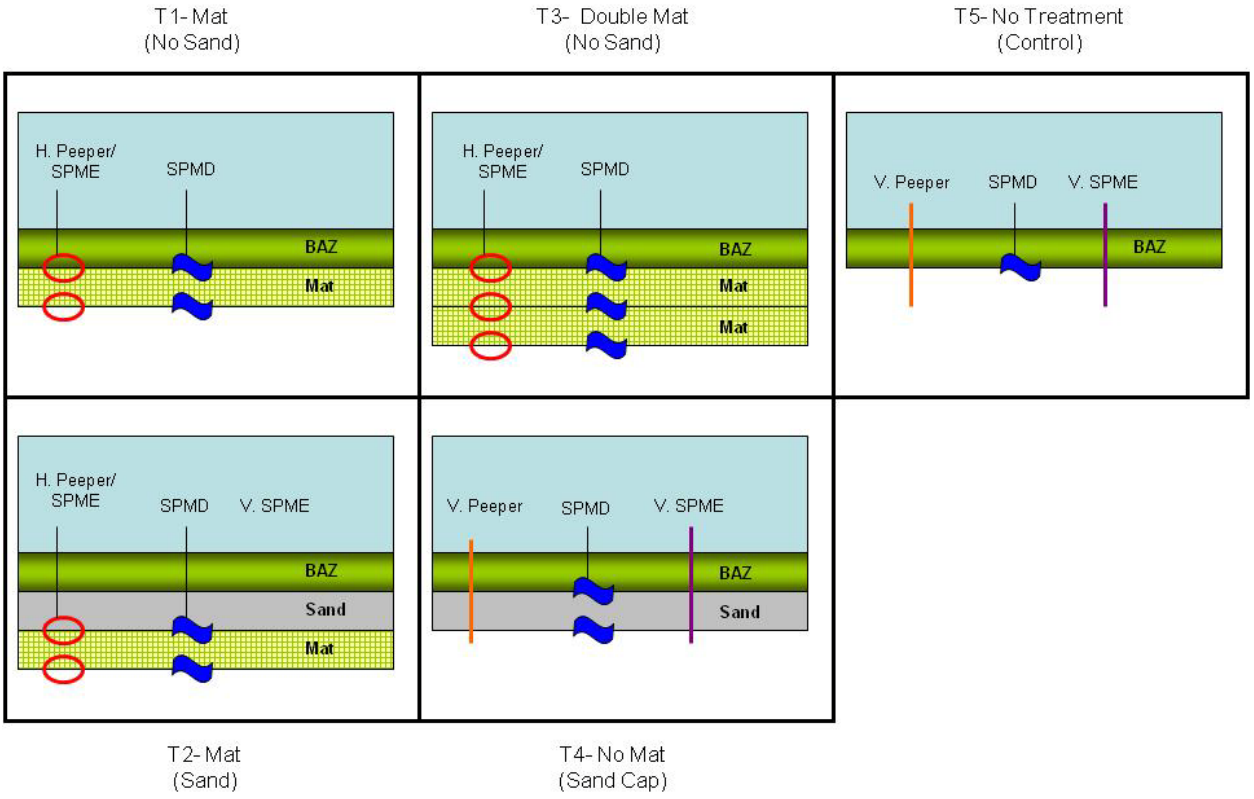

Figure 4.4-3. Vertical passive sampler layout in Cottonwood Bay.

A total of 21 horizontal peeper/SPME combination devices, 30 SPMDs, four vertical peepers and four vertical SPMEs were deployed at unique mat-water, sediment-mat, mat-sand, mat-mat, sand-water, sediment-sand and sediment-water interfaces across the five test areas (including control). The T4 area (sand cap only) and the T5 area (no treatment) received vertical peepers and SPMEs to evaluate conditions over multiple horizons in the absence of a mat. A graphical representation of the final vertical passive sampler layout as deployed in Cottonwood Bay is presented in Figure 4.4-3.

Monitoring Device Deployment – Year 2. In October 2009, after approximately 18 months of soak time, divers again installed three types of in-situ passive diffusion samplers at the prototype mat system to provide a comparative second year contaminant sequestration dataset. The same general sampling design, methods and sampler configuration were followed as in the previous investigation. One exception was that SPMEs were excluded from the second year sampling (based on ubiquitous non-detect results from the first round of sampling); these were replaced with horizontal and vertical polyethylene devices (PEDs) as an alternate experimental form of sampling for organics. The PEDs consist of a strip of low density polyethylene that measures the activity of hydrophobic organic compounds (*e.g.*, PAHs, PCBs, DDT) in the environment based on the partitioning of these compounds between polyethylene and water. The PED is deployed in the same manner as the SPMD such that freely dissolved hydrophobic organic compounds can passively adsorb onto the membrane. As with the SPMEs and SPMDs, equilibrium is reached on the order of days to weeks.

In a new approach, vertical peeper arrays were installed through small slits made into the mats in areas T1 and T2 to provide data over multiple horizons in these treatment areas that were not obtainable during the first round of sampling. A separate peeper and PED were also suspended in the water column using an independent anchor-float system to provide background information on contaminants present in the Cottonwood Bay.

The custom deployment rods holding the peepers, SPMDs and PEDs were modified following the first round of sampling to include a second cross-member designed to keep the SPMD taught on the sediment surface and eliminate some of the folding and tearing that was previously experienced. A total of 21 horizontal peepers, 30 SPMD/horizontal PED combinations, 8 vertical peepers (2 through mats) and 6 vertical PEDs were installed throughout the overall mat system in Year Two.

While installing the samplers, divers also inspected the mats for the presence of sand in the capping areas as well as any slumping affects due to wave and current action or potential air pockets caused by gas buildup below the mats. An air pocket measuring approximately 1-1.5 ft high and 3 ft in diameter was observed below the mat in area T1 (mat only); divers were able to remove the air by applying pressure to the mat until it escaped out the edge. In contrast, only minor air pockets were observed for T2 (mat with sand cap) and T3 (double mat) and if present, were also removed by the divers. Multiple ridges were also observed in area T3 likely caused by the weight of the double mat distorting the underlying soft sediment. The presence of 2-3 inches of coarse sand was observed in both capping areas (T2 and T3), which was consistent with the findings of the sediment cores (see Section 4.4.6).

Monitoring Device Retrieval – Year 1. In December 2008, divers retrieved the peepers, SPMDs and SPMEs from Cottonwood Bay after exactly 50 days of soak/sampling time by extracting the aluminum bars via the polypropylene lines and carefully bringing each array of samplers to the surface. Working from the dive platform/small survey vessel, project personnel extracted porewater from the individual peeper chambers using small syringes and placed the test material in vials for shipment to the analytical laboratory. All vertical peepers were recovered by the divers and processed on the dive platform/small survey vessel in the same manner as the horizontal peepers, with a separate sterile syringe used for extracting porewater from each discrete vertical chamber. The SPME deployment devices were encased in aluminum foil for processing and extraction at a later time.

Recovered SPMDs were carefully sealed in pre-labeled tin cans for shipment to the processing laboratory and the conditions of each sample were recorded on designated SPMD logs. One SPMD was not recovered (*i.e.*, lost) and several other SPMDs contained visible tears and creases upon first inspection. The extent of this damage and the potential effects on sample data quality were later quantified during the extraction process (see below).

During the sampler recovery effort, water quality measurements were also collected from the surface water at the mat system area using a handheld YSI 556 Multi-Probe water analyzer. . The probe was then lowered into Cottonwood Bay approximately one foot below the surface at the mat system area. Readings for temperature, conductivity, dissolved oxygen concentration, pH and oxidation-reduction potential stabilized, were recorded in the field logbook. The process was repeated with the probe lowered into Cottonwood Bay approximately one foot above the mats. Water temperature values were to be used to complete SPMD concentration calculations.

Monitoring Device Retrieval – Year 2. In December 2009, divers returned to retrieve the peepers, SPMDs and PEDs from Cottonwood Bay after 47 days of soak/sampling time following the same procedures used during the Year One recovery (discussed in the previous section). As for the vertical peepers, the vertical PEDs embedded in the sediment were recovered by the divers and processed in the same manner as the horizontal PEDs. Finally, the peeper and PED membranes suspended in the water column to analyze ambient surface water conditions were recovered directly from the survey vessel and processed in the same manner as the horizontal samplers.

All 30 test SPMDs were recovered (*i.e.*, none were lost) and all were found to be taught on the aluminum bars and appeared in good condition upon first inspection. The additional cross-member added to the deployment bars for the second year sampling appeared to have eliminated the tearing and folding that was experienced in Year One (discussed in previous section). While onsite, water temperature measurements were made using a submersible thermometer. At the time of sampler recovery in December, the water temperature in Cottonwood Bay was 7°C (45°F), as compared to 19°C (66°F) at the time of sampler deployment in October.

Finally, divers again inspected the mats for the presence of air pockets below the surface. In contrast to the observations made during passive sampler deployment, when multiple small air pockets (< 3 ft diameter) were observed in areas T1, T2 and T3, no air pockets were found under

any of the mats at this time. These findings were consistent with previous observations of the small-scale test mats that indicated potential gas buildup beneath the mats in the summer, minimal to no buildup in the fall, and no buildup in the winter.

Peeper Extraction and Analysis. Horizontal peepers were deployed in replicates of three at specific target interfaces (sediment-mat, mat-water, mat-sand, mat-mat) in areas T1 (mat only), T2 (mat with sand cap) and T3 (double mat). In contrast, vertical peepers were deployed in replicates of four (Year One) or three (Year Two) spanning specific target interfaces (sediment-sand, sand-water, sediment-water) in areas T4 (sand cap only) and T5 (no treatment/control). In Year Two, a peeper was also suspended in the water column in the middle of the treatments to provide background data on the ambient water column.

Each replicate peeper featured several membrane-bound chambers at each depth containing distilled water into which site porewater contaminants were allowed to equilibrate at that specific horizon. During the sampler recovery process, the peepers were removed from the water and a sterile syringe was used to puncture the membrane for each chamber and extract the contaminant enriched water. The extracted water was then placed directly into a chamber-specific vial for transport and analysis as a typical water sample. All vials containing water extracted from the peepers were sent with wet ice (4°C) to UNH and analyzed for metals by inductively coupled plasma-mass spectrometry (ICP-MS).

SPMD Extraction and Analysis. Semi-permeable membrane devices (SPMDs) consist of a dialysis bag filled with oil (triolein) which essentially mimics the tissue/lipid matrix of aquatic organisms. By measurement of the organic contaminants that accumulate in the oil, the environmental concentration and bioavailability of the contaminant can be determined. Additionally, because the oil will accumulate contaminants at very low concentrations, the method is much more sensitive than traditional surface water or direct porewater analyses.

Extraction of the triolein test material from the recovered SPMD tubes was performed at the processing laboratory (EST Labs, St. Joseph, Missouri). The SPMD extraction process generally involves (1) removal of exterior surficial periphyton and debris; (2) organic solvent dialysis; (3) size-exclusion chromatography (SEC); and (4) chemical class specific fractionation using Florisil, silica gel and/or alumina sorption chromatography (Petty et al. 2000). Cleaned SPMDs were dialyzed in hexane (125 mL of hexane per standard SPMD) for 18 hours at 18°C, followed by a second dialytic period (with 125 mL of fresh hexane) of 6 hours also at 18°C. The two dialysates were then combined and reduced in volume to about 1 ml for SEC cleanup (or an equivalent process) and GC/MS analysis (Petty et al. 2000).

During the extraction process, laboratory personnel observed the conditions of each SPMD tube in terms of the number of holes/tears, site water infiltration, apparent triolein loss and apparent distension. Both triolein loss and site water infiltration would increase uncertainty in SPMD analytical results as true representations of site porewater concentrations by diluting or altering the composition of the internal solvent prior to analysis. All SPMDs holes were sealed prior to extraction to limit the effects of any holes present. During the first round of SPMD sampling, 12 of 30 samplers exhibited at least one hole, with 7 of these samplers also experiencing measurable oil loss or water infiltration. During the second round of SPMD sampling, only 2 of

30 samplers exhibited holes and neither of these samplers experienced measurable oil loss or water infiltration. The data usability for these compromised SPMDs is discussed in the study results (Section 5.4.2).

Following the extraction process, the ampoules containing the resulting hexane dialysates were sent to the analytical laboratory (EnviroSystems, Inc., Hampton, New Hampshire) and analyzed for PAHs by EPA method PAH680. The subsequent analytical results were then entered into an "Estimated Water Concentration Calculator" provided by the SPMD processing laboratory, which converts the concentration of a measured PAH analyte in the SPMD extract (in units of ng/mL hexane) to an estimated porewater concentration at the deployment site (in units of pg/L). The calculation is based on mathematical models developed by the USGS Columbia Environmental Research Center (Version 4.1) as a function of days deployed (~50 days), water temperature (~10°C), mass of SPMD (4.5 g), volume of lipid (0.001 L), volume of membrane (0.0037 L) and volume of SPMD (0.0047 L).

SPME Extraction and Analysis. The SPME process for monitoring PAHs in Cottonwood Bay porewater was consistent with previously established protocol presented in Reible 2008. This sampling technique employed between 10 and 20 cm of 300/200 µm polydimethylsiloxan (PMDS) fiber (Fiberguide) per replicate sample. Fibers were deployed at 10 cm lengths in a protective stainless steel sheath which was slotted on three sides to allow adequate porewater/SPME interaction. Upon recovery, all SPME fibers were kept in their sheaths, immediately cooled below 0°C using dry ice and shipped overnight to the UNH analytical laboratory.

Within 48 hours of field recovery, the SPME fibers were removed from their protective casing, rinsed free of sediment with deionized water and cut to 1 cm increments which were placed in 300 µL of methylene chloride and allowed to desorb PAH analytes into the solvent for seven days. Following desorption, the contaminant-enriched solvent was stored below 0°C until analysis via GC/MS using a Varian 3800GC in line with a Saturn 2200 MS.

During chemical analysis, an external calibration for the 12 PAH compounds of interest for Cottonwood Bay indicated that all concentrations in the SPME solvents were below the reporting limit of the analytical instrument. Using the equation presented below, all porewater concentrations for the various interfaces in the prototype mat system were thus determined to be < 5 ng/mL.

$$C_{PW} = \frac{(C_{Solvent})*(V_{Solvent})*K_f}{(V_{SPME})}$$

Where:
C_{PW} = Porewater Concentration
$C_{Solvent}$ = Solvent Concentration (determined by GC/MS)
$V_{Solvent}$ = Volume of Solvent analyzed in GC/MS method
V_{SPME} = Volume of PDMS on SPME fiber analyzed
K_f = Partition Coefficient between Porewater and SPME fiber

4.4.5 Chemical Flux Survey

After one year of soak time, groundwater seepage measurements through the prototype mat system were made using Ultraseep groundwater seepage meters in order to quantify water flux through the mats from underlying sediments as well as to identify any changes in contaminant concentration with respect to the source (*e.g.*, groundwater flux out of the mat versus overlying water penetration into the mat). The Ultraseep is a modular, state-of-the-art seepage meter designed for direct measurement of groundwater plumes at the sediment-water interface. This unit was invented out of the need to accurately quantify contaminant flux into surface waters in a time-transient manner, as previous methods were not able to locate and quantify these measurements in a reliable way (Chadwick et al. 2003). Not only does the Ultraseep record flow parameters, but it also collects passive samples of groundwater passing through the selected interface to be used for chemical analysis.

Mobilization. Personnel from subcontractor Coastal Monitoring Associates (CMA) arrived at the mat test site on the weekend of 12-14 June to mobilize a portable on demand storage (PODS) unit containing all survey equipment and assemble an approximately 20 ft pontoon barge powered by a small electric trolling motor. Personnel from Specialty Devices, Inc. (SDI) then arrived on the morning of 15 June to launch the pontoon barge and assemble and launch a second 12' dual Jon-boat vessel powered by a small gasoline engine as well as a third single Jon-boat powered by another small electric trolling motor. The survey effort required three Ultraseep units and one Trident Probe unit modified for use in the reactive mat setting.

Ultraseep Groundwater Flow Modeling. Ultraseep meters were deployed at the different treatments within the prototype mat system (T1-single mat only, T2-single mat with sand cap, T3-double mat, T4- sand cap only, T5-no treatment/control) from 15-19 June 2009. During the deployment process, the units were lowered from the pontoon barge using a davit and hand-powered winch. Scuba divers provided underwater support for guiding the Ultraseep to the bottom and ensuring it was resting in place with a tight seal at the desired interface (*e.g.*, mat-water, sand-water, etc.). The Ultraseep meters were allowed to soak for approximately 24 hours to record groundwater flux data as well as collect a passive groundwater plume sample. Following this soak time, the Ultraseep meters were recovered from each treatment area with the aid of scuba divers and brought aboard the pontoon barge using the hand-powered winch. While being raised from the surface but still in the water, divers cleaned the units to remove any sediment or detritus. The units were then brought to shore and fully decontaminated following standard operating procedures. The internal bag containing the groundwater plume sample was removed from the unit and weighed. A small portion of the sample was then extracted and used to test water quality parameters (*e.g.*, temperature, conductivity, pH) using a handheld water quality meter. The remainder of the sample was then transferred to a pre-labeled jar containing 70% HCl as a preservative to be shipped to the UNH analytical laboratory for chemical analysis.

Over the course of the week, Ultraseep meters were deployed twice at each mat-system area (T1, T2, T3, T4) and once at the control area (T5). Sequencing, soak times and sample volume for each Ultraseep replicate are provided in Table 4.4-1. During each sampling event, a single Ultraseep unit was deployed at the treatment area and recovered the following day, with all three units typically being recovered, decontaminated and re-deployed during a full working day.

During the initial deployment attempt at the control area (T5), the native sediment proved too soft to support the Ultraseep unit without it sinking too far into the mud or tipping over. Thus the unit had to be retro-fitted with a thin plywood skirt to provide additional surface area for deployment on the following day. Electronic groundwater flow data were recorded successfully during all nine deployments. However, the second Ultraseep deployment at area T1 failed to produce a groundwater plume sample, which may have resulted from the mat folding over onto the unit, the unit being placed in an area where an air bubble had developed under the mat and prevented contact with the sediment below or the unit being placed in an area where groundwater flow was not percolating upwards into the overlying sediment.

Table 4.4-2. Ultraseep sampling summary for the Cottonwood Bay prototype mat system.

Treatment Area	Deployment (Date; Time)	Recovery (Date; Time)	Soak Time (~hours)	Sample Volume (mL)	Discharge Water in Sample (mL)	Discharge Fraction (%)	Surface Water Fraction (%)	Sample Type
T1 - Deployment 1	06/15/09; 1445	06/16/09; 1425	24	671	113.06	17	83	Composite
T1 - Deployment 2	06/18/09; 1030	06/19/09; 0859	22	2	-	-	-	No Sample
T2 - Deployment 1	06/15/09; 1400	06/16/09; 1412	24	215	13.39	6	94	Composite
T2 - Deployment 2	06/17/09; 1052	06/18/09; 0855	22	10	-	-	-	No Sample
T3 - Deployment 1	06/16/09; 1349	06/17/09; 1124	22	72	-	-	-	No Data Provided
T3 - Deployment 2	06/17/09; 1435	06/18/09; 1125	21	103	18.04	18	82	Composite
T4 - Deployment 1	06/17/09; 0938	06/18/09; 0840	23	868	172.65	20	80	Composite
T4 - Deployment 2	06/18/09; 0950	06/19/09; 0920	24	722	111.85	15	85	Composite
T5 - Deployment 1	06/18/09; 1418	06/19/09; 1306	23	344	34.09	10	90	Composite

Trident Probe Porewater Collection. Concurrent with the Ultraseep deployments, active surface and porewater samples were collected from various depths in each mat-system area using the Trident Probe. The Trident Probe unit is a flexible, multi-sensor water sampling probe used for screening and mapping groundwater plumes discharging from surfaces sediments into the overlying water column. The probe records real-time measurements of porewater temperature and conductivity, which can then be compared to the overlying surface water to find areas of probable groundwater flow (as evidenced by lower temperature and higher conductivity). The probe also features three screened and sand-packed arms through which porewater can be drawn into flexible hoses using a low-flow peristaltic pump. For the present study, the tips of these arms were set at 3.5 in, 11 in and 24 in, respectively, below the base plate to sample various depths within the test areas. A fourth hose (without a screen) was also set 2 inches above the base plate to sample surface water at the treatment-water interface. These sampling horizons were selected to mirror the same interfaces targeted previously by the passive contaminant samplers (*i.e.*, peepers, SPMDs) in order to analyze synoptic vertical chemical gradients.

During each Trident Probe event, the sampler was lowered from the dual Jon-boat vessel by hand and pushed upright into the underlying sediment. In test areas containing a mat, modified cutting tips were attached to each arm of the probe which were able to penetrate the geotextile layers with minimal use of force. Prior to initiating sampling, scuba divers provided visual confirmation that the probe was indeed in a desirable area (*i.e.*, penetrating the mat or sand cap where appropriate, particularly in areas where methane gas bubbles under the mats were problematic) and that the base plate of the probe was flat against the selected interface. A GPS

fix of the exact probe location was obtained and temperature and conductivity data from each arm, as well as a reference sensor in the surface water, were collected.

Active sampling was then initiated by attaching each hose from the various probe arms to a low-flow peristaltic pump and drawing water out of the target matrix (*i.e.*, surface water, sand cap, sediment). Approximately 250 mL of water were immediately purged from the sampling lines in order to eliminate potential contamination. A small sample was then extracted from each line and used to test water quality parameters (*e.g.*, temperature, conductivity, pH) using a handheld water quality meter. An additional 250 mL was then purged and a second water quality measurement was taken. Finally, the analytical sample was collected directly from the line into a pre-labeled jar containing 70% HCl as a preservative to be shipped to the analytical laboratory for chemical analysis. Following each Trident Probe sampling event, the unit was returned to shore and decontaminated following appropriate procedures (*i.e.*, Alconox scrub, nitric acid rinse, and distilled water rinse) prior to occupying a new sampling area.

Sampling from the surface line and the shallow arm (3.5 inches) took less than 10 minutes to fill the 125 mL sample jar. In contrast, sampling from the deeper arms (11" and 24", respectively) took over one hour due to fine sediment at depth and a very slow recharge rate. In the interest of time, sampling from these depths was stopped following collection of approximately 30 mL of porewater, which was the minimum volume identified by the analytical laboratory to successfully conduct the desired metals analyses. Due to extremely long sampling times, the deepest samples (24") were only collected from areas T3, T4 and T5. When attempting to sample the control area (T5), the probe base plate sunk into the very soft native sediment and the surface water sampling line became clogged in the absence of a screen. Here, scuba diver assistance was required to collect a surface water sample directly into a jar at the sediment-water interface. During each Trident Probe sampling event at the double mat area (T3) an additional water sample was taken from between the individual mat layers. In order to accomplish this task, a scuba diver placed a separate probe between the mats that was not attached to the main Trident Probe unit. This additional probe contained its own hose and was sampled in the same manner as the other lines.

Over the course of the week, Trident Probe measurements and samples were collected twice at each mat-system area (T1, T2, T3, T4) and once at the control area (T5). Sequencing and depths for each Trident Probe replicate are provided in the table below.

Chemical Analysis. In total, 8 analytical Ultraseep samples from the treatment-water interface and 32 analytical Trident Probe samples from various depths were collected from the Cottonwood Bay prototype mat system. Single equipment blank samples were also collected from the Ultraseep and Trident Probe units, respectively. These samples were shipped to the UNH analytical laboratory and analyzed for metals by inductively coupled plasma-mass spectrometry (ICP-MS).

Flow Data Processing. Specific discharge, temperature and conductivity data were downloaded from the Ultraseep instrumentation for each individual deployment and plotted as a function of time. These data allowed for determination of the volume of active flow discharge in the Ultraseep sample compared to the amount of instrument purge water also present in the sample.

The results were used to quantify the groundwater flow for each treatment as well as calculate the "discharge fraction" for each analytical sample (Table 4.4-1). This de facto dilution factor was applied to the raw chemistry results from the Ultraseep analytical samples to calculate the concentration of a specific analyte reflective only of the active flow sample (*i.e.*, the discharge; typically 0.1-1.0 L) and not the required volume of deionized water inside the instrument (~0.5L) with which the environmental sample is mixed when sampling is initiated. The following proportion was used to perform the desired calculation:

Equation: $[C_D] = ([C_S]*[V_S]) / [V_D]$

Where: C_D = Discharge water concentration (mg/L)
C_S = Analytical sample concentration (mg/L)
V_S = Analytical sample volume (mL)
V_D = Discharge volume (mL)

4.4.6 Sediment Coring

Core Collection. Concurrent with the second year passive sampler deployment effort, sediment cores were collected from the study site in order to help establish the vertical chemical gradient in the sediment from which previous porewater samples had been extracted. In areas without a mat (T4-sand cap only, T5-control), the sediment core was collected from the center of the treatment. In areas with a mat (T1-single mat only, T2-single mat with sand cap, T3-double mat), the sediment core was collected as close to the edge of the mat as possible without penetrating the mat with the corer barrel. The GPS coordinates of all coring locations were recorded in the field logbook using a handheld Garmin GPSMAP76 navigator with wide area augmentation system (WAAS) enabled.

Sediment coring was conducted using a WILDCO® hand corer consisting of an approximately 4-ft by 2.5-in internal diameter stainless steel tube with an 8-ft extension T-handle. Prior to sampling, a chemically clean 4-ft by 2-in internal diameter transparent butyrate core liner was inserted into the corer barrel and capped with a 2-in internal diameter core cutter at the end. The corer was pushed into the sediment from the sampling vessel by hand using fully leveraged body weight. Upon reaching the maximum possible penetration depth, the corer was recovered by slowly pulling the barrel out of the sediment by hand. The resulting vacuum created by the polyurethane flutter valve on the head assembly retained the material in the butyrate liner. The end of the corer was then covered with a sterile gloved hand, the core cutter removed from the barrel, the liner extracted and the core inspected for integrity. Each successful core, as determined by the presence of a continuous solid sample greater than eight inches in length with no washout (*i.e.*, intact sedimentary material and overlying water without loss due to drainage), was then immediately capped and sealed with electrical tape and stored upright in an ice chest to allow suspended particles to settle prior to processing. Prior to use at each station the core cutter was decontaminated by scrubbing with a solution of distilled water and phosphate-free detergent (Alconox) followed by distilled water and site water rinses.

Core Processing and Subsampling. Following settlement as described above, cores were visually observed with preliminary notes on various sediment layers recorded in the field

logbook. A designated core processing area was established on shore consisting of a small table with clean cover. During processing, the core liner was pierced with a razor knife above the sample to allow drainage of the overlying water. Excess core liner above the drainage point was cut off using a hacksaw and discarded, with special care given to prevent liner shavings from contacting the sample. The core liner was split length-wise into two halves to expose the sediment for observation and sub-sampling. The exposed core was measured and photographed and the physical properties (*e.g.*, color, grain size, and odor) of the core were characterized and recorded in the field logbook.

During sediment core sub-sampling, a stainless steel spoon was used to transfer the top four inches of the core directly into the pre-labeled jar for the surface (0-4") sample and the next four inches directly into the pre-labeled jar for the sub-surface (4-8") sample. The stainless steel spoon was decontaminated between each sub-sample by scrubbing with a solution of distilled water and phosphate-free detergent (Alconox) followed by a distilled water rinse.

All sediment sample jars were immediately sealed with rubber tape, wrapped in bubble-wrap and stored inside a cooler with wet ice at 4°C until overnight shipment to the analytical laboratory. Overall, 12 sediment sample jars from the 6 stations (2 depths per station) were shipped to the analytical laboratory (EnviroSystems, Hampton, New Hampshire) for chemical analysis.

Chemical Analysis. In total, 12 analytical sediment core sub-samples were collected from the Cottonwood Bay prototype mat system. These samples were analyzed for metals following USEPA Method SW6020B, PAHs following USEPA Method SW8270/SIM and TOC following USEPA Method SW9060.

5.0 RESULTS AND DISCUSSION

This section provides results of the tasks described in Section 4 and discussion of how the objectives for SERDP Project Number ER-1493 were met. Figures and tables are provided that highlight the results obtained for each task and support the final conclusions of the overall project. All final project data including raw data tables and intermediate results are provided in the designated appendices or referenced to the appropriate source document.

5.1 Task 1: Composite Material Testing

The purpose of Task 1 was to identify the mixture of amendment materials that would most effectively sequester contaminants as part of a reactive mat when also considering potential interference and complexation caused by interactions with natural organic acids. The reactive mats being developed in this project would be deployed directly over sediment beds, and would therefore be expected to be affected by high concentrations of natural organic matter. Thus the potential presence of organic acids (*e.g.*, humic acid, fulvic acid) originating from natural microbial activity and organic decay was considered a major factor in the design of the reactive mat system and the performance of sorbents to be used in the final amendment mixture.

To identify a suitable amendment, project personnel conducted laboratory tests to characterize different types of activated carbon and organoclay in terms of adsorption and desorption of PCBs

and PAHs in the presence and absence of humic acid. Additional experiments were also conducted to assess the combined effects of humic acid, fulvic acid and NOM on the adsorption properties of these materials. Following the evaluation of different sorbents individually, the preferred amendment mixture was prepared from stock materials and then similarly tested. The results were compared to the performance of a weathered mixture recovered from the small-scale test mats deployed at the Cottonwood Bay pilot site for six months.

Complete results of these experiments, including figures, graphs and tables, are presented in Sharma 2008. A summary of the results as they pertain to SERDP Project Number ER-1493 are presented in the following sections.

5.1.1 Amendment Adsorption Capacity

Preliminary amendment adsorption capacity results presented in the Second Year Annual Progress Report (NAVFAC 2007) showed that CETCO organoclay containing bentonite as the base clay and coconut shell activated carbon were the optimal amendments for achieving maximum contaminant sequestration as compared to other types of organoclay and activated carbon. Final adsorption capacity results in the presence and absence of humic acid, including all relevant plots and tables, after years three and four of laboratory investigation for PCBs on coconut shell activated carbon, PCBs on CETCO organoclay and PAHs on both coconut shell activated carbon and CETCO organoclay are presented in the "isotherm" subsections of Chapters 2, 3 and 4, respectively, in Sharma 2008.

The overall characterization of activated carbon showed that adsorption capacity was greater for higher chlorinated PCB congeners than for lower chlorinated PCB congeners and are affected by the preloading of humic acid. There was minimal desorption of these congeners as well as co-planar PCB congeners when exposed to humic acid over prolonged periods.

The characterization of different organoclays was similar to that of activated carbon, although with the CETCO organoclay the humic acid preloading effect was more pronounced for lower chlorinated congeners. The desorption from organoclays in the presence of humic acid was more pronounced than for activated carbon, however, the effect was not uniform and varied depending on specific contaminant.

Additional testing involving exposure of activated carbon and organoclay to humic acid, fulvic acid, NOM and porewaters from other sites (Passaic River, Hudson River) showed that preloading effects were more pronounced for humic acid than other compounds and that organic acids in sediment porewater have a significant impact on the effectiveness of potential reactive mat amendments in sequestering contaminants. The data showed that the humic fraction of NOM was the primary determinant of adsorption affinity reduction. This factor should be included in the final design and performance estimate of potential reactive mats under typical site conditions.

With regards to PAHs, laboratory results showed that the adsorption capacity of bare activated carbon was found to be higher than that of bare CETCO organoclay for three select PAHs. Within each bare amendment, the adsorption capacities for the three selected PAHs were

naphthalene > phenanthrene > pyrene. Similar to the bare sorbent tests, results when preloading with humic acid were significant and showed that the adsorption capacity of preloaded activated carbon was higher than the adsorption capacity of preloaded CETCO organoclay. Similar preloading studies with humic acid on activated carbon generally indicated negligible effects compared to the bare amendment. For CETCO organoclay, however, preloading with humic acid did change the relative adsorption capacity of the individual PAHs (pyrene > phenanthrene > naphthalene). This contrast shows that if the sorbents are exposed to very high concentrations of natural organics (*e.g.*, >1 g/L), the resulting interactions can affect the performance of the reactive core mat. Additionally, long term exposure of organoclay to natural organic matter might also affect mat performance by causing increased desorption of target compounds.

5.1.2 Amendment Adsorption Kinetics

Kinetic studies were an important laboratory component of this project in order to characterize adsorption equilibrium times for the different sorbents to be used in subsequent equilibrium isotherm experiments as well to assess the potential effectiveness of a thin reactive mat where contaminant residence time may be significantly less than 24 hours. Amendment adsorption equilibrium results after the first two years of work were presented in the Second Year Annual Progress Report (NAVFAC 2007). Final adsorption kinetic results in the presence and absence of humic acid, including all relevant plots and tables, after years three and four of laboratory investigation for PCBs on coconut shell activated carbon, PCBs on CETCO organoclay and PAHs on both coconut shell activated carbon and CETCO organoclay are presented in the "kinetics" subsections of Chapters 2, 3 and 4, respectively, in Sharma 2008.

For PCBs adsorbed on coconut shell activated carbon, preloading with humic acid was found to significantly increase the time required for 2,2',5,5'-tetrachlorobiphenyl to reach equilibrium over the course of the experiment, although these effects gradually decreased over time. Preloading with humic acid also appeared to increase the time required to reach equilibrium for 2,2',4,4',5,5'-hexachlorobiphenyl, but unlike 2,2',5,5'-tetrachlorobiphenyl these effects were found to be very low (due to the very low concentration of hexachlorobiphenyl used in the experiment) and remained consistent over time. These retardation effects could be due to the pore blockage effect and greater complexation of highly chlorinated congeners to humic acid as compared to mono-chloro-congeners. Greater complexation with humic acid is expected for more highly chlorinated congeners as shown by K_{DOC} complexation constants that increase with the increase in hydrophobicity of the compound (Pirbazari *et al*. 1989).

For PCBs adsorbed on organoclay, kinetics experiments showed that the adsorption equilibrium for 2-chlorobiphenyl was reached at approximately 48 hours for the bare amendment, but the presence of humic acid was found to slow the sorption kinetics. This increase in equilibrium time may have been due to the slow diffusivity of 2-chlorobiphenyl into the interlayer spacing of organoclays in the presence of humic acid molecules that can block the path of the contaminants via hydrophobic interactions with organophilic outer layers of the sorbent.

For PAHs, kinetics experiments showed that the effects of preloading with humic acid were less significant compared to that of activated carbon. The adsorption equilibrium times for phenanthrene were found to be approximately 72 hours on both bare sorbents, remained at

72 hours for organoclay preloaded with humic acid, but increased to approximately 120 hours for activated carbon preloaded with humic acid. The adsorption equilibrium times for pyrene were also found to be approximately 72 hours on both bare sorbents, but increased to approximately 100 hours on organoclay and 200 hours on activated carbon following preloading with humic acid.

The equilibrium delaying effects for PAHs caused by preloading the sorbents with humic acid can be attributed to the pore blockage effect on activated carbon and the blocking of interlayer spacing of organoclay resulting from the high loading of humic acid. Because humic acid molecules are $\leq$ 25 Å, they are capable of making bigger aggregates of about 400-500 Å (Osterberg *et al*. 1992 in Sharma 2008). These structures can in turn block the porous structure of activated carbon (<4-250 Å given by Henning and Schafer) and the interlayer spacing (35.74 Å) between the silica layers of organoclay, thus making the internal pore structure of activated carbon and the hydrophobic zone of organoclay less available to the target contaminants. The target compounds then diffuse more slowly through a reduced pore area into the available adsorption sites depending on their diffusivity, availability of sites and partition coefficients for humic acid.

5.1.3 Combined Effects of Humic Acid, Fulvic Acid and Natural Organic Material

Natural organic matter present in sediment porewater can be fractioned into humic acids, fulvic acids, proteins and peptides having both hydrophilic and hydrophobic properties, the ratios of which may affect the solubility, transport and bioavailability of hydrophobic organic contaminants (HOCs) such as PCBs and PAHs (Wu *et al.* 2003 in Sharma 2008). The chemical characteristics of these NOM fractions, including acid/base properties, elemental composition and aromaticity, depend on their origin and are different for freshwater, marine or terrestrial environments (Niederer *et al.* 2007 in Sharma 2008). Because NOM including fulvic acid and humic acid is present in the porewater of a sediment system, these substances will compete with HOCs for amendment sorption sites.

Following the selection of the preferred sorbent types, studies were conducted to evaluate the performance of coconut shell activated carbon and CETCO organoclay in the presence of different fractions of NOM. Additionally, the effects of NOM present in the Cottonwood Bay field site on the performance of the preferred amendment mixture (35% activated carbon, 35% organoclay, 30% apatite) in terms of sequestering two select organic contaminants (2,2',5,5'-tetrachlorobiphenyl and phenanthrene) was assessed.

In these studies, different concentrations of Aldrich humic acid (AldHA), Suwannee River humic acid (SRHA), Suwannee River fulvic acid (SRFA) and Suwannee River NOM (SRNOM), as well as porewater extracted from different locations (Hudson River, Passaic River), were used to assess a range of effects that may be encountered under different site conditions with the goal of quantifying the impact of different fractions of NOM from different origins on the performance of activated carbon, organoclay and an amendment mixture in sequestering organic contaminants. Weathered amendment mixture samples obtained from the reactive mats deployed in a non-contaminated area of Cottonwood Bay for six months were also evaluated to determine the effect of longer term exposure to NOM concentrations present at the pilot site on overall

reactive mat performance. The general results of this experiment indicated that organic acids, which are quite concentrated in sediment porewater, have a significant impact on the efficacy of reactive mat components and should be an essential factor in the final design and ultimate performance evaluation of the reactive mat technology.

Complete results of these experiments through Year Two of the project, including relevant plots and tables, were previously presented in the Second Year Annual Progress Report (NAVFAC 2007). In summary, the adsorption capacity of organoclay was found to be consistently higher than that of activated carbon for 2,2',5,5'-tPCB and phenanthrene. The effects of humic acid were more pronounced than the effects of fulvic acid and NOM, the latter of which were both found to have a negligible influence on the adsorption capacity of both sorbents. The preloading effect of extracted Hudson River porewater on adsorption was found to be important and was attributed to the high humic content of the sample. In contrast, Passaic River pore water (low in humics) had little effect on adsorption (Figure 5.1-1).

Batch adsorption experiments were also conducted at five loadings of a contaminant mixture of 2,2',5,5'-tPCB and phenanthrene on a virgin sorbent mixture, the weathered sorbent mixture recovered from the small-scale reactive mats deployed in Cottonwood Bay for six months, and a virgin sorbent mixture placed in Cottonwood Bay sediment porewater. The weathered sorbent mixture that was obtained from the mats represented the realistic scenario of having sorbents deployed in a geotextile mat over a natural sediment bed for a relatively long period of time. Results showed that there was a negligible effect of natural organics present at the Cottonwood Bay site on the adsorption of 2,2',5,5'-tetrachlorobiphenyl and a slight reducing effect on the adsorption of phenanthrene that was also found to be statistically negligible. Figure 5.1-2 shows the adsorption isotherms for 2,2',5,5'-tetrachlorobiphenyl on virgin sorbent mixture and on the sorbent mixture deployed in Cottonwood Bay for six months. Dotted lines in this figure are spline fits to show data point progressions whereas solid and dashed lines show Freundlich Isotherm fits.

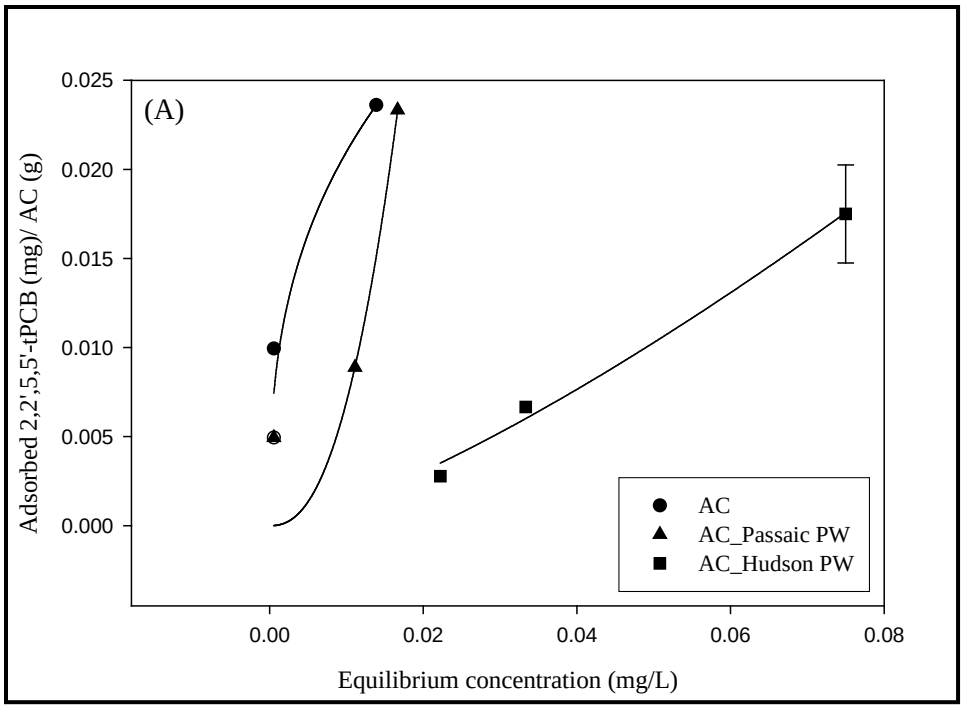

Figure 5.1-1. Adsorption of 2,2',5,5'-tetrachlorobiphenyl on bare activated carbon in the presence of Passaic River and Hudson River porewaters.

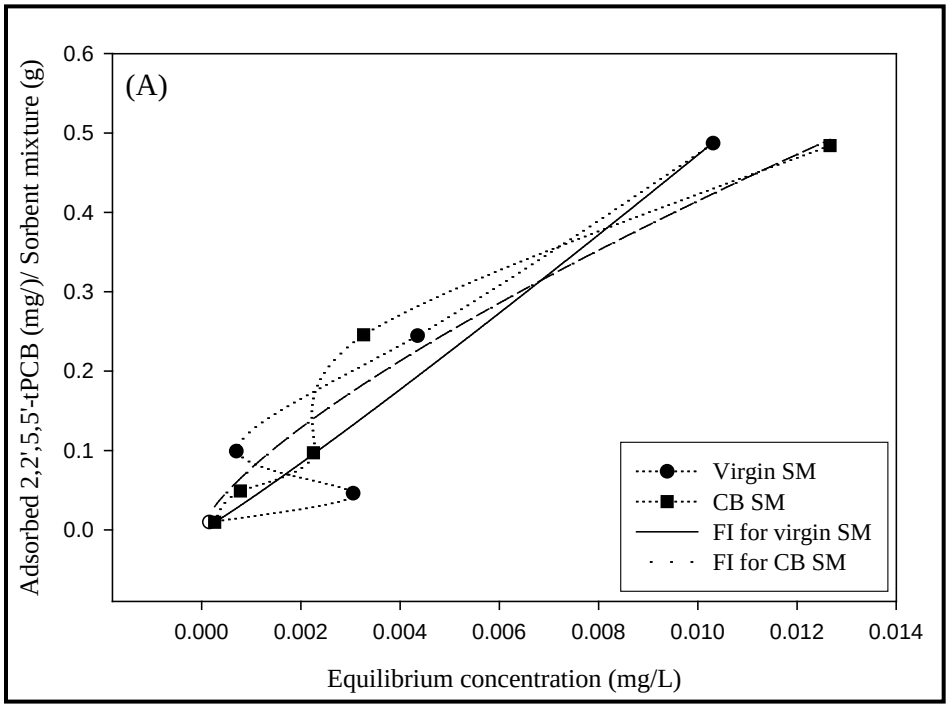

Figure 5.1-2. Adsorption of 2,2',5,5'-tetrachlorobiphenyl on virgin sorbent mixture (virgin SM) and weathered sorbent mixture after six months in Cottonwood Bay (CB SM).

5.2 Task 2: Pilot Site Selection

The purpose of selecting a pilot site for this project was to identify a suitable location for the small-scale field testing of geotextile mats as well as a specific target area for deployment of a prototype mat system. As described in Section 4.2, the pilot site selection process consisted of two phases that involved first narrowing a "long list" of potential Navy sites down to two primary sites. The decision was based on a series of chemical, physical, biological and logistical factors that would provide a suitable environment for geotextile testing and a focused comparison of two candidate sites in terms of history, surficial hydrology, hydrogeologic properties, nature and extent of contamination and past remediation efforts as documented in existing literature. This lead to selection of the primary site, Cottonwood Bay, which was then subjected to phase two of the pilot site selection process which involved conducting geophysical investigations to determine a specific area for prototype mat system deployment based on bottom topography, habitat characteristics and groundwater seepage properties.

5.2.1 Site Selection Overview

Phase One Site Selection. A detailed description of Phase I of the pilot site selection process was provided in the First Year Annual Progress Report for Project Number ER-1493 (NAVFAC 2006). Based on these criteria, Cottonwood Bay in Grand Prairie, Texas (adjacent to the NWIRP and NAS Dallas) and Pearl Harbor in Honolulu, Hawaii (adjacent to the Honolulu Naval Facilities) were identified as the most suitable locations for small-scale geotextile testing and prototype mat deployment.

Phase Two Primary Site Comparisons. The focused literature review for the selected primary sites focused on two reports each for Cottonwood Bay and Pearl Harbor. These documents were *Chemical Quality of Water, Sediment, and Fish in Mountain Creek Lake, Dallas, Texas, 1994-97* (VanMetre *et al*. 2003) provided by the U.S. Geological Survey (USGS), *Texas Natural Resource Conservation Commission Affected Property Assessment Report* (EnSafe 2001) provided by the Navy as part of the requirements of the Texas Risk Reduction Program (TRRP), *Remedial Investigation Report for Pearl Harbor Sediment* (NAVFAC 2006), and *Baseline Ecological Risk Assessment for Pearl Harbor Sediment Remedial Investigation* (NAVFAC 2006). Correspondence and phone conferences with site managers also contributed to the understanding of the conditions and management at each location as well as logistical considerations that would be important for further site assessment.

Detailed results of the focused site comparison between Cottonwood Bay and Pearl Harbor, including several tables and figures, are provided in the First Year Annual Progress Report (NAVFAC 2006). In summary, both sites were found to have sufficiently elevated concentrations of metals and organics to provide a representative test of reactive mat performance, although principal metals of concern at Cottonwood Bay were chromium and lead while principal metals of concern at Pearl Harbor were copper and zinc. At the time of the initial focused comparison, sediments had been more thoroughly and recently characterized at Pearl Harbor. Available data for Cottonwood Bay were all found to be greater than ten years old, thus introducing some uncertainty with regard to current site conditions. More current Cottonwood Bay data was obtained during Year Two to fill existing data gaps which included the document

Computer-model analysis of ground-water flow and simulated effects of contaminant remediation at Naval Weapons Industrial Reserve Plant, Dallas, Texas provided by the USGS (Barker and Braun 2000).

Regarding flow parameters, Cottonwood Bay appeared to have significant groundwater influence while Pearl Harbor is subject to tidal flow and limited groundwater movement. At both sites there is a likelihood of measurable biologically-driven deposition, although Cottonwood Bay was deemed more likely to have a higher accretion rate relative to Pearl Harbor, where turbidity and nutrient loading is expected to be lower. In terms of management planning, both sites have identified needs for remediation and groundwater control measures are currently in place at Cottonwood Bay. Pearl Harbor has been investigated following USEPA guidance for risk assessment and remedial investigations but a Feasibility Study (FS) for remediation alternatives had yet to be completed by the time of this project. Logistically, both Cottonwood Bay and Pearl Harbor were deemed accessible and found to possess the necessary infrastructure to support mobilization and field activities. Security limitations were identified for both sites, however, with water access to the eastern portion of Cottonwood Bay restricted by NAS security and entrance into Pearl Harbor near the Naval Facility berthing areas also restricted.

Final Site Selection. Cottonwood Bay was ultimately deemed more suitable for geotextile testing than Pearl Harbor and thus selected as the final pilot site for this project. Although contaminant conditions at both sites are generally similar, Cottonwood Bay was found to have more thorough mixtures of both metals and organics that would correspond well to overall adsorption goals. Cottonwood Bay was also found to have a significantly greater groundwater flow potential, which made it a more attractive location for evaluating potential groundwater flux through the reactive mats. Although an energetic environment such as the intertidal zones within Pearl Harbor was originally sought in order to provide conditions where a traditional sand cap would be insufficiently stable to provide a permanent form of remediation, the relatively constant conditions and groundwater flow parameter described by USGS for Cottonwood Bay were considered more important in evaluating mat performance than a dynamic setting. Logistical and travel considerations also contributed heavily to the selection of Cottonwood Bay since its location within the contiguous United States would make it more cost effective in terms of transporting equipment and field personnel. Finally, the location of Cottonwood Bay was within the general Mountain Creek Lake area already scheduled for remediation under the TRRP made it an attractive site for further investigation, with results of the proposed geophysical surveys not only applicable to SERDP goals but also to the overall Mountain Creek Lake remedial investigation and FS. Previously established contacts within NAVFAC and EnSafe, Inc. familiar with the Cottonwood Bay site were also able to assist with site access logistics as well as mitigating security concerns with the relevant landowner parties. In general, the criteria initially established for site selection proved effective and therefore applicable to other sites where this technology would be applied.

5.2.2 Selected Site Background Assessment

As discussed above, the majority of information regarding the background conditions at Cottonwood Bay was obtained from a USGS sampling effort (VanMetre *et al*. 2003), a TRRP analysis (EnSafe 2001) and subsequent groundwater modeling (Barker and Braun 2000). Details

about the site that were provided in these documents and compiled during both the Year One and Year Two efforts are described in the following sub-sections.

Site Description and History. Cottonwood Bay is located in northeastern Texas within Dallas County approximately four miles southeast of Grand Prairie between routes I-30 and I-20. The site is adjacent to the Vought Aircraft Industries, Inc. facility (former Naval Weapons Industrial Reserve Plant) and NAS Dallas and was created by fill placement that took place during the original construction of the NAS airstrip. Recreational fishing is popular in the connected Mountain Creek Lake, which is connected to Cottonwood Bay, but consumption of catch is banned due to documented PCB contamination. An overview of the entire Cottonwood Bay site was provided previously in Figure 4.2-1.

***Surficial Hydrology*.** Cottonwood Bay is an artificially constructed stream and groundwater-fed freshwater body that is connected to Mountain Creek Lake by a narrow channel (Figure 4.2-1). The Cottonwood Creek diversion channel feeds directly into the bay and, along with surface runoff, constitutes the main surface water input into the bay (Figure 5.2-1). The east and west lagoons on Vought property to the north of the bay were constructed to contain stormwater runoff but also receive input from groundwater. Cottonwood Bay has relatively consistent water elevations throughout the year (+/- 2 ft) and is not a very dynamic environment given both lack of wind fetch and wave action (i.e., boat wash).

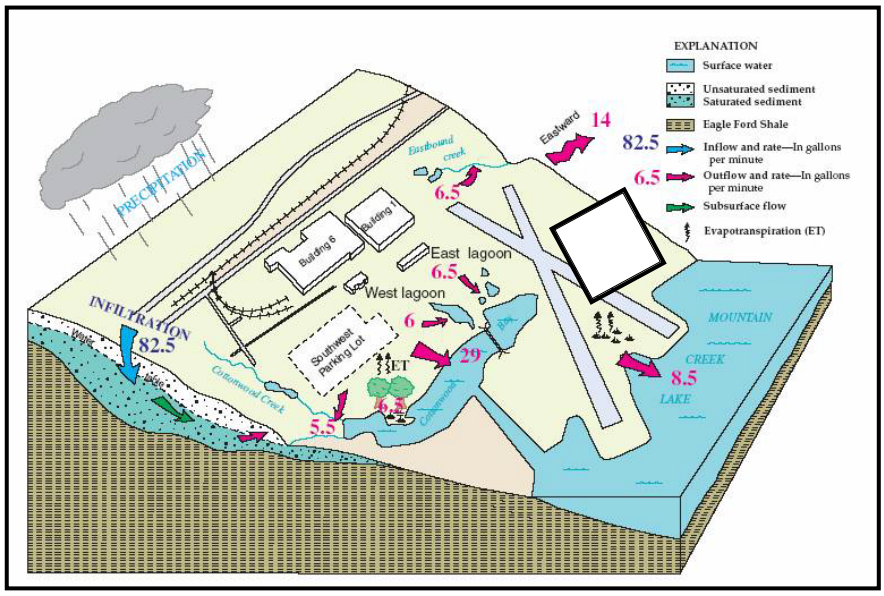

Figure 5.2-1. Conceptual model of the hydrogeologic setting of the Cottonwood Bay site (modified from Barker and Braun 2000).

Hydrogeologic Properties. The source of most groundwater is precipitation which averages about 36 in/yr in Grand Prairie (Owenby and Ezell 1992). Precipitation readily infiltrates the porous higher-altitude areas around the northern limits of the Cottonwood Bay site, while the buildings and impervious surfaces which characterize the lower elevations create runoff instead of infiltration.

As shown in Figure 5.2-1, the water table slopes toward Cottonwood Bay and Mountain Creek Lake. The aquifer is unconfined and composed mostly of silty sand and silty clay, which thins to the south and eventually becomes level with the site's water bodies (EnSafe 1994). Most of the groundwater discharges to Cottonwood Bay and Mountain Creek Lake which maintains the surface water levels of those water bodies. The rest of the ground water either discharges to the east and west retention lagoons, flows out of the site area to the east, or is evapo-transpired back into the atmosphere (Barker and Braun 2000).

Nature and Extent of Contamination. The concentrations of select contaminants of concern (CoCs) in Cottonwood Bay sediments, including three metals (chromium, copper and zinc), PCBs and fluoranthene (representing the highest measured PAH) as determined from previous site investigations are presented in Table 5.2-1. The locations of the historic samples from which these data were generated are shown in Figure 5.2-2. The red markers on this figure indicate previous sampling stations of interest with high concentrations of mixed contaminants that are included in the table below. Two of these stations are in the southwest end of the bay near the terminus of Cottonwood Creek diversion channel, while eight represent stations in the northeastern quadrant in the vicinity of the former NWIRP and current NAS.

Table 5.2-1. Select sediment data available from historic Cottonwood Bay samples showing elevated concentrations of contaminants of interest for the site selection process.

		Historic Cottonwood Bay Sediment Sampling Stations									
Parameter	**Units**	**BG1-01**	**MCL-5**	**OF4-01**	**M2.3**	**M2.4**	**M2.5**	**M2.7**	**Bay 7**	**Bay 11**	**Bay 16**
Metals											
Chromium	mg/Kg	15	83	473	240	255	256	329	349	350	350
Copper	mg/Kg	16	33	71	59	64	61	69	55	53	52
Lead	mg/Kg	25	26	95	95	90	89	96	84	82	61
Nickel	mg/Kg	19	56	34	49	50	51	325	64	NA	46
Zinc	mg/Kg	64	130	502	358	354	364	383	314	NA	280
PAHs											
Anthracene	ug/Kg	62	44	270	226	245	233	143	190	NS	410
Fluoranthene	ug/Kg	960	740	2400	2630	1940	1770	1820	3600	NS	4800
Benzo[a]anthracene	ug/Kg	480	350	1020	1500	1450	1370	996	1220	NS	2100
Other											
PCBs	ug/Kg	NS	6.0	4350*	NS	NS	NS	NS	210	NS	190

* = Sum of 3 Arochlors
NS = Not Sampled
NA = Not Available; Information is forthcoming

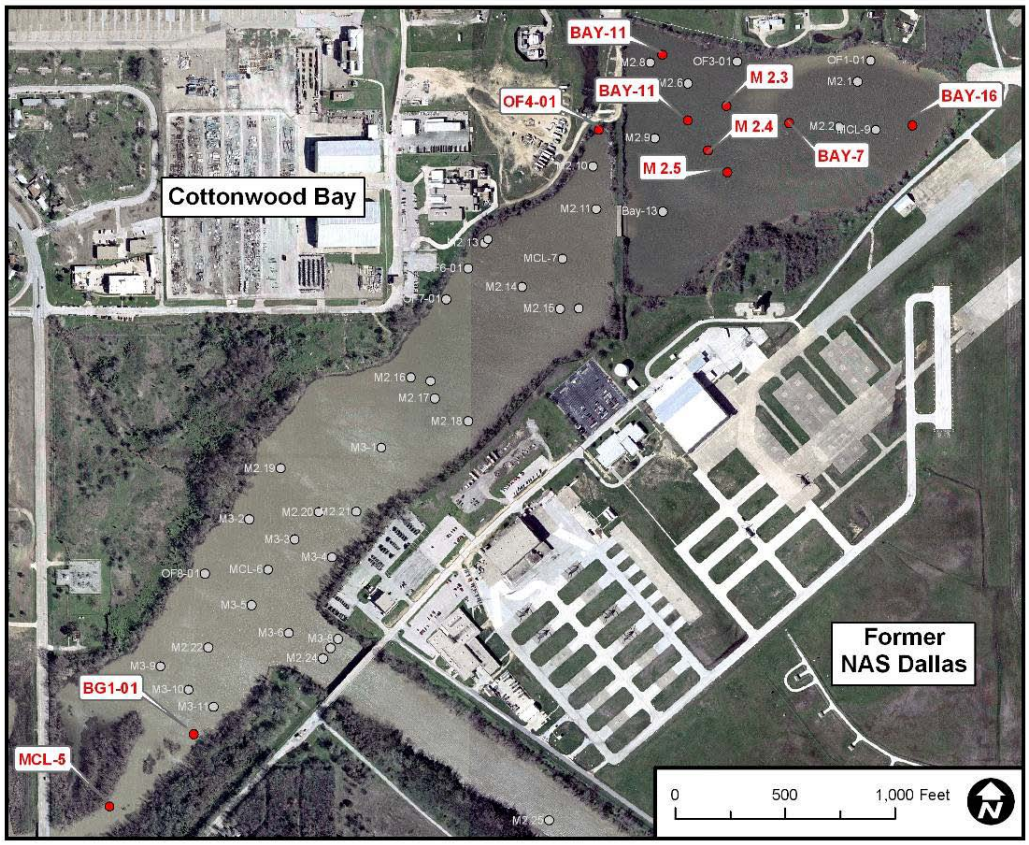

Figure 5.2-2. Historic Cottonwood Bay sampling stations used in the site background assessment (modified from EnSafe 2001).

The highest metals concentrations in the historic Cottonwood Bay sediment samples were found for total chromium and zinc while the greatest organic contaminant loads were found for PAHs. Concentrations of chromium and PCBs were generally higher at Station OF4-01 adjacent to the former NWIRP shoreline while concentrations of PAHs (*e.g.*, fluoranthene) increased with proximity to the NAS. Concentrations of metals and organics were found to be generally lower by a factor of five at the southwestern stations in Cottonwood Bay West where a diversion channel enters the bay as compared to stations in Cottonwood Bay East on the opposite side of the causeway. Groundwater intrusion may also be contributing to lake water and sediment risks because trichloroethene (TCE), dichloroethene (DCE), vinyl chloride (VC), chromium, lead, and other metallic contaminants have been measured in the shallow unconfined aquifer underlying the former NWIRP property (EnSafe 1996).

Remediation Efforts. A series of wells and trenches were installed at the Cottonwood Bay site as early as 1996 with the goal of controlling the flow of groundwater and surface runoff on the NWIRP (now Vought) property (Figure 5.2-3). The specific purpose of these remedial activities was to treat groundwater from the aquifer before it reaches Cottonwood Bay to mitigate VOC contamination. Modeling indicates that the trenches adjacent to Cottonwood Bay East intercept about 827 ft^3/day of groundwater that otherwise would enter the bay. While the trenches intercept groundwater before it can reach Cottonwood Bay, the wells (when actively pumping)

create a depression that reverses the direction of groundwater flow in order to draw contaminated water away from the bay.

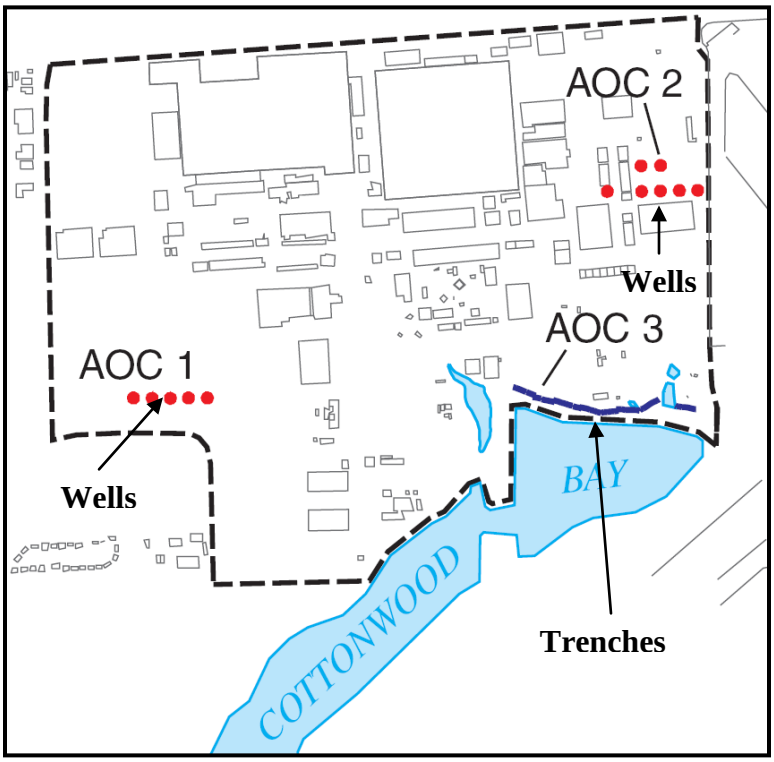

Figure 5.2-3. Locations of remedial wells and trenches at the Cottonwood Bay site (modified from Barker and Braun 2000).

Additional Cottonwood Bay remedial studies were conducted primarily by the USGS and can be characterized as "nature and extent" evaluations that provided data for a Screening Level Risk Assessment (EnSafe 2000). This report was not finalized when the Affected Property Assessment Report was submitted in 2001, but at that time the Texas Natural Resource Conservation Commission (TNRCC) determined that additional studies would be required before additional action could take place at the site.

5.2.3 Geophysical Surveys

The Cottonwood Bay geophysical investigation provided data on water depth, habitat characteristics and lake sediment properties with the goal of selecting a specific location for future prototype mat system deployment. Detailed results of this Phase II evaluation, including all relevant figures, were presented in the Second Year Annual Progress Report (NAVFAC 2007). A summary of the geophysical results is provided in the following sub-sections.

Bathymetry. Bottom topography in the eastern portion of Cottonwood bay ranged from zero along the shorelines to approximately 6.6 ft in the center at the time of the geophysical survey. Depth increases were found to be relatively steep with a majority of the area constituting the

deeper topography. Overall, water depths and gradients were substantially greater in Cottonwood Bay East compared to Cottonwood Bay West. Overall water depths (independent of topography) were found to fluctuate approximately 2 ft based on seasonal rain and drought conditions in northern Texas.

Sub-Bottom Profiling. In the eastern portion of Cottonwood Bay, sub-bottom profiling results showed that sediment thickness ranged from zero along the shorelines to approximately 2.5 ft in the center. Seismic profile cross-sections generated from these data along two select transects in Cottonwood Bay East showed a thin lens of material above the main sediment-water interface. The composition of this lens was unknown at the time, and may represent either a sediment deposit or a layer of leaf detritus. This lens was not confirmed in subsequent sediment vibracores.

Side-Scan Sonar. Side-scan sonar mosaic results for Cottonwood Bay East showed the presence of multiple linear features in the northwest portion of the study area near the Vought shoreline. These features may represent logs or man-made debris that could interfere with potential dredging or mat placement. In addition to these side-scan observations, visual observations indicated the presence of several stumps (approximately six inches in diameter) sticking out of the water and other submerged natural structures (*e.g.*, fallen trees) in both portions of Cottonwood Bay.

Sediment Profile Imaging. Sediment profile images for Cottonwood Bay showed a consistent grain size major mode of >4 phi for all images, which indicates predominantly fine-grained material such as silt or clay according to the Udden-Wentworth size class scale. Mean boundary roughness ranged from 0.00 cm (flat surface) to 2.94 cm, which signifies an uneven surface at some stations. For benthic habitat types, all but one of the 13 stations in Cottonwood Bay East were classified as "Unconsolidated Soft Bottom" (UN). These soft bottom stations were then further classified as either "Silty" (UN.SI) or "Very Soft Mud" (UN.SF). The one station that was not classified as unconsolidated soft bottom (CW-E-12) was considered indeterminate due to low camera penetration caused by the presence of localized debris.

Successional stage could only be determined at three stations in Cottonwood Bay East (CW-E-8, CW-E-9, CW-E-10). Each of these areas was considered a "Stage I" (ST I) infaunal habitat, which in a marine environment often includes the presence of opportunistic, pioneering species with rapid population growth rates that quickly colonize a site following disturbance and generally include smaller species that inhabit the uppermost portion of the substrate, feeding on surface sediments or from the water column (Rhoads and Germano 1982, 1986). Despite being a freshwater site, similar general principals are likely applicable for Cottonwood Bay.

Mean apparent oxygen penetration depth (RPD) depth in Cottonwood Bay East ranged from 1.40 cm to 3.04 cm. These values are generally indicative of moderately well-oxygenated surface sediments. The presence of bubbles was observed in most images, thus signifying gas formation (possibly methane) at depth across the entire study area.

Due to indeterminate data for some of the other parameters, the mean organism-sediment index OSI value, an indicator of macroinvertebrate population health, could only be calculated for

three stations in Cottonwood Bay East (CW-E-8, CW-E-9, CW-E-10). These values ranged from +1.00 to +3.00. In a marine environment, index values in this range would indicate highly degraded or disturbed overall habitat conditions. From the OSI data, the benthic habitat quality (BHQ) index based on a combination of surface and subsurface biogenic features was calculated. Because Cottonwood Bay is a freshwater habitat, the typical interpretation of OSI values based on marine sites are limited since the organic enrichment and disturbance paradigms used to assign benthic successional stage has not been developed. Allowing this uncertainty for consideration of site-specific variation, results in Cottonwood Bay East were similar and ranged from +2.00 to +4.00; these values are typical of pioneering communities in moderately stressed habitats (Iocco *et al*. 2000).

Overall, the SPI photographs collected from Cottonwood Bay revealed a generally consistent soft bottom with degraded habitat conditions. There was some variability between stations in terms of sediment color and amount of gas bubbles present, but this variability was not as substantial as in the adjacent Mountain Creek Lake where a similar SPI survey revealed soft bottom at some stations and shell bottom at other stations within the same cove. The fact that bottom conditions were consistent in Cottonwood Bay put less emphasis on the use of SPI results in determining a specific target area for geotextile testing as compared to other survey parameters.

Sediment Vibracoring. All confirmatory sediment vibracores taken during the original Cottonwood Bay geophysical survey were collected from Cottonwood Bay West due to site access restrictions on the vibracoring vessel. The locations of the Cottonwood Bay West vibracore stations corresponded to previously occupied SPI stations CW-8 and CW-17. Station CW-8 was targeted due to its location in the mouth of the diversion channel, thus making it likely to show historic sedimentation patterns due to potential influx into the bay. Station CW-17 was targeted due to its proximity to the causeway, thus making it more likely to be representative of conditions in Cottonwood Bay East. Core CW-8-C and Core CW-17-C are characterized in Table 5.2-2.

Table 5.2-2. Sediment core characteristics at two stations in Cottonwood Bay West.

Core ID: CW-8-C		**Core ID: CW-17-C**	
Total Length: 38”		Total Length: 36”	
0-16”	Soft reduced silt with clay faction.	0-16”	Soft reduced silt; organic odor.
16-32”	Reduced silty clay.	16-22”	Soft reduced silt with clay faction.
32-34”	Hard yellow clay with pebbles and coarse sand.	22-32”	Reduced silty clay.
34-38”	Hard yellow clay with silt.	32-36”	Hard yellow clay plug.

These characterizations were ultimately used to calibrate and confirm the sub-bottom profiling dataset for Cottonwood Bay. Sediment thickness results from the vibracores were consistent with the soft surface and hard underlying layers identified in the sub-bottom survey. In addition,

the vibracore characterizations were also used to confirm the grain size and habitat conditions identified in the SPI photographs.

Groundwater Seepage Survey. A Cottonwood Bay groundwater seepage survey was conducted by Groundwater Seepage, Inc. in 2007 with results provided in the *Final Data Report, Groundwater Upwelling Survey, Naval Weapons Industrial Reserve Plant, Cottonwood Bay, Dallas, Texas*. For this survey, horizontal mapping of elevated groundwater conductivity and decreased temperature data at the groundwater-surface water interface were used to identify likely areas of groundwater discharge and the potential relationship to increased contaminant loads being transported from upland properties within the groundwater flow. The seepage survey was designed to cover areas of suspected elevated sediment contamination as determined by the historic sampling dataset (Figure 5.2-2). Final Trident Probe stations for the Cottonwood Bay groundwater seepage survey are shown in Figure 5.2-4.

During the summer (2007) when the Cottonwood Bay seepage survey was conducted, groundwater in this region was expected to be cooler than the surface water. Groundwater temperatures in a monitoring well along the shore averaged 23°C during the course of the survey while Cottonwood Bay surface water temperatures as determined with the Trident Probe ranged from 27.8-29.8°C with an average 28.5°C across stations. Subsurface temperatures as determined by the Trident Probe ranged from 24.8-28.2°C and averaged 26.9°C across stations. Accordingly, areas with subsurface water temperatures less than the surface water minimum (27.8°C) were considered zones of potential groundwater upwelling.

Surface water conductivity as determined with the Trident Probe ranged from 0-0.5 mS/cm and averaged 0.39 mS/cm across stations. Subsurface water conductivity as determined with the Trident Probe ranged from 0-3.1 mS/cm and averaged 1.09 mS/cm across stations. All areas with subsurface conductivity measurements greater than the surface water maximum were considered zones of potential groundwater upwelling. Complete Trident Probe temperature and conductivity statistics for Cottonwood Bay are summarized in Table 5.2-3.

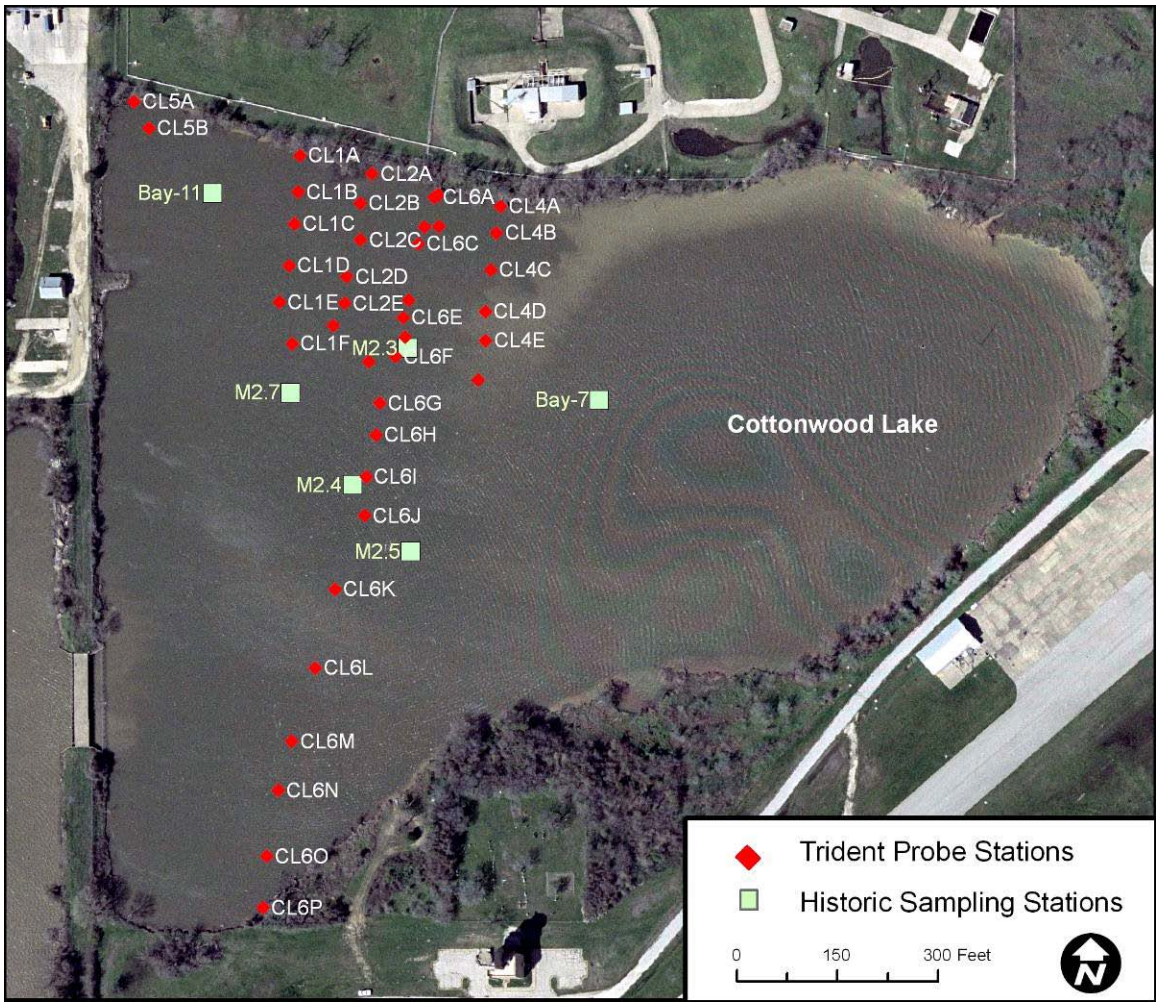

Figure 5.2-4. Trident Probe stations for the Cottonwood Bay groundwater seepage survey.

Table 5.2-3. Trident Probe subsurface temperature and conductivity results for Cottonwood Bay.

	Subsurface Temperature (°C)	Subsurface Conductivity (mS/cm)	Surface Temperature (°C)	Subsurface Conductivity (mS/cm)
Minimum	24.82	0.6	27.81	0.38
Maximum	28.23	2.1	29.84	0.5
Average	26.88	1.1	28.49	0.39
St. Dev.	1.15	0.39	0.51	0.02

Spatial results from the relative subsurface temperature and conductivity mapping process were used to define three zones of increasing groundwater discharge potential as shown in Figure 5.2-5. In general, cooler subsurface temperatures were observed in association with higher subsurface conductivity for several of the outer transect stations (E,F,G,H; Figure 5.2-4). The majority of these areas were found to be located approximately 200 feet from the northern shoreline, but similar conditions were also observed in one area near the southern shoreline. The zone with the highest potential for groundwater seepage (blue) begins approximately 200 feet

offshore. Lithology of an upland monitoring well coupled with observed resistance to Trident Probe penetration at some of the inshore stations seemed to indicate the presence of a clay layer deflecting terrestrial groundwater flow further offshore.

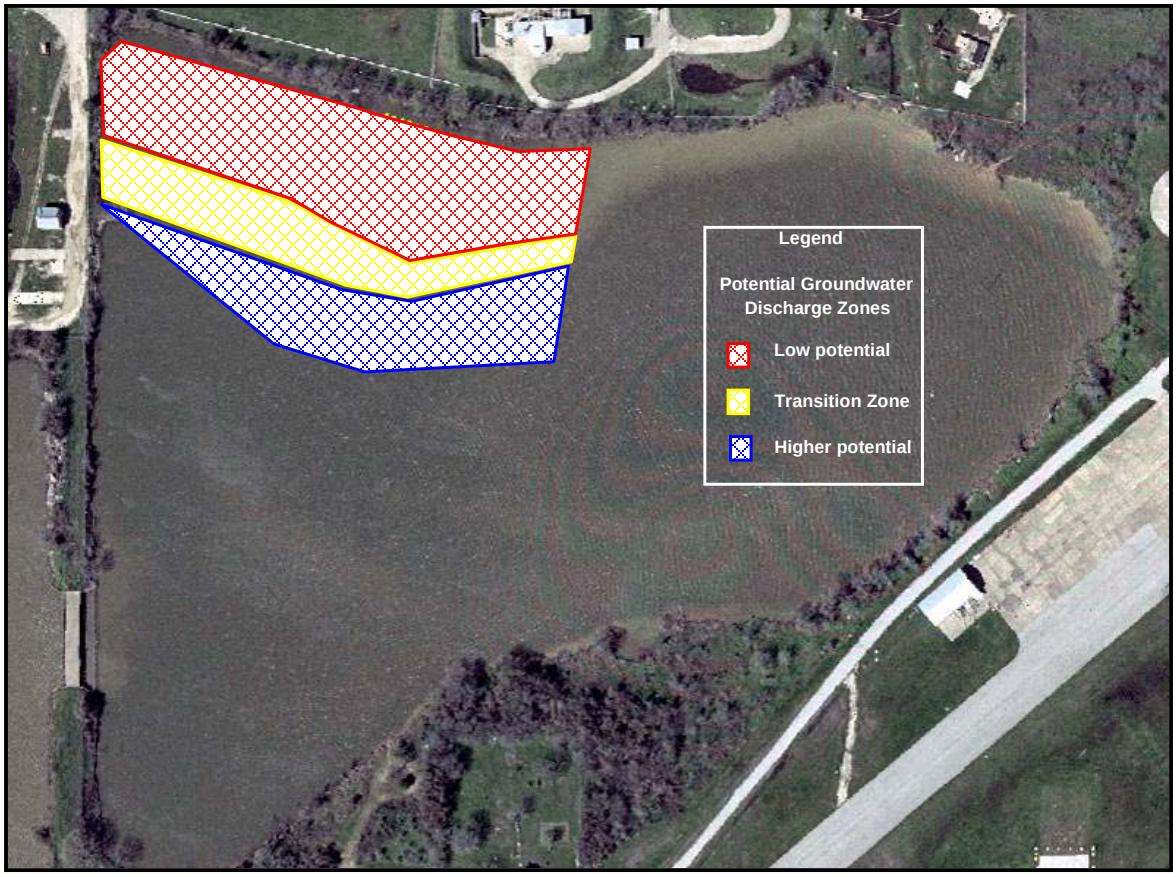

Figure 5.2-5. Potential groundwater discharge zones for Cottonwood Bay.

5.2.4 Target Area Establishment

Based on the overall results of the Cottonwood Bay geophysical investigation completed in summer 2007, the eastern portion of the bay was selected as the general area of focus for further prototype geotextile testing due to greater water depths, increased sediment layer thickness, consistent bottom characteristics and the presence of confirmed groundwater plumes that would allow for accurate assessment of flux through the various test mat arrangements. These parameters were then considered both individually and in combination to select a specific target area within Cottonwood Bay East to serve as the deployment for Task 4. The side-scan sonar survey did not generally identify any major obstacles in Cottonwood Bay East such as debris or hard bottom, save for some linear features of note nearby (possibly submerged logs) which should be avoided. The SPI photographs showed a consistently unconsolidated soft bottom environment with generally degraded habitat conditions, and therefore did not provide any site discriminators. Therefore, groundwater seepage results and sediment chemistry data from previous sampling events were the key factors for selecting a target area compatible with project goals.

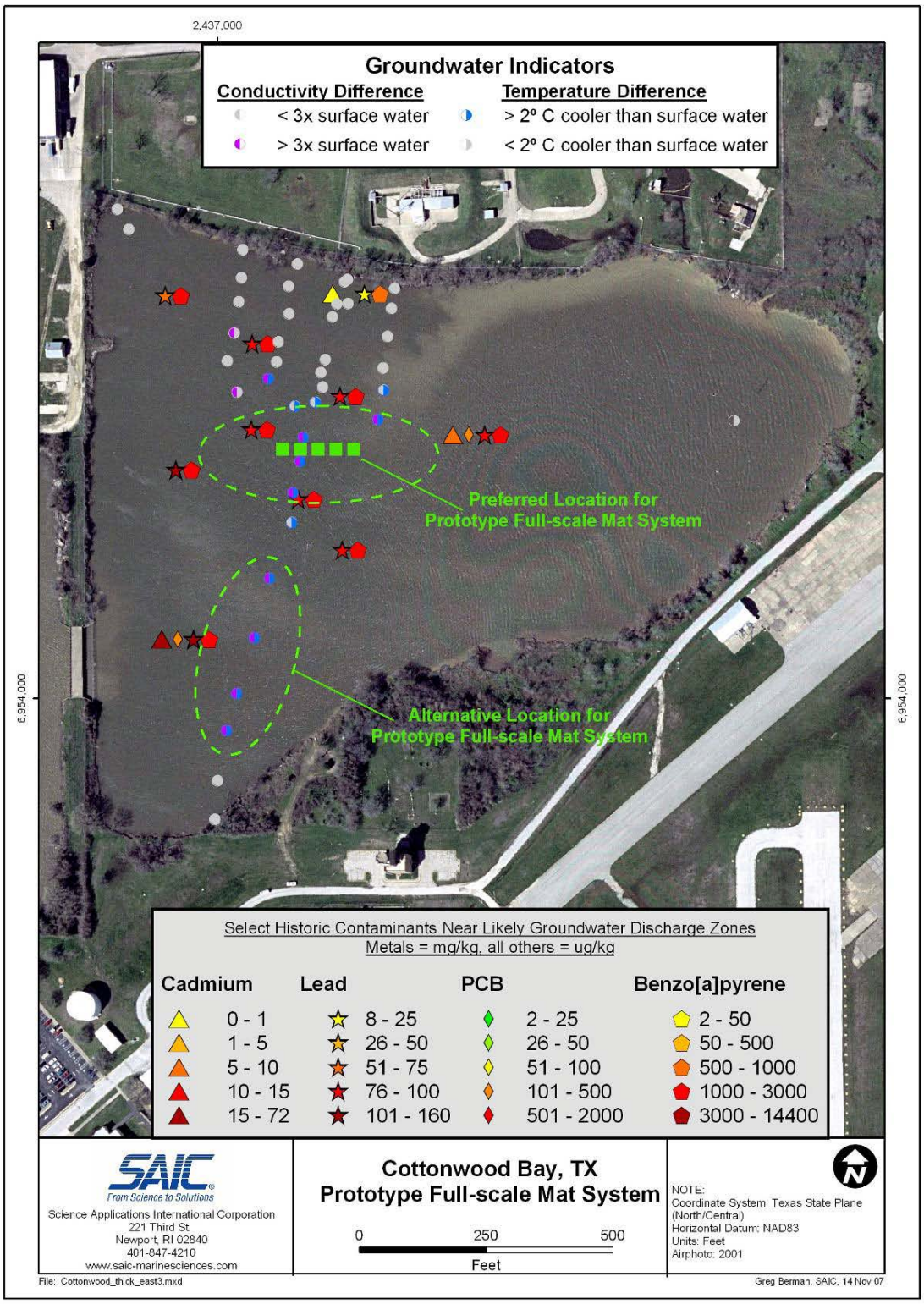

Figure 5.2-6. Preferred target areas for prototype mat system deployment based on the results of the Cottonwood Bay geophysical surveys.

The preferred target area determined from the geophysical investigation is located in the western portion of Cottonwood Bay East approximately 200 feet south of the Vought shoreline (Figure 5.2-6) and corresponds to a region of high potential groundwater discharge (Figure 5.2-5). Historical chemistry results for this area indicated consistently elevated concentrations of lead (>75 mg/kg) and benzo[a]pyrene (>1000 µg/kg) as well as indications of relatively high and consistent groundwater seepage based on temperature and conductivity data. Sub-bottom profiling and SPI results did not show any major obstructions that could impede groundwater flow or contaminant transport in this area. Challenges inherent in use of this location included water depths of approximately six feet at the time of the bathymetry survey, which would necessitate use of divers for mat system deployment and monitoring as opposed to wading. The location of this target area was also in the middle of the bay and therefore posed additional logistical challenges related to deploying the sand cap from the NAS shoreline staging area. On balance, the identified mat placement target was selected for meeting technical requirements despite the logistical challenges presented.

5.3 Task 3: Geotextile Testing

The purpose of the geotextile testing task for this project was to field test different types of geotextile material at the selected pilot site to assess (a) whether sediment clogging, and biofouling and biofilm formation would adversely affect the ability of the fabric to allow water to pass through the final mat design, (b) whether environmental weathering compromises the ability of the mat to retain the amendment material, and (c) whether environmental weathering compromises the reactivity of the sequestration agents. This task also included laboratory gradient ratio testing and finite element analysis to assess stability, clogging potential and prospective sediment deformation for clean, non-fouled mats before the weathered test mats are retrieved. A summary of the accomplishments for each component of this task are provided in the following sections.

5.3.1 Field Evaluation

Fourteen test mats of various compositions were deployed for field testing in Cottonwood Bay East in June 2007 as described in Section 4.3. The first group of mats were collected in December 2007 and shipped to UNH for performance testing with a geotechnical test column system via the ASTMD 5101 method. The mats were shipped wet in sealed tubes to maintain the surface conditions as well as possible. The second group of mats were retrieved in December 2008 and June 2009, but based on column testing results from the first group of mats the second group has not been tested and will be held indefinitely pending further instruction.

5.3.2 Gradient Ratio Testing

Preliminary laboratory gradient ratio testing conducted during Year One showed that trapped bubbles are a significant impediment to groundwater flux through a fine grained matrix. Purging the systems with carbon dioxide gas is the standard procedure for eliminating bubbles as the CO_2 forces the air from the system and then dissolves into solution. However, the fine-grained nature of the sediment made it impossible to pass CO_2 through the column, necessitating the attempt of different approaches. The most successful approach involved soaking the geotextiles under a

light vacuum to minimize air trapped in the fabric. In addition, the sediment was slurried for placement in the column, and a light vacuum was used to remove air bubbles prior to placement.

Gradient ratio testing was conducted on three stock CETCO geotextile fabrics (GT-1, GT-2 and GT-3) and a fourth geotextile (GT-4) chosen to represent an extreme case for clogging (thick fabric and small opening size). Two clean mats (one with organoclay, one with activated carbon) and three weathered mats were also tested. All tests followed the methods described in Section 4.3.2.

Single Geotextiles. Table 5.3-1 presents the physical properties of the four single layer geotextile fabrics used for gradient ratio testing. Gradient ratio tests were carried out on these geotextiles using three hydraulic gradients, i = 1, 4 and 8. The gradient ratio (GR) was measured over time for each geotextile and the results are shown in Figures 5.3-1 to 5.3-4, respectively. Each of these figures includes the results for the three hydraulic gradients; the first two curves are replicates of the same test and the last curve corresponds to a test starting at i = 0.5 for one day, followed by the i = 1, 4 and 8 tests. The objective of this later test was to study the effect of very low hydraulic gradients on the clogging potential of geotextiles.

Table 5.3-1. List of non-woven geotextiles used for reactive core gradient ratio testing applications.

Geotextile ID	Mass per unit area [g/m^2] (oz/yd^2)	Apparent Opening Size	Polymer Type
GT-1	170 (5)	170	Polyester – White
GT-2	203 (6)	70	Polypropylene – White
GT-3	271 (8)	80	Polypropylene – Black
GT-4	265 (7.8)*	170	Polypropylene – Grey

The GR was relatively stable for any hydraulic gradient after only one day, which falls into the recommendation of the ASTM standard for "some recognizable equilibrium or stabilization of the system." Although in some cases (Figure 5.3-1 and Figure 5.3-2) the GR was not fully stable after 24 hours at a constant hydraulic gradient, it is clear the system was not prone to clogging because the GR was less than 3 as recommended by the USACE. In general, all gradient ratio tests showed that no clogging potential of the four geotextiles would be expected in the field when used with similar fine-grained sediment.

The gradient ratio tests carried out on the finer geotextiles AOS 170 (Figure 5.3-1 and Figure 5.3-4, for GT-1 and GT-4, respectively) reached GR-values in the range of 1.2 to 2.2. The lower range of GR values were measured with the less dense geotextiles, which can be interpreted to be of lower tortuosity (degree of pathway meandering). In addition, piping conditions were also measured on lighter geotextiles. Under piping conditions some fine sediment particles move towards the geotextile, leaving small voids that eventually will interconnect to each other, forming small preferential flow paths for the water to pass through. This behavior can improve the performance of the reactive mat because it accelerates the flow of contaminated water from the sediment to the reactive material. Moreover, the transport of fine sediment particles is controlled so a stable filter system can develop.

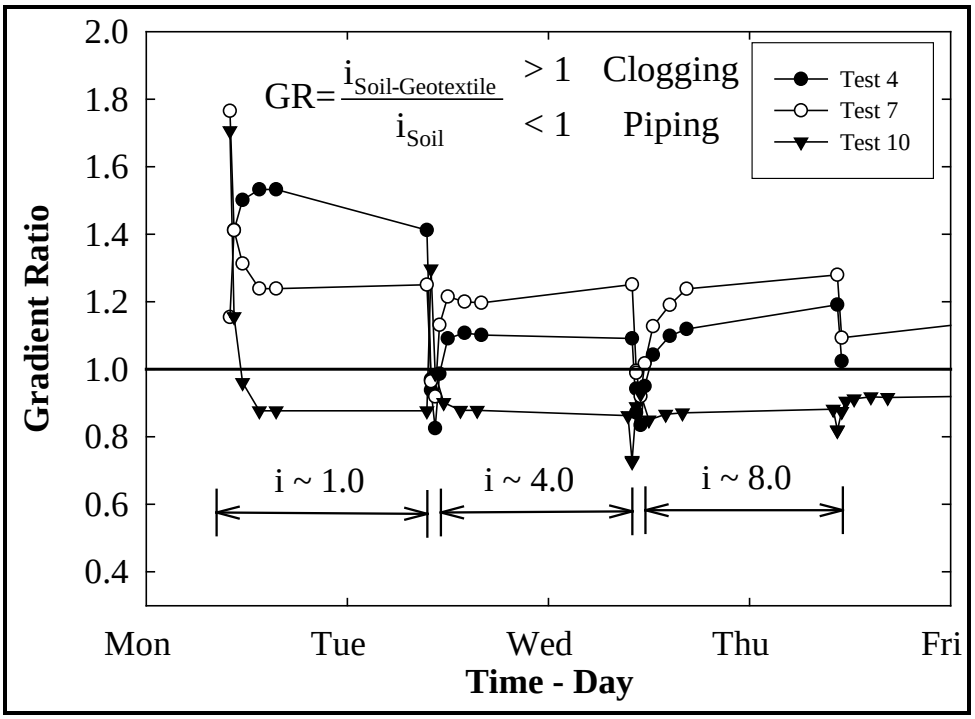

Figure 5.3-1. Gradient ratio test results for geotextile GT-1 (AOS 170).

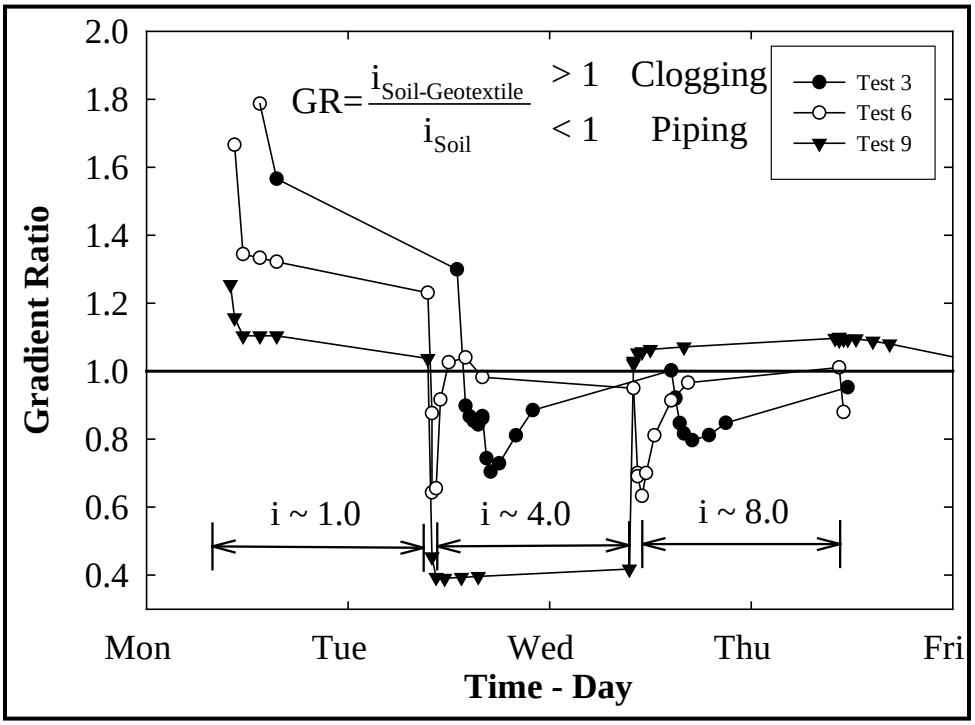

Figure 5.3-2. Gradient ratio test results for geotextile GT-2 (AOS 70).

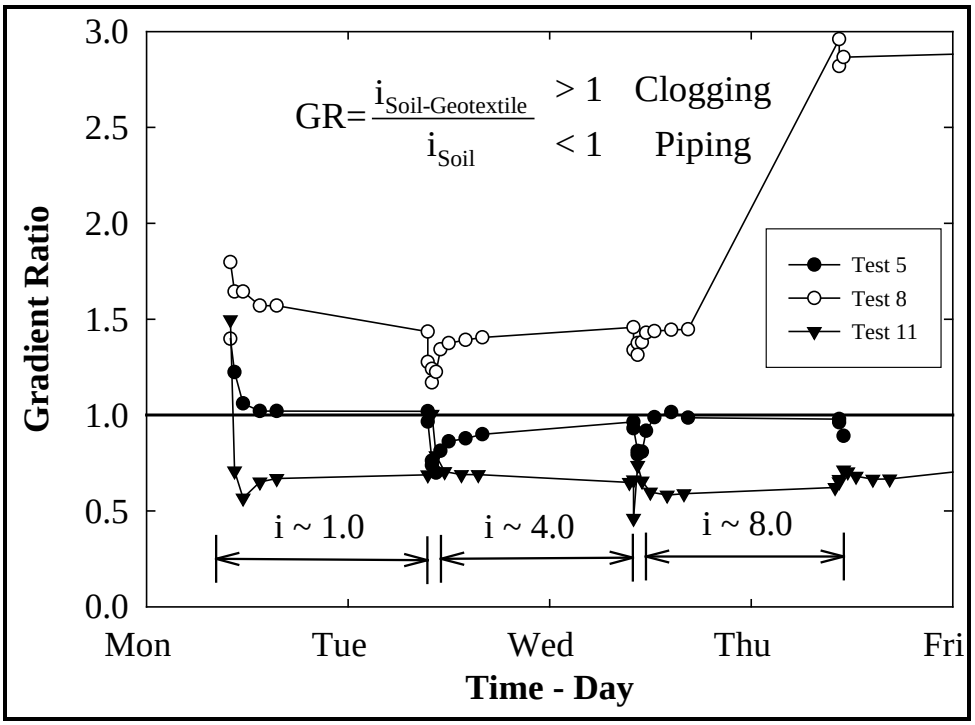

Figure 5.3-3. Gradient ratio test results for geotextile GT-3 (AOS 80).

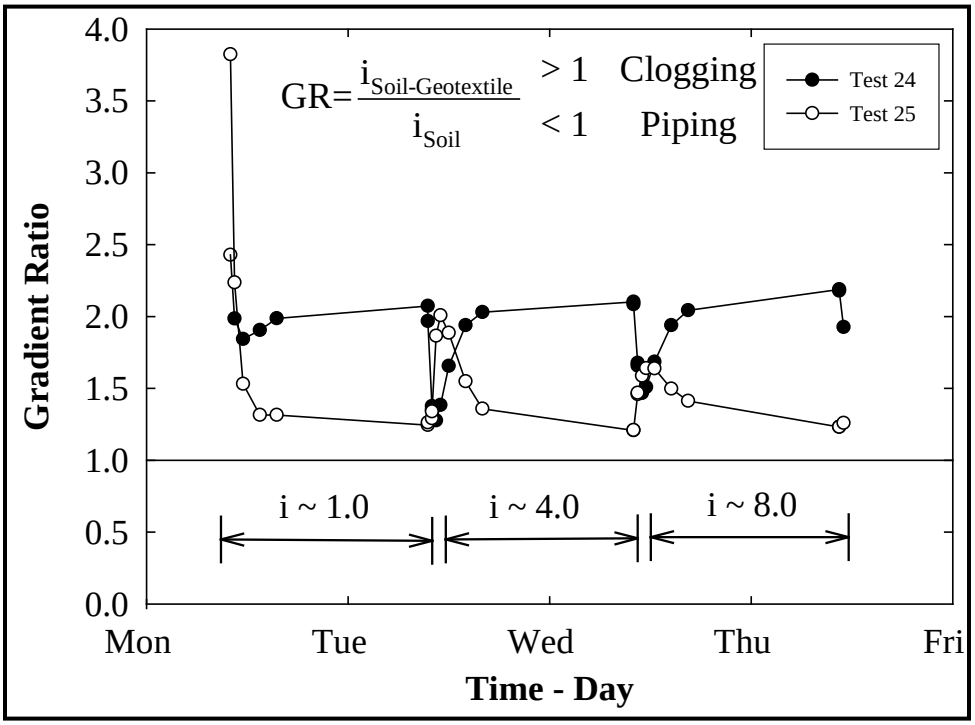

Figure 5.3-4. Gradient ratio test results for geotextile GT-4 (AOS 170).

The results on geotextiles with coarse AOS (70-80) (Figure 5.3-2 and Figure 5.3-3, for GT-2 and GT-3, respectively) showed smaller GR values than the finer geotextiles. In general, the final GR-values for coarse geotextiles ranged from 0.6 to 1.1, with the majority of values at the lower end of the range. These values indicate the geotextiles performed under piping conditions, with a GR value close to one or slightly less as recommended by the ASTM standard. Reactive core mats are typically constructed by CETCO using the geotextile GT-2 (AOS 70) as listed in Table 5.3-1.

Geotextile Mats. The clogging potentials of two clean reactive core mats, one containing organoclay as the reactive material and the other containing activated carbon, were also measured using the gradient ratio test. This process provided verification of the influence of swelling of the clay on the clogging potential of the reactive core mat.

Each mat has one non-woven and one woven side. The mats are typically deployed over the contaminated sediment with the woven geotextile facing the sediment; therefore, the reactive mats were placed in the test chamber with the woven geotextile facing the sediment to represent the most likely field conditions. Figure 5.3-5 shows the results of the GR tests on the clean reactive core mats featuring the GT-2 (AOS 70) geotextile.

The results showed no clogging potential for the reactive core mats under the test conditions. In addition, the overall tendency of the GR-value for the double geotextile mat arrangement was similar to the behavior exhibited by the single geotextiles discussed above. This result indicates that the presence of the second geotextile in the mat does not significantly affect the filtration behavior of the system. Finally, the GR-value stabilized at slightly less than unity as recommended by the USACE for slight piping conditions.

The first group of small-scale reactive test mats listed on Table 4.3-1 was deployed in Cottonwood Bay for a period of six months. Only the mats deployed with the woven geotextile in contact with the sediment were evaluated using the gradient ratio test (RCM-1, RCM-3 and RCM-5), because installation procedures for commercial applications prevent deployment with the non-woven geotextile facing the sediment. The results of the gradient ratio tests with duplicates for the reactive core mat RCM-1, RCM-3 and RCM-5 are shown in Figure 5.3-6 to 5.3-8, respectively.

These results showed no clogging potential on any of the weathered reactive core mats under the tests conditions. The mat with the finer geotextile (RCM-1, AOS 170) showed strong piping conditions (GR-value = 0.5), but eventually stabilized at a GR-value close to unity. The mats with coarser geotextiles (RCM-3, AOS 70 and RCM-5, AOS 80) showed stable gradient ratio values close to unity, ranging from 0.9 to 1.2, which is in agreement with the recommendations of the ASTM standard and the USACE.

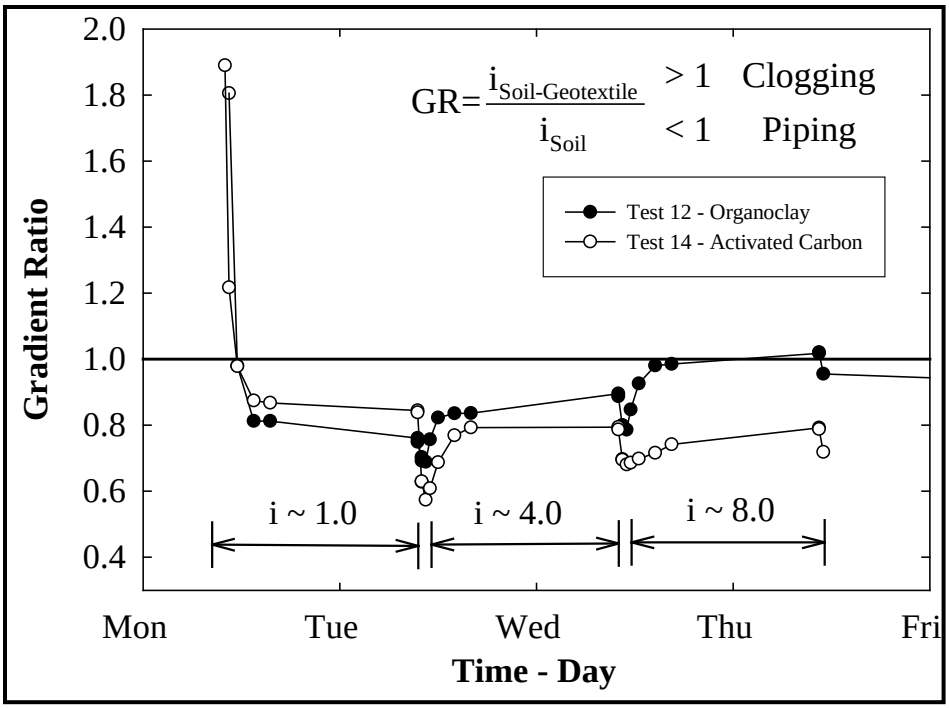

Figure 5.3-5. Gradient ratio test results for clean mats featuring the GT-2 (AOS 70) geotextile and containing organoclay and activated carbon as the reactive material.

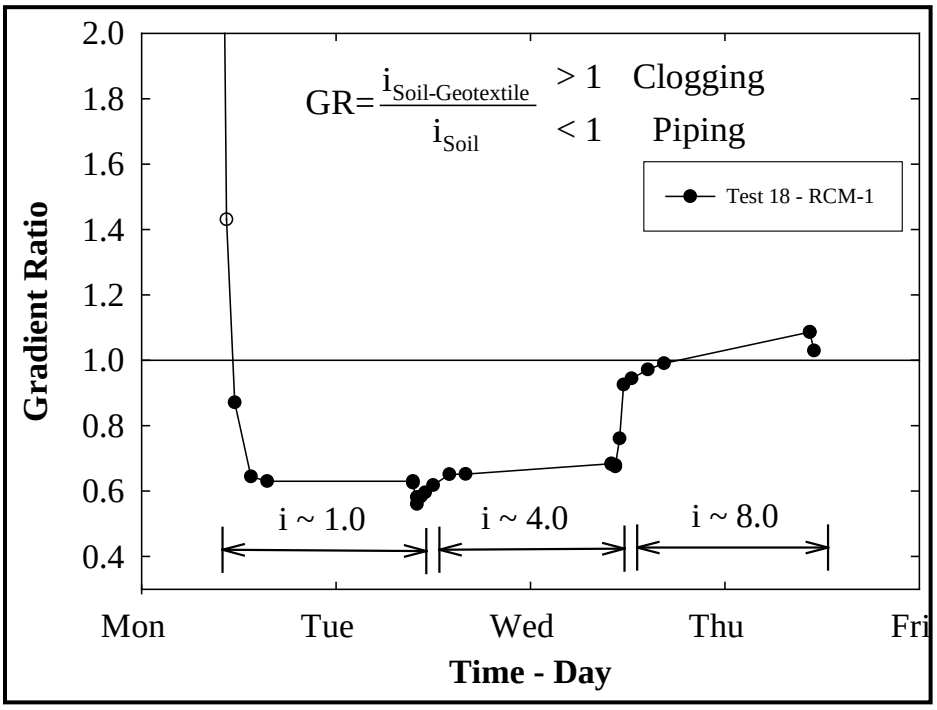

Figure 5.3-6. Gradient ratio test results for weathered geotextile mat RCM-1 after six months of soak time in Cottonwood Bay.

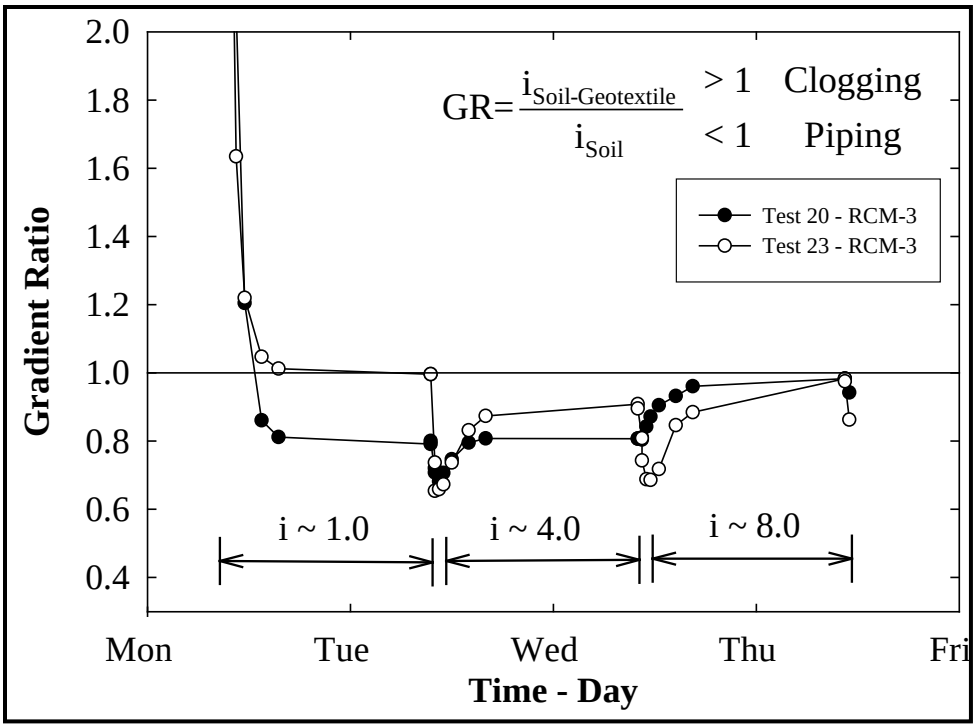

Figure 5.3-7. Gradient ratio test results for weathered geotextile mat RCM-3 after six months of soak time in Cottonwood Bay.

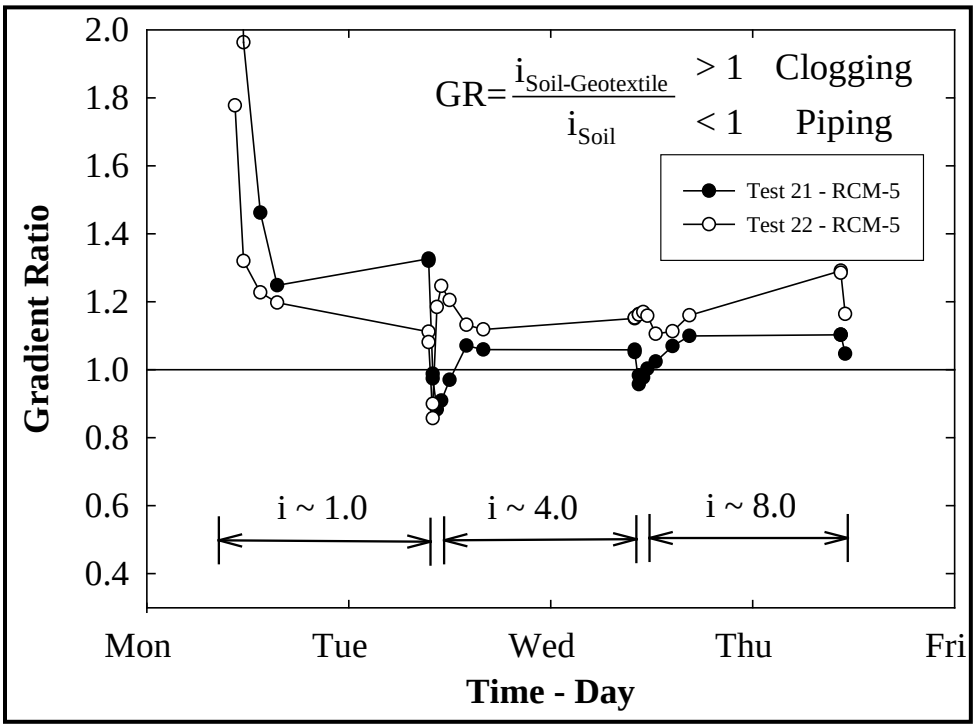

Figure 5.3-8. Gradient ratio test results for weathered geotextile mat RCM-5 after six months of soak time in Cottonwood Bay.

Long-Term Clogging Behavior of Geotextiles. Additional long-term gradient ratio tests were also carried out to evaluate the long-term performance of sediment-geotextile systems under expected field conditions. This type of extended gradient ratio test is initiated at a hydraulic gradient of $i = 1$ that is gradually increased to cover the hydraulic gradients expected in field applications. General site characteristics and seepage measurements from a previous pilot reactive capping project conducted in the Anacostia River (Melton *et al*. 2005) indicated maximum hydraulic gradients in the range of $i = 4$ to 5 for the type of sediment encountered in Cottonwood Bay. In addition, a hydraulic gradient of $i = 5$ represents a conservative condition for the modeling of most geotextile filter applications (Fischer *et al*. 1999). Two long term gradient ratio tests were conducted at $i = 4$ to 6 for nearly 30 days on geotextiles GT-2 and GT-3, with AOS 70 and 80, respectively. The results are shown in Figure 5.3-9.

The results of the long-term test on the geotextile GT-3 show a strong disturbance in the system after 25 days ($i = 6$), which results in a sudden jump of the GR-value from 1.01 to 1.18 followed by a gradual increase to 1.6. The GR-value step increment followed by a gradual increase was caused by the disturbance of the soil near the manometer ports, which promoted seepage along of the wall of the permeameter (Figure 5.3-10).

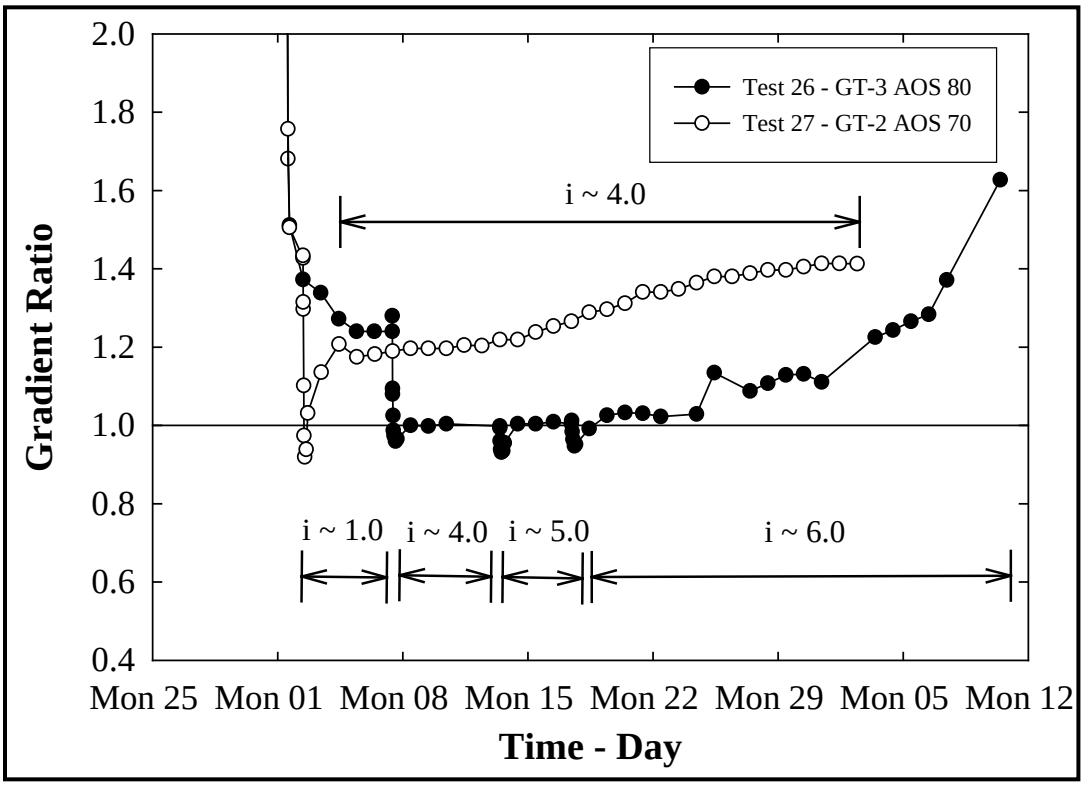

Figure 5.3-9. Long-term gradient ratio test results for geotextiles GT-2 and GT-3.

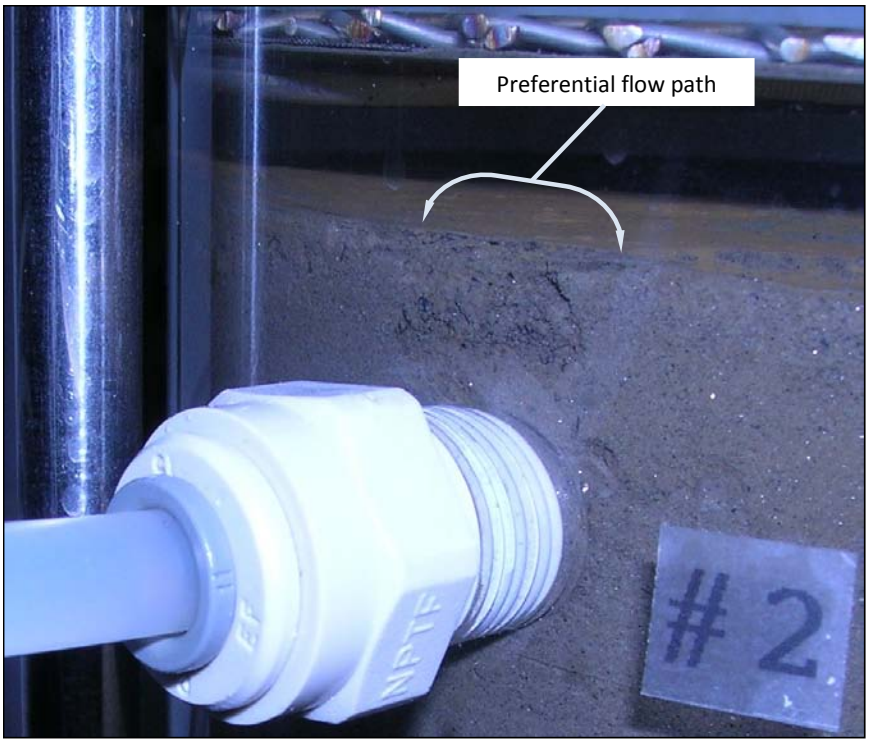

Figure 5.3-10. Evidence of wall seepage near the manometer port during the long-term gradient ratio test for single geotextile GT-3.

The long term GR test on the geotextile GT-2 (AOS 70) showed a GR-value of 1.2 after 24 hours at $i = 4.0$. This test was carried out for 30 days and the GR-value slowly leveled at 1.4, thus indicating that geotextile GT-2 is not prone to clogging according to the USACE recommendations (GR-value < 3.0). In addition, the difference in the results from running the test for 30 days versus only 1 day does not appear to be significant.

Numerical Modeling. The gradient ratio tests carried out on single geotextiles as well as on both clean and weathered reactive core mats did not show evidence of significant clogging that would adversely affect the filtration behavior of the system. However, given the uncertainty of the reactive mat installation process and the actual compatibility between the sediment and the reactive core mats at a given site, it was necessary to develop a numerical model to simulate the eventual clogging of the mat.

Gradient ratio testing results indicated that a significant hydraulic head would be required to force sediment particles into any of the test geotextiles to the extent that they would become clogged and thus impermeable to groundwater flow. Because such drastic hydraulic conditions are not expected to occur in the field, the use of geotextiles as planned to contain reactive material should be appropriate for achieving project goals. Overall results from the finite element modeling process (to be discussed below) indicated that soft underlying sediment will undergo some compression directly beneath a reactive mat following deployment, but this compression will not extend greatly beyond the mat edges. Porewater displacement caused by this consolidation will be confined mainly to the sediment directly below the mat. When using a fully permeable geotextile as the starting point for the models, results indicated that a

permeability decrease of several orders of magnitude would be required to greatly impact groundwater flow around the reactive mat. This level of clogging is not expected to occur under field conditions based on the results of the gradient ratio testing. Biofouling data from weathered test mats can ultimately be used to refine the finite element models with actual permeability values.

Given the fact that the sediment particles are contaminated and that it takes some time for the filter structure to develop at the interface between the sediment and the geotextile, it is important to control and verify that the amount of piped sediment does not compromise the retention efficiency of the system. As previously discussed, the gradient ratio test requires the flow of water through the sediment-geotextile system for several days. Also, the gradient ratio test column was modified to run water from top to bottom of the permeameter, while the geocomposite was placed beneath the sediment. Laboratory observations indicated that the water flow transported a measurable amount of fine particles of sediment through the geocomposite within the first day of the test but by the second day of the test only water passed through. Figure 5.3-11 shows an example of the sediment collected on the bottom plate of the permeameter at the end of a typical gradient ratio test.

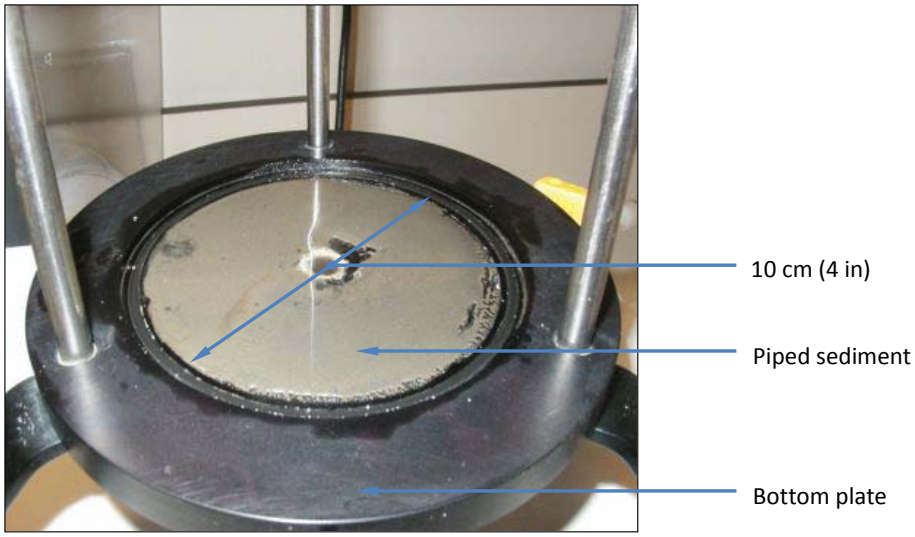

Figure 5.3-11. Example of sediment passing through the geotextile during a typical gradient ratio test.

A stable geotextile/soil system limits the amount of fine soil particles able to pass through the geotextile. The recommended limit for a stable system is 2500 g/m^2 (Lafleur *et al*. 1989), which for the area of a gradient ratio test permeameter amounts to 20 g. In order to determine whether the different geocomposites for this project met such goals, all sediment passing through the geotextile or reactive core mats during the gradient ratio tests was collected, weighed and analyzed in terms of the physical properties of the geocomposite. Figure 5.3-12 shows the weight of the piped sediment versus the mass per area and AOS of each geotextile for gradient ratio tests starting at a hydraulic gradient of $i = 5$. These results indicate that the geocomposite-

sediment filter system is stable in terms of its retention capabilities, and that all geocomposites tested for this project allow less than 2500 g/m^2 to move through the geotextiles.

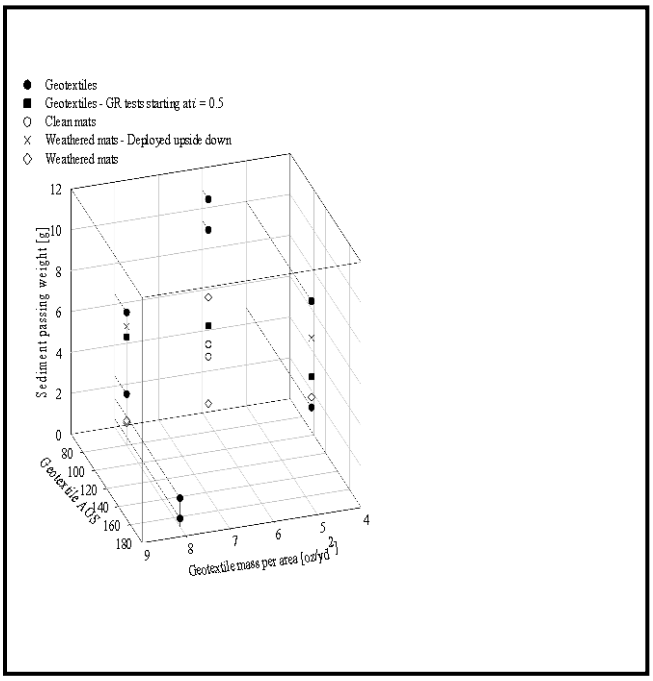

Figure 5.3-12. Sediment mass passing through different geotextiles and reactive core mats during gradient ratio tests starting at hydraulic gradient of *i* = 5.

These results also show that the use of a finer AOS (180) or a heavier geotextile (8 oz/yd^2), or a combination of both, drastically reduces the amount of sediment that is able to pass through the geocomposite. Furthermore, the model proves that reactive mats allow less material to pass through than single geotextiles, mainly because the flow path in reactive core mats is longer and expectedly more tortuous than in single geotextiles.

Conclusion. The main questions about mat design to be addressed by the gradient ratio testing and numerical modeling were how to balance the choice of the geotextile fabric such that the clogging potential was minimized while also preventing the loss of reactive amendment materials and sediment transport into the mat. Results of the numerical modeling influenced the prototype mat design by showing that clogging would have to be severe, with the permeability reduced to two orders of magnitude less than the sediment, before there would be significant adverse impacts on mat performance, thus providing a lower limit for success. The gradient ratio testing was then specifically designed to determine how the geotextile/sediment system and reactive mat/sediment system would actually behave under controlled conditions. Results showed that the coarser geotextiles (AOS 70 and 80) did not clog and did not lose amendment while also experiencing relatively little sediment transport into the cap. Based on these results, the AOS 80 geotextile was chosen for the cap. Subsequent testing on weathered tests mats confirmed that this geotextile size was resistant to clogging and would not reach the lower limit predicted by the model. The variability of the consolidation (*i.e.*, bathymetry) and groundwater

flow (*i.e.*, Trident Probe) field data made it difficult to draw conclusions about how the laboratory data and modeling compare to the field.

5.3.3 Consolidation Testing

In order to model the sediment deformation to be caused by the weight of an overlying geotextile mat system as accurately as possible, a series of consolidation tests were carried out on reference sediment from the Cottonwood Bay pilot site. The consolidation curves for this sediment were obtained from one dimensional and seepage consolidation tests. However, it is important to mention that only one seepage consolidation step was possible on the Cottonwood Bay sediment due to its low permeability, which promoted water flow alongside the permeameter wall instead of through the sediment sample after 30 days of test time. Though only one step was carried out, the results still followed the observed trends for one dimensional tests. Inspection of the results showed that the pressure caused by the porous stone, loading plate and bearing ball (2.457 kPa) induces 33% of strain on the sample.

The results of the consolidation tests performed on the Cottonwood Bay sediments are presented in the series of figures below. Figures 5.3-13 and 5.3-14 presents these results in terms of strain and void ratio as a function of effective stress, respectively.

Figure 5.3-15 shows the variation of the coefficient of consolidation with effective stress for this sediment, and Figure 5.3-16 presents the variation of the coefficient of volumetric compressibility. The inflexion point in the compressibility of the sediment occurs at 6-7 kN/m^2. Moreover, the coefficient of volumetric compressibility indicates stiffening of the sample.

The variation of the coefficient of consolidation with the void ratio is shown in Figure 5.3-17 and the variation of the coefficient of volumetric compressibility is shown in Figure 5.3-18. The variation of the permeability with effective stress is presented in Figure 5.3-19 and in terms of void ratio in Figure 5.3-20.

Overall, consolidation testing results for Cottonwood Bay sediment show a critical void ratio of 5.8 where the rate of permeability change has an inflexion point. Furthermore, this critical void ratio corresponds to an effective stress of 6-7 kN/m^2 and matches the results shown on Figure 5.3-15. In geotechnical engineering practice, the compression index (*Cc*) and recompression index (*Cr*) is commonly used to estimate the settlement and the rate of consolidation of soils. The corresponding parameters of both sediments are calculated from the *Log(σ') vs. e* curves obtained from the consolidation tests.

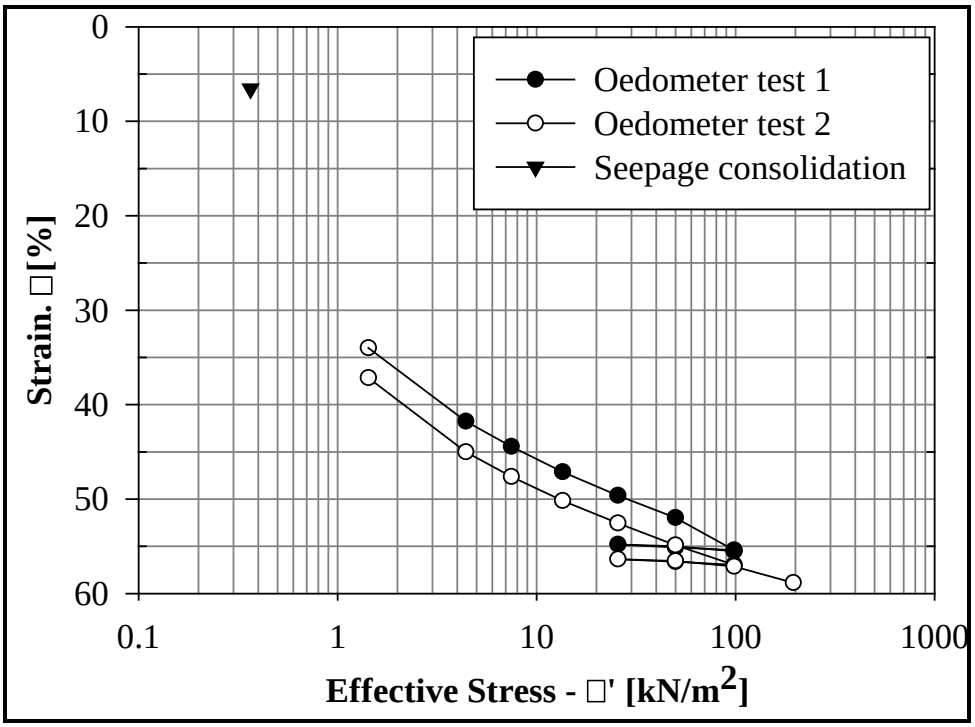

Figure 5.3-13. Consolidation of Cottonwood Bay sediment; strain versus effective stress.

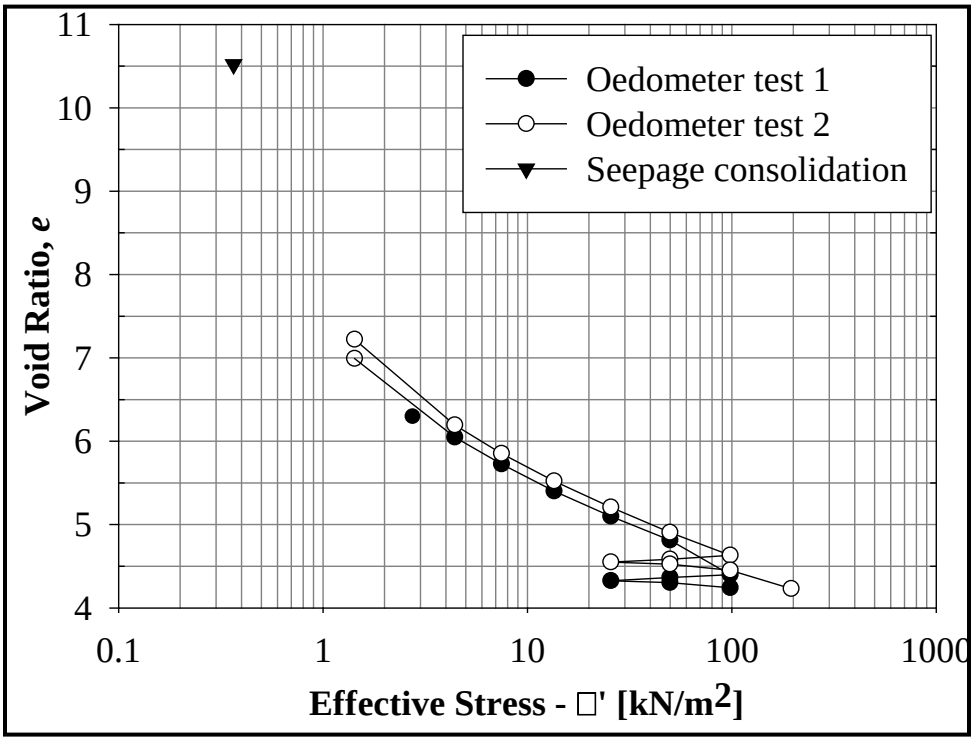

Figure 5.3-14. Consolidation of Cottonwood Bay sediment; void ratio versus effective stress.

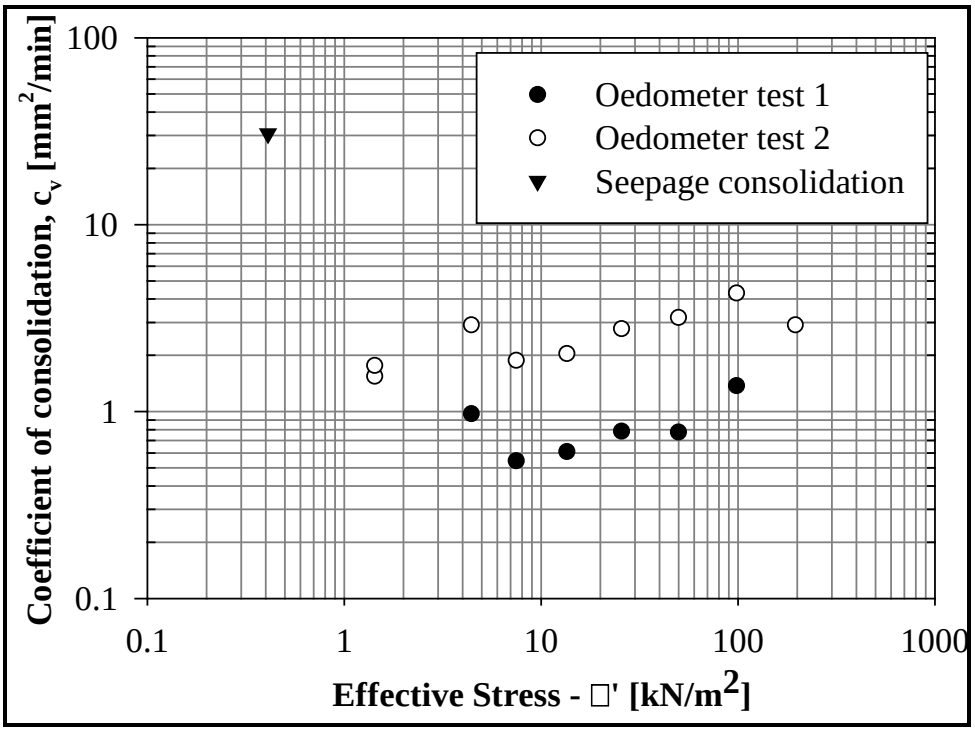

Figure 5.3-15. Coefficient of consolidation of Cottonwood Bay sediment.

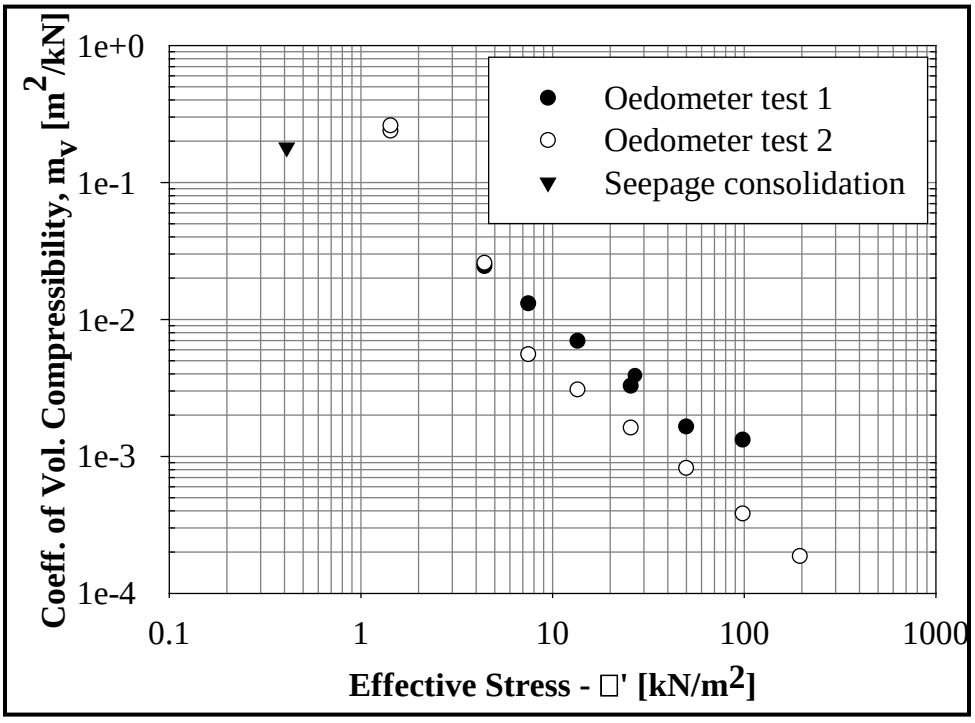

Figure 5.3-16. Coefficient of volumetric compressibility of Cottonwood Bay sediment.

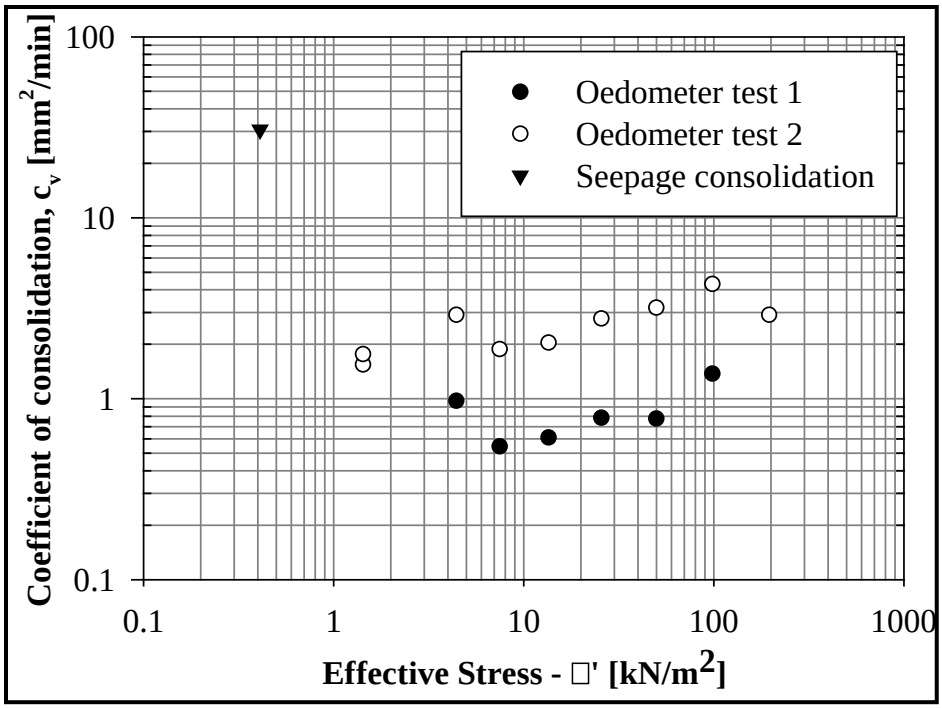

Figure 5.3-17. Variation in coefficient of consolidation with void ratio for Cottonwood Bay sediment.

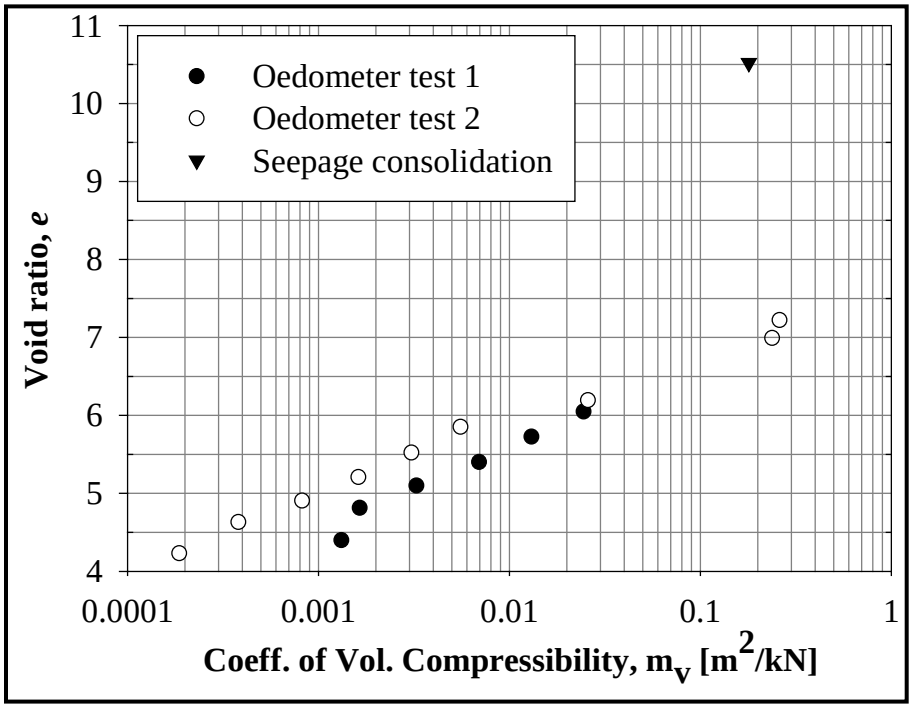

Figure 5.3-18. Variation in coefficient of volumetric compressibility for Cottonwood Bay sediment.

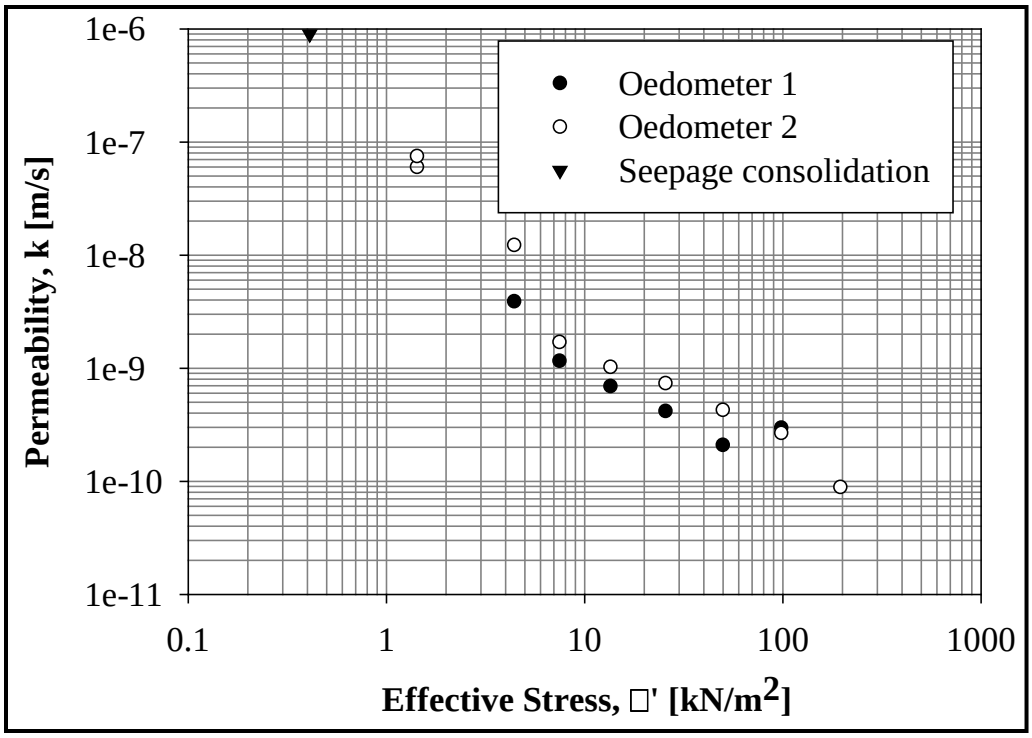

Figure 5.3-19. Permeability versus effective stress for Cottonwood Bay sediment.

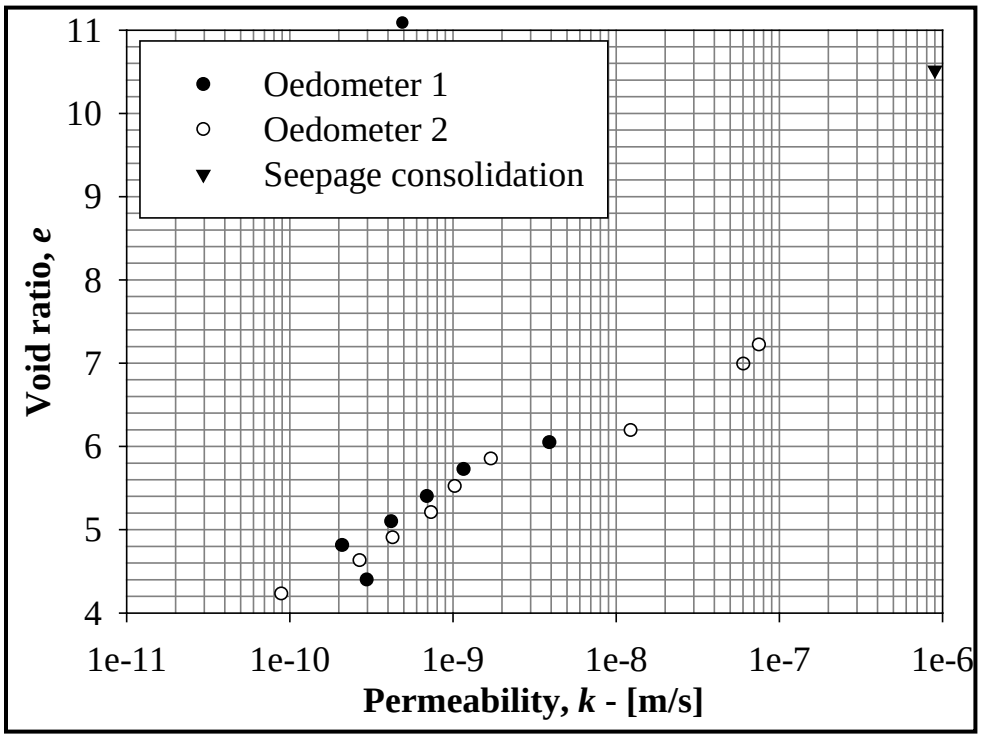

Figure 5.3-20. Void ratio versus permeability for Cottonwood Bay sediment.

5.3.4 Finite Element Analysis

Finite element analyses conducted for this project incorporated various geotextile components to assess increasingly sophisticated deformation and porewater pressure scenarios beyond the basic sand cap investigated in the preliminary models discussed in the First Year Annual Progress Report (NAVFAC 2006). Final results from the various finite element models generated using PLAXIS v8.0 software are presented in the following sub-sections.

Uncoupled Consolidation Model. The uncoupled consolidation model computed the *in situ* stress state of the underlying sediment assuming no steady state or transient groundwater flow. Figure 5.3-21 below shows how the excess pore pressure dissipates with time for this model and that 90% of the consolidation occurs at 400 days, while the 95% consolidation is reached after 600 days.

Confirmation of this curve can be performed by comparing the pressure induced by the mat and the maximum excess pore pressure beneath the sediment through the following equation:

$$ExcessPP = \gamma' \cdot thickness_{mat} = (17 - 9.81)\frac{kN}{m^3} \cdot 0.3m = 2.1\frac{kN}{m^2}$$

The slight difference (2.0 vs. 2.1) is due to stress redistribution.

At the end of consolidation the corresponding displacements can be computed to find the total settlement caused by the potential mat deployment. Figure 5.3-22 below shows the final settlement of the sediment after 600 days and 95% consolidation.

Results indicate that a maximum sediment compression of 9.58 cm occurs beneath the mat. Because the consolidation time estimates are based on a linear stress-strain relationship and assume a constant permeability for the entire model over time, they should be evaluated according to these limitations. Results also show that outside the mat area the maximum displacements of the sediment are nearly 20% and less of the maximum value is caused by the mat deployment.

Figure 5.3-23 shows a horizontal profile of the maximum sediment displacement across the entire uncoupled consolidation model. The maximum settlement occurs directly beneath the mat at nearly 7 m from the mat edge and is constant towards the inside of the mat. The settlement on the sediment surface rapidly decreases beyond the mat edge and reaches a zero displacement at 6.5 m outside the mat limits. The volumetric strain of the sediment serves as an indicator of the area affected by the mat deployment.

Figure 5.3-24 below shows the volumetric strain distribution in the uncoupled model after 95% consolidation. This distribution is similar to the void ratio distribution when the volume of solids is constant. The maximum volumetric strain is 0.98%. These results indicate that the sediment directly below the mat has a final volumetric strain between 100% and 50% of the maximum strain induced by the mat deployment. Due to the soft nature of the material, the uncoupled consolidation model shows that sediment directly beneath the mat is displaced by compressive

effects similar to punching shear effects in foundation design. The pore water displaced by these consolidation effects will occur mainly in the sediment area directly below the mat.

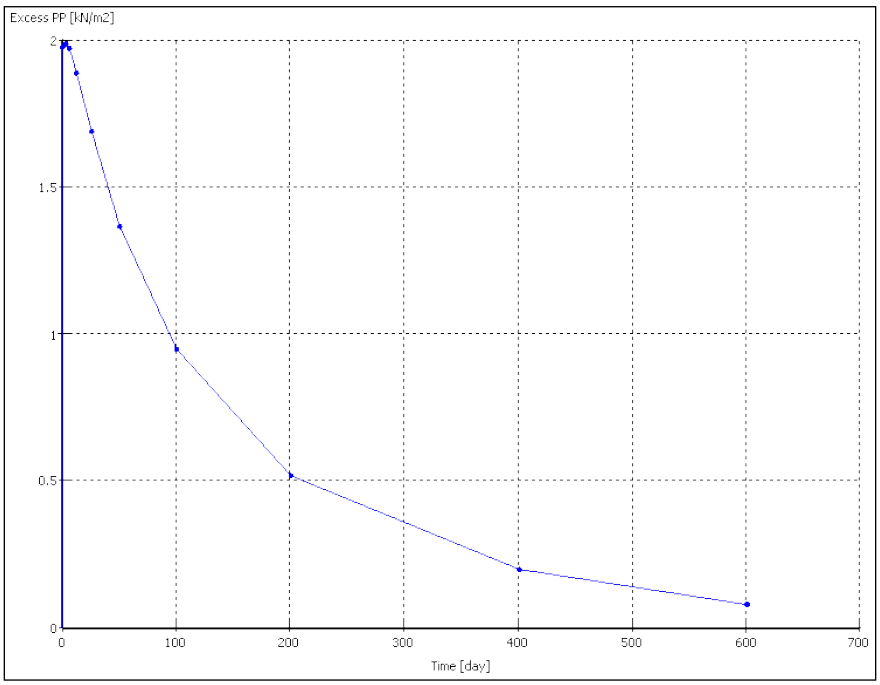

Figure 5.3-21. Excess pore pressure dissipation in the underlying sediment for the uncoupled consolidation finite element model.

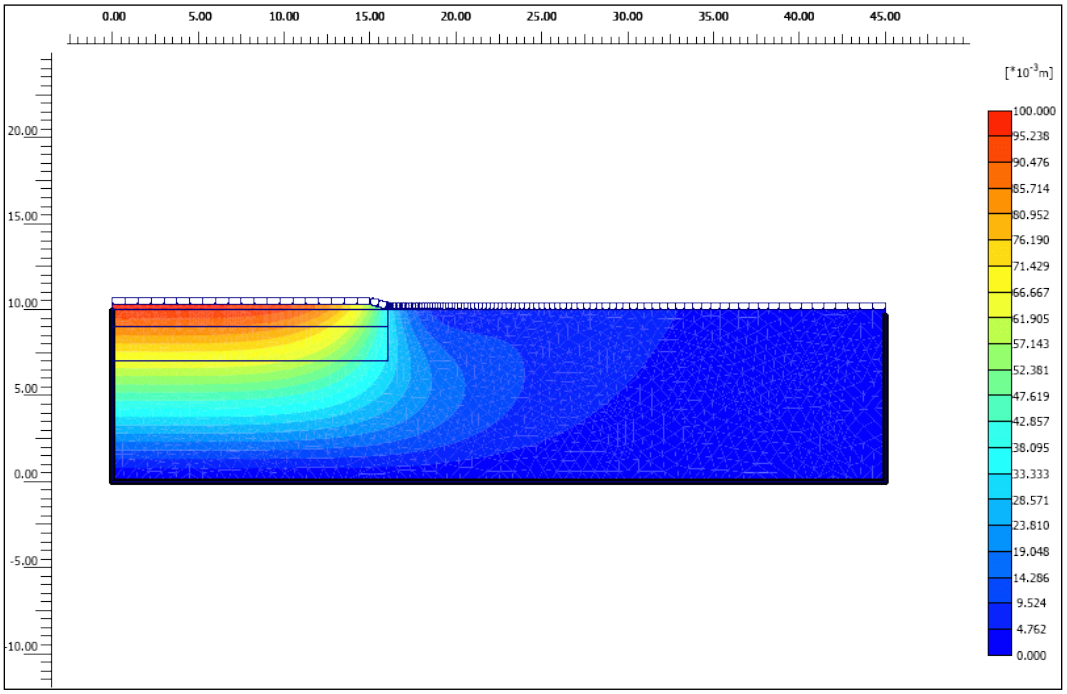

Figure 5.3-22. Settlement due to mat deployment after 95% sediment consolidation under the uncoupled model.

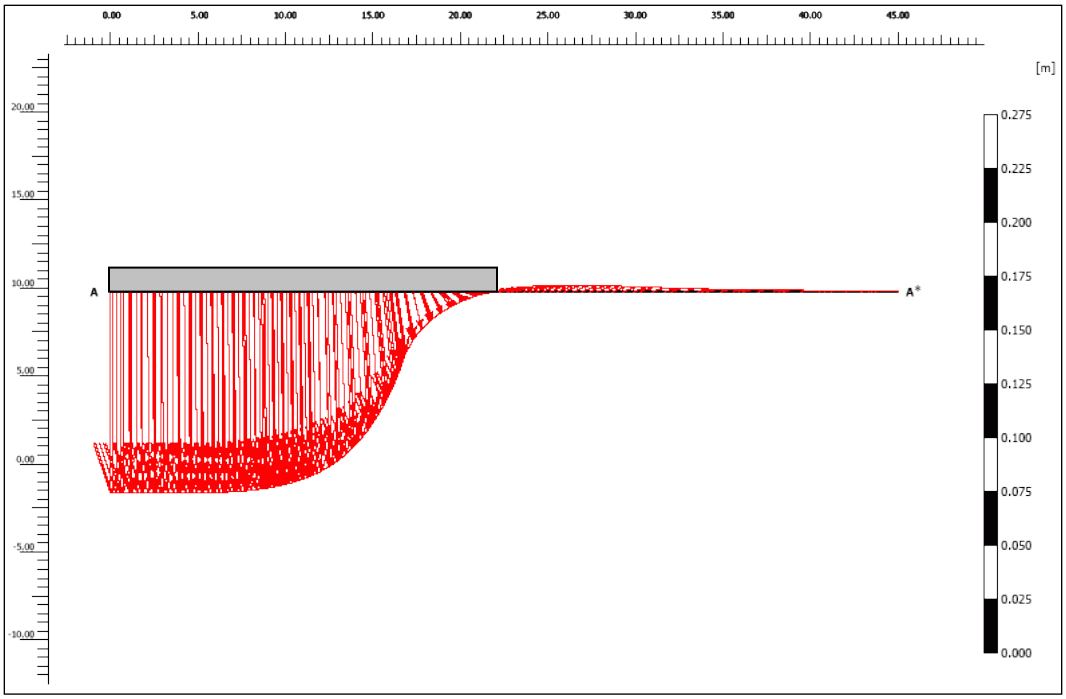

Figure 5.3-23. Horizontal profile of maximum sediment displacement under the uncoupled consolidation model.

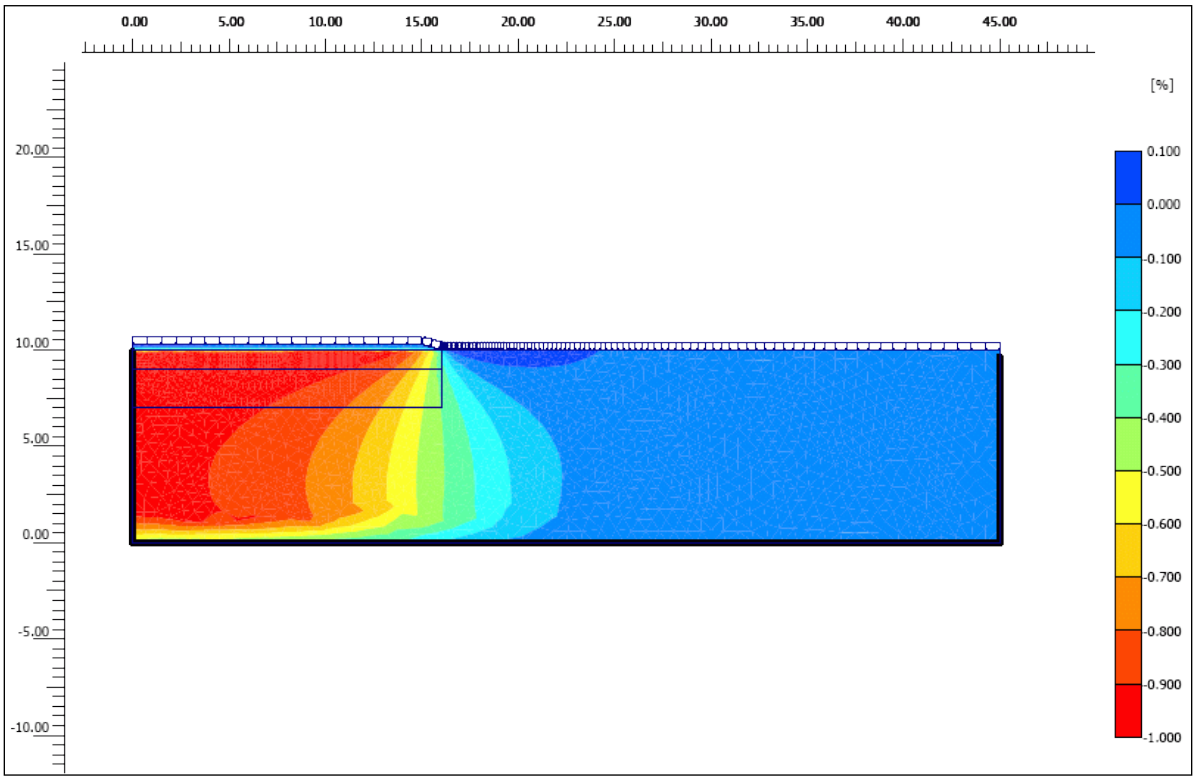

Figure 5.3-24. Volumetric strain after 95% consolidation under the uncoupled consolidation model.

Uncoupled Seepage Model. The uncoupled seepage model assessed potential changes in groundwater flow properties following mat placement for both unclogged and clogged geotextiles. Figure 5.3-25 shows the total water pore pressure distribution for both clogging scenarios. Results indicate that despite having a clogged mat on the second model, the flow of water still moves through the mat albeit at slower rates as shown by the increase in separation between contours from the clogged to the unclogged case. The increase of separation between successive contours indicates lower hydraulic gradient and thus lower seepage velocity. The region near the mat edge shows that the flow is slightly deviated from crossing the mat perpendicularly when the mat is clogged. This result may be of particular interest in selecting the overall extension of the final mat design.

The specific discharge computed for any cross section gives the total water discharge flowing through that section of the model. Figure 5.3-26 shows the specific discharge distribution for both the unclogged and clogged scenarios corresponding to the combined XY direction discharge.

Assuming that 100% of the groundwater flows in the upward direction at the mat deployment site, 35% of the total flow in this model passes through the mat for the unclogged condition. This fraction is slightly reduced to 31% for a clogged mat, thus indicating that ~4% of the groundwater flow was deviated from its original path. It should be noted, however, that the average magnitude of the discharge does not vary significantly from the unclogged to the clogged mat condition and still averages approximately 36-40 m^3/day outside the mat area. The specific discharge distribution varies because the overall boundary conditions change after the mat clogs, but the percentages of groundwater flow moving through and around the mat do not vary significantly.

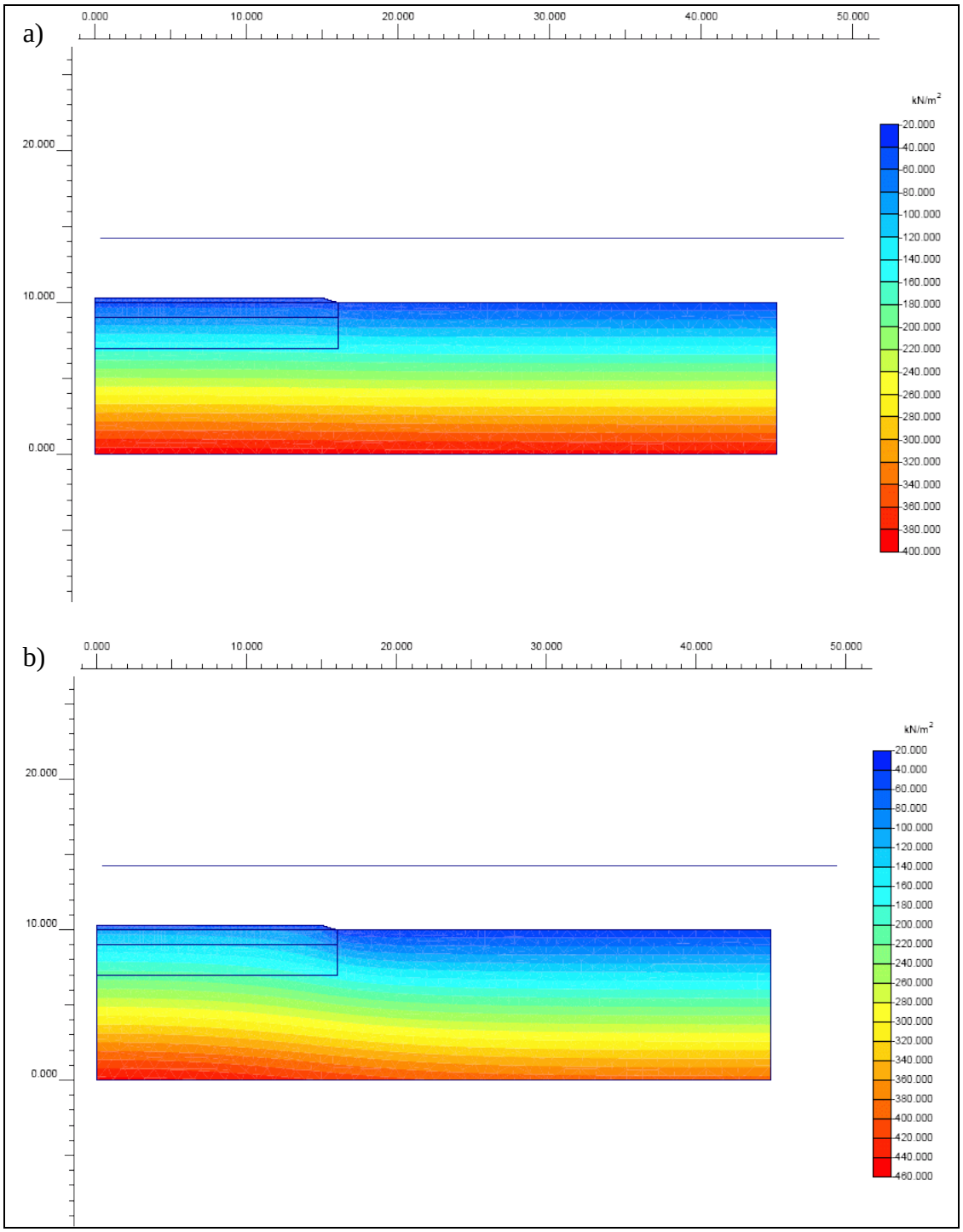

Figure 5.3-25. Total water pore pressure for an unclogged mat (a) and a clogged mat (b) under the uncoupled seepage model.

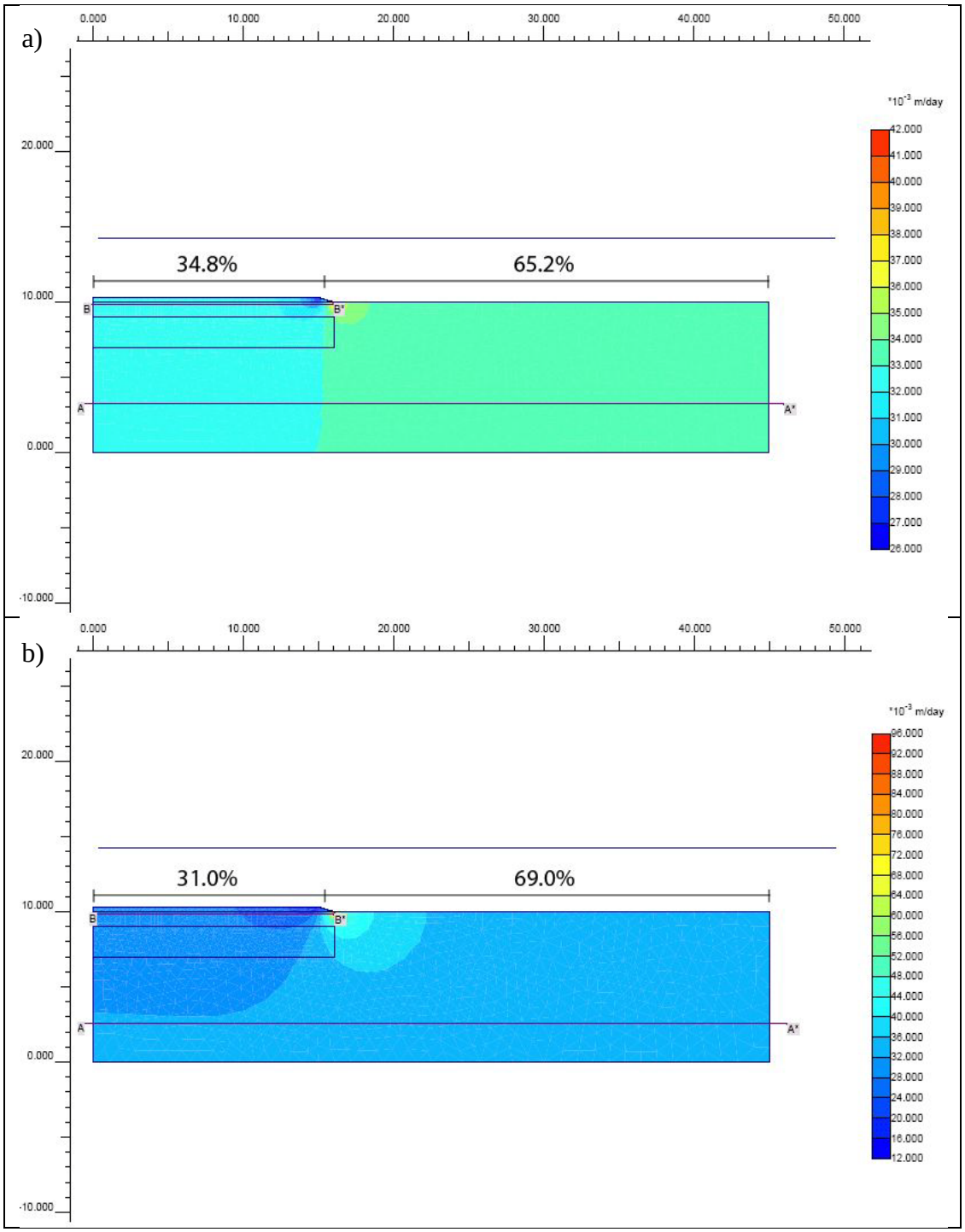

Figure 5.3-26. Specific discharge for an unclogged mat (a) and a clogged mat (b) under the uncoupled seepage model.

Coupled Model. The coupled model merges potential sediment consolidation and groundwater seepage conditions, essentially combining the two uncoupled models, by applying sequential parameters that first define the initial sediment stress caused by mat deployment followed by application of a groundwater flow component that results in a new sediment stress state. Figure 5.3-27 shows the final displacement distribution due to mat deployment under the coupled model.

The maximum displacement for the coupled solution is 9.87 cm, which is close to 9.58 cm obtained without including the groundwater flow in the uncoupled consolidation solution. The 3% increase is the result of the sequential groundwater flow parameter being added following initial sediment consolidation in the coupled solution.

Figure 5.3-28 shows a horizontal profile of the maximum sediment displacement across the entire coupled model. The small increase of the estimated maximum settlement compared to the uncoupled consolidation model and shown in the previous figure does not significantly affect the shape of the settlement profile. The maximum displacement of the mat still occurs 7 m from the edge and remains constant towards the inside of the mat.

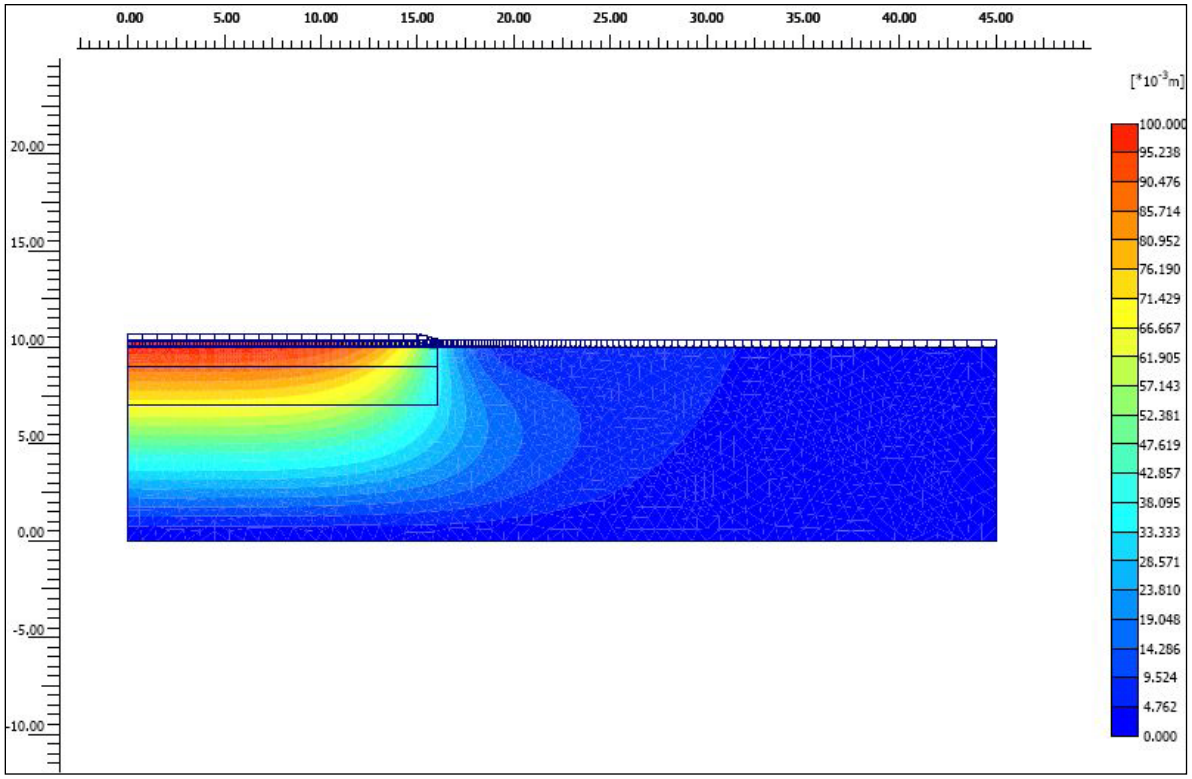

Figure 5.3-27. Sediment settlement due to mat deployment under the coupled model.

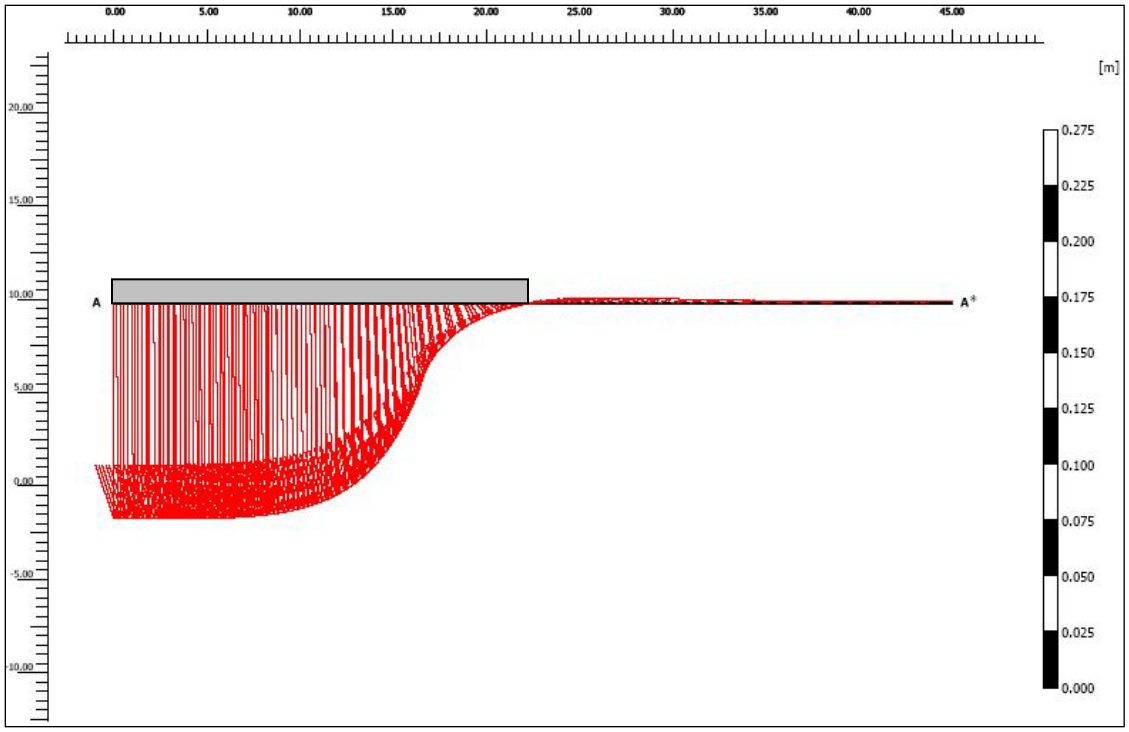

Figure 5.3-28. Horizontal profile of the maximum sediment displacement under the coupled model.

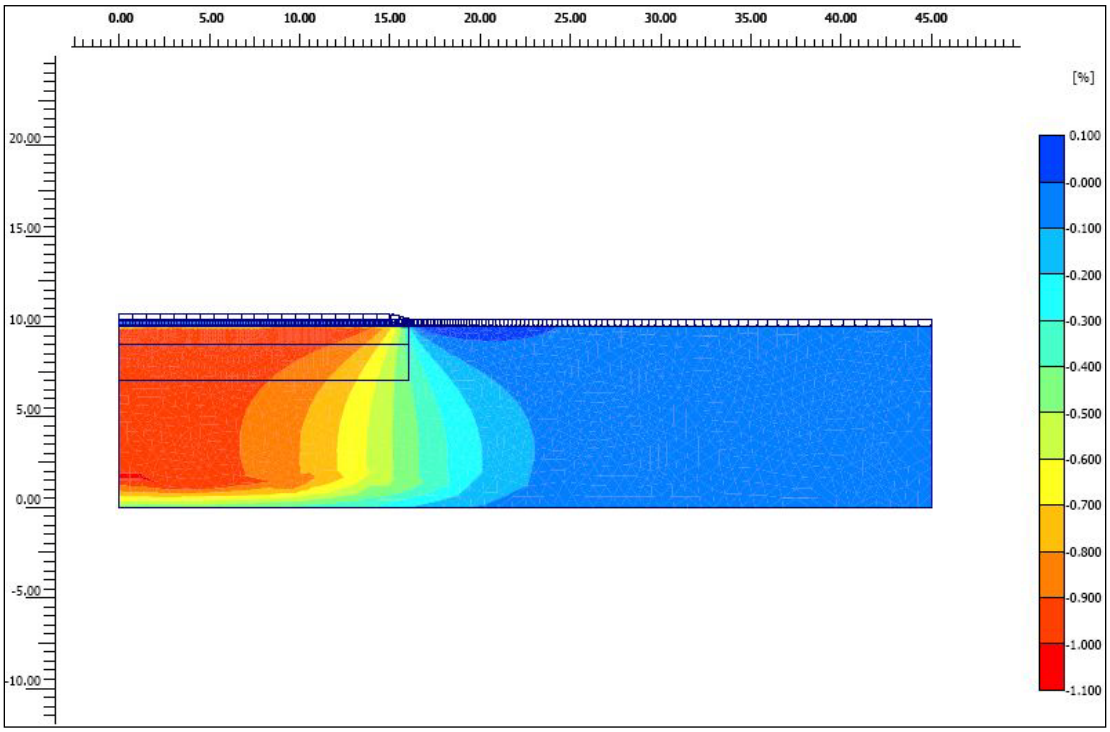

Figure 5.3-29. Volumetric strain under the coupled model.

The volumetric strain distribution for the coupled model is presented in Figure 5.3-29. The maximum volumetric strain was found to be 1.03% for the coupled solution as compared to 0.98% for the uncoupled consolidation solution. The estimated final volumetric strain increases 5% from the uncoupled to the coupled solution. Because the sediment and mat permeabilities as well as the flow rate and water level are constant throughout the coupled solution, there is no change in the amount of flow passing through and around the mat. Similar specific discharge results as the uncoupled seepage model (Figure 5.3-25) are expected for the coupled model when the sediment permeability is varied according to the consolidation tests results.

Summary. Overall results from the FEA process indicate that the soft nature of the underlying sediment will result in significant compression directly beneath the mat following deployment. The porewater displacement caused by this consolidation will be confined mainly to the sediment directly below the mat and a relatively low level of geotextile clogging will not significantly alter groundwater flow patterns. Model results show that a permeability decrease of several orders of magnitude would be required to greatly impact groundwater flow, but this level of clogging is not expected under field conditions based on the results of the gradient ratio testing. Data collected from laboratory tests to be performed on the field weathered small-scale test mats following retrieval will ultimately be used to refine both the uncoupled and coupled finite element models with real permeability data rather than clogging assumptions. The FEA does not favor selection of any particular geotextile at this stage.

Seepage Consolidation Testing. Continued low stress sediment consolidation tests were performed during year three on unweathered geotextiles in order to provide compression curves (e vs. σ') that indicate a reduction of the void ratio as effective stress increases. Nevertheless, permeability tests carried out at each sediment load increment show an inverse behavior, essentially increasing permeability with a decrease in voids. This result indicates seepage along the wall of the cylinder due to radial consolidation. A solution is currently being developed to remedy the seepage problem. A seepage consolidation test has been running for 43 days with favorable results in that wall seepage has not been observed after data reduction.

Consolidation Modeling. Results of the consolidation modeling are provided in Appendix C. Figure C-1 shows the geometry of the 2D model and Table B-1 lists the geotechnical properties used to define the Modified Cam-Clay model. Figure C-2 shows the excess pore pressure profiles during consolidation along the center of the model. The results indicate that 90% of the consolidation process would occur within 120 days of mat deployment.

The settlement of the sediment surface along the mat during consolidation is presented in Figure C-3. The results show uniform settlement of 1.5 cm within the capped area and that most of the sediment distortion occurs within 0.5 m of the border of the mat. The voids within the soil mass are squeezed during the consolidation of the soft sediment.

Figure C-4 shows the rate of water expulsion from the sediment into the water column and along the mat surface during consolidation. The results show that after nearly 10 days of consolidation the magnitude of water flow from the sediment is reduced by two orders of magnitude from its maximum initial value.

Groundwater Flow Modeling. Results of the groundwater flow modeling are also provided in Appendix C; Figure C-5 shows the geometry of the 2D model. The USACE recommends limiting the GR-value of geotextile-soil systems to 3.0 for filtration applications. Replacing GR = 3.0 in the definition of the GR value given by the ASTM standard and using Darcy's law leads to the following definition of clogging in terms of the permeability of the sediment and the sediment-geotextile interface:

$$k_{\text{Sediment}-\text{Geotextile}} = 0.33 \cdot k_{\text{Sediment}}$$

Table B-2 lists the permeability of the soft sediment (measured using the falling head test) and the permeability of the reactive core mat layer used to simulate different degrees of geotextile clogging. The results of the simulations are better represented by the contours of pressure head (meters of water) and the flow paths of water beneath the reactive mat. These results for the five simulations listed are presented in Figure C-6 to C-11.

The results in Figure C-8 show that even a two orders of magnitude reduction of the geotextile permeability does not significantly affect the direction of the flow paths, and the majority of the water still flows through the reactive core mat. A significant deviation of the flow paths is observed in Figure C-9 when the geotextile permeability is three orders of magnitude less than the sediment permeability.

The amount of water actually passing through the mat can be obtained by integrating the water velocities along the mat and assuming a 1 m thickness of the model. The volume of water crossing the reactive core mat for the different clogging scenarios is shown in Figure C-11.

The results shown in Figure C-11 also indicate that the reduction of water flow under USACE clogging conditions (GR = 3.0) is not significant (less than 1%). A 50% reduction of the flow crossing the reactive core mat occurs when the permeability of the geotextile is about 0.004 of the sediment permeability, and a 75% reduction when the mat permeability is 0.001 of the sediment permeability.

In addition to field evaluation, Task 3 also included gradient ratio testing to evaluate geotextile flow properties under laboratory conditions as well as a finite element analysis to evaluate sediment deformation and porewater pressure increases caused by the weight of a potential reactive mat. Preliminary flow-through column experiments were used to evaluate flux for three stock geotextiles and one unweathered organoclay mat by closely mimicking expected processes in the field, thus providing baseline data to which the results of similar testing on the recovered small-scale geotextile mats can be compared.

5.3.5 Gas Permeability Testing

During the course of the geotextile gas permeability testing described in Section 4.3.4, images of the state of the bubble underneath the geotextile were taken daily until the gas bubble had completely disappeared either by flow through the geotextile, by dissipation in the water or by a combination of both mechanisms. Table 5.3-2 below lists the approximate daily volume of the gas bubble during the test and Figure 5.3-30 shows the most detailed images taken at day zero

and day twelve of the experiment. These pictures were taken approximately from the same distance, which allows a rough estimation of the bubble volume over time by comparing the initial dimensions to subsequent observations. Figure 5.3-31 shows a graph of the measured bubble volume during the test with the best exponential fit to the data.

Table 5.3-2. Approximate gas bubble volume over time during the gas permeability test.

Day	Volume of gas bubble [cm^3]
1	1.000
2	0.990
3	0.990
4	0.830
5	0.800
6	0.730
7	0.550
8	0.450
9	0.290
10	0.200
11	0.110
12	0.100
13	0.040
14	0.010
15	0.001

Figure 5.3-30. Biogas bubble flow/dissipation at Day 0 (left) and Day 12 (right) of the gas permeability test.

Gas was flowing/dissipating during this experiment over an area of nearly 2 cm^2 (the initial bubble had a volume of 1 cm^3 and an average thickness of 0.5 cm). The rate of gas flow/dispersion over time per square meter of geotextile was then obtained from the volume versus time fitted curve and normalized to the square meter of geotextile. The rate of gas flow/dispersion over time per square meter of geotextile is shown in Figure 5.3-32.

The rate of gas flow/dissipation was found to vary over time from 3000 to 100 cm^3/day per square centimeter of the fine AOS 170 geotextile. This result indicated that the volume of the gas bubble affects the rate of gas flow through the geotextile and it is possible that the greater buoyant force from the bubble on the geotextile at the beginning of the experiment promotes a greater gas flow rate passing through the geotextile. However, this buoyant force must be compared to the submerged weight of the potential reactive mat to prevent overturning of the system.

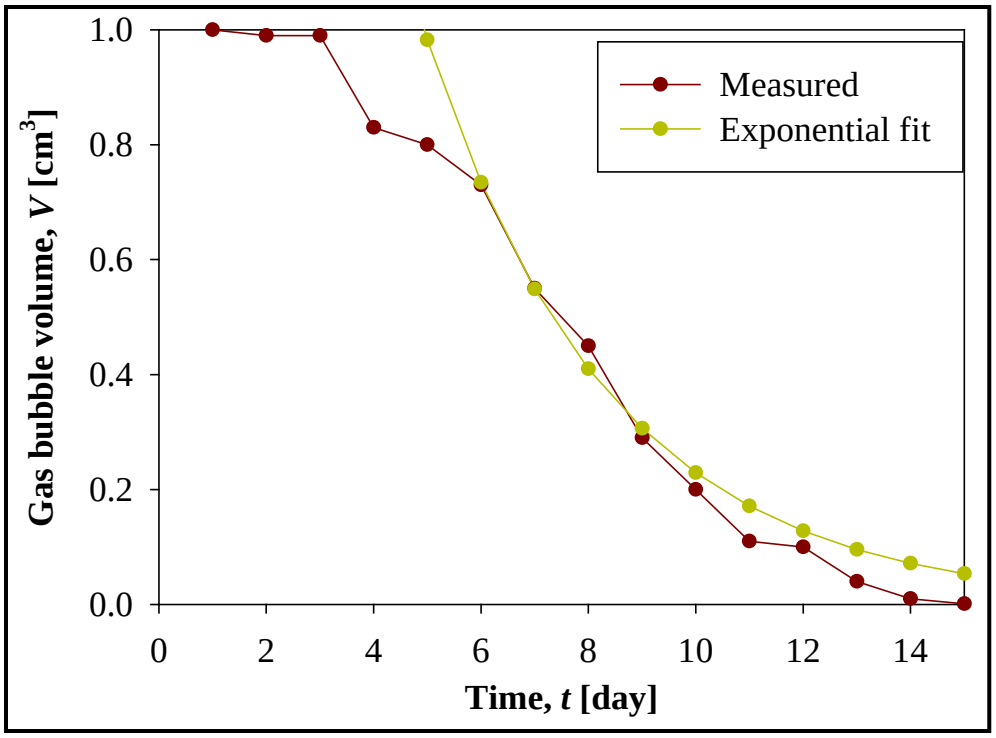

Figure 5.3-31. Volume of the gas bubble beneath the geotextile versus time.

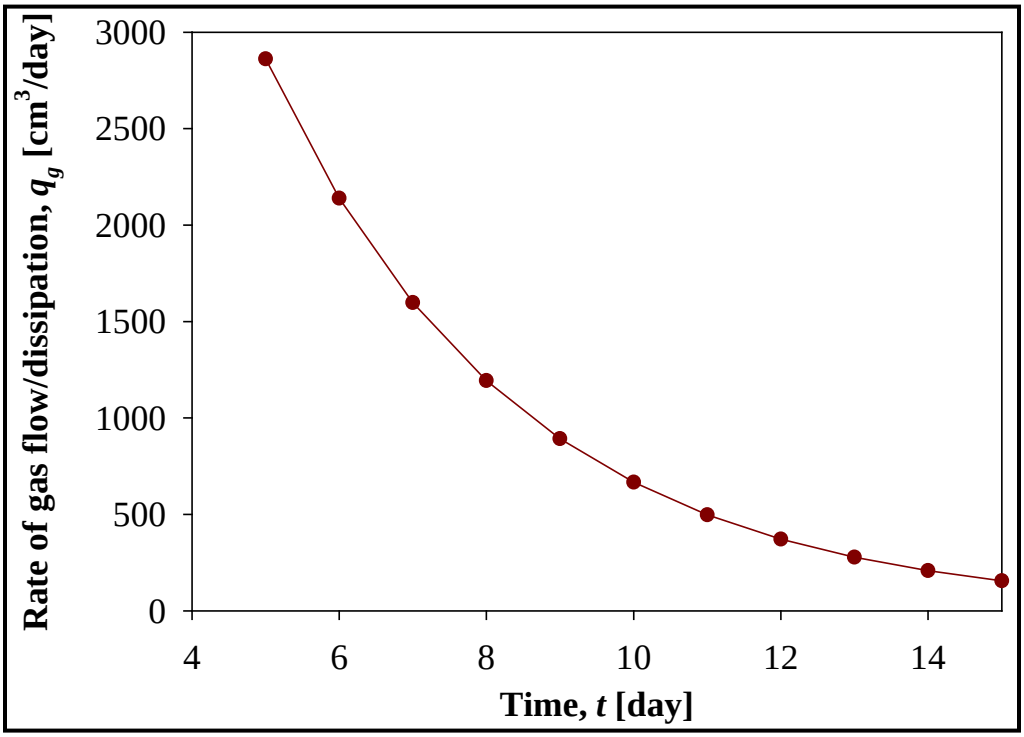

Figure 5.3-32. Flow/dissipation rate of gas versus time per square meter of geotextile.

Comparing the peak gas flow/dissipation rate measured for the heaviest and finest geotextile (AOS 170, 8 oz/yd^2) shown in Figure 5.3-32 (3000 cm^3/day) to the maximum freshwater sediment gas production rates reported in the literature (up to 2640 cm^3/day) (Qingzhong *et al*. 2007) showed that gas accumulation beneath the geotextile is not expected to represent a main hazard to the stability and integrity of a geotextile deployed over sediment under the assumed conditions as long as there is a sand/sediment protective layer providing additional weight to the cap. Reactive core mats used for full-scale implementation are expected to be built using geotextiles with a coarser opening size (AOS 70 to 80), which would transfer gas even faster compared to the geotextile tested in the laboratory gas permeability experiment (AOS 170). Therefore, the rate of gas flow/dissipation in the field is expected to be greater than the values presented above, which would provide an additional margin of safety to the structural integrity of the mat system independent of the weight of a potential sand cap. Regardless, a sand cap component should still be included even with a coarse geotextile to ensure ultimate stability of the system.

In the case of the small test mats deployed in Cottonwood Bay without an overlying sand layer, field observations indicated that the initial buoyant force generated by gas buildup were sufficient to lift the mat, particularly for the finest geotextile (AOS 170). As this gas buildup eventually dispersed over time and further gas production decreased with decreasing temperature, the test mats ultimately returned to the lake floor during the winter months. Similar conditions occurred at the larger prototype mat system, with gas buildup and mat lifting being observed in the summer at the two mat areas without an overlying sand layer (T1 and T3). When compared to these two treatments, the gas buildup and mat lifting at the mat with sand cap area (T2) was found to be negligible, thus confirming the laboratory conclusions stated above.

5.4 Task 4: Prototype Mat Testing

The purpose of Task 4 was to field test a prototype mat system in order to assess *in-situ* chemical sequestration effectiveness and flux properties of various reactive mat/sand cap arrangements.

The final design specifications for the prototype mat system are discussed in Section 4.4.1. This mat system was deployed in April 2008 following the methodology described in Section 4.4.2. Following successful deployment, confirmation and monitoring events in the form of geophysical surveys, passive contaminant sampling (two rounds), groundwater flow surveys, sediment coring and sediment cap sampling were conducted to evaluate the success of the various mat/cap treatments in achieving overall project goals. The analytical results of these individual tasks are provided in the following sub-sections and referenced to the appropriate appendices.

5.4.1 Geophysical Investigation

Final images from the prototype mat system confirmatory geophysical investigation are presented in Appendix D. Raw side-scan sonar, bathymetry and sub-bottom data were processed to provide a pictorial view of the prototype mat system area and the post-cap surfaces.

Side-Scan Sonar. The final side-scan mosaic produced a clear planview image of the prototype mat system layout and identified the acoustic signature unique to this type of geotextile (Appendix D, Figure D-1). The side-scan data also confirmed the horizontal distribution of sand capping material (dark patches with a different reflective signature), thus allowing for an evaluation of the success of sand placement techniques in construction goals. Sand capping material settled in areas T2 and T4 over the desired width of the treatment.

Bathymetry. Bathymetry data for the prototype mat system indicated that water depths ranged from 4.5 ft to 5.8 ft at the time of collection (December 2008), with 5.0 ft deep areas directly over the mats and deeper areas generally to the north (Appendix D, Figure D-2). However, deeper points (5.6-5.8 ft) were also present underneath the mats in areas T1 and T3, which may represent local sediment depressions.

Sub-Bottom Profiling. Sub-bottom profiling data for the prototype mat system indicated that the isopach depth below the sediment-water interface (*i.e.*, thickness) of the uppermost sediment layer ranged from 0.2 ft to 1.25 ft (Appendix D, Figure D-3). Points of decreased sediment layer thickness (0.20-0.25 ft) in areas T1 and T3 may provide evidence of localized variability in depositional history.

Sediment Profile Imaging. Visual analysis of the SPI images taken at the prototype mat system allowed for an evaluation of sediment buildup on the mats, confirming sand capping thickness in appropriate areas, and a description of control area conditions. By definition, the use of the SPI measurement method was limited in areas T1 and T3 because the camera prism could not penetrate the geotextile mats in these mat only treatments. Thus images from these areas depicted only conditions on the mat surfaces at six months. In contrast, images from areas T2, T4 and T5 were able to depict sediment cross-sections above the mats or natural substrate, thus confirming the vertical distribution of sand capping material to confirm what had previously been documented by diver observations.

The SPI images from each mat treatment area included the following notable features after six months of soak time:

- **T1 (Single Mat Only)** – Substantial natural sediment buildup, biofilm formation or capping material overflow deposited on top of the single layer mat in a non-capping area (Appendix D, Figure D-5).
- **T2 (Single Mat with Sand Cap)** – Sand capping thickness >2" over the single layer mat; apparent redox potential discontinuity (RPD) depth (*i.e.*, the depth of oxygen penetration into the sediment indicative of microorganism activity) of approximately 0.23" (Appendix D, Figure D-6).
- **T3 (Double Mat)** – Poor image quality; also likely substantial natural sediment buildup, biofilm formation or capping material overflow deposited on top of the single layer mat in a non-capping area (Appendix D, Figure D-7).
- **T4 (Sand Cap Only)** – Sand capping thickness of approximately 1.85" before mixing of cap material with natural tan and gray soft mud; apparent RPD depth of approximately 0.85" (Appendix D, Figure D-8).

- **T5 (No Treatment/Control)** – Some capping material overflow present above the natural tan and gray soft mud; apparent RPD depth of approximately 0.58" (Appendix D, Figure D-9).

The fact that the apparent RPD depth was two times greater in the T5 control area and four times greater in the T4 capping only area than in the T2 mat capping area indicates slightly diminished microorganism activity in the engineered substrate when placed over a cap as compared to the natural substrate after six months, but colonization was occurring.

Modeling Verification. Geophysical data collected at the prototype mat system were ultimately compared to the laboratory consolidation testing and finite element analysis results to evaluate the success of these modeling exercises in predicting mat performance in a freshwater, soft-sediment environment. The side-scan sonar mosaic was used to identify the specific mat/sand cap locations via their unique acoustic signature within the general target area. Bathymetry data was collected from the treatment deployment areas both before (July 2007) and after (December 2008) mat placement in order to allow an evaluation of any appreciable changes in bottom topography and water depth that might have occurred due to the placement of the capping materials.

Bathymetry data collected in Cottonwood Bay both before and after mat placement are shown concurrently in Figure 5.4-1. The bathymetry data was corrected to the same hydrographic control point to account for yearly fluctuations in lake water levels and then plotted as specific data points along the survey lanes. Results of the July 2007 bathymetry survey conducted prior to mat placement indicated that the study area was relatively flat with a gradual increase in depth from south to north. Less consistent trends were observed after the mats had been in place for 16 months (Dec 2008), suggesting some disturbance and/or deformation in the natural sediment due to mat placement activities.

The 2007 bathymetry survey was designed to cover the entire placement area in Cottonwood Bay, which resulted in robust survey lanes that did not ultimately pass directly over the future mat treatment areas. Thus the comparison of pre-mat to post-mat changes in bathymetry was not possible. However, the December 2008 survey conducted 16 months after mat placement did reflect changes in elevation due to mats as compared to adjacent non-treatment areas. The placement of the half-inch (1.3 cm) thick mat with an additional three-inch (7.6 cm) sand cap in area T2 would be expected to add 3.5 inches (8.9 cm) of total relief to the ambient surface, assuming solid conditions without compression. In soft substrate such as the conditions experienced in Cottonwood Bay, however, the weight of the mat/sand could exceed the load-bearing capacity of the underlying natural sediment causing compression and therefore subsidence of the mat and sand treatments.

Modeling efforts predicted maximum sediment compression of 9.6-9.9 cm due to consolidation (Section 5.3.3). Post-mat bathymetry data collected at the center of area T2 revealed relief of up to 4 cm above the surrounding sediments one year after mat deployment (Figure 5.4.1). When subtracted from the expected 8.9 cm relief to be caused by the thickness of the mat/sand cap, this finding suggests at actual net sediment compression at this location of approximately 5 cm. Compression of this magnitude is within the expected range as predicted by the model. In

comparison, the sand-only treatment (T4) was uniformly level with the surrounding environment, such that potentially greater consolidation occurred in this treatment than T2.

As far as the mat-only treatments, results were highly variable, with areas of noticeable elevation change up to 20 cm observed in some portions of areas T1 and T3. As the bathymetry survey was conducted during the winter when biological activity is at its lowest, this added relief is not believed to have been caused by gas accumulation lifting the mats off the surface. Instead, the changes were attributed to localized irregularities in the mat surface possibly resulting from a fold or crease in the mat geotextile (which seems apparent from the side scan data) or other sources of roughness caused by monitoring activities (*e.g.*, SPI survey, passive sampler deployment, Trident and Ultraseep survey). The SPI images taken on top of the mats showed sediment accumulation ranging from approximately 0-0.5" (~1.27 cm) for the treatments without a sand cap, thus suggesting relatively negligible impacts of sediment deposition on the topography of the overall mat system. In general the geophysical data revealed changes within the range of modeled expectations and exhibited sufficient sensitivity to be a useful tool for monitoring mat conditions.

With regard to the Trident Probe and Ultraseep groundwater flow data (discussed in Section 5.4.3), the control area showed essentially no flow while the various mat/sand treatments showed approximately 0-3 cm/day. This discrepancy is likely due to the nature of clay sublayers in the natural sediment where groundwater escapes through cracks in a non-uniform manner across the area. A lack of consistency observed at the local mat level makes it difficult to compare the field and model groundwater flow results with any certainty.

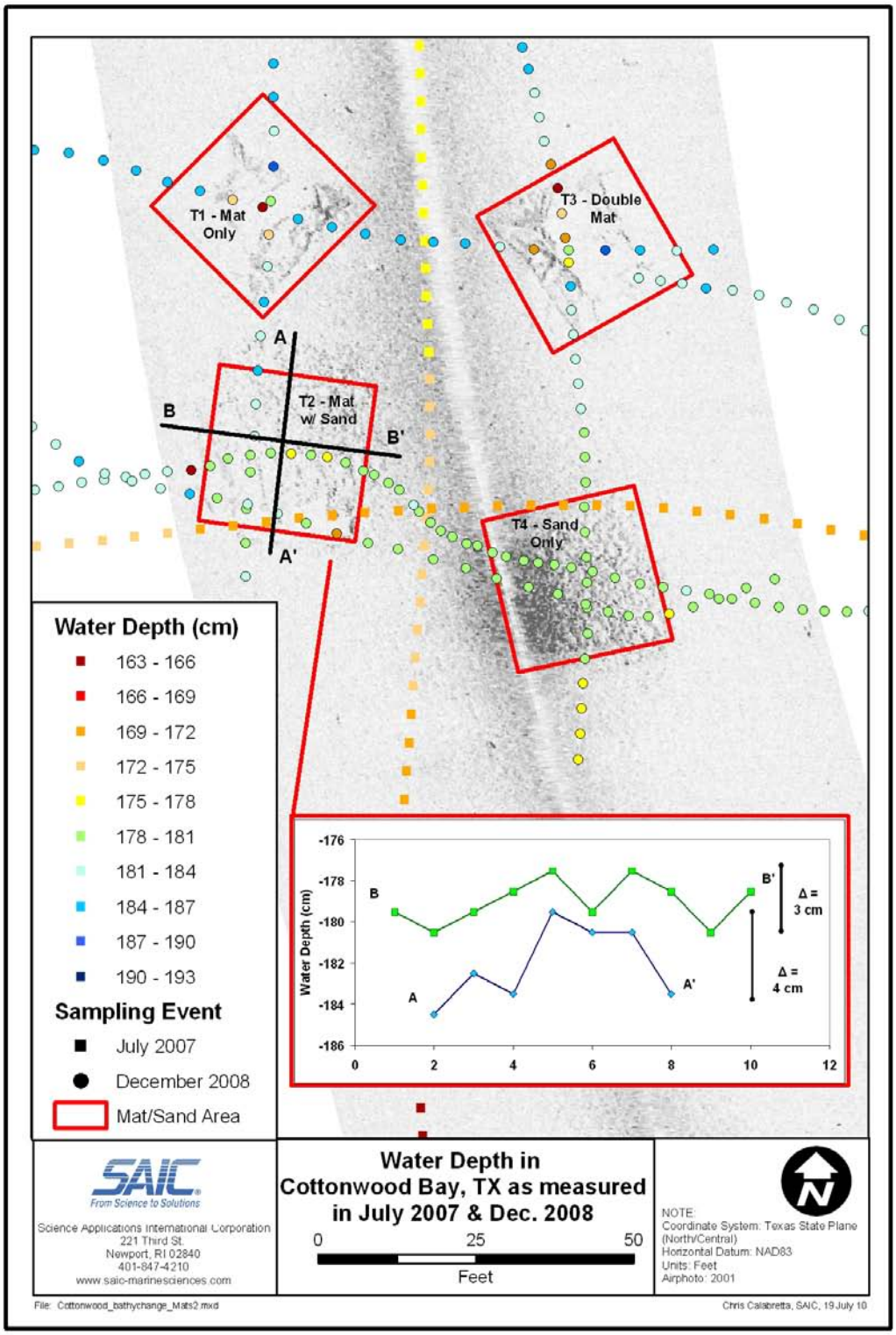

Figure 5.4-1. Water depth comparison in Cottonwood Bay from bathymetry collected both before and after placement of the prototype mat system.

5.4.2 Diffusion Sampling Results

In evaluating the passive sampling data to determine whether the reactive mat technology achieved the project goal of demonstrating significant contaminant reduction across the treatment boundary, a set of conditions was established that must be met for each test parameter in order for the resulting analytical values to be considered relevant and applicable to the effects of the prototype mat system. Data trends that did not meet these conditions were considered artifacts of the test site exhibited independent of the reactive mat influence and the associated analytes were not considered suitable subjects on which to base project conclusions. These test conditions were defined as follows.

- *The analyte must be detected in the below treatment samples*. It is impossible to determine the reduction capabilities of the mat technology on contaminants that are non-detect or otherwise non-existant in the natural sediment environment.
- *The below treatment concentration must be greater than or equal to the above treatment concentration*. In order for sampler data to accurately depict mat effects on contaminant levels at the site based on the known properties of the technology, these data must demonstrate either a contaminant reduction or no change across the treatment boundary. Because the mats themselves, including the reactive core, were constructed from virgin materials, and only clean material was used for the sand cap, the technology did not contribute any contaminants to the test environment. It is therefore impossible for concentrations to increase across the treatment boundary without non-treatment influences, which would then make the resulting gradient irrelevant. Contaminants can either be blocked by the mats (concentrations elevated below treatment, non-detect above), sequestered within the mat amendments (concentrations greater below treatment than above) or flow through the mats unimpeded (concentrations equal below and above).
- *The below treatment concentration must be greater than the ambient surface water concentration*. In order for the below treatment samples to demonstrate true contaminant levels in the natural sediment, these concentrations must be independent of the overlying water column prior to encountering the mat technology. A situation in which ambient surface water concentrations were greater than or equal to below treatment concentrations would suggest contributions from outside sources or contaminant dilution within the sediment. The resulting contaminant gradient would then decrease from the overlying water into the sediment opposite of groundwater flow, which would make an accurate assessment of mat effects on flow concentrations impossible.

Peeper Analytical Results. Raw horizontal and vertical peeper analytical results for the prototype mat system collected during the first round (December 2008) and second round (December 2009) of passive contaminant sampling are presented in Appendix E. Analytical results from the three chambers (*i.e.*, sub-replicates) within each horizontal peeper were averaged to produce a single value for that replicate at a particular horizon within a treatment. These three replicate values were then averaged to produce a single summary value for that particular horizon in the treatment. In contrast, analytical results from the fifteen chambers within each vertical peeper were treated as independent values for each discrete horizon, but three replicate values were still averaged to produce a single summary value for that horizon within a treatment.

Prior to performing any calculations, non-detect results were substituted with one half the method detection limit (MDL) following standard USEPA protocol. A summary of the final Year One and Year Two peeper data showing mean results for all non-lithogenic metals of concern at each treatment is presented in Table 5.4-1.

Table 5.4-1. Summary of first year (top) and second year (bottom) peeper mean analytical results for all metals of concern at the prototype mat system.

Year 1 Peeper Results: Metals

		T1 - Mat Only		T2 - Mat w/ Sand		T3 - Double Mat			T4 - Sand Only		T5 - No Treatment
Analyte	Units	Below Treatment	Above Treatment	Below Treatment	Above Treatment	Below Treatment	Between Treatment	Above Treatment	Below Treatment	Above Treatment	Above Treatment
Arsenic	ug/L	20	29	6.9	6.9	29	6.9	6.9	6.9	6.9	13
Barium	ug/L	110	65	98	67	146	47	52	61	58	54
Cadmium	ug/L	2.4	0.99	0.93	1.9	2.2	0.16	0.16	0.16	0.16	0.55
Chromium	ug/L	7.7	3.0	7.7	10	10	2.0	5.5	0.66	0.71	0.65
Copper	ug/L	5.7	2.2	3.4	7.2	2.2	2.1	3.6	1.6	1.7	0.67
Lead	ug/L	19	3.5	3.5	20	5.9	3.5	3.5	3.5	3.5	3.5
Nickel	ug/L	4.2	2.2	8.9	5.1	5.8	1.3	2.2	1.5	1.5	1.6
Silver	ug/L	0.21	0.21	0.21	0.21	0.21	0.21	0.21	0.21	0.21	0.21
Vanadium	ug/L	8.5	3.5	1.8	9.5	7.3	0.76	2.1	0.49	0.49	0.89
Zinc	ug/L	45	8.2	24	47	33	9.3	5.6	2.4	2.5	2.8

Year 2 Peeper Results: Metals

		T1 - Mat Only		T2 - Mat w/ Sand		T3 - Double Mat			T4 - Sand Only		T5 - No Treatment
Analyte	Units	Below Treatment	Above Treatment	Below Treatment	Above Treatment	Below Treatment	Between Treatment	Above Treatment	Below Treatment	Above Treatment	Above Treatment
Arsenic	ug/L	31	6.9	6.9	6.9	42	6.9	6.9	6.9	6.9	11
Barium	ug/L	122	41	104	71	181	43	41	60	55	49
Cadmium	ug/L	1.5	0.16	0.47	0.16	3.5	0.16	0.16	0.74	0.34	0.97
Chromium	ug/L	3.7	1.6	13	1.0	1.8	1.4	1.2	0.39	0.32	0.32
Copper	ug/L	0.4	1.2	1.6	0.82	0.33	0.6	1.1	0.33	0.33	0.33
Lead	ug/L	3.5	3.5	3.5	3.5	4.0	3.5	3.5	3.5	3.5	3.5
Nickel	ug/L	2.6	1.1	3.6	1.9	3.1	1.0	4.6	0.73	0.73	0.73
Silver	ug/L	0.41	0.21	0.8	0.29	0.68	0.21	0.21	0.41	0.21	0.34
Vanadium	ug/L	4.9	0.96	1.6	0.85	6.6	0.62	0.95	0.49	0.49	0.49
Zinc	ug/L	11	3.2	11	4.3	16	1.5	2.2	2.0	1.2	1.2

In order to provide a quantitative basis for evaluating the efficacy of the different mat treatments, hypothesis testing was performed to compare the below and above datasets for each analyte and determine whether any observed reductions were statistically significant. This hypothesis testing consisted of a simple two-sample t-test conducted at the 95% confidence coefficient (alpha = 0.05). The null hypothesis was defined as the above treatment mean being greater than or equal to the below treatment mean (*i.e.*, no treatment effect on contaminant reduction). In contrast, the alternative hypothesis was defined as the above treatment mean being less than the below treatment mean (*i.e.*, contaminant reduction occurred across treatment). A p-value less than 0.05 would reject the null hypothesis and conclude that statistically significant contaminant reduction occurred at the treatment. A p-value greater than 0.05 would fail to reject the null hypothesis and effective treatment by the mats could not be accurately concluded. Each above/below treatment dataset consisted of three peeper replicates with no data points excluded. All hypothesis testing calculations were performed using USEPA ProUCL software and population variances for each dataset were determined automatically within the context of the t-test application, which in turn determined whether the pooled (equal variance) or Satterthwaite

(unequal variance) was selected. The results for the hypothesis testing of each analyte at each treatment are shown in Table 5.4-2.

Table 5.4-2. Results of hypothesis testing to determine the statistical significance of contaminant reductions across treatment boundaries for all metals of concern at the prototype mat system.

Significance Level: Alpha = 0.05
Null Hypothesis: Above Treatment >= Below Treatment (p-value > 0.05)
Alternative Hypothesis: Above Treatment < Below Treatment (p-value < 0.05)

	T1 - Mat Only				T2 - Mat w/ Sand				T3 - Double Mat (Below to Between)			
Analyte	Replicate Variance (n=3)	p-value	Reject Null? (Above < Below)	Conclusion Explanation	Replicate Variance (n=3)	p-value	Reject Null? (Above < Below)	Conclusion Explanation	Replicate Variance (n=3)	p-value	Reject Null? (Above < Below)	Conclusion Explanation
Year 1 Peeper Results												
Arsenic	EQUAL	0.645	NO	b	EQUAL	N/A	NO	a	UNEQUAL	0.174	NO	c
Barium	EQUAL	0.072	NO	c	EQUAL	0.087	NO	c	UNEQUAL	0.084	NO	c
Cadmium	EQUAL	0.170	NO	c	EQUAL	0.693	NO	b	EQUAL	0.106	NO	c
Chromium	UNEQUAL	0.187	NO	c	EQUAL	0.698	NO	b	UNEQUAL	0.112	NO	c
Copper	UNEQUAL	0.254	NO	c	EQUAL	0.789	NO	b	EQUAL	0.421	NO	c
Lead	EQUAL	0.187	NO	c	EQUAL	0.813	NO	a	EQUAL	0.187	NO	c
Nickel	UNEQUAL	0.236	NO	c	UNEQUAL	0.165	NO	c	EQUAL	0.046	YES	d
Silver	EQUAL	N/A	NO	a	EQUAL	N/A	NO	a	EQUAL	N/A	NO	a
Vanadium	EQUAL	0.189	NO	c	UNEQUAL	0.802	NO	b	UNEQUAL	0.142	NO	c
Zinc	UNEQUAL	0.173	NO	c	UNEQUAL	0.687	NO	b	EQUAL	0.092	NO	c
Year 2 Peeper Results												
Arsenic	UNEQUAL	0.211	NO	c	EQUAL	N/A	NO	a	UNEQUAL	0.211	NO	c
Barium	UNEQUAL	0.134	NO	c	EQUAL	0.086	NO	c	UNEQUAL	0.114	NO	c
Cadmium	EQUAL	0.187	NO	c	EQUAL	0.187	NO	c	EQUAL	0.187	NO	c
Chromium	UNEQUAL	0.211	NO	c	UNEQUAL	0.208	NO	c	EQUAL	0.358	NO	c
Copper	EQUAL	0.999	NO	b	EQUAL	0.269	NO	c	EQUAL	0.813	NO	a
Lead	EQUAL	N/A	NO	a	EQUAL	N/A	NO	a	EQUAL	0.187	NO	c
Nickel	EQUAL	0.117	NO	c	EQUAL	0.067	NO	c	EQUAL	0.027	YES	d
Silver	EQUAL	0.059	NO	c	EQUAL	0.034	YES	d	EQUAL	0.001	YES	d
Vanadium	UNEQUAL	0.210	NO	c	EQUAL	0.045	YES	d	UNEQUAL	0.202	NO	c
Zinc	UNEQUAL	0.146	NO	c	EQUAL	0.061	NO	c	UNEQUAL	0.09	NO	c

	T3 - Double Mat (Below to Above)				T4 - Sand Only			
Analyte	Replicate Variance (n=3)	p-value	Reject Null? (Above < Below)	Conclusion Explanation	Replicate Variance (n=3)	p-value	Reject Null? (Above < Below)	Conclusion Explanation
Year 1 Peeper Results								
Arsenic	UNEQUAL	0.174	NO	c	EQUAL	N/A	NO	a
Barium	UNEQUAL	0.092	NO	c	EQUAL	0.326	NO	c
Cadmium	EQUAL	0.138	NO	c	EQUAL	N/A	NO	a
Chromium	UNEQUAL	0.207	NO	c	EQUAL	0.749	NO	b
Copper	EQUAL	0.986	NO	b	EQUAL	0.565	NO	b
Lead	EQUAL	0.187	NO	c	EQUAL	N/A	NO	a
Nickel	UNEQUAL	0.106	NO	c	EQUAL	0.178	NO	b
Silver	EQUAL	N/A	NO	a	EQUAL	N/A	NO	a
Vanadium	UNEQUAL	0.183	NO	c	EQUAL	N/A	NO	a
Zinc	UNEQUAL	0.094	NO	c	EQUAL	0.707	NO	b
Year 2 Peeper Results								
Arsenic	UNEQUAL	0.211	NO	c	EQUAL	0.211	NO	a
Barium	UNEQUAL	0.112	NO	c	EQUAL	0.379	NO	c
Cadmium	EQUAL	0.187	NO	c	EQUAL	0.099	NO	c
Chromium	UNEQUAL	0.299	NO	c	EQUAL	0.211	NO	c
Copper	EQUAL	1.000	NO	a	EQUAL	N/A	NO	a
Lead	EQUAL	0.187	NO	c	EQUAL	N/A	NO	a
Nickel	EQUAL	0.661	NO	b	EQUAL	N/A	NO	a
Silver	EQUAL	0.001	YES	d	EQUAL	0.015	YES	d
Vanadium	UNEQUAL	0.110	NO	c	EQUAL	N/A	NO	b
Zinc	UNEQUAL	0.095	NO	c	EQUAL	0.211	NO	a

Conclusion Explanation:
a - Analyte not detected in sediment porewater (below treatment); no contamination to be treated.
b - Below treatment mean concentration not greater than above treatment mean concentration; potential non-treatment influences.
c - Below treatment mean concentration greater than above treatment mean concentration but reduction not statistically significant.
d - Below treatment mean concentration greater than above treatment mean concentration and reduction is statistically significant.

Key summary plots showing average concentrations above (yellow), between (red) and below (blue) treatment boundaries for select metals (nickel, zinc, copper) for the first year and second

year peeper sampling efforts are provided in Figure 5.4-2. These specific analytes were chosen as the primary metals of interest for the mat system assessment because they were previously identified as CoCs in the USGS Cottonwood Bay dataset (EnSafe 2001) and produced consistently detected results in the horizontal peeper analysis, suggesting that observed trends are real and not artifacts of variability in non-detect results. Ambient surface water contaminant concentrations determined from the peeper suspended in the water column were also included in the Year Two plots to provide a point of comparison for final reduction data and background values.

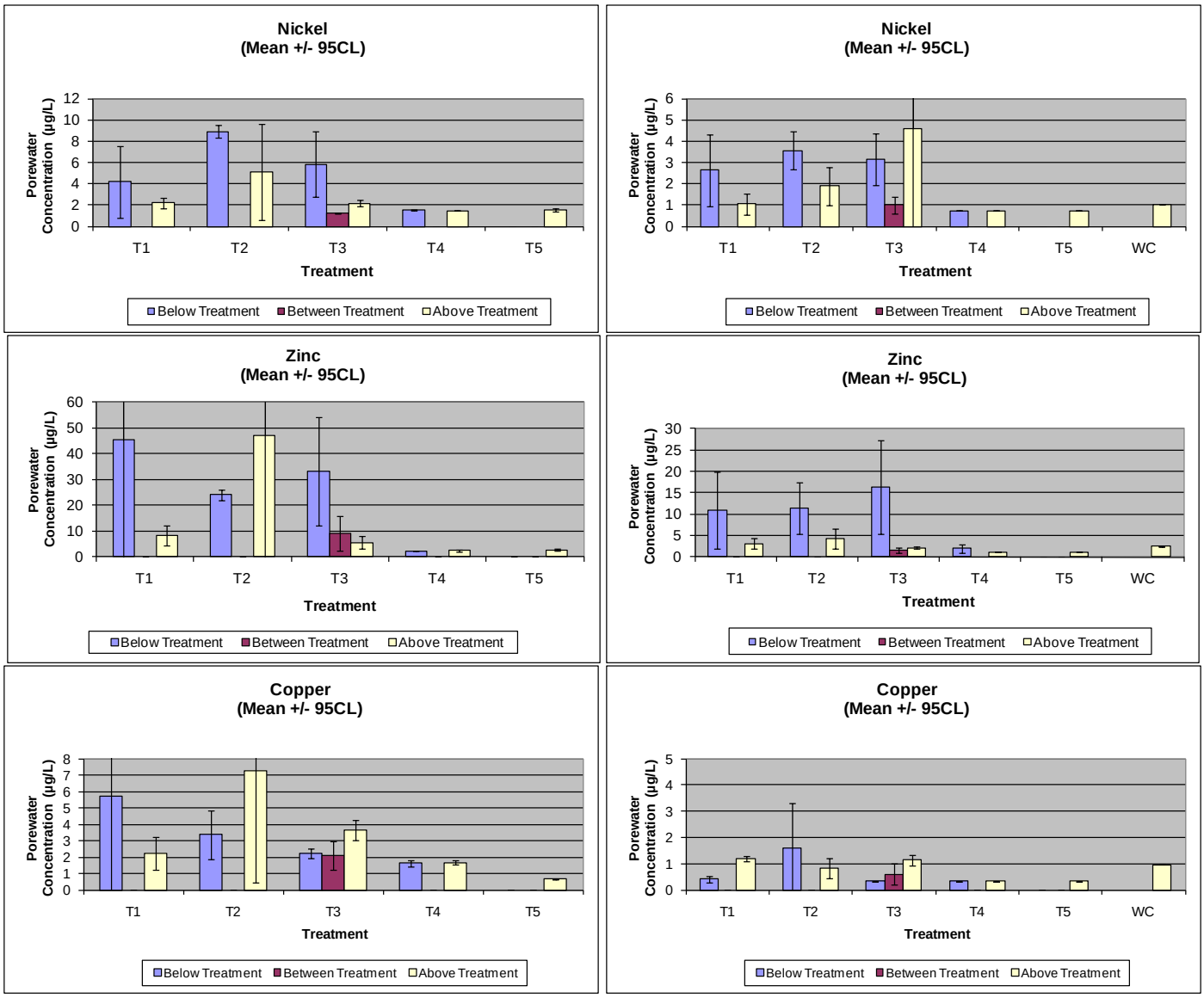

Figure 5.4-2. First year (left column) and second year (right column) peeper analytical results for select metals (nickel, zinc, copper) at the prototype mat system.

Results from the hypothesis testing and summary plots indicated certain trends that were not consistent over the two sampling years and did not appear logical based on the expected

properties of the test site. One notable anomaly was that zinc and copper concentrations below treatment in area T1 were much higher in Year One than Year Two and these values were also substantially greater than the below treatment concentrations in other areas; logic dictates that below treatment concentrations should be relatively consistent in all areas since they all contain the same natural sediment, with some leeway allowed for local variation. A second notable anomaly was that the Year One zinc and copper concentrations above treatment in area T2 and the Year Two nickel concentration above treatment in area T3 were substantially greater than the ambient water column concentration, an illogical result considering the mats could not add contaminants to the environment. Because these anomalies could not be explained through a typical uncertainty analysis, the decision was made to further inspect the entire raw peeper dataset at the most robust level for the presence of potential outliers which, due to the limited number of peeper replicates (n = 3) in each test area, would skew the final treatment data in a manner unrepresentative of true mat behavior and thus erroneously impact final conclusions regarding mat efficacy in sequestering metals. The outlier investigation was performed as an alternative approach to standard regulatory protocol and was not intended to replace the full dataset provided above.

The outlier investigation was conducted by compiling the peeper sub-replicate (*i.e.*, chambers within each peeper) data at each horizon within each treatment into one dataset with nine values (n = 9). Treating all sub-replicate concentrations as independent values in this manner was considered appropriate because increasing sample size would strengthen the power of the outlier test and true large variations would not be expected between different chambers located only centimeters apart within the same sampler. A Dixon's Q-test for detection of a single outlier was then performed on each population using USEPA ProUCL software. This simple test is based on the statistical distribution of "subrange ratios" of ordered data samples drawn from the same normal population and allows one to examine if one (and only one) observation from a small set of replicate observations (typically 3 to 10) can be "legitimately" rejected or not at different significance levels. For the purposes of this investigation, a significance level of 5% was selected as the cutoff point for outlier identification. A list of the suspected outliers identified with this technique along with the maximum significance level (< 5%) of each identification is provided for both Year One and Year Two in Table 5.4-3. The raw sub-replicate data used for this evaluation is provided in Appendix E.

As shown in Table 5.4-3, excluding these sub-replicate outliers from the overall peeper dataset substantially decreases the mean concentrations for the replicates in which they were contained, which would in turn decrease the summary mean for that horizon in that particular treatment. Depending on whether the outlier was identified in a below mat or above mat sample, its presence was explained by either potential particulate contamination within the peeper chamber (below) or non-treatment influences (above).

As an alternative approach to standard regulatory protocol, these outliers were removed from the peeper dataset at the sub-replicate level and the adjusted replicate means were rolled up into the final treatment summary values. The hypothesis testing described above was then re-run with the new replicate means (still n = 3) to provide a more accurate assessment of statistically significant contaminant reductions across the various treatments. The results of this second

round of hypothesis testing are provided in Table 5.4-4; all analytes affected by outlier exclusion are highlighted.

Table 5.4-3. Suspected outliers for metals of concern in the peeper dataset identified at the sub-replicate level.

Statistical Outliers: Metals

Analyte	Treatment	Horizon	Replicate (n=3)	Sub-Replicate (n=9)	Result (ug/L)	Dixon's Test Statistic	Outlier @ 5% Significance?	Max Outlier Significance Level	Replicate Mean w/ Outlier	Replicate Mean w/o Outlier	Outlier Explanation
Year 1 Outliers											
Copper	T1 - Mat Only	Below Mat	Rep 1 (A)	A-3	37	0.911	YES	1%	5.7	1.9	a
Zinc	T1 - Mat Only	Below Mat	Rep 1 (A)	A-3	267	0.938	YES	1%	45	18	a
Copper	T2 - Mat w/ Sand	Above Mat	Rep 3 (L)	L-1	42	0.975	YES	1%	7.2	2.8	b
Nickel	T2 - Mat w/ Sand	Above Mat	Rep 3 (L)	L-1	20	0.840	YES	1%	5.1	1.8	b
Zinc	T2 - Mat w/ Sand	Above Mat	Rep 3 (L)	L-1	251	0.978	YES	1%	47	5.4	b
Year 2 Outliers											
Nickel	T3 - Double Mat	Above Mat	Rep 2 (R)	H2a	25	0.815	YES	1%	4.6	2.2	b

Outlier Explanation:
a - Value 10x greater than colocated sub-replicates; suggesting potential particulate sample contamination.
b - Value 10x greater than colocated below treatment data; suggesting non-treatment influences.
Source:
See Appendix E for full peeper sub-replicate dataset.

Table 5.4-4. Results of hypothesis testing to determine the statistical significance of contaminant reductions across treatment boundaries for all metals of concern at the prototype mat system with the exclusion of sub-replicate outliers.

Significance Level: Alpha = 0.05
Null Hypothesis: Above Treatment >= Below Treatment (p-value > 0.05)
Alternative Hypothesis: Above Treatment < Below Treatment (p-value < 0.05)

	T1 - Mat Only					T2 - Mat w/ Sand					T3 - Double Mat (Below to Between)				
Analyte	Sub-Rep Outliers Removed?	Replicate Variance (n=3)	p-value	Reject Null? (Above < Below)	Conclusion Explanation	Sub-Rep Outliers Removed?	Replicate Variance (n=3)	p-value	Reject Null? (Above < Below)	Conclusion Explanation	Sub-Rep Outliers Removed?	Replicate Variance (n=3)	p-value	Reject Null? (Above < Below)	Conclusion Explanation
Year 1 Peeper Results															
Copper	YES	EQUAL	0.609	NO	b	YES	EQUAL	0.309	NO	c	NO	EQUAL	0.421	NO	c
Nickel	NO	UNEQUAL	0.236	NO	c	YES	EQUAL	0.000	YES	d	NO	EQUAL	0.046	YES	d
Zinc	YES	EQUAL	0.040	YES	d	YES	EQUAL	0.001	YES	d	NO	EQUAL	0.092	NO	c
Year 2 Peeper Results															
Nickel	NO	EQUAL	0.117	NO	c	NO	EQUAL	0.067	NO	c	NO	EQUAL	0.027	YES	d

	T3 - Double Mat (Below to Above)					T4 - Sand Only				
Analyte	Sub-Rep Outliers Removed?	Replicate Variance (n=3)	p-value	Reject Null? (Above < Below)	Conclusion Explanation	Sub-Rep Outliers Removed?	Replicate Variance (n=3)	p-value	Reject Null? (Above < Below)	Conclusion Explanation
Year 1 Peeper Results										
Copper	NO	EQUAL	0.986	NO	b	NO	EQUAL	0.565	NO	b
Nickel	NO	UNEQUAL	0.106	NO	c	NO	EQUAL	0.178	NO	b
Zinc	NO	UNEQUAL	0.094	NO	c	NO	EQUAL	0.707	NO	b
Year 2 Peeper Results										
Nickel	YES	EQUAL	0.226	NO	c	NO	EQUAL	N/A	NO	a

Conclusion Explanation:
a - Analyte not detected in sediment porewater (below treatment); no contamination to be treated.
b - Below treatment mean concentration not greater than above treatment mean concentration; potential non-treatment influences.
c - Below treatment mean concentration greater than above treatment mean concentration but reduction not statistically significant.
d - Below treatment mean concentration greater than above treatment mean concentration and reduction is statistically significant.
Notes:
= Result affected by outlier removal.

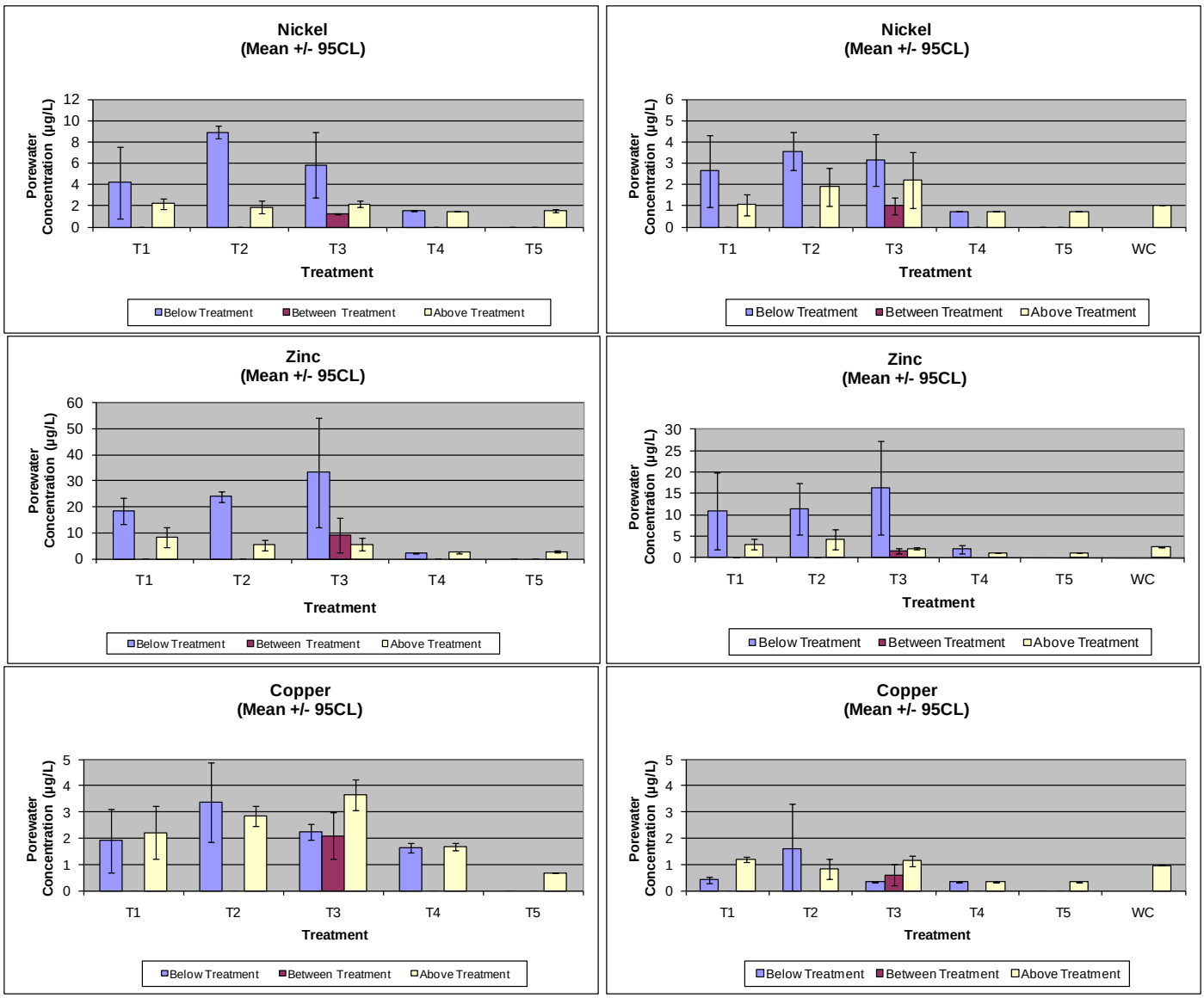

Figure 5.4-3. First year (left column) and second year (right column) peeper analytical results for select metals (nickel, zinc, copper) at the prototype mat system with the exclusion of sub-replicate outliers.

A second set of summary plots for select metals (nickel, zinc, copper) generated with the exclusion of the outliers was also generated for comparison purposes and is shown in Figure 5.4-3. When compared to the previous plots above, it is clear that the outlier removal produces mean zinc and copper concentrations below treatment in area T1 that are more akin to the below treatment concentrations observed in the other areas and the nickel, copper and zinc concentrations above treatment in areas T2 and T3 are more in line with the concentrations observed in the overlying water column. These changes also had the effect of reversing the reduction trends in areas T2 and T3 to be more consistent with expected results based on the nature of the technology (*i.e.*, the mats do not add contaminants to the environment).

Findings from the peeper dataset included the following:

- Hypothesis testing on the full dataset indicated that of all the analytes that satisfied the test conditions described above (*i.e.*, excluding conclusions "a" and "b" in Table 5.4-2), only silver and vanadium in area T2, silver in area T3 and silver in area T4 showed statistically significant concentration reductions across the treatment boundary from below to above (*i.e.*, conclusion "d" in Table 5.4-2). In addition, nickel and silver showed statistically significant reductions in area T3 (double mat) from below the mats to between the mats, suggesting that the double mat array sequesters contaminant contributions emanating from both below and above the treatment. All other analytes satisfying the test conditions showed some reduction of mean concentrations, but replicate data was insufficient to prove that these reductions were significant. However, changing the significance level of the hypothesis test by reducing the confidence coefficient from 95% to 90% (alpha = 0.1) would also demonstrate significant reductions for barium (T1, T2, T3), nickel (T2) and zinc (T3).
- When taking the alternative step of repeating the hypothesis testing with the exclusion of statistically proven sub-replicate outliers from the peeper dataset, zinc in area T1 as well as nickel and zinc in area T2 then also show statistically significant concentration reductions across the treatment boundary (*i.e.*, conclusion "d" in Table 5.4-4). Due to the nature of the sampler design (*i.e.*, multiple sub-replicate chambers within each peeper only centimeters apart), these outliers were considered true anomalous values and excluding them in this manner was deemed an important step in accurate data analysis.
- Nickel. All three mat treatments (T1, T2, T3) had mean nickel and zinc concentrations generally two to four times greater in the natural porewater below the treatment (*i.e.*, reactive mat/sand cap) than in the porewater above the treatment, suggesting effective sequestration by the mat system. Results for area T3 further indicated a general decrease in porewater concentration between the two mat layers while for area T4, concentrations in porewater in sediment below the sand-only cap were not elevated above the cap or water-only control concentrations.
- Zinc. All three mat treatments (T1, T2, and T3) had zinc concentrations generally two to four times greater in the natural porewater below the treatment (*i.e.*, reactive mat/sand cap) than in the porewater above the treatment, suggesting effective sequestration by the mat system. Again, results for area T3 indicate a general decrease in porewater concentration between the mats and in area T4, concentrations in sediment porewater were not elevated above the sand cap porewater or surface water control concentrations.
- Copper. None of the three mat treatments (T1, T2, and T3) showed a decrease in porewater concentrations in sediments below the mat compared to above the mat, thus suggesting that the mat system is less effective at sequestering copper than nickel and zinc. However, measurements between mats of the T3 treatment did indicate a general decrease in porewater concentration, suggesting some sequestration of copper by the mat system is occurring.
- The second year horizontal peeper dataset closely replicated the first year horizontal peeper results, confirming that the findings presented for nickel, zinc and copper are indicative of real trends as opposed to random processes or analytical error.

All peeper data has been presented above in a manner consistent with application in a regulatory environment (*i.e.*, one half MDL substituted for non-detect values, no suspected outliers excluded). In order to evaluate the potential influence of method MDLs on peeper trends, however, an additional alternative evaluation was conducted in which the non-detect values in the "below treatment" samples from the Year Two dataset were removed while the non-detect values in the "above treatment" samples were retained (Table 5.4-5). This adjustment followed the logic that the mat system would not show any tangible reduction effects on ambient contaminant concentrations that are already below MDLs but would be capable of reducing elevated contaminant concentrations to levels below those same detection limits. For the select metals of concern, removing non-detect values significantly increased the "below treatment" concentrations in some areas. It also resulted in the removal of copper from areas T3 and T4 and nickel from area T4 as all replicates were non-detect. Although most of the absolute increases were small, these effects cannot be considered negligible because the overall results were generally very low and small differences in values resulted in appreciable differences in trends across treatments. The presence of non-detect values increases uncertainty in the interpretation of the peeper data because lowering the "below treatment" results in turn decreases the calculated difference from "above treatment" results which is the measure of contaminant sequestration efficacy of the mat treatments.

Table 5.4-5. Comparison of "below treatment" peeper concentrations with and without non-detect values included in the mean calculations.

			T1 - Mat Only		T2 - Mat w/ Sand		T3 - Double Mat		T4 - Sand Only	
Analyte	Units	MDL	Below Treatment (w/o NDs)	Above Treatment (w/ NDs)	Below Treatment (w/o NDs)	Above Treatment (w/ NDs)	Below Treatment (w/o NDs)	Above Treatment (w/ NDs)	Below Treatment (w/o NDs)	Above Treatment (w/ NDs)
Cadmium	ug/L	0.31	4.2	0.16	1.1	0.16	10	0.16	0.74	0.34
Chromium	ug/L	0.64	3.7	1.6	13	1.0	2.5	1.2	0.47	0.32
Copper	ug/L	0.67	0.54	1.2	2.2	0.82	N/A	1.1	N/A	0.33
Nickel	ug/L	1.5	3.6	1.1	3.6	1.9	3.1	1.5	N/A	0.73
Zinc	ug/L	2.3	11	3.2	11	4.3	16	2.2	2.8	1.2

N/A = Data not available; all replicates non-detect

Key vertical summary plots showing average porewater concentrations at different depths in each treatment area for select metals (cadmium, chromium) are provided in Figure 5.4-4. These particular metals were chosen for the vertical plots in place of nickel, zinc and copper because the concentrations of the latter CoCs were entirely non-detect in the Year Two vertical peeper dataset. Discrete data points in the vertical plots correspond to porewater concentrations in each peeper chamber when deployed upright and reflect the fine-scale contaminant concentration differences in the sediment horizons immediately below or within the treatment interface. The results do show overall differences in metals concentrations over depth, confirming that local spatial variation is occurring and would complicate the interpretation of treatment effectiveness.

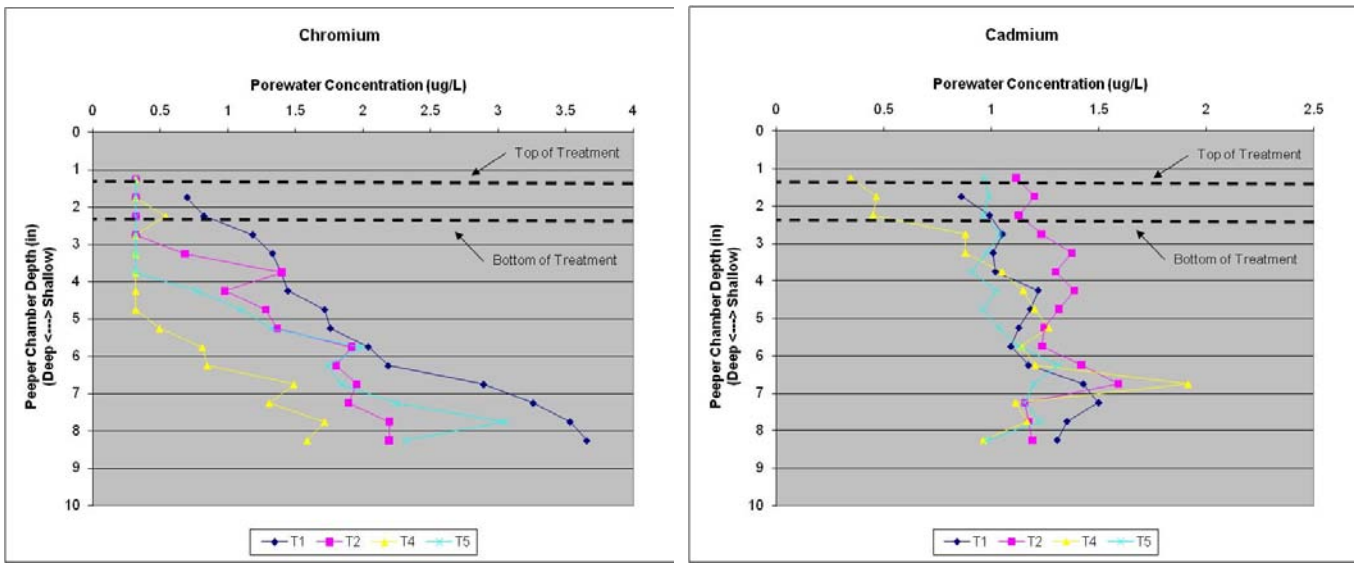

Figure 5.4-4. Second year vertical peeper analytical results for select metals (cadmium, chromium) at the prototype mat system.

SPMD Analytical Results. Raw SPMD analytical results for the prototype mat system collected during the first round (December 2008) and second round (December 2009) of passive contaminant sampling are provided in Appendix F. Similar to the peeper data, non-detect results were substituted with one half the method detection limit (MDL) following standard USEPA protocol. A summary of the final Year One and Year Two SPMD data showing mean results for PAHs at each treatment is presented in Table 5.4-6. Hypothesis testing was conducted in the same manner as for the peeper analysis to determine whether observed reductions across the treatment boundaries were statistically significant. The results for the hypothesis testing of each PAH compound at each treatment are shown in Table 5.4-7.

As stated in Section 4.4.4, seven SPMDs from Year One experienced tearing with measurable water infiltration and/or oil loss during the deployment process, which in turn increased uncertainty in the analytical results. These samplers were heat sealed prior to extraction and extra care was taken during the analytical cleanup process to minimize the effects of oil carryover. Based on communication from the extraction laboratory, the impact of SPMD damage on final Year One analytical results was considered negligible within the scope of the overall dataset, especially since damaged replicates showed similar results when compared to pristine replicates from the same area. No SPMDs from Year Two experienced measurable water infiltration and/or oil loss. Thus potential SPMD damage had no effect on that dataset. The fact that the Year Two data showed similar trends to the Year One data despite significantly less damage further supports the conclusion that the effects of SPMD damage on the Year One dataset were minimal.

Table 5.4-6. Summary of first year (top) and second year (bottom) SPMD mean analytical results for all PAHs at the prototype mat system.

Year 1 SPMD Results: PAHs

		T1 - Mat Only		T2 - Mat w/ Sand		T3 - Double Mat			T4 - Sand Only		T5 - No Treatment
Analyte	Units	Below Treatment	Above Treatment	Below Treatment	Above Treatment	Below Treatment	Between Treatment	Above Treatment	Below Treatment	Above Treatment	Above Treatment
Naphthalene (L)	pg/L	N/A	N/A	N/A	N/A	N/A	N/A	N/A	N/A	N/A	N/A
Acenaphthylene (L)	pg/L	129	129	129	129	602	129	129	129	129	129
Acenaphthene (L)	pg/L	1203	295	6830	206	4890	88	283	543	236	271
Fluorene (L)	pg/L	1743	705	6060	665	5707	417	593	1138	858	1306
Phenanthrene (L)	pg/L	1508	1765	17508	1357	13254	935	2531	1512	1392	1596
Anthracene (L)	pg/L	476	234	2342	151	1452	62	182	224	151	177
Fluoranthene (H)	pg/L	3302	4279	9674	2636	9519	912	4310	2171	2822	3256
Pyrene (H)	pg/L	3725	4732	10562	2928	10902	1046	4627	3059	3294	3634
Benzo(a)anthracene (H)	pg/L	539	589	1915	404	2148	178	507	448	511	630
Chrysene (H)	pg/L	595	923	2263	443	2143	253	1033	470	623	683
Benzo(b)fluoranthene	pg/L	856	1042	1450	817	1950	363	946	829	817	925
Benzo(k)fluoranthene	pg/L	324	553	647	451	847	173	557	424	522	573
Benzo(a)pyrene (H)	pg/L	223	225	549	175	598	72	187	290	427	343
Indeno(1,2,3-c,d)pyrene	pg/L	212	238	287	206	364	97	218	214	194	251
Dibenzo(a,h)anthracene (H)	pg/L	91	84	136	78	267	58	99	64	84	96
Benzo(g,h,i)perylene	pg/L	326	337	470	295	625	126	309	309	281	358
Total LMW PAHs	pg/L	5060	3128	32869	2509	25905	1632	3719	3545	2766	3480
Total HMW PAHs	pg/L	8476	10832	25099	6664	25578	2519	10763	6501	7761	8641
Total LMW+HMW PAHs	pg/L	13536	13961	57968	9173	51483	4151	14482	10046	10527	12121

Year 2 SPMD Results: PAHs

		T1 - Mat Only		T2 - Mat w/ Sand		T3 - Double Mat			T4 - Sand Only		T5 - No Treatment
Analyte	Units	Below Treatment	Above Treatment	Below Treatment	Above Treatment	Below Treatment	Between Treatment	Above Treatment	Below Treatment	Above Treatment	Above Treatment
Naphthalene (L)	pg/L	N/A	N/A	N/A	N/A	N/A	N/A	N/A	N/A	N/A	N/A
Acenaphthylene (L)	pg/L	327	256	404	232	260	129	355	129	129	177
Acenaphthene (L)	pg/L	2862	299	4119	330	1309	87	259	227	325	232
Fluorene (L)	pg/L	2736	495	3483	723	3003	167	464	873	896	715
Phenanthrene (L)	pg/L	6313	2697	8574	1639	4287	761	2697	1314	1473	1590
Anthracene (L)	pg/L	1150	228	1286	208	932	65	218	248	238	279
Fluoranthene (H)	pg/L	8379	7752	9566	4222	8478	1122	8082	3925	4189	5509
Pyrene (H)	pg/L	3922	3171	4589	1863	4172	567	3560	1697	1863	2420
Benzo(a)anthracene (H)	pg/L	1273	619	1379	532	1166	191	776	473	512	607
Chrysene (H)	pg/L	1301	1348	1500	706	1099	220	1383	613	674	897
Benzo(b)fluoranthene	pg/L	997	975	1223	771	1472	305	1454	869	1068	1090
Benzo(k)fluoranthene	pg/L	567	680	655	505	642	193	713	459	451	588
Benzo(a)pyrene (H)	pg/L	355	195	421	182	365	69	219	166	174	336
Indeno(1,2,3-c,d)pyrene	pg/L	112	101	206	137	224	62	193	138	146	172
Dibenzo(a,h)anthracene (H)	pg/L	46	46	92	46	84	46	46	46	46	46
Benzo(g,h,i)perylene	pg/L	228	165	358	235	351	105	269	231	225	269
Total LMW PAHs	pg/L	13387	3975	17866	3132	9790	1208	3992	2790	3061	2993
Total HMW PAHs	pg/L	15276	13129	17548	7552	15364	2215	14066	6921	7459	9815
Total LMW+HMW PAHs	pg/L	28663	17105	35413	10684	25155	3424	18058	9711	10520	12808

N/A = Data not available.

Table 5.4-7. Results of hypothesis testing to determine the statistical significance of contaminant reductions across treatment boundaries for PAHs at the prototype mat system.

Significance Level: Alpha = 0.05
Null Hypothesis: Above Treatment >= Below Treatment (p-value > 0.05)
Alternative Hypothesis: Above Treatment < Below Treatment (p-value < 0.05)

	T1 - Mat Only				T2 - Mat w/ Sand				T3 - Double Mat (Below to Between)			
Analyte	Replicate Variance (n=3)	p-value	Reject Null? (Above < Below)	Conclusion Explanation	Replicate Variance (n=3)	p-value	Reject Null? (Above < Below)	Conclusion Explanation	Replicate Variance (n=3)	p-value	Reject Null? (Above < Below)	Conclusion Explanation
Year 1 Peeper Results												
Naphthalene (L)	EQUAL	N/A	NO	a	EQUAL	N/A	NO	a	EQUAL	N/A	NO	a
Acenaphthylene (L)	EQUAL	N/A	NO	a	EQUAL	N/A	NO	a	EQUAL	0.187	NO	c
Acenaphthene (L)	UNEQUAL	0.225	NO	c	UNEQUAL	0.078	NO	c	EQUAL	0.154	NO	c
Fluorene (L)	EQUAL	0.064	NO	c	UNEQUAL	0.094	NO	c	UNEQUAL	0.102	NO	c
Phenanthrene (L)	UNEQUAL	0.633	NO	b	UNEQUAL	0.103	NO	c	UNEQUAL	0.158	NO	c
Anthracene (L)	EQUAL	0.168	NO	c	UNEQUAL	0.117	NO	c	UNEQUAL	0.162	NO	c
Fluoranthene (H)	EQUAL	0.761	NO	b	UNEQUAL	0.138	NO	c	UNEQUAL	0.142	NO	c
Pyrene (H)	EQUAL	0.736	NO	b	UNEQUAL	0.131	NO	c	UNEQUAL	0.140	NO	c
Benzo(a)anthracene (H)	EQUAL	0.592	NO	b	UNEQUAL	0.148	NO	c	UNEQUAL	0.118	NO	c
Chrysene (H)	EQUAL	0.957	NO	b	EQUAL	0.101	NO	c	UNEQUAL	0.121	NO	c
Benzo(b)fluoranthene	EQUAL	0.726	NO	b	UNEQUAL	0.228	NO	c	EQUAL	0.030	YES	d
Benzo(k)fluoranthene	UNEQUAL	0.870	NO	b	UNEQUAL	0.273	NO	c	EQUAL	0.023	YES	d
Benzo(a)pyrene (H)	EQUAL	0.508	NO	b	UNEQUAL	0.160	NO	c	UNEQUAL	0.125	NO	c
Indeno(1,2,3-c,d)pyrene	EQUAL	0.619	NO	b	UNEQUAL	0.273	NO	c	EQUAL	0.028	YES	d
Dibenzo(a,h)anthracene (H)	EQUAL	0.440	NO	c	EQUAL	0.179	NO	c	EQUAL	0.145	NO	c
Benzo(g,h,i)perylene	EQUAL	0.537	NO	b	UNEQUAL	0.232	NO	c	EQUAL	0.035	YES	d
Total LMW PAHs	EQUAL	0.171	NO	c	UNEQUAL	0.097	NO	c	UNEQUAL	0.152	NO	c
Total HMW PAHs	EQUAL	0.751	NO	b	UNEQUAL	0.135	NO	c	UNEQUAL	0.135	NO	c
Total LMW+HMW PAHs	EQUAL	0.533	NO	b	UNEQUAL	0.112	NO	c	UNEQUAL	0.144	NO	c
Year 2 Peeper Results												
Naphthalene (L)	EQUAL	N/A	NO	a	EQUAL	N/A	NO	a	EQUAL	N/A	NO	a
Acenaphthylene (L)	EQUAL	0.376	NO	c	EQUAL	0.082	NO	c	EQUAL	0.060	NO	c
Acenaphthene (L)	UNEQUAL	0.156	NO	c	UNEQUAL	0.097	NO	c	EQUAL	0.067	NO	c
Fluorene (L)	UNEQUAL	0.122	NO	c	UNEQUAL	0.097	NO	c	UNEQUAL	0.051	NO	c
Phenanthrene (L)	UNEQUAL	0.258	NO	c	UNEQUAL	0.183	NO	c	UNEQUAL	0.071	NO	c
Anthracene (L)	UNEQUAL	0.166	NO	c	UNEQUAL	0.137	NO	c	UNEQUAL	0.048	YES	d
Fluoranthene (H)	UNEQUAL	0.477	NO	c	UNEQUAL	0.139	NO	c	EQUAL	0.015	YES	d
Pyrene (H)	EQUAL	0.366	NO	c	UNEQUAL	0.130	NO	c	UNEQUAL	0.041	YES	d
Benzo(a)anthracene (H)	UNEQUAL	0.232	NO	c	UNEQUAL	0.132	NO	c	EQUAL	0.019	YES	d
Chrysene (H)	UNEQUAL	0.522	NO	b	UNEQUAL	0.183	NO	c	EQUAL	0.501	NO	c
Benzo(b)fluoranthene	EQUAL	0.479	NO	c	EQUAL	0.034	YES	d	EQUAL	0.006	YES	d
Benzo(k)fluoranthene	EQUAL	0.691	NO	b	UNEQUAL	0.180	NO	c	UNEQUAL	0.019	YES	d
Benzo(a)pyrene (H)	UNEQUAL	0.238	NO	c	UNEQUAL	0.117	NO	c	EQUAL	0.006	YES	d
Indeno(1,2,3-c,d)pyrene	EQUAL	0.433	NO	c	EQUAL	0.022	YES	d	EQUAL	0.005	YES	d
Dibenzo(a,h)anthracene (H)	EQUAL	N/A	NO	a	EQUAL	0.063	NO	c	EQUAL	0.065	NO	c
Benzo(g,h,i)perylene	EQUAL	0.291	NO	b	EQUAL	0.031	YES	d	EQUAL	0.007	YES	d
Total LMW PAHs	UNEQUAL	0.199	NO	c	UNEQUAL	0.143	NO	c	UNEQUAL	0.031	YES	d
Total HMW PAHs	UNEQUAL	0.406	NO	c	UNEQUAL	0.139	NO	c	EQUAL	0.016	YES	d
Total LMW+HMW PAHs	UNEQUAL	0.281	NO	c	UNEQUAL	0.141	NO	c	UNEQUAL	0.035	YES	d

Table 5.4.7. Continued.

Analyte	T3 - Double Mat (Below to Above)				T4 - Sand Only			
	Replicate Variance (n=3)	p-value	Reject Null? (Above < Below)	Conclusion Explanation	Replicate Variance (n=3)	p-value	Reject Null? (Above < Below)	Conclusion Explanation
Year 1 Peeper Results								
Naphthalene (L)	EQUAL	N/A	NO	a	EQUAL	N/A	NO	a
Acenaphthylene (L)	EQUAL	0.187	NO	c	EQUAL	N/A	NO	a
Acenaphthene (L)	UNEQUAL	0.190	NO	c	UNEQUAL	0.166	NO	c
Fluorene (L)	UNEQUAL	0.107	NO	c	EQUAL	0.078	NO	c
Phenanthrene (L)	UNEQUAL	0.184	NO	c	EQUAL	0.348	NO	c
Anthracene (L)	UNEQUAL	0.179	NO	c	EQUAL	0.103	NO	c
Fluoranthene (H)	UNEQUAL	0.237	NO	c	EQUAL	0.897	NO	b
Pyrene (H)	UNEQUAL	0.225	NO	c	EQUAL	0.629	NO	b
Benzo(a)anthracene (H)	UNEQUAL	0.149	NO	c	EQUAL	0.735	NO	b
Chrysene (H)	UNEQUAL	0.218	NO	c	EQUAL	0.985	NO	b
Benzo(b)fluoranthene	UNEQUAL	0.114	NO	c	EQUAL	0.476	NO	c
Benzo(k)fluoranthene	UNEQUAL	0.160	NO	c	EQUAL	0.798	NO	b
Benzo(a)pyrene (H)	UNEQUAL	0.169	NO	c	EQUAL	0.790	NO	b
Indeno(1,2,3-c,d)pyrene	EQUAL	0.096	NO	c	EQUAL	0.342	NO	c
Dibenzo(a,h)anthracene (H)	UNEQUAL	0.661	NO	c	EQUAL	0.741	NO	b
Benzo(g,h,i)perylene	UNEQUAL	0.118	NO	c	UNEQUAL	0.334	NO	c
Total LMW PAHs	UNEQUAL	0.168	NO	c	EQUAL	0.143	NO	c
Total HMW PAHs	UNEQUAL	0.217	NO	c	EQUAL	0.839	NO	b
Total LMW+HMW PAHs	UNEQUAL	0.189	NO	c	EQUAL	0.622	NO	b
Year 2 Peeper Results								
Naphthalene (L)	EQUAL	N/A	NO	a	EQUAL	N/A	NO	a
Acenaphthylene (L)	EQUAL	0.874	NO	b	EQUAL	N/A	NO	a
Acenaphthene (L)	UNEQUAL	0.124	NO	c	EQUAL	0.792	NO	b
Fluorene (L)	UNEQUAL	0.061	NO	c	UNEQUAL	0.544	NO	b
Phenanthrene (L)	EQUAL	0.174	NO	c	EQUAL	0.789	NO	b
Anthracene (L)	UNEQUAL	0.068	NO	c	EQUAL	0.411	NO	c
Fluoranthene (H)	UNEQUAL	0.437	NO	c	EQUAL	0.681	NO	b
Pyrene (H)	UNEQUAL	0.322	NO	c	EQUAL	0.717	NO	b
Benzo(a)anthracene (H)	EQUAL	0.144	NO	c	EQUAL	0.739	NO	b
Chrysene (H)	EQUAL	0.834	NO	b	EQUAL	0.745	NO	b
Benzo(b)fluoranthene	EQUAL	0.481	NO	c	EQUAL	0.810	NO	b
Benzo(k)fluoranthene	EQUAL	0.970	NO	b	EQUAL	0.410	NO	c
Benzo(a)pyrene (H)	EQUAL	0.051	NO	c	EQUAL	0.710	NO	b
Indeno(1,2,3-c,d)pyrene	EQUAL	0.196	NO	c	EQUAL	0.685	NO	b
Dibenzo(a,h)anthracene (H)	EQUAL	0.065	NO	c	EQUAL	N/A	NO	a
Benzo(g,h,i)perylene	EQUAL	0.072	NO	c	EQUAL	0.338	NO	c
Total LMW PAHs	UNEQUAL	0.062	NO	c	EQUAL	0.789	NO	b
Total HMW PAHs	UNEQUAL	0.387	NO	c	EQUAL	0.704	NO	b
Total LMW+HMW PAHs	UNEQUAL	0.185	NO	c	EQUAL	0.760	NO	b

Conclusion Explanation:

a - Analyte not detected in sediment porewater (below treatment); no contamination to be treated.

b - Below treatment mean concentration not greater than above treatment mean concentration; potential non-treatment influences.

c - Below treatment mean concentration greater than above treatment mean concentration but reduction not statistically significant.

d - Below treatment mean concentration greater than above treatment mean concentration and reduction is statistically significant.

Key summary plots for one low molecular weight PAH (anthracene) and one high molecular weight PAH (benzo[a]anthracene) showing average concentrations above (yellow), between (red) and below (blue) treatment boundaries are provided in Figure 5.4-5. Findings from the SPMD dataset included the following:

- All above-treatment samples replicated well and indicated contaminant concentrations comparable to the control area.
- Hypothesis testing on the full dataset indicated that of all the analytes that satisfied the test conditions described above (*i.e.*, excluding conclusions "a" and "b" in Table 5.4-7), only benzo[b]fluoranthene, indeno(1,2,3-c,d)pyrene and benzo(g,h,i)perylene in area T2 showed statistically significant concentration reductions across the treatment boundary from below to above (*i.e.*, conclusion "d" in Table 5.4-7). In addition, several PAHs including totals showed statistically significant reductions in area T3 (double mat) from below the mats to between the mats, suggesting that the double mat array sequesters contaminant contributions emanating from both below and above the treatment. All other analytes satisfying the test conditions showed some reduction of mean concentrations, but replicate data was insufficient to prove that these reductions were significant. However, changing the significance level of the hypothesis test by reducing the confidence coefficient from 95% to 90% (alpha = 0.1) would also demonstrate significant reductions for several additional PAHs in areas T2 and T3.
- The single mat with sand cap (T2) and double mat (T3) treatments achieved five to six times greater contaminant sequestration (below vs. above mat concentration).
- Reduced PAH concentrations in the middle layer of the double mat treatment (T3) confirms the efficacy of the mats in reducing flux of chemical from either sediment or surface water sources.
- Treatment effectiveness was comparable for both low and high molecular weight compounds.
- Effectiveness of mat only (T1) and sand only (T4) treatments in sequestering PAHs could not be assessed as below treatment concentrations were not different from surface water.

Overall, the SPMD deployments were fully effective in measuring changes in chemical gradients of PAHs as a function of various test treatments. Conclusions generated from the SPMD data indicated that the deployment configuration of a single layer geotextile mat with sand capping (T2) could be an effective means of reducing PAH exposure in the surface sediments. Patterns observed were generally comparable to metals findings indicating similar groundwater flux processes at each of the treatments.

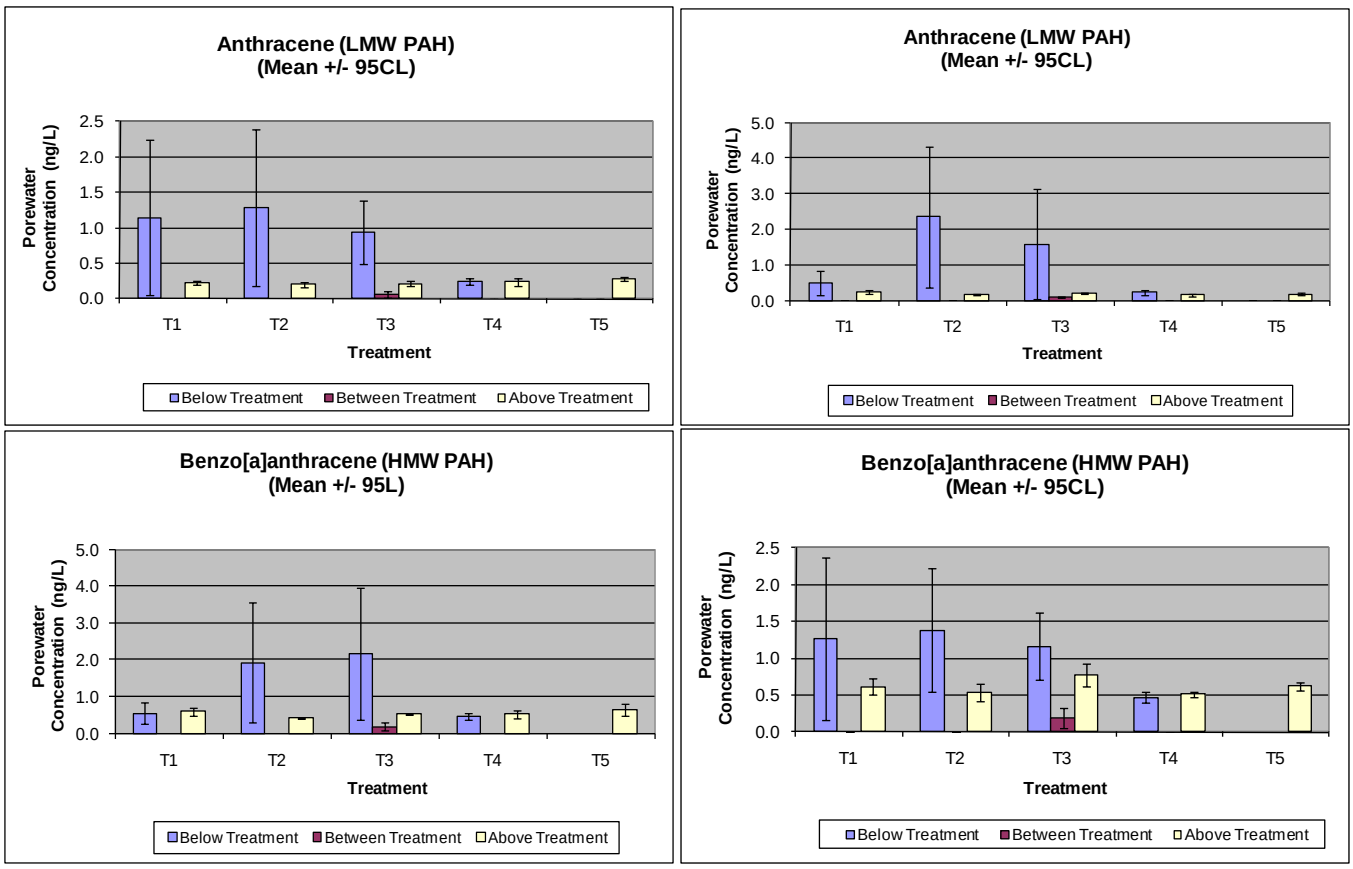

Figure 5.4-5 First year (left column) and second year (right column) SPMD analytical results for select low molecular weight (anthracene), high molecular weight (benzo[a]anthracene) and total PAHs at the prototype mat system.

SPME Analytical Results. Because the entire SPME dataset for the prototype mat system was non-detect (*i.e.*, concentrations < 5 µg/L), no conclusions could be generated from this sampling method regarding the success of the various treatments in sequestering PAH contaminants. The SPME results were not tabulated and are not included in this report. The lack of adequate exposure concentrations for measurable uptake by SPME fibers is consistent with the historical data used in the study design which suggests elevated sediment PAH concentrations (*i.e.*, 2000 ng/g BaP = 0.2 µg/L @ 1% TOC), but at concentrations below SPME detection.

Discussion. Final passive sampler data showed that contaminant sequestering trends, in terms of above versus below treatment concentrations, were generally consistent for metals and PAHs in each of the five treatment areas. Statistically significant retardation of chemical flux for both metals (*e.g.*, nickel, zinc) and PAHs (*e.g.*, anthracene, benzo[a]anthracene) by the mats was indicated by statistically higher (non-overlapping 95% UCL bars) contaminant concentrations maintained immediately beneath the mat than above the mat. These contaminant treatment/sequestration results were particularly relevant for the mat/sand (T2) and double mat (T3) treatments. Additional evidence of mat performance was also revealed by in porewater contaminants observed between mat layers in the double mat treatment (T3), the reductions being significantly ($p = 0.05$) less than background sediment or water column concentrations.

The repeatability of results between sampling years provided additional certainty in reliable performance, at least over the two year duration of the tests.

In general, greater porewater concentration gradients were maintained by mats with a cover (*e.g.*, sand in area T2 or another mat in area T3). This effect was attributed to better bottom contact compared to the other treatments where methane gas releases from the sediment below the treatment was observed to cause gas uplift of a single mat. Such mat uplift likely allowed the advecting porewater chemicals to be diluted by surface water under the floating mat. In contrast to the mats, the sand-only treatment did not exhibit a similar porewater concentration gradient, though this effect may have been due to the thin sand layer applied and/or overall lower porewater concentrations within the sediments being capped (*i.e.*, same as the water column concentration). From these results, it can be concluded that the reactive mat technology, when deployed with sufficient weighting (*e.g.*, sand cover), is an effective technology for sequestering contaminants in sediments.

5.4.3 Volumetric Sampling Results

Volumetric sampling conducted at the prototype mat system included passive flow sampling using Ultraseep technology as well as active draw sampling using the Trident Probe. The concurrent use of these two sampling techniques was designed to provide a comparison between groundwater-mediated contaminant concentrations passing upward through the various mat treatments and contaminant concentrations in porewater at various layers beneath the treatments.

Trident Probe Analytical Results. The ultimate goal of the Trident Probe effort was to collect porewater samples from various target treatment layers (*e.g.*, deep sediment, shallow sediment, mat interface, sand cap, overlying water). Whereas vertical sampling using the vertical peeper arrays was only previously conducted in non-mat areas, the three-pronged Trident Probe was inserted through the mat layers (via surgical cuts made by divers at appropriate locations) to simultaneously collect samples from three depths. Based on the limitations of the Trident Probe hardware, the final sample depths were 2 inches above the treatment interface, 3.5 inches below the treatment interface, 11 inches below the treatment interface and 24 inches below the treatment interface (in select areas only). Similar to the Ultraseep sample analyses, Trident Probe porewater samples were analyzed only for metals because previous SPMD results indicated that organics concentrations would be significantly below detection limits that could be achieved with the volume of water likely to be collected by the sampler.

The Trident Probe data provided synoptic chemical gradients for metals and were used to validate the concentrations previously observed in the peepers. Raw analytical chemistry results from the Trident Probe samples are presented in Appendix H and summarized for metals of concern in Table 5.4-8. Because the Trident Probe base plate rested flat against the mat/sediment surface during sampling, the depths provided in this table represent sample location relative to the treatment-water interface and include the thickness of the mats where applicable (*e.g.*, T1, T2, T3). To determine absolute depth of each sample relative to the mud line, the thickness of a single mat (0.5") is subtracted from the sample depths in areas T1 and T2 and twice the thickness of a single mat (double mat; 1") is subtracted from the sample depths in area T3.

Graphical results for nickel showing porewater concentrations drawn directly from various horizons at each mat system treatment represent the common trends in the Trident Probe data (Figure 5.4-6). Results of the Trident Probe measurements in general revealed substantial reductions in metals concentrations below mats (T1-T3) as well as the sand cover (T4) as compared to the control treatment (Figure 5.4-7). This finding demonstrates that only a thin layer of sand will act as a vertical barrier to porewater advection (10-20X reduction) and allows diffusion to dominate the exchange process, which is the basis for the predicted effectiveness of thin layer capping in low advection environments. However, the addition of mats shows that the reactive materials will sequester the metals to a far greater extent (80-300X reduction) and thus provide a far more effective barrier. This effect was noted in SERDP project ER-1501 and described as the amendment-induced "zone-of-influence" (Knox *et al.* 2011). As a result, porewater containing PAHs (*e.g.*, benzo(a)anthracene) and metals (*e.g.*, zinc) does not readily escape the cap, though perhaps a trend of slightly higher above treatment values is observed relative to the no cap control (Figure 5.4-3). This interpretation is corroborated by further concentration reductions observed in porewater samples taken between mat layers of treatment T3 at which measured levels were typically less than respective background and water column concentrations. Meanwhile, a concentration gradient was not established in the control treatment because the diffusion process allows rapid equilibrium with the overlying surface water. These results also indicate that isolation of the above treatment samples from the surface water is needed to detect the cap sequestration effectiveness, particularly in low concentration, low advection environments. Overall findings from the Trident Probe dataset include the following:

- Large reservoirs of metals existed within the deeper, subsurface sediments (>11") for all treatment locations.
- Concentrations in shallow sediments (< 3") appeared to be depressed in the treatment areas (T1, T2, T3, T4) relative to the control location (T5).
- Trident Probe data were generally corroborated by peeper measurements; nickel occurred at 4-8 µg/L in the treatment areas (0-2" data not available for the control).
- Chemical gradients observed in Trident Probe data indicated reductions in metals concentrations below reactive mats 6-8X higher than the sand cap only treatment. This reduction may be due to a "halo" effect wherein porewater metals (and presumably organics) are sequestered into the amendment cap at depths deeper than the point of physical contact, possibly due to diffusion.

Table 5.4-8. Summary of Trident Probe mean analytical results for all metals of concern at the prototype mat system.

Trident Probe Data: Metals
Treatment Summary - Replicate Averages

		T1 - Mat Only			T2 - Mat w/ Sand			T3 - Double Mat			
Analyte	Units	Below Trtmnt -11 in	Below Trtmnt -3.5 in	Above Trtmnt +2 in	Below Trtmnt -11 in	Below Trtmnt -3.5 in	Above Trtmnt +2 in	Below Trtmnt -11 in	Below Trtmnt -3.5 in	Btwn Trtmnt +0 in	Above Trtmnt +2 in
Arsenic (As)	ug/L	38	6.9	6.9	38	48	6.9	42	6.9	6.9	6.9
Barium (Ba)	ug/L	408	50	42	440	231	40	507	79	68	39
Cadmium (Cd)	ug/L	54	0.156	0.286	65	0.772	0.156	77	0.156	0.489	0.156
Chromium (Cr)	ug/L	1128	2.1	4.2	1608	2.1	2.0	1797	2.2	7.6	3.4
Copper (Cu)	ug/L	212	1.6	2.8	227	1.4	2.0	290	2.2	3.8	3.1
Lead (Pb)	ug/L	290	3.5	3.5	261	3.5	3.5	336	3.5	3.5	3.5
Nickel (Ni)	ug/L	79	1.3	2.1	75	1.6	1.7	111	3.4	2.4	1.9
Silver (Ag)	ug/L	1.5	0.206	0.206	2.0	0.206	0.206	2.3	0.206	0.206	0.206
Vanadium (V)	ug/L	133	1.6	5.2	94	1.3	4.1	146	1.0	5.1	4.8
Zinc (Zn)	ug/L	727	8.2	11	619	10	9.7	856	28	23	18

		T4 - Sand Only				T5 - No Treatment			
Analyte	Units	Below Trtmnt -24 in	Below Trtmnt -11 in	Below Trtmnt -3.5 in	Above Trtmnt +2 in	Below Trtmnt -24 in	Below Trtmnt -11 in	Below Trtmnt -3.5 in	Above Trtmnt +2 in
Arsenic (As)	ug/L	89	25	30	6.9	52	51	78	6.9
Barium (Ba)	ug/L	1118	307	891	38	1073	822	960	38
Cadmium (Cd)	ug/L	475	10.0	0.569	0.156	81	386	59	0.156
Chromium (Cr)	ug/L	50000	232	2.9	2.8	812	7317	902	3.7
Copper (Cu)	ug/L	592	40	1.6	3.3	250	546	397	3.0
Lead (Pb)	ug/L	675	47	3.5	3.5	144	495	471	3.5
Nickel (Ni)	ug/L	139	18	1.6	1.3	117	109	166	2.5
Silver (Ag)	ug/L	4.0	0.575	0.206	0.206	1.1	1.1	0.69	0.206
Vanadium (V)	ug/L	187	25	2.8	4.5	404	116	368	4.4
Zinc (Zn)	ug/L	2700	143	9.4	11	468	1744	1926	7.6

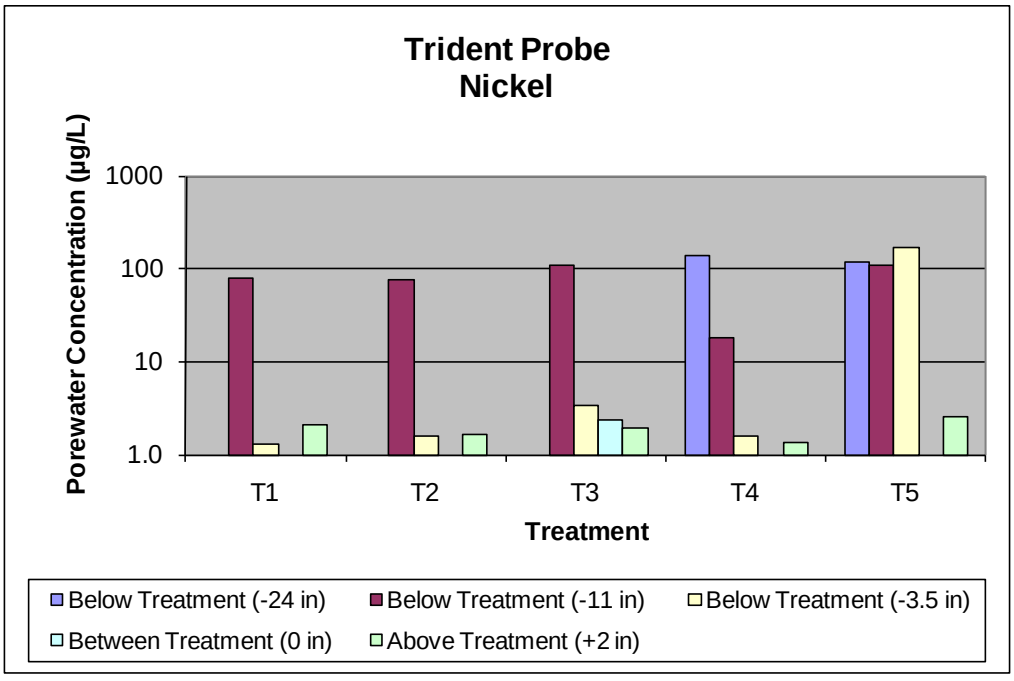

Figure 5.4-6. Trident Probe analytical results for a select metal (nickel) at the prototype mat system relative to the treatment-water interface (thickness of mat included where applicable).

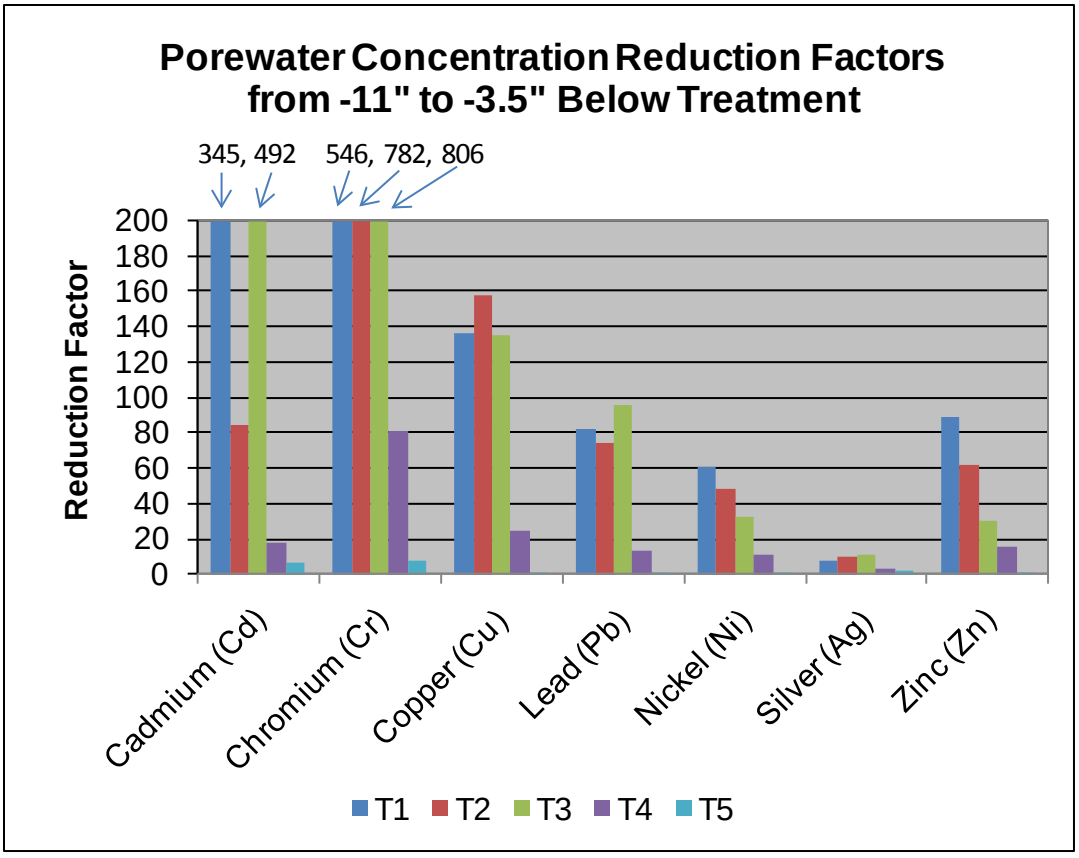

Figure 5.4-7. Reduction factors for deep (-11") versus shallow (-3.5", directly below treatment) porewater concentrations for various metals below the mat system treatments as measured by the Trident Probe.

Ultraseep Analytical Results. The ultimate goal of the Ultraseep measurements was to directly quantify the groundwater-mediated transport of contaminants upward through the various treatments. Because the SPMD approach quantified PAH concentrations at very low concentrations (*i.e.*, pg/L), analyzing Ultraseep groundwater samples for organics was deemed impractical (*i.e.*, a large volume of water, >100 L, would be required to achieve reliable detection limits). Thus the Ultraseep groundwater samples were analyzed only for metals. All electronic groundwater flux data and raw Ultraseep sample analytical results for the prototype mat system collected during the groundwater flow survey (June 2009) are presented in Appendix G. The mean analytical chemistry results for metals of concern at each treatment area are summarized in Table 5.4-9.

All tabulated results presented here for the Ultraseep technology reflect a "discharge fraction" calculation wherein the resulting metals concentrations for that sample are reflective of only the volume of porewater collected while flowing from the treatment (*i.e.*, the discharge; typically 0.1-1.0 L) and not the required volume of deionized water inside the Ultraseep machine (~0.5L) with which the environmental sample is mixed when sampling is initiated (Figure 5.4-8). Findings from the Ultraseep dataset shown in Figure 5.4-5 reveal the following: 1) Nickel: 30-115 µg/L; 2) Zinc: 45-135 µg/L; and 3) Copper: 10-105 µg/L. An inverse relationship

between discharge fraction and overall metal concentration is loosely apparent. As will be discussed below, observed Ultraseep are substantially higher that either peeper or trident data; this uncertainty is discussed in Section 5.4.5, below.

Table 5.4-9. Summary of Ultraseep mean analytical results for all metals of concern at the prototype mat system adjusted to reflect the discharge sample.

Ultraseep Sample Results: Metals
Treatment Summary - Replicate Averages

Analyte	Units	T1 - Mat Only Average	T2 - Mat w/ Sand Average	T3 - Double Mat Average	T4 - Sand Only Average	T5 - No Treatment Average
Arsenic (As)	ug/L	41	111	39	40	70
Barium (Ba)	ug/L	238	485	191	295	373
Cadmium (Cd)	ug/L	0.924	2.5	0.889	0.894	1.6
Chromium (Cr)	ug/L	6.7	22	5.8	4.7	9.2
Copper (Cu)	ug/L	13	107	13	10.0	16
Lead (Pb)	ug/L	21	57	20	20	36
Nickel (Ni)	ug/L	87	115	34	29	42
Silver (Ag)	ug/L	1.2	3.3	1.2	1.2	2.1
Vanadium (V)	ug/L	13	50	15	13	30
Zinc (Zn)	ug/L	114	135	80	47	98

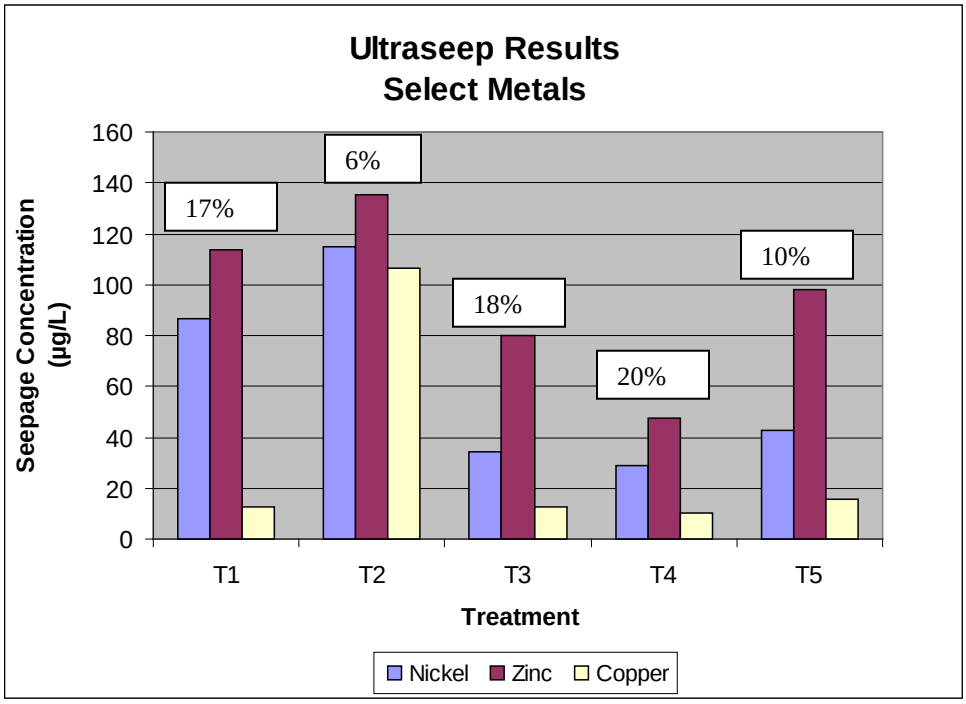

Figure 5.4-8. Ultraseep analytical results for select metals for the prototype mat system treatments. Discharge fraction (%) values indicated in text boxes (see text).

5.4.4 Sediment Coring

Mat System Sediment Data. The goal of the sediment coring effort was to collect sediment cores from each mat system treatment area and analyze the surface (0-4") and subsurface (4-8") intervals for characterization of the natural sediment and confirmation of the potential chemical flux through the various mat/sand layers. The resulting sediment data were also used to calculate the approximate PAH porewater concentrations (via equilibrium-partitioning) and therefore validate the previous SPMD results as well as partly address the data gap left by absence of Ultraseep and Trident Probe organics data. Sediment core locations, photos and raw analytical chemistry data are provided in Appendix I. A summary of the sediment core chemistry results for non-lithogenic metals of concern and PAHs at each treatment is presented in Table 5.4-10.

Table 5.4-10. Summary of sediment core chemistry for all metals of concern and PAHs at the prototype mat system.

Sediment Core Analytical Results

		T1 - Mat Only		T2 - Mat w/ Sand		T3 - Double Mat		T4 - Sand Only		T5 - No Treatment		T0 - Between Treatments	
Analyte	Units	Surface (0-4 in)	Subsurface (4-8 in)	Surface (0-4 in)	Subsurface (4-8 in)	Surface (0-4 in)	Subsurface (4-8 in)	Surface (0-4 in)	Subsurface (4-8 in)	Surface (0-4 in)	Subsurface (4-8 in)	Surface (0-4 in)	Subsurface (4-8 in)
Metals													
Arsenic	mg/kg	11	10	10	9.5	9.5	9.3	4.2	8	10	9.9	8.8	8.4
Barium	mg/kg	120	120	120	110	110	110	57	100	110	120	110	110
Cadmium	mg/kg	4.7	6.2	4.7	5.9	4.2	5.1	1.9	4.7	4.6	5.9	4.2	4.7
Chromium	mg/kg	190	270	180	250	170	210	75	190	190	240	170	190
Copper	mg/kg	38	37	36	38	34	35	16	32	37	39	34	35
Lead	mg/kg	60	72	63	68	56	65	25	58	64	72	54	61
Mercury	mg/kg	0.16	0.2	0.15	0.19	0.16	0.19	0.07	0.17	0.17	0.18	0.14	0.17
Nickel	mg/kg	35	32	32	32	31	31	14	27	33	34	30	30
Silver	mg/kg	3.4	4.5	3.7	4.1	2.8	3.8	1.2	3.3	3.1	4	2.9	3.3
Vanadium	mg/kg	41	36	39	35	35	37	16	29	39	37	33	34
Zinc	mg/kg	220	190	200	200	200	190	91	170	210	220	200	190
Polycyclic Aromatic Hydrocarbons													
Naphthalene (L)	ug/kg	11	9.0	11	8.7	11	9.3	5.8	7.4	11	9.0	10	8.7
Acenaphthylene (L)	ug/kg	11	9.0	11	8.7	11	9.3	5.8	7.4	11	9.0	10	8.7
Acenaphthene (L)	ug/kg	29	29	30	24	23	31	5.8	28	28	26	39	25
Fluorene (L)	ug/kg	23	25	23	18	11	24	5.8	21	11	23	31	19
Phenanthrene (L)	ug/kg	440	430	450	360	390	430	170	400	390	470	550	320
Anthracene (L)	ug/kg	73	51	82	67	81	80	31	73	70	81	110	46
Fluoranthene (H)	ug/kg	0.0	9.0	2300	1800	1500	1700	640	1600	1300	1800	1100	1500
Pyrene (H)	ug/kg	0.0	9.0	1700	1400	1000	1200	400	1100	960	1200	770	1000
Benzo[a]anthracene (H)	ug/kg	690	860	1000	840	710	730	260	680	620	820	490	530
Chrysene (H)	ug/kg	710	930	1100	910	730	880	270	780	660	890	550	540
Benzo[b]fluoranthene	ug/kg	0.0	890	1100	860	820	1000	340	790	790	860	490	710
Benzo[k]fluoranthene	ug/kg	550	880	1100	860	620	590	230	700	630	770	480	520
Benzo[e]pyrene	ug/kg	0.0	9.0	1400	1100	850	1000	350	1000	810	1100	710	860
Benzo[a]pyrene (H)	ug/kg	710	9.0	1000	830	680	740	280	720	690	760	480	590
Indeno[1,2,3-cd]pyrene	ug/kg	570	700	770	630	540	700	220	590	560	670	690	430
Dibenz[a,h]anthracene (H)	ug/kg	180	270	230	190	180	220	68	220	180	240	240	140
Benzo[g,h,i]perylene	ug/kg	550	640	690	560	450	600	190	610	480	630	700	390
2-Methylnaphthalene (L)	ug/kg	11	9.0	11	8.7	11	9.3	5.8	7.4	11	9.0	10	8.7
Total LMW PAHs	ug/kg	598	562	617	495	537	593	230	544	531	627	761	436
Total HMW PAHs	ug/kg	2290	2087	7330	5970	4800	5470	1918	5100	4410	5710	3630	4300
Total LMW+HMW PAHs	ug/kg	2888	2649	7947	6465	5337	6063	2148	5644	4941	6337	4391	4736

Graphical results for select metals (nickel, copper, zinc) and PAHs (anthracene, benzo[a]anthracene) showing sediment concentrations in each horizon for the various treatment areas are provided in Figure 5.4-9. Because zinc concentrations were fundamentally greater than nickel and copper, these values were divided by ten in order to allow all data to be plotted on the same axis. Stand-alone findings from the sediment core dataset included the following:

- Metals (nickel, copper, zinc) and PAHs (anthracene, benzo[a]anthracene) in surface (solid bars) and subsurface (shaded bars) sediments generally showed greater than two times the range in concentration across treatment areas (note T4 surface includes 3" sand cap and 1" of underlying surface sediment) (Figure 5.4-9).
- Concentration gradients were generally not observed in surface versus subsurface sediments, suggesting that the more variable porewater concentrations are likely driven by partitioning dynamics (*e.g.*, TOC concentration) and not bulk chemical concentration.

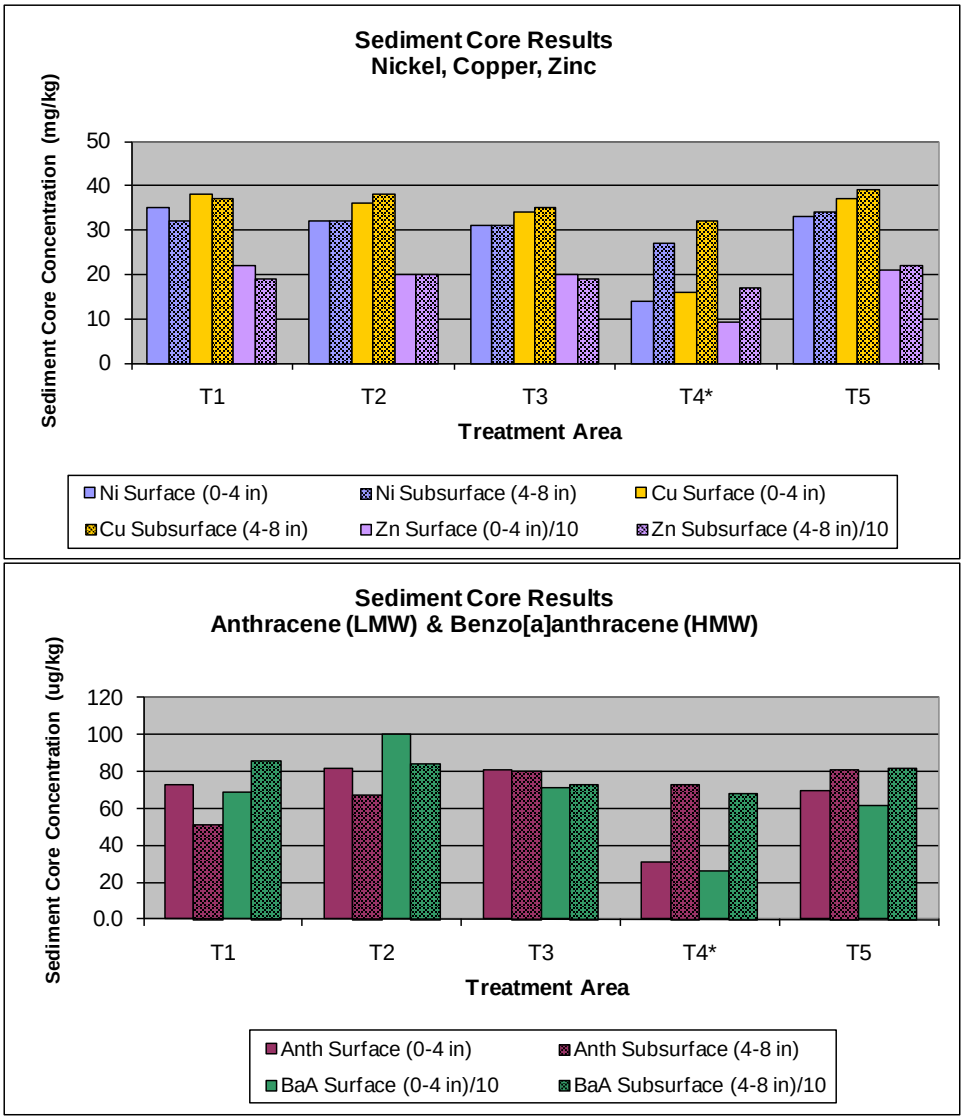

*****_For area T4, the 0-4 in horizon represents predominantly the sand cap material and the 4-8 in horizon represents the natural sediment comparable to the surface horizon in other areas._

Figure 5.4-9. Sediment core analytical results in surface (0-4") and subsurface (4-8") layers for select metals (nickel, copper, zinc) and PAHs (anthracene, benzo[a]anthracene) at various treatments in the prototype mat system.

When jointly considering both the sediment core data and the diffusion sampler data, metals and PAHs in area T4 were found to have relatively lower (2-3X) concentrations in both the below and above treatment diffusion samples as compared to the other test areas (*e.g.*, nickel, zinc, PAHs; Figure 5.4-1). This trend cannot be explained by a lack of contaminant loading or partitioning as comparable surface sediment concentrations and TOC across all treatments were observed. The lack of vertical concentration trends across the cap suggests the thin cap layer did not sequester porewater constituents within the sediments and that equilibration across the cap may be occurring. It is notable that the observed background water column concentrations for nickel and zinc (see WC, Figure 5.4-1) trended higher than the above treatment concentrations, such that the observed patterns appear treatment-related and not due to background influences. Although the cap was constructed of fine-grained material of an appreciable (2-3") thickness, the overall binding capacity of the cap material and/or its porosity may not have been sufficient to provide a discrete buffer between the natural sediment and the overlying water column in the absence of a reactive mat.

5.4.5 Sources of Uncertainty

In order to reach a final evaluation of mat system performance, data from each of the subsequent sampling and monitoring events were integrated and reviewed concurrently to assess sources of uncertainty in the conclusions regarding mat performance. Cross-comparison of different datasets allowed for a valid assessment of the success of each specific mat/cap treatment in achieving contaminant flux and sequestration goals in context with the properties of the native sediment at the selected pilot site and the potential geophysical impacts of the treatment on the surrounding natural conditions.

Historic Sediment Data Comparison. Surface sediment data collected during the Year Two mat system monitoring process were compared to historic bulk surface sediment data for the general prototype mat system area in Cottonwood Bay collected during previous site evaluations in order to assess the consistency of current contaminant concentrations with historic conditions documented for the chosen pilot site. In order to perform this comparison, historic Cottonwood Bay sediment data provided by the USGS as described in First Year Annual Progress Report (NAVFAC 2006) were filtered to only include surface values from 1999 stations (Bay-7) and 1996 stations (M2.3, M2.4, M2.5, M2.7) in the immediate vicinity of the final mat system construction area. The average of these historic concentrations was then plotted against the average of the 2009 surface concentrations at five locations adjacent to the control area and mat system treatments (Figure 5.4-10). Sediment core data collected from area T4 were removed from the 2009 averages because surface subsample data from this point reflected mostly clean sand cap material and not natural sediment conditions.

Results indicated that historical (1996-1999) surface sediment contaminant concentrations in Cottonwood Bay were approximately twice that observed in 2009, suggesting natural attenuation through deposition of cleaner sediment has occurred over the past ten years. Such recent reduction in sediment values likely explain the low-level porewater concentrations observed in surface sediments as well as sharp increases in some metals with depth below. This phenomenon introduces extra sensitivity to the effect that placement/depth of diffusion samplers has on the apparent differences among the treatments.

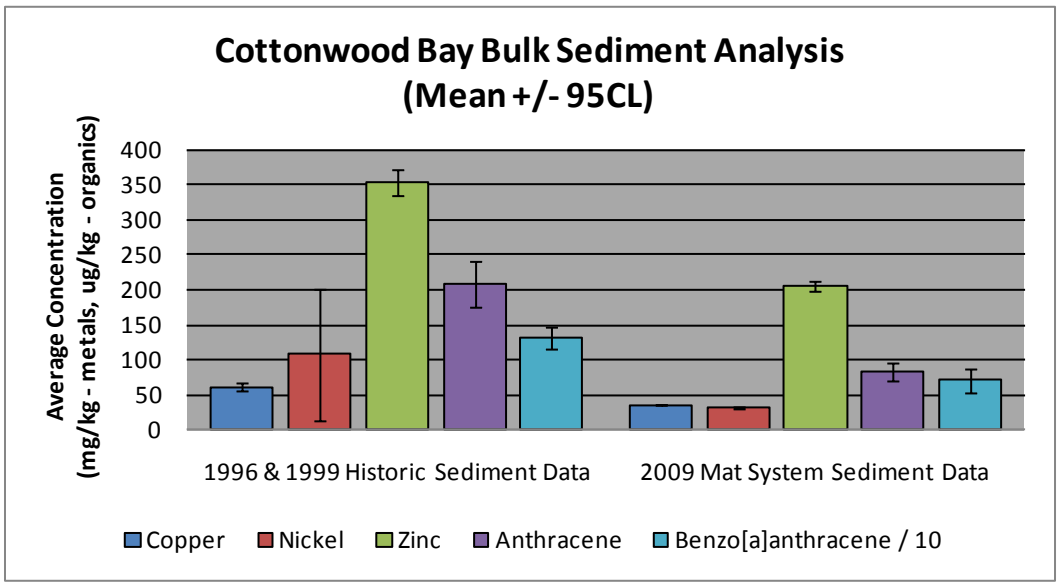

Figure 5.4-10. Historic and recent bulk sediment analytical results for select metals and organics at the prototype mat system area in Cottonwood Bay.

Porewater Monitoring Methodologies. Peeper, Trident Probe and Ultraseep porewater samples collected from the prototype mat system were all analyzed for metals by the same laboratory methodology. Representative results for zinc are tabulated in Table 5.4-11 including the "above treatment" measures for Ultraseep, Trident +2", and Peeper above treatment, as well as the "below treatment" measures consisting of the "peeper below treatment" and trident -3.5" values for comparison. Respective trident and peeper findings for each horizon which exhibited 3X agreement. In contrast, the Ultraseep concentrations were 10X higher than both of the above treatment results. Because this difference included both the sand-only and control areas, the observed trends do not appear to reflect upon mat performance. The explanation for this trend is unclear, but such enrichment could be related to minor amounts of turbidity retained in the samples.

Table 5.4-11. Ultraseep, deep Trident Probe and "below treatment" peeper results for zinc in the prototype mat system.

Analyte	Units	T1 Mat Only	T2 Mat w/ Sand	T3 Double Mat	T4 Sand Only	T5 No Treatment
Zinc						
Ultraseep	ug/L	114	135	80	47	98
Peeper Above Treatment (Year One)	ug/L	7.0	6.6	5.6	2.5	2.8
Trident Probe (+2 in)	ug/L	11	9.7	18	11	7.6
Peeper Below Treatment (Year One)	ug/L	15	24	33	2.4	N/A
Trident Probe (-3.5 in)	ug/L	8.2	10	28	9.4	1926

Low Contaminant Concentrations. Because porewater contaminant concentrations measured in the passive contaminant samplers (peepers for metals, SPMDs for PAHs) were substantially low compared to the expected contaminant concentrations based on historically documented site conditions, there was some uncertainty as to whether the chosen sampling techniques were

accurately quantifying current site contamination before and after treatment. In order to investigate this potential discrepancy, bulk sediment analyses were added to the second year passive contaminant sampling effort as described in Section 5.4.4. Results from these analyses proved that contaminant concentrations during the year two sampling event were significantly less than historic levels (see Figure 5.4-10), likely due to years of deposition on top of previous hotspots, and thus were accurately reflected by the sampler results. Furthermore, the relative contaminant trends observed in the surface sediment samples across treatments closely resembled the relative trends observed in the sampler data for both metals and organics, particularly for an increase in LMW PAHs in area T2 and a predictable contaminant void in the sand capping horizon in area T4. These correlations offers further evidence that passive sampler data were accurately documenting local contaminant conditions for the treatment areas relative to each other even if overall contaminant concentrations were within a range that made precise quantification difficult.

Variability in Contaminant Concentrations. The fact that porewater contaminant concentrations as determined by the various mat system sampling techniques (peepers, SPMDs, Ultraseep, Trident Probe) were relatively low (metals < 30 µg/L in peepers; PAHs < 5 ng/L in SPMDs) compared to what was expected at the Cottonwood Bay pilot site based on available historic data leads to the question of whether these samples reflect true differences in treatment effects or random variation in fine scale values. In order to address this question of true treatment effects versus random variation, passive contaminant sampling with peepers (metals) and SPMDs (PAHs) was repeated after one year to provide a second dataset featuring the same number of replicates designed to strengthen the overall conclusions. Reduction trends for select analytes in the Year Two data showed a strong correlation to trends in the Year One data across treatments (see Section 5.4.2); such replication suggests that the apparent effects of each treatment are true and not an artifact of random sample variation. Additionally, 95% upper confidence limit (UCL) and lower confidence limit (LCL) error bars added to the peeper and SPMD plots are often found to be non-overlapping or nearly so, which implies true statistical differences between treatments. Thus, generally speaking, adequate replication was performed in order to elucidate the treatment effects of interest.

Background Influences on Sample Data. Another point of uncertainty in the mat system sampling dataset was whether the "above treatment" samples were more reflective of the overlying water column (*i.e.*, background conditions) than the concentrations of chemicals in groundwater upwelling through the treatments. In order to test this hypothesis, an additional peeper was suspended in the water column during the second round of passive contaminant sampling and the resulting equilibrium concentrations were compared to the porewater data across the treatment interfaces from the same dataset (Table 5.4-12). Results show that background concentrations were less than or approximately equal to "above treatment" porewater values for the same analytes. For example, data from area T2 (mat with sand cap) showed that the "above treatment" concentrations for nickel and zinc were less than the "below treatment" concentrations but still greater than the water column concentrations, thus suggesting that the sand layer provided a buffer from the overlying water concentrations. A comparable relationship was also present but less evident for areas T1 (mat only) and T3 (double mat only) where the "above treatment" peepers were placed directly on top of the mat with no capping material to serve as a buffer between the treatment and the water column. Thus, influence of

background conditions on "above treatment" passive sampler responses does not appear problematic.

Table 5.4-12. Comparison of Year One and Year Two "above treatment" peeper concentrations with background water column peeper concentrations.

		T1 - Mat Only		T2 - Mat w/ Sand		T3 - Double Mat		T4 - Sand Only		T5 - No Treatment		Background
Analyte	Units	Above Treatment (Year 1)	Above Treatment (Year 2)	Above Treatment (Year 1)	Above Treatment (Year 2)	Above Treatment (Year 1)	Above Treatment (Year 2)	Above Treatment (Year 1)	Above Treatment (Year 2)	Above Treatment (Year 1)	Above Treatment (Year 2)	Water Column
Copper	ug/L	2.2	1.2	3.0	0.82	3.6	1.1	1.7	0.33	0.67	0.33	0.96
Nickel	ug/L	2.0	1.1	2.1	1.9	2.0	1.5	1.5	0.73	1.6	0.73	1.0
Zinc	ug/L	7.0	3.2	6.6	4.3	5.6	2.2	2.5	1.2	2.8	1.2	2.5

6.0 CONCLUSIONS AND IMPLICATIONS FOR FUTURE RESEARCH/IMPLEMENTATION

The overall project goal was to determine the most successful mat arrangement for sequestering contaminants. Based on the findings from these comprehensive studies, the reactive core mat technology has been determined to be effective at sequestering metals and PAH compounds in fine-grained sediments at a quiescent site with low groundwater flow. Therefore, it would be suitable to use the system for full-scale demonstration/validation under similar conditions. The combined results of the laboratory chemical and geotechnical testing, field mini-mat testing and finally mat prototype testing involving different reactive mat arrangements provide a solid foundation to support further expansion of testing in a pilot scale demonstration (*e.g.*, increase mat size tested from 400 ft^2 to 10,000 ft^2). The substantive conclusions are as follows:

1. Laboratory batch and column testing with contaminants and mixtures of dissolved phase natural organic matter (humic and fulvic acids) indicated that the mat amendments should remain effective in adsorption of metals and organics in marine environments of low to moderate dissolved organic matter levels;
2. Geotextile testing and modeling have identified a material and mesh size that are effective in the retention of the amendment material but sufficiently porous to allow the free flow of groundwater through the mats;
3. Repeated testing of field acclimated amendments contained in mini-mat systems deployed over a two year period did not show any reduction in adsorptive capacity, lending confidence to longer term effectiveness of the mat system as presently designed;
4. Field observations revealed that methane accumulations can lift the reactive mats from the sediment surface, but these effects can be mitigated if an overlying sand layer is used to provide additional weight and stability to the system. This expectation was confirmed by gas permeability testing conducted on geotextiles in a controlled laboratory setting, the results of which indicated that a coarse opening geotextile (*e.g.*, AOS 80) should be sufficient in allowing the maximum methane production found in freshwater environments to pass through the mat without experiencing uplift if such additional weighting is in place.
5. Conclusions regarded as relevant in assessment of whether mats did serve as an effective barrier to advection/diffusion were focused on select contaminants that were (1) detected

in the below treatment samples, (2) had a below treatment mean concentration greater than or equal to the above treatment concentration and (3) had a below treatment concentration greater than the ambient surface water concentration. Statistically significant (at 90-95% confidence) below/above reductions were observed in primarily two treatments (mat/sand and double mat) for select metals (nickel, zinc, barium, silver, vanadium) and several PAHs (benzo[b]fluoranthene, indeno[1,2,3-c,d]pyrene, benzo[g,h,i]perylene, anthracene, benzo[a]anthracene), thus demonstrating that contaminant sequestration had occurred. Maintenance of two- to four-fold concentration gradients across the prototype mat boundary for both metals and organics were well replicated over a two year period which suggests that the mats did serve as an effective barrier to diffusion for these contaminants.

6. Chemical gradients observed in Trident Probe data indicated reductions in metals concentrations below reactive mats 6-8X higher than the sand cap only treatment. This reduction may be due to a "halo" effect wherein porewater metals (and presumably organics) are sequestered into the amendment cap at depths deeper than the point of physical contact, possibly due to diffusion.

7. Demonstrated mat performance for other metals of ecological concern (*e.g.*, copper) was less robust because of overall low environmental concentrations relative to detection limits.

In conclusion, the reactive mats were proven to be generally effective in sequestering chemicals in sediment and are significantly thinner than non-reactive caps that may require a thickness of a meter or more as needed to ensure effective cover. This lightweight design did prove somewhat problematic due to uplift caused by methane accumulation beneath the mats, but this situation can be rectified by adding an additional sand layer coating. Conclusive (*i.e.*, statistically significant) results were observed for a small number of contaminants, but these cases were generally limited by the number of positive detections rather than mat effectiveness. More definitive results are expected if a follow-on test site has higher porewater constituent concentrations (*i.e.*, in the ecological risk range) so as to allow for documentation of larger gradients/reductions across the mat boundary.

The findings from this study represent significant evolution in the maturity of amendment technology. A mat with sand cover is expected to be an effective treatment in the majority of cases, although double mats may be applied if extra reduction in contaminant flux is desired. Presently, a mixture of apatite, organoclay and activated carbon in roughly equal proportions will address both metals and non-polar organics (PCBs and PAHs); depending on site contaminants one or more amendments could be replaced with extra amendment of the remaining type to likely boost effectiveness as needed.

Finally, promoting the use of reactive mats as a far more environmentally sustainable remedy relative to traditional dredging would be achieved by a pilot scale demonstration. Reactive mat capping (assuming sand capping alone would be insufficient) when used as a remedy would largely eliminate greenhouse gas (CO-, CO_2) emissions otherwise released during excavation by dredge barge and trucking equipment, and would increase the life expectancy of landfills not otherwise depleted with dredged material. Lastly, the use of reactive mats may also provide a

starting point to monitored natural attenuation (MNA), wherein the initial benthic recolonization made possible by the mats would jump-start further sediment deposition and therefore eventual re-establishment of infaunal communities.

ACKNOWLEDGEMENTS

Ms. Amy L. Hawkins:	Naval Facilities Engineering Service Center Lead Investigator Specialist in Sediment Risk Assessment
Dr. Gregory A. Tracey:	Science Applications International Corporation Specialist in Contaminated Sediment Assessment
Dr. Kevin H. Gardner:	University of New Hampshire Expertise in Laboratory Evaluation of Contaminated Sediments and Reactive Capping Materials
Dr. Jeffrey S. Melton:	University of New Hampshire Expertise in Reactive Cap Design and Performance Evaluation

This page is intentionally left blank.

REFERENCES

Adams, R.G., R. Lohmann, L.A. Fernandez, J.K. MacFarlane, P.M. Gschwend. 2007. Polyethylene Devices: Passive Samplers for Measuring Dissolved Hydrophobic Organic Compounds in Aquatic Environments. *Environ. Sci. Technol*., 2007, 41 (4), pp 1317-1323. January.

Barker, R.A. and C.L. Braun. 2000. Computer-model analysis of ground-water flow and simulated effects of contaminant remediation at Naval Weapons Industrial Reserve Plant, Dallas, Texas. U.S. Geological Survey Water-Resources Investigations Report 00–4197, 44 p.

Chadwick, D.B., J. Groves, C. Smith, and R. Paulsen. 2003. Hardware description and sampling protocols for the Trident Probe and UltraSeep system: Technologies to evaluate contaminant transfer between groundwater and surface water. Technical Report #1902, SSC San Diego, United States Navy.

Colwell, F.S., S. Boyd, M.E. Delwiche, D.W. Reed, T.J. Phelps, and D.T. Newby. 2008. Estimates of Biogenic Methane Production Rates in Deep Marine Sediments at Hydrate Ridge, Cascadia Margin. *Appl. Environ. Microbiol*. Vol. 74, No. 11, pp 3444-3452.

EnSafe/Allen & Hoshall. 1994. Comprehensive long-term environmental action-Navy stabilization work plan. Revision I: Memphis, Tenn. 83 p.

EnSafe/Allen & Hoshall. 1996. Draft RCRA, facility investigation report, Naval Weapons Industrial Reserve Plant, Dallas, Texas. Volume I: Memphis, Tenn.

EnSafe. 2000. Ecological Risk Assessment Screening Level, Mountain Creek Lake, Dallas, Texas. Prepared for SOUTNAVFACENGCOM, Charleston, SC.

EnSafe. 2001. Affected Property Assessment Report, Mountain Creek Lake, Dallas, Texas. Prepared for NAVFAC under contract N62467-89-D-0318, CTO 0025.

Fischer, G.R., A.D. Mare and R.D. Holtz. 1999. Influence of Procedural Variables on the Gradient Ratio Test. *Geotechnical Testing Journal*. Vol. 22, No. 1, pp 22–31.

Groundwater Seepage, Inc. 2007. Final. Data Report. Groundwater Upwelling Survey, Naval Weapons Industrial Reserve Plant, Cottonwood Bay, Dallas, Texas. November.

Iocco, L.E., P. Wilber and R.J. Diaz. 2000. Final Report. Benthic Habitats of Selected Areas of the Hudson River, NY Based on Sediment Profile Imagery. September.

Knox, A.S., M.H. Paller, D.D. Reible, X.Ma, I.G. Petrisor. 2008. Sequestering Agents for Active Caps-Remediation of Metals and Organics. *Soil and Sediment Contamination*, 17 (5) 516-532 (2008).

Knox, A.S., M.H. Paller, K. Dixon, D.D. Reible. 2011. Field Performance of Active Caps – Assessment of Contaminant Immobilization, Erosion Resistance, and Toxicity. SERDP Project ER-1501.

Lafleur, J., J. Mlynarek and A.L. Rollin. 1989. Filtration of Broadly Graded Cohesionless Soils. *Journal of Geotechnical Engineering*. Vol. 115, No. 12, pp 1747-1768.

McDonough, K.M., P. Murphy, J. Olsta, Y. Zhu, D. Reible, G. Lowry. 2007. Development and Placement of a Sorbent-amended Thin Layer Sediment Cap in the Anacostia River. *Journal of Soil and Sediment Remediation*. 16:3, 313-322 (2007).

Qingzhong, Y., K. T. Valsaraj, D.D. Reible and C.S. Willson. 2007. A Laboratory Study of Sediment and Contaminant Release during Gas Ebullition. *Journal of the Air & Waste Management Association (1995).* Vol. 57, No. 9, pp 1103-1111.

Reible, D.D., D. Lampert, W. D. Constant, R.D. Mutch, and Y. Zhu. 2006. Active Capping Demonstration in the Anacostia River, Washington, DC. *Remediation: The Journal of Environmental Cleanup Costs, Technologies and Techniques*. Vol. 17(1).

Melton, J.S., B.S. Crannell, K.H. Gardner, T. Eighmy and D.D. Reible. 2005. Apatite-Based Reactive Barrier Technology in the Anacostia River Study. In: *Remediation of Contaminated Sediments 2005: Finding Achievable Risk Reduction Solutions. Proceedings of the Third International Conference on Remediation of Contaminated Sediments*. R.F. Olfenbuttel and P.J. White, Eds. Battelle Press, Columbus, OH.

NAVFAC. 2006. Annual Progress Report. Reactive Capping Mat Development and Evaluation for Sequestering Contaminants in Sediment. Prepared for SERDP Project Number ER-1493. With Science Applications International Corporation and the University of New Hampshire. December.

NAVFAC. 2007. Second Year Annual Progress Report. Reactive Capping Mat Development and Evaluation for Sequestering Contaminants in Sediment. Prepared for SERDP Project Number ER-1493. With Science Applications International Corporation and the University of New Hampshire. December.

Niederer, C., R.P. Schwarzenbach and K. Goss. 2007. Elucidating Differences in the Sorption Properties of 10 Humic and Fulvic Acids for Polar and Nonpolar Organic Chemicals. *Environ. Sci. Tech*. 2007, 41, 6711 – 6717.

Osterberg, R. and K Mortense. 1992. Fractal dimension of Humic Acids. *European Biophysics Journal*. 1992, 21, 163-167.

Owenby, J.R. and D.S. Ezell. 1992. Climatography of the United States-Monthly station normals of temperature, precipitation, and heating and cooling degree days, 1961–91. Asheville, N.C. National Climatic Data Center no. 81, 65 p.

Petty, J.D., C.E. Orazio, J.N. Huckins, R.W. Gale, J.A. Lebo, J.C. Meadows, K.R. Echols, W.L. Cranor. 2000. Considerations involved with the use of semipermeable membrane devices for monitoring environmental contaminants. *Journ. of Chrom.* A Vol. 879, pp. 83-95.

Pirbazari, M., V. Ravindram, S.P. Wong and M.R. Stevens. 1989. Adsorption of Micropollutants on Activated Carbon. Aquatic Humic Substances – Influence on Fate and Treatment of Pollutants. ACS publishers. 1989, 549-578.

Reible, D. and G. Lotufo. 2008. Lab Demonstration Plan, Summary and Results ER-0624, Demonstration and Evaluation of Solid Phase Microextraction for the Assessment of Bioavailability and Contaminant Mobility. June 5.

Rhoads, D.C. and J.D. Germano. 1982. Characterization of organism-sediment relations using sediment profile imaging: An efficient method of remote ecological monitoring of the seafloor (Remots™ System). *Mar. Ecol. Prog. Ser.* 8: 115-128.

Rhoads, D.C., and J.D. Germano. 1986. Interpreting long-term changes in benthic community structure: A new protocol. *Hydrobiologia.* 142: 291-308.

Saparpakorn, P., J.H. Kim and S. Hannongbua. 2007. Investigation on the Binding of Polycyclic Aromatic Hydrocarbons with Soil Organic Matter: A Theoretical Approach. *Molecules*. 2007, 12, 703-715.

Sharma, B. 2008. Evaluation of Reactive Cap Sorbents for In-Situ Remediation of Contaminated Sediments. Submitted to the University of New Hampshire. September.

VanMetre, P.C., S.A. Jones, J.B. Moring, B.J. Mahler and J.T. Wilson. 2003. Chemical Quality of Water, Sediment, and Fish in Mountain Creek Lake, Dallas, Texas, 1994-97. Geological Survey Water-Resources Investigations Report 03-4082, 69 p.

Wu , F. C., R.D. Evans and P.J. Dillon. 2003. Separation and Characterization of NOM by High-Performance Liquid Chromatography and On-Line Three Dimensional Excitation Emission Matrix Fluorescence Detection. *Environ. Sci. Tech.* 2003, 37, 3687-3693.

Zhao, X., P. Viana, K. Yin, K. Rockne, D. Hey, J. Schuh, R. Lanyon. 2007. Combined Active Capping/Wetland Demonstration in the Chicago River. Paper D-019 in: E.A. Foote and G.S. Durell (Conference Chairs), Remediation of Contaminated Sediments 2007. Proceedings of the Fourth International Conference on Remediation of Contaminated Sediments (Savannah, Georgia; January 2007). Battelle Press, Columbus, OH.

This page is intentionally left blank.

APPENDIX A

"SERDP Project Number ER-1493 First Year Annual Progress Report (December 2006)"

This page is intentionally left blank.

APPENDIX B

"SERDP Project Number ER-1493 Second Year Annual Progress Report (December 2007)"

This page is intentionally left blank.

APPENDIX C

"Mat System Consolidation and Groundwater Flow Modeling Results"

This page is intentionally left blank.

APPENDIX D

“Prototype Mat System Geophysical Results (December 2008)”

This page is intentionally left blank.

APPENDIX E

"First and Second Year Peeper Analytical Results (December 2008 & December 2009)"

This page is intentionally left blank.

APPENDIX F

"First and Second Year Semi-Permeable Membrane Device (SPMD) Analytical Results (December 2008 & December 2009)"

This page is intentionally left blank.

APPENDIX G

“Prototype Mat System Ultraseep Flow and Analytical Data (June 2009)”

This page is intentionally left blank.

APPENDIX H

"Prototype Mat System Trident Probe Analytical Results (June 2009)"

This page is intentionally left blank.

APPENDIX I

“Prototype Mat System Sediment Core Results (October 2009)”

This page is intentionally left blank.

ATTACHMENT 1

"Evaluation of Reactive Cap Sorbents for In Situ Remediation of Contaminated Sediments"

Bhawana Sharma

Submitted to the University of New Hampshire

September 2008

This page is intentionally left blank.